

**BIOGEOCHEMISTRY OF PALEOZOIC BRACHIOPODS
FROM
NEW YORK STATE AND ONTARIO**

A Thesis Presented
to the Department of Geological Sciences
Brock University

In Partial Fulfillment
of the Requirements for the Degree
Master of Science
in Geology

by

Nicholas R. Bates

©1989

Dr. Uwe Brand

Thesis Supervisor

In Praise of Limestone

If it form the one landscape that we, the inconstant ones,
Are consistently homesick for, this is chiefly
Because it dissolves in water.....

W.H. Auden, 1951.

Abstract

A comprehensive elemental, isotopic and microstructural analyses was undertaken of brachiopod calcites from the Hamilton Group (Middle Devonian), Clinton Group (Middle Silurian) and Middle to Upper Ordovician strata of Ontario and New York State. The majority of specimens were microstructurally and chemically preserved in a pristine state, although a number of specimens show some degree of post-depositional alteration. Brachiopod calcites from the Hamilton and Clinton Groups were altered by marine derived waters whereas Trenton Group (Middle Ordovician) brachiopods altered in meteorically derived fluids.

Analysis of the elemental and isotopic compositions of pristine Hamilton Group brachiopods indicates there are several chemical relationships inherent to brachiopod calcite. Taxonomic differentiation of Mg, Sr and Na contents was evident in three co-occurring species from the Hamilton Group. Mean Mg contents of pristine brachiopods were respectively *Athyris spiriferoides* (1309ppm), *Mucrospirifer mucronatus* (1035ppm) and *Mediospirifer audacula* (789ppm). Similarly, taxonomic differentiation of shell calcite compositions was observed in co-occurring brachiopods from the Clinton Group (Middle Silurian) and the Trenton Group (Middle Ordovician). The taxonomic control of elemental regulation into shell calcite is probably related to the slightly different physiological systems and secretory mechanisms.

A relationship was observed in Hamilton Group species between the depth of respective brachiopod communities and their Mg, Sr and Na contents. These elements were depleted in the shell calcites of deeper brachiopods compared to their counterparts in shallower reaches. Apparently shell calcite elemental composition is related to environmental conditions of the depositional setting, which may have controlled the secretory regime, mineral morphology of

shell calcite and precipitation rates of each species. Despite the change in Mg, Sr and Na contents between beds and formations in response to environmental conditions, the taxonomic differentiation of shell calcite composition is maintained. Thus, it may be possible to predict relative depth changes in paleoenvironmental reconstructions using brachiopod calcite. This relationship of brachiopod chemistry to depth was also tested within a transgressive-regressive (T-R) cycle in the Rochester Shale Formation (Middle Silurian). Decreasing Mg, Sr and Na contents were observed in the transition from the shallow carbonates of the Irondequoit Formation to the deeper shales of the lowest 2 m of Rochester Shale. However, no isotopic and elemental trends were observed within the entire T-R cycle which suggests that either the water conditions did not change significantly or that the cycle is illusory.

A similar relationship was observed between the Fe and Mn chemistries of shell calcite and redox/paleo-oxygen conditions. Hamilton Group brachiopods analysed from deeper areas of the shelf are enriched in Mn and Fe relative to those from shallow zones. The presence of black shales and dysaerobic faunas, during deposition of the Hamilton Group, suggests that the waters of the northern Appalachian Basin were stratified. The deeper brachiopods were marginally positioned above an oxycline and their shell calcites reflect periodic incursions of oxygen depleted water. Furthermore, analysis of *Dalmanella* from the black shales of the Collingwood Shale (Upper Ordovician) in comparison to those from the carbonates of the Verulam Formation (Middle Ordovician) confirm the relationship of Fe and Mn contents to periodic but not permanent incursions of low oxygen waters.

The isotopic compositions of brachiopod calcite found in Hamilton Group ($\delta^{13}\text{C}$; +2.5‰ to +5.5‰; $\delta^{18}\text{O}$ -2.5‰ to -4.0‰) and Clinton Group ($\delta^{13}\text{C}$; +4.0‰ to +6.0; $\delta^{18}\text{O}$; -1.8‰ to -3.6‰) are heavier than previously reported.

Uncorrected paleotemperatures (assuming normal salinity, 0‰ SMOW and no fractionation effects) derived from these isotopic values suggest that the Clinton sea temperature (Middle Silurian) ranged from 18°C to 28°C and Hamilton seas (Middle Devonian) ranged between 24°C and 29°C. In addition, the isotopic variation of brachiopod shell calcite is significant and is related to environmental conditions. Within a single time-correlative shell bed (the *Demissa* Bed; Hamilton Group) a positive isotopic shift of 2-2.5‰ in $\delta^{13}\text{C}$ compositions and a positive shift of 1.0-1.5‰ in $\delta^{18}\text{O}$ composition of shell calcite is observed, corresponding with a deepening of brachiopod habitats toward the axis of the Appalachian Basin. Moreover, a faunal succession from deeper *Ambocoelia* dominated brachiopod association to a shallow *Tropidoleptus* dominated association is reflected by isotopic shifts of 1.0-1.5‰. Although, other studies have emphasized the significance of ± 2 ‰ shifts in brachiopod isotopic compositions, the recognition of isotopic variability in brachiopod calcite within single beds and within depositional settings such as the Appalachian Basin has important implications for the interpretation of secular isotopic trends. A significant proportion of the variation observed isotopic distribution during the Paleozoic is related to environmental conditions within the depositional setting.

Table of Contents

ABSTRACT.....	i
LIST OF FIGURES.....	ix
LIST OF TABLES.....	xvi
INTRODUCTION.....	xviii

Chapter 1. **Preliminary considerations and methodology**

THEORETICAL CONSIDERATIONS.....	1
DIAGENETIC CONSIDERATIONS.....	5
GEOCHEMISTRY OF BRACHIOPOD SHELL CALCITE.....	8
BRACHIOPOD ECOLOGY.....	10
METHODOLOGY	
Area of study.....	11
Sampling procedure.....	15
Sample preparation.....	15
Trace and minor element analysis.....	16
Carbon and oxygen isotopic analysis.....	17
Scanning electron microscopy.....	17
Thin section studies.....	18
Statistical analysis of chemical data.....	18

Chapter 2. **Primary and diagenetic microstructures of brachiopod shell calcite**

INTRODUCTION.....	20
-------------------	----

BRACHIOPOD SECRETION AND SHELL MICROSTRUCTURE.....	20
MODERN BRACHIOPOD SHELL CALCITE MICROSTRUCTURE.....	26
PALEOZOIC BRACHIOPOD MICROSTRUCTURE	
Primary structure.....	26
Diagenetic structure.....	34
CONCLUSIONS.....	38

Chapter 3. **Diagenetic and paleoenvironmental investigation of
brachiopod shell calcite from the Middle Devonian
Hamilton Group; New York State and Ontario.**

INTRODUCTION.....	41
GENERAL GEOLOGY.....	45
RESULTS.....	48
Diagenetic trends.....	50
Diagenetic waters of the Hamilton Group.....	56
Selection of best preserved material.....	57
BRACHIOPOD SHELL CALCITE CHEMISTRY	
Generic trends.....	61
<i>Fractionation of Mg</i>	61
<i>Fractionation of Sr</i>	64
<i>Fractionation of Na</i>	66
Relationship of shell chemistry to biofacies and environmental conditions.....	67
Isotopic trends.....	70
PALEOENVIRONMENTAL ANALYSIS OF THE "DEMISSA " BED.....	71
Chemical trends.....	73
Isotopic trends.....	76

PALEOENVIRONMENTAL ANALYSIS OF THE LOWER WINDOM SHALE.....	78
Chemical trends.....	79
Isotopic trends of the Lower Windom Shale.....	81
PALEOENVIRONMENTAL ANALYSIS OF THE KASHONG.....	82
PALEOENVIRONMENTAL ANALYSIS OF THE HUNGRY HOLLOW, ARKONA AND WIDDER FORMATIONS.....	84
BRACHIOPODS AND LOW OXYGEN CONDITIONS.....	86
CONCLUSIONS.....	89

Chapter 4. **Diagenetic and paleoenvironmental study of brachiopod
shell calcite from the Clinton Group (Middle Silurian);
New York State and Ontario.**

INTRODUCTION.....	92
GENERAL GEOLOGY.....	93
RESULTS AND DISCUSSION	
Chemical trends.....	95
Elemental fractionation and taxonomic trends.....	98
Isotopic trends.....	98
DIAGENETIC EVALUATION OF CLINTON GROUP BRACHIOPODS	
Merritton Formation.....	101
Reynales Formation.....	103
Irondequoit and Rochester Shale Formation diagenetic waters.....	104
PALEOENVIRONMENTAL ANALYSIS OF THE IRONDEQUOIT FORMATION.....	106
PALEOENVIRONMENTAL ANALYSIS OF THE ROCHESTER SHALE FORMATION	
Introduction.....	110

Stratigraphic setting of the Lewiston Member.....	110
Chemical trends.....	114
Isotopic trends.....	118
Geochemistry of brachiopods from the Burleigh Hill Member.....	125
CONCLUSIONS.....	131

Chapter 5. **Diagenetic and paleoenvironmental study of brachiopod calcite from the Middle and Upper Ordovician; southern Ontario and Manitoulin Island.**

INTRODUCTION.....	133
GENERAL GEOLOGY.....	133
RESULTS	
Chemical trends.....	137
Isotopic trends.....	141
Lithology and preservation potential.....	141
Diagenetic waters of the Middle and Upper Ordovician.....	144
PALEOENVIRONMENTAL ANALYSIS OF MIDDLE TO UPPER ORDOVICIAN.....	149
Taxonomic differences in shell calcite composition.....	150
Relationship of depth to Mg, Sr, and Na compositions of brachiopod calcite.....	150
Brachiopod calcite and low oxygen conditions.....	152
Depositional waters.....	154
Isotope trends.....	154
CONCLUSIONS.....	156

Chapter 6. **Secular trends of oxygen and carbon isotopes**

INTRODUCTION.....	158
CARBON ISOTOPES.....	159
OXYGEN ISOTOPES.....	162
CONCLUSIONS.....	165
ACKNOWLEDGEMENTS.....	166
REFERENCES.....	167
APPENDIX I Locality description and sampling horizons.....	195
APPENDIX II Species identification.....	226
APPENDIX III Isotopic and elemental data.....	227
APPENDIX IV Statistical tables.....	248
APPENDIX V Taphonomic summary table.....	257

List of Figures

Figure 1.1	Locality map of Middle and Upper Ordovician sampling sites.....	12
Figure 1.2	Locality map of Middle Silurian sampling sites in Ontario and New York State.....	13
Figure 1.3	Locality map of Hamilton Group (Middle Devonian) sampling sites.....	14
Figure 2.1	Generalized cross-section of an articulate brachiopod exoskeleton.....	21
Figure 2.2	S.E.M. micrograph of primary and secondary calcite layers of <i>Laqueus vancouverensis</i>	23
Figure 2.3	S.E.M. micrograph cross section of foliated secondary shell layer around punctae.....	23
Figure 2.4	S.E.M. micrograph of the imbricate internal surface of <i>L.</i> <i>vancouverensis</i>	27
Figure 2.5	S.E.M. micrograph of regularly-spaced punctal openings on the internal surface of a <i>L.vancouverensis</i> shell.....	27
Figure 2.6	S.E.M. micrograph close up of fibrous secondary shell layer.....	28
Figure 2.7	S.E.M. micrograph of the secondary layer of <i>Mediospirifer audacula</i> (#400; Hamilton Group).....	28
Figure 2.8	S.E.M. micrograph of the secondary layer of <i>Mucrospirifer mucronatus</i> (#178; Hamilton Group).....	30
Figure 2.9	S.E.M. micrograph of the secondary layer of <i>Eospirifer radiatus</i> (#2301; Lewiston Member, Middle Silurian, New York State.....	30
Figure 2.10	S.E.M. micrograph of the imbricated internal valve surface of <i>Athyris spiriferoides</i> (#403, Wanakah Shale, New York State).....	31
Figure 2.11	S.E.M. micrograph of the internal surface of an etched <i>Athyris</i>	31

Figure 2.12	S.E.M. micrograph of primary, secondary and tertiary layer shell calcite layers of <i>Mediospirifer audacula</i> (#71, Wanakah Shale).....	32
Figure 2.13	S.E.M. micrograph cross section of prismatic trabecular calcite morphology in <i>Whitfieldella nitida</i> valves (#2108, Irondequoit Formation).....	32
Figure 2.14	S.E.M. micrograph of the internal surface of an etched <i>Tropidoleptus carinatus</i> (#409, Wanakah Shale, New York State).....	33
Figure 2.15	S.E.M. micrograph cross section of the secondary shell layer of <i>Tropidoleptus</i> (#409, Wanakah Shale, New York State).....	33
Figure 2.16	S.E.M. micrograph of the internal valve surface of <i>Rhipidomella vanuxemi</i> (#412, Wanakah Shale, New York State).....	35
Figure 2.17	S.E.M. micrograph of micropores on the internal valve surface of <i>Eospirifer radiatus</i> (#2195, Lewiston Member, New York).....	35
Figure 2.18	S.E.M. micrograph of the secondary fibrous shell layer of altered <i>Athyris spiriferoides</i> (#5, Wanakah Shale, Middle Devonian, New York).....	36
Figure 2.19	S.E.M. micrograph of the secondary fibrous shell layer of altered <i>Athyris spiriferoides</i> (#61, Wanakah Shale, Middle Devonian, New York).....	36
Figure 2.20	S.E.M. micrograph of recrystallized <i>Pentameroides</i> sp. from the Merritton Formation (#2007, Middle Silurian, Ontario).....	37
Figure 2.21	S.E.M. micrograph of laminar secondary shell structure of <i>Rafinesquina deltoidea</i> (#794, Verulam Formation, Ontario).....	37
Figure 2.22	S.E.M. micrograph of secondary shell structure of orthid <i>Dalmanella rogata</i> (#754, Verulam Formation, Ontario).....	39
Figure 2.23	S.E.M. micrograph of punctate brachiopod <i>Tropidoleptus</i> showing punctal filling cements (#409, Wanakah Shale, New York State).....	39

Figure 3.1	Generalized paleoecological model relating Hamilton Group biofacies to inferred gradients of depth-related parameters, turbidity and/or sedimentation rates and oxic conditions.....	43
Figure. 3.2	Diagrammatic cross-section of the Upper Hamilton Group (Middle Devonian) across New York State.....	44
Figure 3.3	Paleogeographic reconstruction of the Appalachian Basin during deposition of the Middle Devonian Hamilton Group.....	46
Figure 3.4	Generalized stratigraphic section of the Ludlowville and Moscow Formations of the Hamilton Group.....	47
Figure 3.5	Scatter plot of Fe vs Mn for all Devonian brachiopods.....	52
Figure 3.6	Scatter diagram of Na vs Mg for brachiopods and matrix of the Hamilton Group (Middle Devonian).....	53
Figure 3.7	Scatter plot of Fe vs Mn for <i>Tropidoleptus</i> and <i>Rhipidomella</i> brachiopods from the Hamilton Group (Middle Devonian).....	55
Figure 3.8.	Scatter plot of Na vs Mg for <i>Tropidoleptus</i> and <i>Rhipidomella</i> brachiopods from the Hamilton Group.....	55
Figure 3.9	The mean and standard deviations of unaltered elemental chemistries of three Hamilton Group brachiopod species.....	63
Figure 3.10	Routes of elemental transport from the external environment toward the site of carbonate secretion.....	65
Figure 3.11	Mean and standard deviations of unaltered brachiopod elemental chemistries related to brachiopod biofacies and depth.....	68
Figure 3.12	Mean and standard deviation of unaltered chemistries; <i>Athyris</i> and <i>Mediospirifer</i> from the <i>Demissa</i> Bed across the Hamilton Shelf.....	74
Figure 3.13	Isotopic compositions of <i>Athyris</i> and <i>Mediospirifer</i> brachiopods from the Hamilton Group.....	77
Figure 3.14	Scatter plot of Fe vs Mn for Lower Windom brachiopods	

	from western New York State.....	80
Figure 3.15	Scatter diagram of Fe vs Mn contents of upper and lower Kashong Shale Member brachiopods (upper Hamilton Group).....	83
Figure 3.16	Scatter plot of Fe vs Mn for <i>Mucrospirifer</i> brachiopods from the Arkona, Hungry Hollow and Widder Formations (Middle Devonian).....	85
Figure 3.17	Scatter plot of Na vs Mg for <i>Mucrospirifer</i> brachiopods from the Arkona, Hungry Hollow and Widder Formations (Middle Devonian).....	87
Figure 4.1	Middle Silurian stratigraphy of southern Ontario and New York State.....	94
Figure 4.2	Scatter plot of Fe vs Mn for all species from the Middle Silurian Clinton Group (Wenlockian).....	97
Figure 4.3	Diagenetic trend of isotopic compositions of Middle Silurian Clinton Group brachiopods.....	100
Figure 4.4	Isotopic compositions of <i>Eospirifer</i> from Irondequoit, Rochester Reynales and Merritton Formations of the Middle Silurian Clinton Group.....	102
Figure 4.5	Scatter plot of Na vs Mg for all species from the Middle Silurian Clinton Group (Wenlockian).....	105
Figure 4.6	Rochester Shale/Irondequoit Formation brachiopod associations with reference to inferred gradients of depth-related parameters and turbidity and/or sedimentation rates.....	108
Figure 4.7	Diagenetic trend of Irondequoit Formation brachiopods (Middle Silurian).....	109
Figure 4.8	Scatter plot of Na vs Mg contents of Irondequoit brachiopods illustrates two diagenetic trends.....	109
Figure 4.9	Rochester Shale stratigraphic section at Niagara Gorge.....	111
Figure 4.10	Facies map of the Rochester Shale across southern Ontario and western New York State.....	113

Figure 4.11	Scatter plot of Fe vs Mn for all species from the Lewiston Member of the Rochester Shale Formation.....	116
Figure 4.12	Na vs Mg scatter plot of Lewiston Member brachiopods.....	116
Figure 4.13	Plot of mean Sr, Mn and Fe contents of <i>Atrypa reticularis</i> and <i>Eospirifer radiatus</i> against height within the Lewiston Member section.....	117
Figure 4.14	Plot of mean Mg and Na contents of pristine <i>Atrypa reticularis</i> and <i>Eospirifer radiatus</i> height within the Lewiston Member section.....	119
Figure 4.15	Plot of mean Mg and Na contents of pristine <i>Atrypa reticularis</i> from the Lewiston Member subunits A and B.....	120
Figure 4.16	Mean isotopic composition (in per mil; PDB) of pristine <i>Eospirifer radiatus</i> from the Irondequoit Formation and Lewiston Member of western New York State (Clinton Group Middle Silurian).....	123
Figure 4.17	Plot of oxygen isotopes versus Mg contents within pristine <i>Eospirifer radiatus</i> from the Irondequoit Formation and Lewiston Member (Clinton Group, Middle Silurian).....	124
Figure 4.18	Burleigh Hill Member stratigraphic section at the type locality in St. Catharines, Ontario.....	126
Figure 4.19	Scatter plot of Fe vs Mn for all species from the Burleigh Hill Member (Clinton Group).....	129
Figure 4.20	Scatter plot of Sr vs Mg for all brachiopod species of the Burleigh Hill Member (Clinton Group).....	130
Figure 5.1	Generalized stratigraphic section of southern central Ontario.....	135
Figure 5.2	Middle and Upper Ordovician Stratigraphy of Manitoulin Island.....	136
Figure 5.3	Scatter plot of Fe vs Mn for all brachiopods from the Middle and Upper Ordovician of south Ontario and Manitoulin Island.....	140
Figure 5.4	Diagenetic trend of oxygen isotopic composition for Middle and	

	Upper Ordovician <i>Dalmanella rogata</i> and <i>Rafinesquina deltoidea</i> brachiopods of southern Ontario.....	142
Figure 5.5	Diagenetic trend of oxygen isotopic composition for Middle and Upper Ordovician <i>Dalmanella rogata</i> and <i>Rafinesquina deltoidea</i> brachiopods of southern Ontario and Manitoulin Island.....	142
Figure 5.6	Scatter plot of Sr vs Mn for <i>Dalmanella rogata</i>	143
Figure 5.7	Scatter plot of Sr vs Mn for <i>Sowerybella</i> sp.....	145
Figure 5.8	Scatter diagram of Na vs Mg for brachiopods from Manitoulin Island and from southern Ontario.....	147
Figure 5.9	Mean and standard deviation of unaltered chemistries of <i>Dalmanella</i> <i>rogata</i> , <i>Rafinesquina deltoidea</i> and <i>Sowerybella</i> sp. of the Verulam Formation.....	152
Figure 5.10	Scatter plot of Fe vs Mn for <i>Dalmanella rogata</i>	155
Figure 6.1	Secular trend of carbon isotopes during the Paleozoic.....	161
Figure 6.2	Secular trend of oxygen isotopes during the Paleozoic.....	161
Figure A-1	Stratigraphic section of Hamilton Group (Middle Devonian) units at Hungry Hollow Quarry.....	196
Figure A-2	Stratigraphic section of Wanakah and Windom Shale Members at Eighteen Mile Creek.....	197
Figure A-3	Stratigraphic section of Hamilton Group strata exposed at Penn Dixie Quarry.....	200
Figure A-4	Stratigraphic section of Hamilton Group strata exposed at Cazenovia Creek.....	202
Figure A-5	Section of Hamilton Group strata exposed at Murder Creek.....	205
Figure A-6	Section of Hamilton Group strata exposed at Jaycox Creek.....	208
Figure A-7	Stratigraphic section of Verulam Formation from the Bolsover roadcut.....	219

Figure A-8	Stratigraphic section of Verulam Formation at Kirkfield Quarry.....	220
Figure A-9	Stratigraphic section of Verulam Formation at Lakefield Quarry near Peterborough.....	224
Figure A-10	Stratigraphic section of Verulam Formation outcropping along roadcuts at the intersection of Highways 33 and 401.....	225

List of Tables

Table 3.1	Middle Devonian chemical data of all brachiopods and pristine brachiopods.....	49
Table 3.2	Comparison of microstructural preservation and chemical contents for selected brachiopods from the Middle Devonian Hamilton Group of western New York State and southern Ontario.....	52
Table 3.3	T-test: Upper Hamilton Group unaltered brachiopods.....	62
Table 3.4	T-test: Demissa bed (upper Wanakah Shale) unaltered brachiopod chemical data.....	62
Table 3.5	T-test: Demissa bed (Wanakah Shale) unaltered brachiopods.....	75
Table 4.1	Summary of chemical data for all Clinton Group brachiopods and for pristine specimens.....	96
Table 4.2	Comparison of microstructural preservation and chemistry for selected brachiopods, representing different species and lithologies.....	96
Table 4.3a	Summary of pristine brachiopod calcites from the Rochester Shale and Irondequoit Formations.....	99
Table 4.3b	Unpaired T-test: pristine brachiopod chemistry (Clinton Group).....	99
Table 4.4	Unaltered brachiopod chemistries from locality 36 (Burleigh Hill Member).....	128
Table 4.4	Unaltered brachiopod chemistries from locality 34 (Burleigh Hill Member).....	128
Table 5.1	Geochemical data of Middle and Upper Ordovician brachiopods from Ontario and Manitoulin Island.....	138
Table 5.2.	Comparison of microstructural preservation and chemistry for selected brachiopods, representing different species and lithologies.....	139
Table 5.3	T-test: Verulam Formation unaltered brachiopods.....	151

Table A-1	Factor analysis of Devonian brachiopod elemental chemistries.....	249
Table A-2	Factor analysis of <i>Athyris spiriferoides</i>	249
Table A-3	Factor analysis of <i>Mucrospirifer mucronatus</i>	250
Table A-4	Factor analysis of <i>Mediospirifer audacula</i>	250
Table A-5	Factor analysis of <i>Tropidoleptus carinatus</i>	251
Table A-6	Factor analysis of <i>Rhipidomella vanuxemi</i>	251
Table A-7	Factor analysis of Middle Devonian brachiopod elemental chemistries.....	252
Table A-8	Factor analysis of Silurian brachiopod elemental chemistries.....	252
Table A-9	Factor analysis of <i>Eospirifer radiatus</i> elemental chemistries.....	253
Table A-10	Factor analysis of <i>Whitfieldella nitida</i> elemental chemistries.....	253
Table A-11	Factor analysis of <i>Atrypa reticularis</i> elemental chemistries.....	254
Table A-12	Factor analysis of Ordovician brachiopod elemental chemistries.....	254
Table A-13	Factor analysis of <i>Dalmanella rogata</i> elemental chemistries.....	255
Table A-14	Factor analysis of <i>Rafinesquina deltoidea</i> elemental chemistries.....	255
Table A-15	Factor analysis of <i>Sowerybella</i> sp. elemental chemistries.....	256

GENERAL INTRODUCTION

Articulate brachiopods were a common faunal element of Paleozoic shelf communities. Their abundance, and the fact that they secrete a low-Mg calcite shell that is quite resistant to diagenetic alteration makes them suitable for paleochemical investigations (Brand and Veizer, 1980; Popp et al., 1986a; Brand, 1982, 1983, 1989a). Brachiopods are generally assumed to incorporate stable isotopes in equilibrium with their external environment and shell calcite can provide a chemical record of changes in ocean and atmosphere chemistry during the Phanerozoic. As such, brachiopods have been used to investigate isotopic shifts at stratigraphic boundaries (e.g., Permo-Trias, Gruszczynski et al., 1989), extinction events (e.g., Frasnian-Famennian; Brand, 1989c) and the secular changes in isotopic compositions of Paleozoic oceans (Veizer 1985; Popp et al., 1986; Veizer et al., 1986; Brand, 1989a). For example, a post Devonian-Carboniferous change in brachiopod calcite $\delta^{18}\text{O}$ compositions has been attributed to either global cooling (Kump, 1989a) or to a change in the isotopic composition of oceans (Veizer et al., 1986). A further use of brachiopod calcite may be in the paleoenvironmental reconstruction of depositional settings and conditions (e.g., Adlis, 1988).

Although brachiopods are used in isotopic investigation, there is at present, little empirical data on their chemical composition. The composition of brachiopod calcite has been assumed to be singularly uniform for the purpose of selecting chemically pristine specimens for use in isotopic interpretations (Veizer et al., 1986). However, fractionation of Mg and Na contents into shell calcite has been reported previously (Popp et al., 1986; Brand, 1989a) which indicates that the chemistry of their shell calcite is variable and needs further scrutiny. As yet there is no comparative study of the chemistry of co-occurring

brachiopod species within the context of strict paleoecological and stratigraphic criteria. The spatial distribution of brachiopods upon a shelf is in part controlled by the environmental conditions (e.g., depth, turbidity, nutrient supply; Fursich and Hurst, 1974), and if a relationship between brachiopod chemistry and environmental conditions can be determined, brachiopod calcite may be useful in paleoenvironmental reconstructions and constraining isotopic interpretations. It is therefore the purpose of this thesis to investigate the trace element and isotopic geochemistry of ancient brachiopods in the context of their paleoecologic and stratigraphic settings.

The objectives of this study are as follows;

1. Assess the microstructural preservation of articulate brachiopod shell calcites from the Middle Devonian (Hamilton Group), Middle Silurian (Clinton Group), and Middle and Upper Ordovician of Ontario and New York State and illustrate the textural changes in shell calcite accompanying post-depositional alteration.

2. Evaluate the chemical preservation of shell calcites and determine the degree and direction of alteration of brachiopod calcite.

3. Investigate the elemental and isotopic trends in co-occurring brachiopod species, in order to illustrate: i) elemental fractionation; ii) taxonomic differentiation of shell calcite compositions and; iii) the relationship of shell calcite chemistry to environmental conditions such as depth and low oxygen conditions.

4. Evaluate the isotopic trends in brachiopod shell calcite within: i) a single shell bed that deepens across a basin and; ii) a transgressive-regressive cycle.

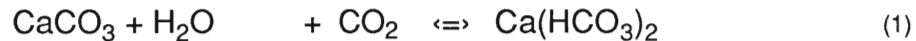
5. Evaluate the isotopic compositions of pristine brachiopod shell calcites in context with secular variations of mean oceanic $\delta^{13}\text{C}$ and $\delta^{18}\text{O}$ compositions during the Paleozoic.

CHAPTER 1

Preliminary considerations and methodology

THEORETICAL CONSIDERATIONS

The precipitation of calcium carbonate can be described by six simple chemical equilibria (Bathurst, 1975). Overall the reaction can be written;



Biogenic and inorganic carbonates contain other cations and anions beside Ca and the incorporation of minor and trace elements into calcium carbonate minerals can occur through five recognized processes (McIntire, 1963; Zemann, 1969; Veizer 1983a, b). These are:

1. Diadochic substitution of Ca^{2+} in the CaCO_3 lattice by minor (Mg^{2+} , Sr^{2+}) and trace elements (e.g., Fe^{2+} , Mn^{2+} , Zn^{2+} , Cu^{2+}).
2. Incorporation interstitially between lattice planes;
3. Occupation of vacant lattice positions due to crystal structural defects (e.g., point, line defects);
4. Adsorption to lattice surfaces due to remanent ionic charges;
5. Presence of non-carbonate components within silicate impurities and fluid inclusions;

The theory of diadochic substitution for Ca^{2+} (factor 1) is reasonably well understood and is a general basis for fossil biogeochemical studies (Brand and Veizer, 1980; Al-aasm and Veizer, 1982; 1986a, b; Veizer et al., 1986). The influence of other factors on chemical distribution is less certain (Veizer, 1983 a, b). Divalent metallic ions, such as Cd^{2+} , Cu^{2+} , Mn^{2+} and Co^{2+} , can be actively adsorbed onto the calcite lattice (Zachara et al., 1988) although this and the

influence of processes 2 to 4 are suggested to be random and negligible when compared to factor 1 (Veizer, 1983a). The fifth process, elemental leaching of Fe, Mn and Al from non-carbonate fractions, can be significant (Brand and Veizer, 1980; Boyle, 1981), but its contribution to the overall chemical composition can be minimized by refinements of the geochemical analysis, such as removal of all adhering matrix and the reduction of digestion times (Brand and Veizer, 1980; Veizer 1983a, 1983b; Morrison and Brand, 1986). Similarly, the presence of minute organic-rich fluid inclusions (1000Å or less in size) in biogenic carbonates may contribute to the analysis but these constitute less than 1% by volume (Bruni and Wenk, 1985; Gaffey, 1988). The significance of these chemical biases remain difficult to determine and quantify.

Carbonate mineralogy and crystal structure will partly determine the concentration of lattice bound minor and trace elements (Pingitore, 1976, 1978; Brand and Veizer, 1980; Veizer, 1983a, b; Morrison and Brand, 1986). Orthorhombic aragonite selectively incorporates larger cations (Sr^{2+} , Ba^{2+} , and Pb^{2+}) into lattice sites (Okumura and Kitano, 1986) whereas rhombohedral calcite favours smaller cations (Mg^{2+} , Fe^{2+} , Mn^{2+} , Zn^{2+} , Cu^{2+} , Ni^{2+} , and Cd^{2+} ; Reeder, 1983).

The incorporation of minor and trace elements into the CaCO_3 lattice is governed by a distribution coefficient (**D**) between solution and the particular mineralogical phase. It is defined as (McIntire, 1963; Kinsman, 1969);

$$({}^m\text{Me}/ {}^m\text{Ca}) \text{ (s)} = \mathbf{D} ({}^m\text{Me}/ {}^m\text{Ca}) \text{ (aq)} \quad (2)$$

where (^m) indicates molar concentration, Me is trace/minor element concentration, **D** is the distribution coefficient and (s) and (aq) represent solid and aqueous phases of calcium carbonate, respectively. This relationship is

only valid when the system is at equilibrium (constant temperature and pressure) and there are no concentration gradients between the phases (Veizer, 1983a, b). If a gradient exists, a heterogenous distribution law applies (Gordon et al., 1959; Morrison and Brand, 1986),

$$\log ({}^m\text{Me}_i / {}^m\text{Me}_f) = \mathbf{D} \log ({}^m\text{Ca}_i / {}^m\text{Ca}_f) \quad (3)$$

where **i** and **f** indicate initial and final concentrations of trace and minor elements and Ca in solution.

The trace and minor element distribution in carbonate, relative to the major elements Ca and Mg, will be governed by conditions of the distribution coefficient **D**. When **D** is equal to 1, the carbonate will incorporate Me in equilibrium with the aqueous phase. If **D** is greater than 1, the solid phase will contain higher Me concentrations than the aqueous phase and when **D** is less than 1, the carbonate precipitate will contain lower Me concentrations than the aqueous phase. Experimentally derived distribution coefficients for most elements in aragonite and calcite are listed in Veizer (Table ?, 1983a). Equilibrium conditions (**D** = 1) occur only when the amount of precipitate is minor compared to the volume of fluid (Veizer, 1983a). Partitioning of minor and trace elements into carbonates is dependant on certain physico-chemical conditions related to temperature (Bordine et al., 1965; Kinsman, 1969), coupled substitution (Mucci and Morse, 1983; Busenberg and Plummer, 1985), rate of precipitation (Lorens, 1981), and the nature of the overall reaction such as replacement, seeded growth or nucleation and growth (Reeder and Grams, 1987). For example, the partitioning of elements is less pronounced with increasing precipitation rates of carbonate (Lorens, 1981). The incorporation of Sr into non-lattice sites affects calculations of **D**_{sr} calcite at low Sr

concentrations (Pingitore and Eastman, 1985), and differential partitioning was observed in different crystal growth sectors of calcite cements (Reeder and Grams, 1987). Skeletal carbonates are assumed to incorporate Me in equilibrium with ambient conditions, however, biological fractionation occurs when the organism physiologically controls partitioning of elements into biogenic calcite. In molluscs and coral ectoderm, manipulation of extrapallial fluids by ionic regulation will be reflected in positively or negatively fractionated elemental contents of their carbonate.

The incorporation of oxygen and carbon isotopes into carbonate minerals is similarly governed by a fractionation factor (α);

$$R (s.) = \alpha_{(s.)-(aq.)} R (aq.) \quad (4)$$

where R is the isotopic ratio ($^{18}\text{O}/^{16}\text{O}$, $^{13}\text{C}/^{12}\text{C}$) in solid and liquid phases. Equilibrium isotopic fractionation in natural systems is significantly affected by kinetic factors, precipitation rates and temperature (Faure, 1986). Tarutani et al. (1969) have observed an ^{18}O enrichment of about 0.6‰ in aragonite compared to calcite during inorganic precipitation at 25°C. Similarly, changes in salinity may influence incorporation of ^{13}C and ^{18}O into calcium carbonate and positive correlations of skeletal $\delta^{13}\text{C}$ and $\delta^{18}\text{O}$ with salinity (Mook, 1971). The fractionation factor for carbon isotopes is only slightly temperature sensitive (Veizer, 1983b). The fractionation factor of oxygen is temperature dependant (Faure, 1986) and paleotemperature determinations for calcite were derived by Urey et al. (1951). This equation is;

$$T^{\circ} (\text{C}) = 16.9 - 4.14 (\delta_{\text{c}} - \delta_{\text{w}}) + 0.13 (\delta_{\text{c}} - \delta_{\text{w}})^2$$

where $\delta_c = \delta^{18}O$ value of CO_2 generated from carbonate samples at $25^\circ C$ (relative to PDB) and $\delta_w = \delta^{18}O$ value of CO_2 in equilibrium with ambient seawater at $25^\circ C$ (relative to SMOW).

Many organisms, such as bryozoa and gastropods, apparently secrete calcium carbonate in equilibrium with seawater conditions (Lowenstam, 1961; Veizer, 1983a; Morrison and Brand, 1986). However, the calcification process in some biogenic carbonates, such as corals and foraminifera, produces non-equilibrium isotopic fractionation (McConnaughey, 1989a). Isotopic deviation from equilibrium may be the result of 'metabolic' or 'kinetic' effects. There may be changes in the $\delta^{13}C$ of dissolved inorganic carbon (DIC) near calcification nucleation sites that result from photosynthetic or respiratory processes (Swart, 1983); respiration may decrease skeletal $\delta^{13}C$ by selective additions of metabolic ^{12}C . Kinetic effects result in discrimination against heavy isotopes during the hydration and hydroxylation of CO_2 (McConnaughey, 1989a; 1989b). Strong kinetic disequilibrium occurs with rapid skeletal growth (Land et al., 1975) and there appears to be a convergence towards isotopic equilibrium with slower calcification rates (McConnaughey, 1989a; 1989b).

DIAGENETIC CONSIDERATIONS

Metastable aragonites, high-Mg and intermediate-Mg calcites on exposure to diagenetic waters, dissolve partially or fully, in response to chemical gradients (Veizer, 1983a, b) and surface reactivity (Walter, 1985). Trace and minor elements are repartitioned into a secondary, diagenetic low-Mg calcite product (dLMC) in single or multiple dissolution-reprecipitation events (Bathurst, 1975; Brand and Veizer, 1980). Low-Mg calcites are relatively resistant to alteration in the presence of diagenetic fluids (Veizer, 1983a, b) but

even this mineralogical phase will re-equilibrate with diagenetic waters (Al-Aasm and Veizer, 1982; Veizer et al, 1986; Popp et al., 1986a; Brand, 1988).

The rate and magnitude of alteration is influenced by a number of factors;

1. The partition coefficient (**k**). This is influenced by rates of precipitation, kinetic, temperature effects and a mineralogical control (i.e. calcite rhombohedra will more readily accept small cations, Mn^{2+} , Fe^{2+} , etc). Depending on the deviation of a particular partition coefficient from unity, the diagenetic product will be elementally or isotopically enriched or depleted in the direction of equilibrium with diagenetic waters (Brand and Veizer, 1980; Veizer, 1983a).
2. The chemistry of the diagenetic waters. Alteration below the permanent water table occurs with waters of meteoric, mixed meteoric or marine phreatic origin (Veizer, 1983a; James and Choquette, 1984). Chemistries of any diagenetic product will reflect the complexities and compositional differences of single or mixed sources (e.g., ionic strengths, redox conditions; Veizer, 1983a). Isotopic repartitioning depends on temperature and salinity, altitude, latitude, seasonal changes, superimposed on pertinent global seawater isotopic secular variations (Brand, 1981b; 1982; 1989b).
3. Rock-water ratios. Dissolution-reprecipitation across a messenger film (Pingitore, 1976; 1978; Brand and Veizer, 1980) is partly a function of host lithology and rock-water volume. Diffusion of ions is controlled by: i) diffusion coefficients; ii) pore geometry and pathway between aquifer and reaction zone; and iii) the concentration gradient between aquifer and reaction zone (Pingitore, 1982). Furthermore, Pingitore (1982) correlates an increase in dissolution rates to lithofacies in the following order of

mudstone < wackestones < grainstones. Variance of rock-water volumes will result in a spectrum of diagenetic products reflecting grain reaction-controlled dissolution-reprecipitation to fluid-controlled dissolution-reprecipitation (Brand and Veizer, 1980; Pingitore, 1978; 1982; Drever, 1982; Veizer, 1983a).

Diagnostic elements such as Sr^{2+} , Mn^{2+} , Fe^{2+} , Na^{2+} , and Mg^{2+} are used to establish the degree and direction of diagenetic alteration within fossil allochems (Brand and Veizer, 1980; Brand 1989a, b). Textural indicators, such as microstructural preservation, may give support to these chemical trends. The bound and free water contents of skeletal carbonates is a potential indicator of diagenetic alteration especially in aragonite and high-Mg calcite, although even low-Mg calcite may lose free H_2O from fluid inclusions and possibly bound H_2O (Gaffey, 1988). Re-equilibration of biogenic carbonates with diagenetic waters may be reflected isotopically. Meteorically derived waters are generally enriched in light isotopes (Siegenthaler, 1979; Anderson and Arthur, 1983; Faure, 1986) and a diagenetic low-Mg calcite product will generally become depleted in $\delta^{13}\text{C}$ and $\delta^{18}\text{O}$. Alteration in the presence of marine- or mixed-waters will reflect higher oceanic $\delta^{13}\text{C}$ and $\delta^{18}\text{O}$ values (Baker et al., 1982; Elderfield et al., 1982). Once a determination of the degree of post-depositional alteration of fossils is made, chemical distribution can be used to decipher paleoenvironments and possible changes in paleocean chemistry (Veizer et al., 1986; Popp et al., 1986b; Morrison and Brand, 1988; Brand, 1988).

GEOCHEMISTRY OF BRACHIOPOD SHELL CALCITE

Calcite is subdivided into: low-Mg calcite (LMC) with approximately 0-5 mol% MgCO_3 ; intermediate-Mg calcite (IMC) with 5-8 mol% MgCO_3 ; and high-Mg calcite (HMC) with 8-28 mol% MgCO_3 (Milliman, 1974, p. ?). All articulate brachiopods secrete low-Mg calcite shells (Chave, 1954), with less than 5 mol% MgCO_3 and usually 3000-5000 ppm Mg (Morrison and Brand, 1986). Two exceptions to this are mentioned in the literature (Brand and Veizer, 1980; Morrison and Brand, 1987), but they are inarticulate species. The recent brachiopod *Crania* and the order Trimerellidae are possible exceptions to the above rule (Brand and Veizer, 1980; Morrison and Brand, 1986). The fossil Trimerellidae, may have secreted aragonite (Jaanusson, 1966), and Recent *Crania* are unusual inarticulate brachiopods (Laverack, 1987; Stricker and Reed, 1985; Gorjansky and Popov, 1986).

The application of partitioning theory to ancient biogenic carbonates gives indications of original water chemistries or diagenetic regimes (Brand, 1981a, 1983, 1987a, b). However, equilibrium physicochemical conditions for skeletal carbonates are complicated by possible physiological controls exerted by carbonate precipitating organisms. Biological fractionation appears to be ubiquitous to most taxa and is well documented for bivalves (Rosenberg, 1980), gastropods (Milliman, 1974; Bathurst, 1975), ammonites (Buchardt and Weiner, 1981) and other taxa (see Morrison and Brand 1986; Brand and Morrison, 1987a). Brachiopods fractionate Mg and Na with respect to inorganic low-Mg calcite precipitated in equilibrium with ambient conditions, discriminating against Mg and preferentially incorporating Na into shell calcite (Brand and Veizer, 1980; Brand, 1988). Sodium contents in brachiopod calcite are 5-10

times greater than in inorganic low-Mg calcite (White, 1977; Brand and Morrison, 1987a).

There may be other factors involved in the partitioning of elements into brachiopod calcite. Lowenstam (1961) suggested that Sr contents in brachiopod calcite reflect changes in salinity. In a subsequent paper, he proposed that Recent and Pliocene to Mississippian brachiopods discriminate physiologically against Sr (Lowenstam, 1963). In addition, he also suggested that Mg contents increased proportionately with respect to salinity. Morrison and Brand (1984) and Popp et al., (1986) have observed potential taxonomic differences in Sr between spirifers and productids, and data from the latter study (Popp et al, 1986a, b) suggests that there may also be a taxonomic control of Mg. The fractionation of Mg contents in shell calcite may also be related to shell mineral morphology. In a few Recent (Stricker and Reed, 1985; Rowell and Grant, 1987; Hiller, 1988) and fossil brachiopods, primary prismatic layer calcite is enriched in Mg relative to secondary layer fibrous calcite (Foster, 1974). Differential pH, T° and/or metabolic activity at the mantle generative zone may be responsible for different secretory regimes, growth rates and differential partitioning between shell layers.

Isotopic disequilibria ("vital effects") are common in foraminifera (Grossman, 1984; 1987; Grossman et al., 1986) and corals (Land et al., 1975; Gonzalez and Lohmann, 1985; McConnaughey, 1989a; 1989b) but, empirical data concerning brachiopods is limited. A study on three specimens of *Argyrotheca bermudana* suggest that they discriminate against the incorporation of ^{13}C by 4-5‰ (Wefer, 1985) whereas extant brachiopods are observed to incorporate ^{18}O in equilibrium with ambient conditions (Lowenstam, 1961; Wefer, 1985). The incorporation of oxygen isotopes is temperature dependant (Lowenstam, 1961) and has been used as a basis for

paleotemperature determinations and evaluation of secular trends of $\delta^{18}\text{O}$ reservoirs.

BRACHIOPOD ECOLOGY

Ancient brachiopods were lophophorate suspension feeders (Rudwick, 1970; Tasch, 1973) and proliferated in a great variety of substrate and habitat settings on Paleozoic shelves. Areal and spatial distribution are related to physical and biological parameters of their environment, such as salinity, temperature, substrate, agitation, turbidity, fugacity of epiplanktic reproduction. Depth related brachiopod communities are recognized from the Ordovician (e.g., Lockley, 1983), Silurian (e.g., Zeigler, 1965; Cocks, 1967; Hancock et al., 1974), Devonian (e.g. Brett et al., 1986a; Miller, 1985). Fursich and Hurst (1974) suggest that food supply, lophophore surface area and morphological adaptations are factors controlling Silurian brachiopod community distribution. Brachiopods with thick shells and large pedicle openings may prefer more turbulent settings (e.g., *Pentamerus*). In contrast, brachiopods with either a) a fairly large, median sulcus; b) alae; or c) thin, smooth shells prefer quiet water environments. Since brachiopods are high level suspension feeders (Walker and Bambach, 1974), the direction of inhalent and exhalent currents (Jones, 1982) and the orientation and hydrodynamic stability of modern and ancient brachiopods may have determined substrate preferences (Alexander, 1975; LaBarbera, 1977; 1978, 1981a; Alexander, 1984, 1986). Modern species appear to tolerate a wide range of mud, sand or semi-cryptic substrates and physical conditions (Richardson, 1981a, b; Campbell and Fleming, 1981; Chapman and Richardson, 1981; Richardson and Mineur, 1981; Aldridge, 1981, Stewart, 1981; Witman and Cooper, 1983; Foster, 1989), which may be

partially related to pedicle structure (Richardson, 1981a). Articulate brachiopods have often been assumed as stenohaline (Rudwick, 1970; Tasch, 1973). However, Fursich and Hurst (1980) demonstrated that brachiopods as a taxon were able to tolerate both hypersaline and brackish conditions. Paleoecological study of brachiopod communities provides information about the physical and chemical conditions of their environment. Complementary information about their chemical environment is potentially discernible from brachiopod shell calcite.

METHODOLOGY

Area of study

A succession of Paleozoic limestones and shales, outcropping in Ontario and New York State, were sampled for this study. Middle Ordovician brachiopods were collected from Trenton Group carbonates of southern Ontario and Manitoulin Island (Fig. 1.1), whereas Upper Ordovician Whitby and Georgian Bay Formations were sampled from Manitoulin Island and along the shore of Georgian Bay (Fig. 1.1). Clinton Group (Middle Silurian) specimens were collected from the Merritton, Reynales, Irondequoit and Rochester Shale Formations, which outcrop along the Niagara Escarpment in Ontario and western New York State (Fig. 1.2). Brachiopods of Middle Devonian age were collected from shales of the Ludlowville and Moscow Formations (Hamilton Group, Givetian) exposed in western New York State. Additional material was obtained from the Arkona, Hungry Hollow and Widder Formations (Hamilton Group) in Ontario (Fig. 1.3).

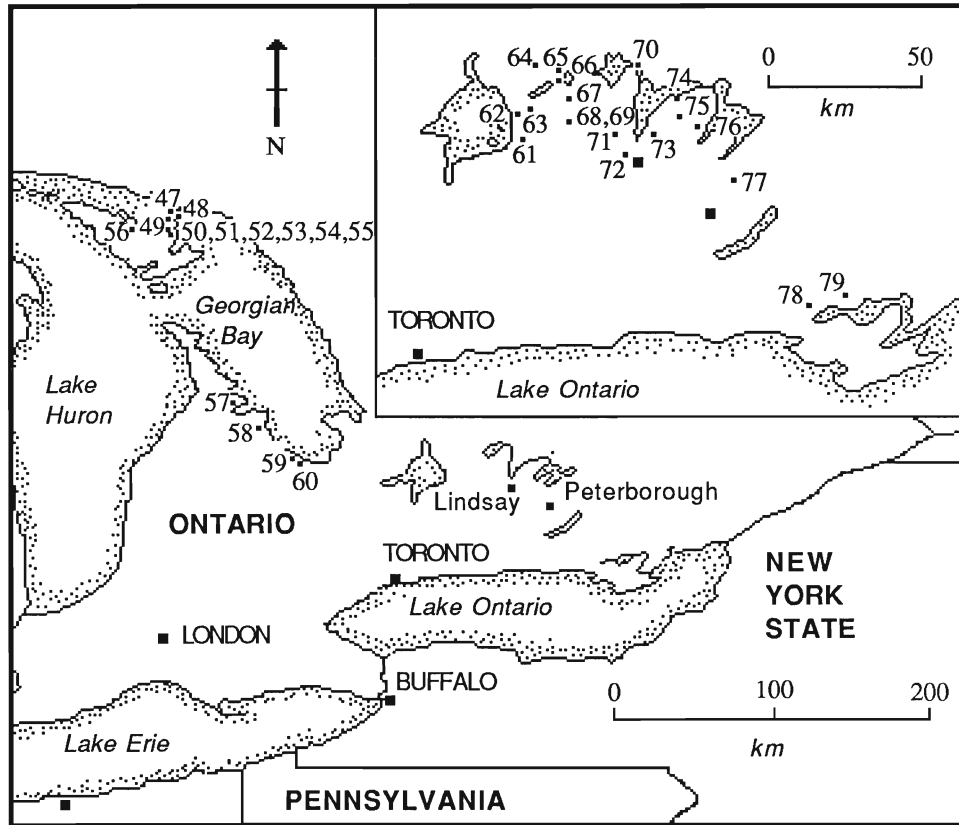


Figure 1.1. Locality map of Middle and Upper Ordovician sampling sites. Respectively; 47. Goat Island; 48, 49. Little Current; 50, 51. South of Little Current; 52, 53, 54. Sheguiandah; 55. High Falls; 56. Kagawong; 57. Keppel Township; 58. East Meaford Creek; 59. Craigleith; 60. Collingwood; 61. Beaverton; 62. Mara Quarry; 63. Bolsover; 64. Dalrymple; 65. Kirkfield Quarry; 66. Trent Lock Canal; 67. Kirkfield; 68. Glenarm; 69. Eldon Hill; 70. Fenelon Falls; 71. County Road 21; 72. Lindsay; 73. Dunsford; 74. Cedar Glen Road; 75. Highway 36; 76. County Road 7; 77. Lakefield Quarry; 78. Trenton; 79. Belleville. Complete description of each section and sampling horizons, lithology and brachiopods is listed in Appendix I.

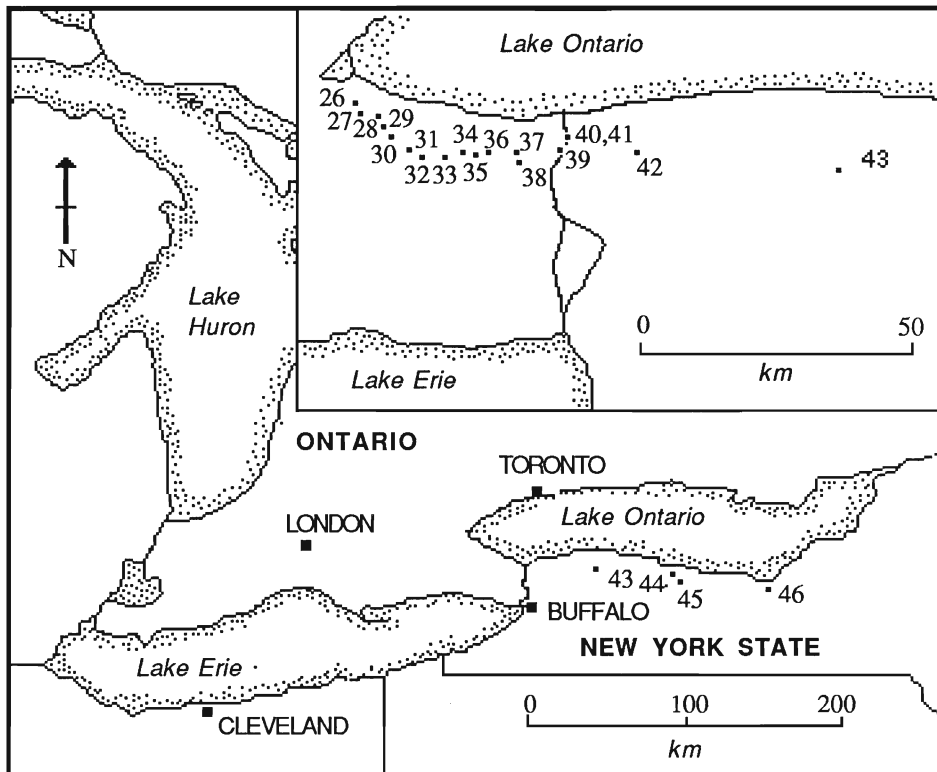


Figure 1.2. Locality map of Middle Silurian sampling sites in Ontario and New York State. Localities are; 26. Stoney Creek; 27. Dewitt Road; 28. Vinemount; 29. Wolverton Road; 30. Beamers Falls; 31. 15 Mile Creek; 32. Rockway Falls; 33. Decew Falls; 34. Brock-Decew; 35. Highway 406; 36. Burleigh Hill; 37. Lock 5 Thorold; 38. Old Welland Canal; 39. Niagara Falls Gorge (Ontario); 40. Niagara Falls Gorge (Artpark); 41. Niagara Falls Gorge (Robert Moses Hydroelectric); 42. Bree Road; 43. Lockport; 44. Brewer Street Rochester; 45. Hydro Road Rochester; 46. Sodus Creek. Complete description of each section and sampling horizons, lithology and brachiopods is listed in Appendix I.

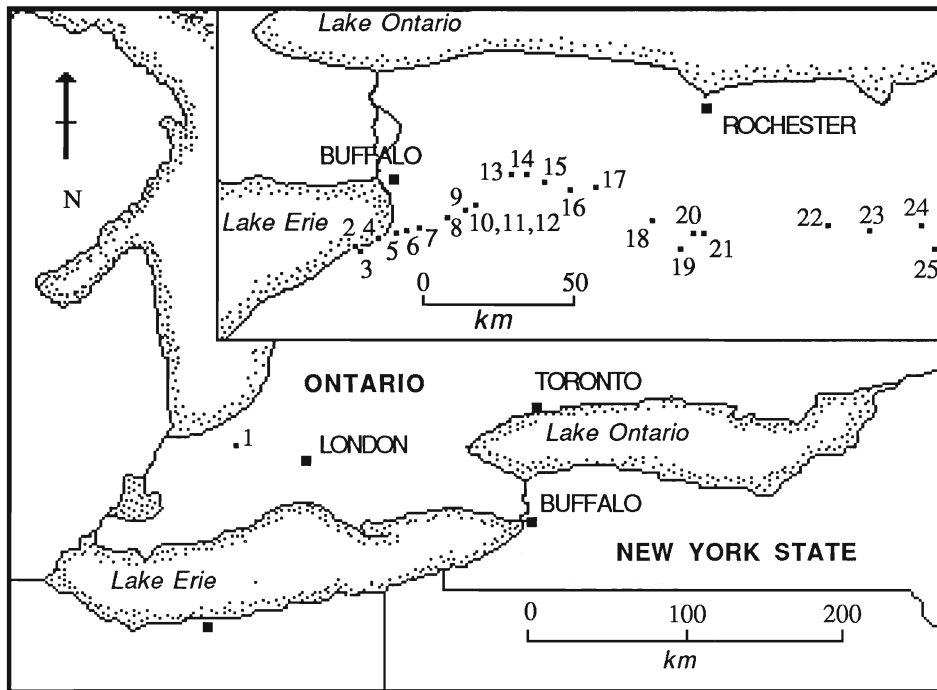


Figure.1.3. Locality map of Hamilton Group (Middle Devonian) sampling sites. These are; 1. Hungry Hollow; 2. Lake Erie shoreline; 3. Eighteen Mile Creek; 4. Athol Springs; 5. Big Tree Road shale pit; 6. Penn Dixie Quarry; 7. Smoke Creek; 8. Cazenovia Creek. 9. to 12. Buffalo Creek; 13. Eleven Mile Creek; 14. Spring Creek; 15. Murder Creek; 16. Bowen Creek; 17. Bethany Railcut; 18. Retsof; 19. Fall Brook Creek; 20. Jaycox Creek; 21. Wheeler Gully; 22. Menteth Creek; 23. Kashong Creek; 24. Indian Creek; 25. Big Hollow Creek. Complete description of each section and its sampling horizons, lithology and collected brachiopods, are listed in Appendix I.

Sampling Procedure

Specific stratigraphic horizons and sampling localities were identified from a variety of sources (Liberty, 1969; Liberty and Bolton, 1971; Liberty, 1975; Barnes et al., 1978; Telford, 1978; Baird and Brett, 1981; Telford et al., 1981; Brett and Cottrell 1982; Brett, 1983a, b; Grasso, 1983; Brett and Brookfield, 1984; Speyer and Brett, 1985, 1986; Grasso et al., 1986; Miller 1986; Wygant, 1986; Brett et al, 1986a, b; Landing and Brett, 1987; Brookfield and Brett, 1988; Liebe and Grasso, 1988; Miller et al., 1988; Parsons et al., 1988). Where possible, entire bedding plane samples were collected for thin sectioning and taphonomic data, such as the state of articulation, corrosion, abrasion, and life position. Confirmation of brachiopod species identification was based on the relevant literature (e.g., Williams et al., 1965; Bolton, 1966; Shimer and Shrock, 1972; Sinclair, 1971; Cottrell and Brett, 1982; Brett, 1983a, 1989; Sinclair et al., 1984; Rowell and Grant, 1987; Brett et al., 1986a). A complete list of sampling localities, precise stratigraphic position of units and specific horizons, lithologies and dominant brachiopod species is compiled in Appendix I.

Sample Preparation

Individual brachiopods were separated from their enclosing matrix to reduce matrix and iron oxide contamination in chemical analysis. Brachiopods from shale, calcareous shales or calcisiltite lithologies were manually separated from most of the adhering matrix. In some instances, matrix was removed from brachiopod shells by cleaning in water and final rinsing with deionized water. Dental picks and a Dremel moto-tool drill were used to remove more resistant matrix from shell material and adhering epibionts were completely removed. While cleaning, brachiopods were periodically immersed in 10% (v/v) HCl solution for 30-45 seconds to aid in the cleaning process. The presence of

delicate costae in some taxa (e.g., *Mucrospirifer mucronatus*) necessitated the removal of shell material during cleaning to ensure removal of all matrix; similarly, cracks and borings (e.g., *Athyris spiriferoides*) required the drilling out of both matrix and surrounding shell material. After a final HCl rinse and followed by a deionized water rinse, the brachiopods were allowed to air dry.

Cleaning of some brachiopods from Middle Ordovician units presented additional problems. Trenton Group strophomenids, sampled from wackestones and packstones, were difficult to separate from their matrix. Exposed brachiopod shell surfaces (e.g., *Rafinesquina deltoidea*.) were thoroughly cleaned with water and 10% HCl washes. Each brachiopod was washed with a final deionized water rinse and left to air dry. Shell material was then picked and drilled out of the sample and collected. Between drilling, the brachiopods were washed with HCl and deionized water and left to dry, in order to ensure that the drill had not passed through to the matrix beneath. The drill tool (steel alloy) was cleaned of powder after each sampling. These protracted cleaning processes assured that contamination by matrix and iron oxides were minimized.

Trace and minor element analysis

Six hundred and twenty six brachiopods, fifteen crinoids, fifteen matrix and eight cement samples were analysed for Ca, Mg, Sr, Mn, Na, Fe and Al by atomic absorption spectrophotometry (AAS) using a Varian 1475-HP 85. Shell fragments of each sample were separated for later S.E.M. study and individual brachiopod, matrix and cement samples were then carefully powdered. Approximately 0.1g of each sample was digested in 10mL of 5% (v/v) HCl for 70-80 minutes. Insoluble residue (I.R.) was determined gravimetrically by ashing the filter paper and residue at 800°C for 1 h. Mean insoluble residue

was less than 6%; data and discussions in the text are based on concentrations recalculated to 100% (insoluble residue-free; Brand and Veizer, 1980). Filtrates were analysed by AAS against reference standards and National Bureau of Standards solutions. Mean accuracy relative to N.B.S. 634 and 636 was Ca (4.0; 1.6); Mg (6.6; 3.9); Sr (2.5; 9.0); Mn (3.4; 4.3); Na (9.0; 4.2); Fe (10.5; 14.8); and Al (8.1; 14.9) percent respectively. Average precision was Ca (0.6); Mg (1.5); Sr (2.7); Mn (2.9); Na (1.8); Fe (3.0); and Al (4.8) percent. A compilation of chemical data is presented in Appendix III.

Carbon and oxygen isotopic analysis

Seventy-three brachiopod samples were analysed for stable isotopes. Analyses were performed on a 602 VG Micromass Spectrophotometer at the University of Waterloo. Approximately 10 mg of powdered sample was reacted with 100% phosphoric acid at 50°C for 30 min. The isotopic ratios are reported in the standard notation (δ) relative to the PDB standard in ‰. Reproducibility of results was (0.13‰) for $\delta^{18}\text{O}$ and (0.25‰) for $\delta^{13}\text{C}$. The ^{17}O correction was applied to the data (Craig, 1957) and isotopic data is reported relative to PDB (Epstein et al., 1953).

Scanning Electron Microscopy

The preservation of brachiopod skeletal calcite microstructure was investigated using an International Scientific Instruments scanning electron microscope (S.E.M.), and approximately 23% of all brachiopod specimens were analysed; representative of different species, lithologies and ages. Fractured shell material allowed cross-sectional views of primary and secondary shell calcite-layers and internal and external surfaces were examined for punctal and other biomineralization structures. Initially, fragments were cleaned in deionized

water and dried in an oven at 50°C, then after cooling in a dessicator, fragments were mounted on metal stubs and coated with gold/palladium prior to examination. Microstructures were identified and later compared to those reported by Williams (1968a, 1968b, 1971), Popp (1981), Brand (1981, 1983, 1987), Curry, 1983b), Stricker and Reed (1985), Rowell and Grant (1987), and Hiller (1988).

Thin section studies

Petrography of each sampled horizon was studied by thin-section, which were stained in accordance with the procedures of Lindholm and Finkelman (1972). Folk's (1962) classification was used to denote the grain and matrix type and Dunham's (1962) classification is used to denote depositional texture.

Statistical Analysis of Chemical Data

Unpaired T-tests were used to compare the means of chemical populations. Trace element distribution in carbonates is log normally distributed (Veizer and Demovic, 1974; Brand, 1989), therefore chemical data were log transformed for factor analytic calculations. The recognition of chemical alteration in biogenic carbonates has been successfully confirmed by factor analysis of geochemical data (e.g., Brand and Veizer, 1980; Al-Aasm and Veizer, 1982; Waasenaar, 1986; Morrison, 1986; Veizer et al., 1986; Al-Aasm and Veizer, 1986a, b; Brand, 1989a, b.). Three controls of chemical distribution have been recognized; 1. the re-equilibration of skeletal carbonate with diagenetic waters (Mn, Fe); 2. biological fractionation (Sr, Na, Mg); and 3. leaching of aluminosilicates (I.R., Al). The distribution of elements in crystal lattices is dependant upon relatively few physicochemical parameters and may justify the original underlying factor analytic hypothesis of a small number of

factors (Temple, 1978). Computations were performed using the statistics program Statview 512™ on an Apple Macintosh microcomputer.

CHAPTER 2

Primary and diagenetic microstructures of brachiopod shell calcite

INTRODUCTION

The structural characteristics of articulate brachiopod valves has remained constant since the Cambrian (Rowell and Grant, 1987). Similarly, it can be assumed that the secretory mechanisms and the processes controlling calcification remain unchanged. As a consequence, a comparative analysis of modern and ancient brachiopod shell calcite can provide the basis for determining the preservation states and degree of post-depositional alteration of brachiopod calcite. As such, microstructural analysis can augment chemical and isotopic trends that are indicative of diagenetic alteration. The identification of pristine shell calcite and the elimination of altered material is essential to the investigation of ancient shell calcite compositions and paleoenvironmental reconstructions. Use of altered material can lead to misinterpretation of chemical data (Brand, 1989a).

This purpose of this chapter is to identify primary and diagenetic microstructures within brachiopod shell calcites collected from the Paleozoic of New York State and southern Ontario and illustrate the textural changes accompanying post-depositional alteration.

BRACHIOPOD SHELL SECRETION AND MICROSTRUCTURE

Modern brachiopods possess an exoskeleton composed of a thin outer proteinaceous layer, the periostracum, which is underlain by primary and secondary layers of calcite (Fig. 2.1; Rudwick, 1970; Tasch, 1973; Rowell and Grant, 1987). These foliated calcite layers are recognized in ancient brachiopods but the outer organic periostracum degrades quickly after death

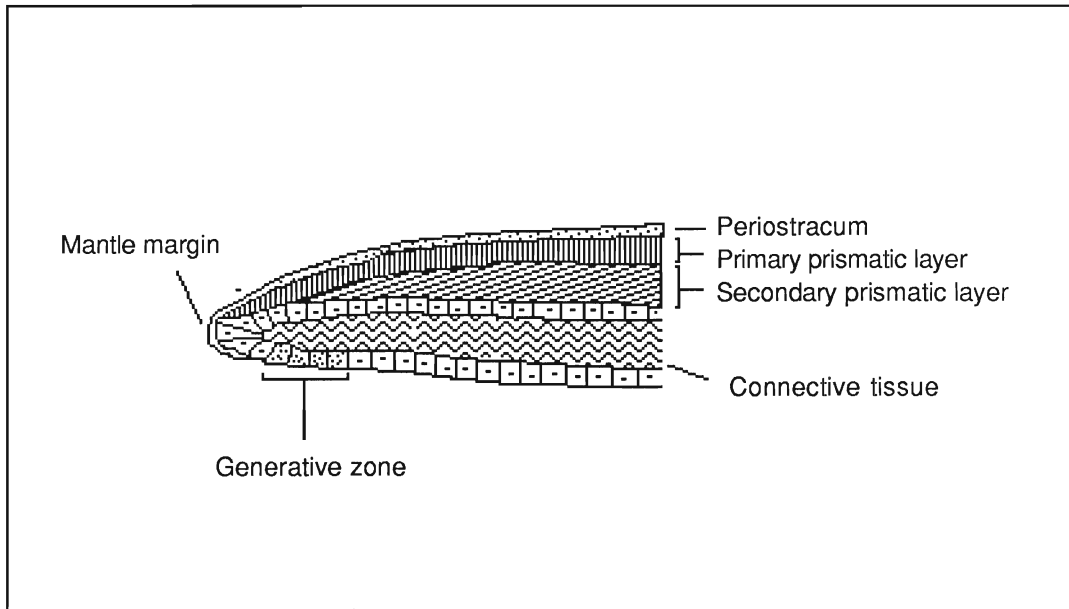


Figure 2.1. Generalized cross section of an articulate brachiopod exoskeleton. Modified from Rudwick (1970), Grant and Rowell (1987.).

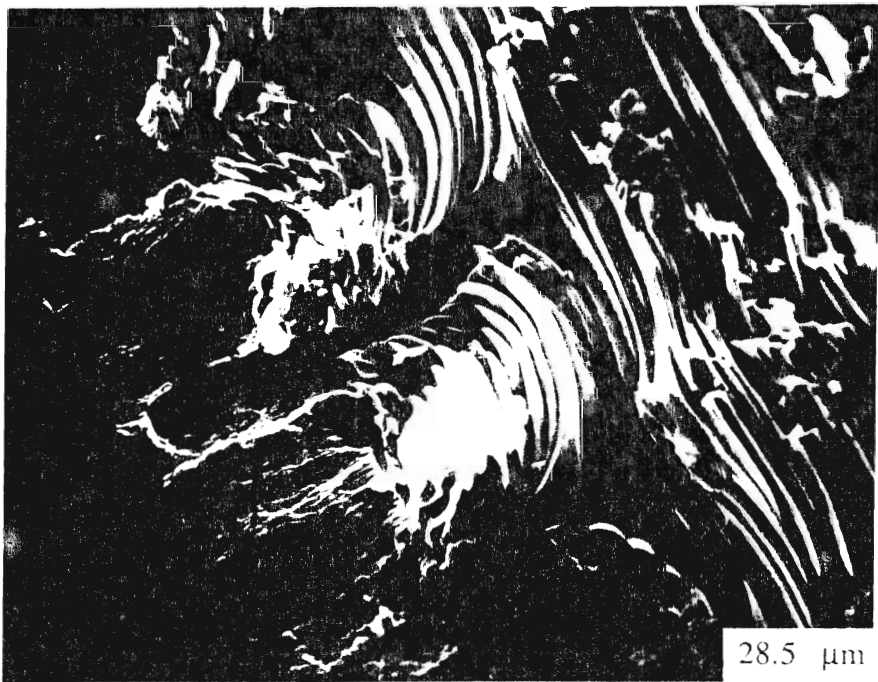
and is not fossilized (Williams, 1966; 1968a, b; Rowell and Grant, 1987; Brand, 1988). Shell calcite secretion is controlled by epithelial cells within a generative zone close to each valves mantle edge (Fig. 2.1; Rowell and Grant, 1987). Initially these cells assemble a thin organic meshwork periostracum which is composed of conchiolin, a protein-polysaccharide complex (Rosenberg et al., 1988). The cells then switch to secretion of a thin calcitic primary shell layer, constructed of small fused prismatic crystallites, oriented tangentially to the shell surface: the primary layer is secreted without benefit of an organic matrix (Williams, 1968a).

The secretory regime changes once more as the epithelial cells moves further away from the generative zone and thick layers of foliated calcite are constructed as the secondary shell layer. In ancient brachiopods, differentiation of this layer into fibrous or laminar foliation is recognized. Fibrous shell layers consist of long calcite rods ensheathed in membranous organic matrices, oriented about 10° to the primary layer (Fig. 2.2). In contrast, laminar shell structure is constructed of thin platy laths of calcite fused to form individual separated lamina; orientation is roughly parallel to the shell surface. This type of structure is restricted to brachiopods of the order Strophomenida. Cells secreting the secondary layer may intermittently cease depositing an organic matrix causing layers or lenses of prismatic calcite, arranged normally to the mantle, to build up within the fibrous layer (Rowell and Grant, 1987). Alternately, some taxa secrete distinct tertiary layers of prismatic calcite, which may thicken and strengthen the valve in response to physiological, ontogenetic or environmental demands.

Growth lines, similar to those observed in bivalves, are recognized in modern (e.g., *Terebratulina retusa*; Curry, 1982) and ancient brachiopods

Figure 2.2. Scanning electron micrograph of the primary and secondary calcite layers of the modern brachiopod *Laqueus vancouverensis*. The primary shell layer is composed of small, stacked prismatic calcites oriented at 90° to the outer valve surface. The secondary layer is composed of rounded elongate calcite fibres. The organic matrix between each fibre is not visible. The shell structure is modified by punctal openings that terminate just below the prismatic layer upper surface. Crystallites on the internal surfaces of each punctae are fused.

Figure 2.3. S.E.M. micrograph cross section of foliated secondary shell layer around punctae. Individual calcite fibres are rounded, oblate and curve upward to meet punctal surface. (*Laqueus vancouverensis*).



(Williams, 1968a; Jones, 1982). Some modern species apparently dissolve portions of their inner shell in response to metabolic anaerobiosis, although this does not extend to the outer shell (Hughes et al., 1989). The Recent rhynchonellid *Notosaria nigricans* exhibits three types of recognizable growth lines, which result from cessation of shell growth in response to diurnal, seasonal and disturbance controls (Hiller, 1988). Growth increments in bivalves are the subject of numerous conflicting studies (e.g., Crenshaw, 1980; Carter, 1980; Brand et al., 1987; Rollins et al., 1987) which indicate that skeletal growth lines may be the result of either anaerobic or physiological processes. The Lutz and Rhoads (1977) theory of anaerobiosis explains growth increments as the result of cycles of aerobic calcite precipitation and anaerobic dissolution controlled by a complex interaction of physiological and environmental interactions (Crenshaw, 1980). Alternately, inherent cyclic protein and calcite deposition may be the cause for growth increments (see discussion by Rosenberg et al., 1988). Future ontogenetic and environmental analysis of brachiopod valves may be possible with the evolution of microprobe analysis and microsampling techniques.

Punctate brachiopods possess structural modifications of shell microstructure. In Recent articulate brachiopods, punctae are small cylindrical pores (15 μm diameter) within the primary and secondary layers, which are generally uniformly distributed over the surface of the shell (Kemyzys, 1965). They extend from the inner surface of the valve to just below the outer primary layer where growth of the mantle epithelial tissue (caeca) into the punctae connects with the periostracum via fine organic strands (Rowell and Grant, 1987). The majority of shell organic matter in modern species, *Liothyrella uva*, is located within the caeca (Peck et al., 1989) and it has been suggested that

caecal contents inhibit boring organisms and function in a nutrient storage capacity (Curry, 1983b). Several authors suggest that punctae have a respiratory function (Shumway, 1982; Curry, 1983a, 1983b) because they effectively communicate with the external environment (Thayer, 1986b). When the valves are closed, caecal respiratory needs can be met by simple diffusion through the punctae. However, observations on closed *Liothyrella uva* have shown that internal tissues are not supplied by punctal diffusion and must rely on oxygen enclosed within the body cavity (Peck et al., 1986; 1989). Metabolic needs in mantle tissues are apparently switched from aerobic pathways to anaerobic pathways after prolonged oxygen deprivation of about 15 hours (Peck et al., 1986). Brachiopods have been described as oxygen "minimal organisms" (Thayer, 1986b) because they metabolize slowly and efficiently (LeBarbera, 1981b). Consequently ATP generation by anaerobiosis may enable them to survive extensive periods of oxygen deprivation (Hammen, 1977; Shumway, 1982). There are no long-term studies of oxygen deprivation and it is not known how or if oxygen depleted environments affect the ultimate viability of brachiopod communities. Tunnicliffe and Wilson (1988) observed that although modern *Terebratulina* survive prolonged periods of anoxia (20-35% of time) there is a slow retreat by the community from deeper, more persistent anoxic conditions. Absence of ancient and modern brachiopod populations from anaerobic and strongly dysaerobic facies, suggests that permanent low oxygen conditions were lethal to individual brachiopods and brachiopod communities.

MODERN BRACHIOPOD SHELL CALCITE MICROSTRUCTURE

SEM analysis of a Recent brachiopod *Laqueus vancouverensis* clearly illustrates the primary calcite layer of prismatic crystallites, which is oriented normally to the external surface (Fig. 2.2). Tangentially oriented calcite fibres of the secondary shell layer are also evident; each fibre is rounded and oblate in cross section (Fig. 2.3). Rounded and stacked calcite fibres of the secondary layer are exposed on internal surfaces of several Recent brachiopods, including *Laqueus vancouverensis*, (Fig. 2.4), rhyconellid *Notosaria nigricans* (Hiller, 1988, p. 180), terebratulids, *Waltonia* and *Liothyrella* (Rowell and Grant, 1986, p. 472) and this primary structural feature is informally termed "imbricate structure" here. Furthermore, observation of the protegulum of juvenile *Terebratalia transversa* indicates that this internal valve microstructure is present shortly after metamorphosis (Stricker and Reed, 1985, p. 297).

Punctae are recognized in many modern brachiopod species. In *Laqueus vancouverensis*, small regularly spaced punctal openings (Fig. 2.5) transverse the entire secondary fibrous layer into the primary layer, but terminate just below the upper surface of the primary layer (Fig. 2.6). Furthermore, strong foliation of secondary shell layers around each punctae is evident (Fig. 2.6).

PALEOZOIC BRACHIOPOD MICROSTRUCTURE

Primary structures

In general, excellent microstructural detail is preserved in the majority of Paleozoic brachiopods from New York State and southern Ontario. The foliated

Figure 2.4. S.E.M. micrograph of the imbricate internal surface of *L. vancouverensis*. Oblate and flattened calcite fibres of the secondary layer are exposed at the internal valve surface. Punctal openings are also common.

Figure 2.5. S.E.M. micrograph of regularly-spaced punctal openings on the internal surface of a *L.vancouverensis* shell. Openings are not filled and exposed fibres of the secondary layer can be seen.

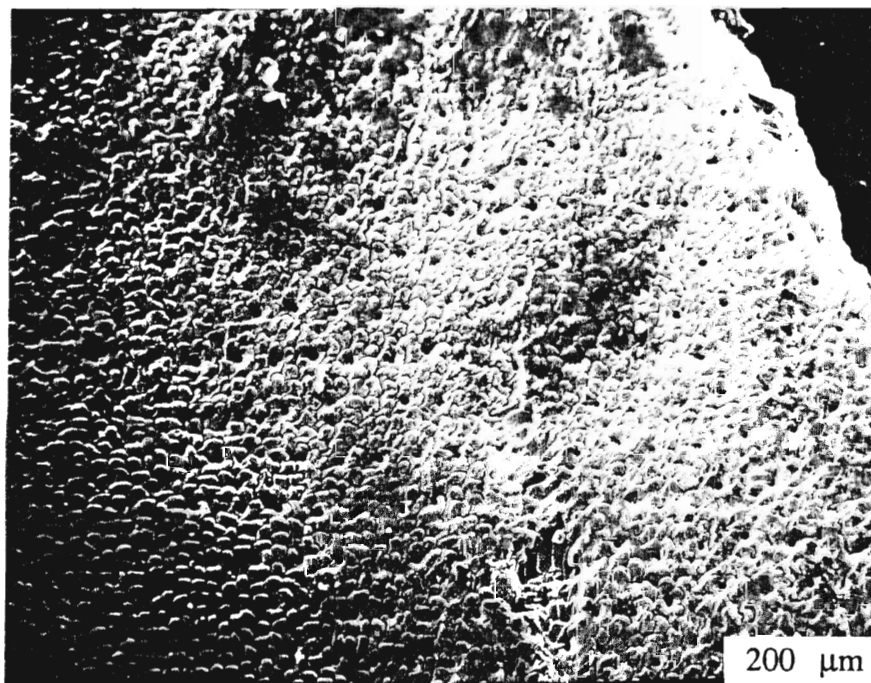
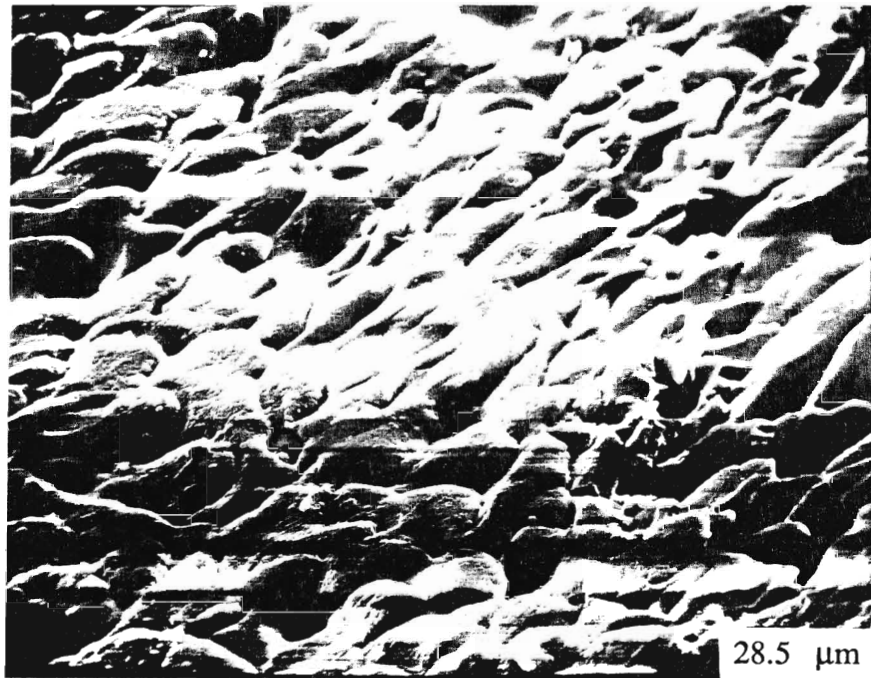


Figure 2.6. S.E.M. micrograph close up of fibrous secondary shell layer. Ultrastructure of *Laqueus vancouverensis*. shows stacked nature of secondary calcite fibres, which are elongate, rounded and oblate in section.

Figure 2.7. S.E.M. micrograph of the secondary layer of *Mediospirifer* (#400; Hamilton Group). Stacked nature of rounded, oblate calcite fibres is evident and separation between fibres is a few micrometres. Fractures in this layer are probably the result of sample preparation.



secondary layer is the most common feature observed by S.E.M. Comparisons between calcite fibres of modern brachiopods and many Paleozoic specimens offers no visible difference in their preservation state (compare Figs. 2.2, 2.3, with 2.7). Tangential and obliquely broken shell fragments of many Paleozoic specimens commonly display regularly stacked elongate fibres which are rounded and oblate with no dissolution features (Figs. 2.8, 2.9). Imbricate structure is present on the internal valve surfaces of Paleozoic specimens (e.g., *Athyris spiriferoides*; Figure 2.10; Middle Devonian, Hamilton Group). Furthermore, the internal stacked nature of secondary calcite fibres is evident in the majority of etched brachiopod valves (Figure 2.11).

The primary shell layer is rarely seen in Paleozoic brachiopods, which may reflect removal of outer shell layers by sample preparation, natural abrasion or superficial thickness. A thin, outer prismatic primary layer has been observed in *Mediospirifer audacula* (Hamilton Group; Middle Devonian) together with a second prismatic layer underlying the foliated secondary layer (Figure 2.12). Prismatic calcite fibre structure, termed trabecular calcite, is common to Recent and ancient brachiopods (e.g., Recent *Neothyris lenticularis* and Carboniferous *Neospirifer* sp., *Composita*, and *Spirifer gorei* ; Brand, 1989). In valves of *Whitfieldella nitida* (Fig. 2.13; Clinton Group, Middle Silurian) trabecular structure may represent modification of prismatic shell calcite. Only along the mantle edge does this species exhibit the secondary fibrous-calcite layers.

Punctal structures are recognized in two species from the Middle Devonian Hamilton Group. Etched inner surfaces of *Tropidoleptus carinatus* reveal regularly spaced punctae (Fig. 2.14), which have dimensions similar to those seen in Recent specimens (Figs. 2.5). Foliation of the fibrous secondary

Figure 2.8. S.E.M. micrograph of the secondary layer of *Mucrospirifer mucronatus* (#178; Hamilton Group). Stacked calcite fibres do not show signs of dissolution or reprecipitation of pore-filling cements.

Figure 2.9. S.E.M. micrograph of the secondary layer of *Eospirifer radiatus* (#2301; Lewiston Member, Middle Silurian, New York State). Close up reveals rounded and elongate calcite fibres similar to those in Figure 2.3, 2.7 and 2.8.

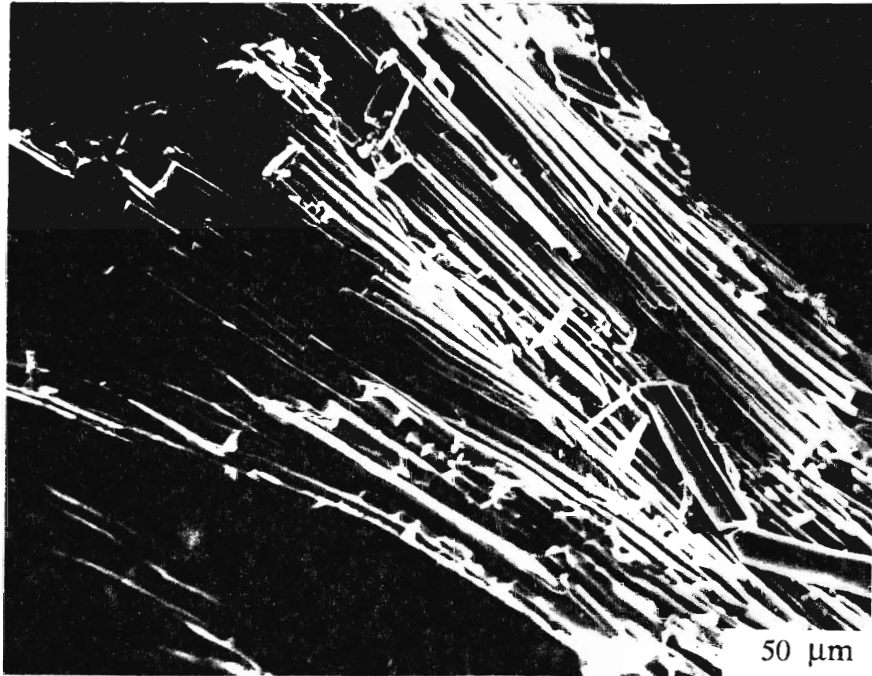


Figure 2.10. S.E.M. micrograph of the imbricated internal valve surface of *Athyris spiriferoides* (#403, Wanakah Shale, New York State). This primary structure on the internal surfaces of ancient valves is also observed in Recent brachiopods and results from modification of oblate fibres oriented at $\sim 10^\circ$ by epithelial cells.

Figure 2.11. S.E.M. micrograph of the internal surface of an etched *Athyris spiriferoides*. Etching of inner surfaces reveals stacked calcite inclined at low angle from the surface (#445, Wanakah Shale, New York State).

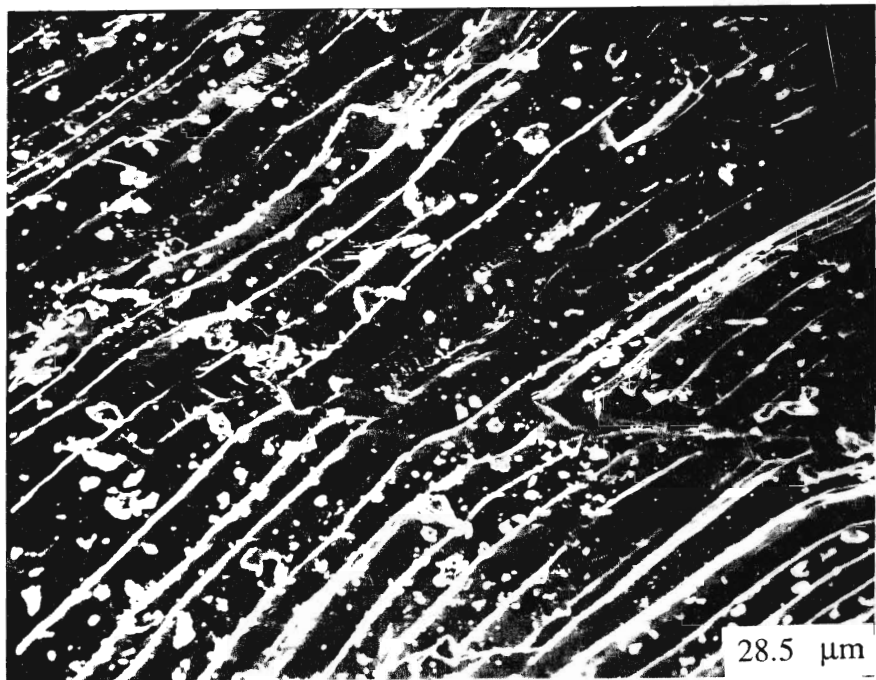
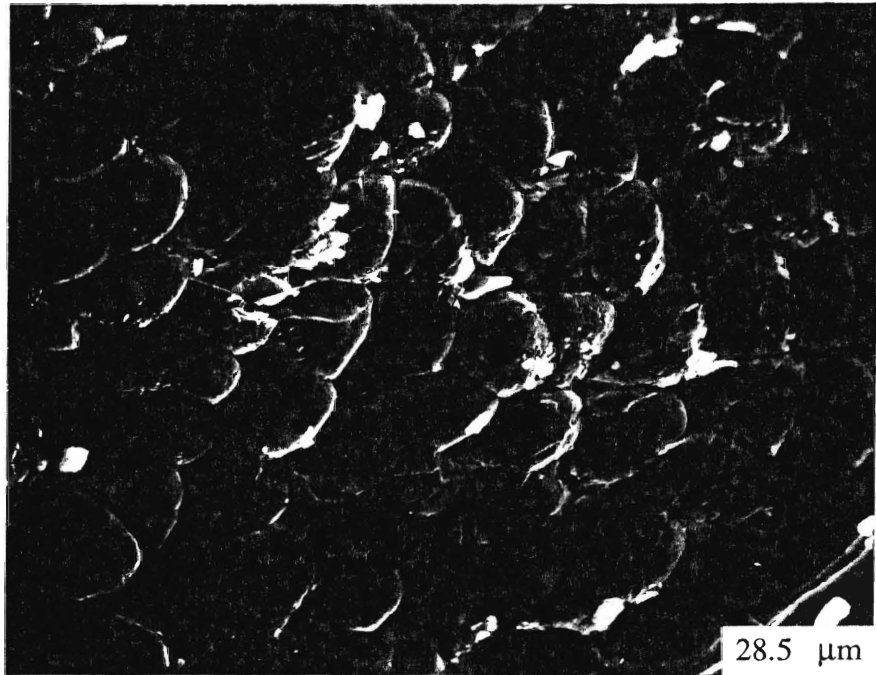


Figure 2.12. S.E.M. micrograph of primary, secondary and tertiary layer shell calcite layers of *Mediospirifer audacula* (#71, Wanakah Shale)

Figure 2.13. S.E.M. micrograph cross section of prismatic trabecular calcite morphology in *Whitfieldella nitida* valves (#2108, Irondequoit Formation). Similar primary structure are reported by Brand (1981, 1983, 1989a).

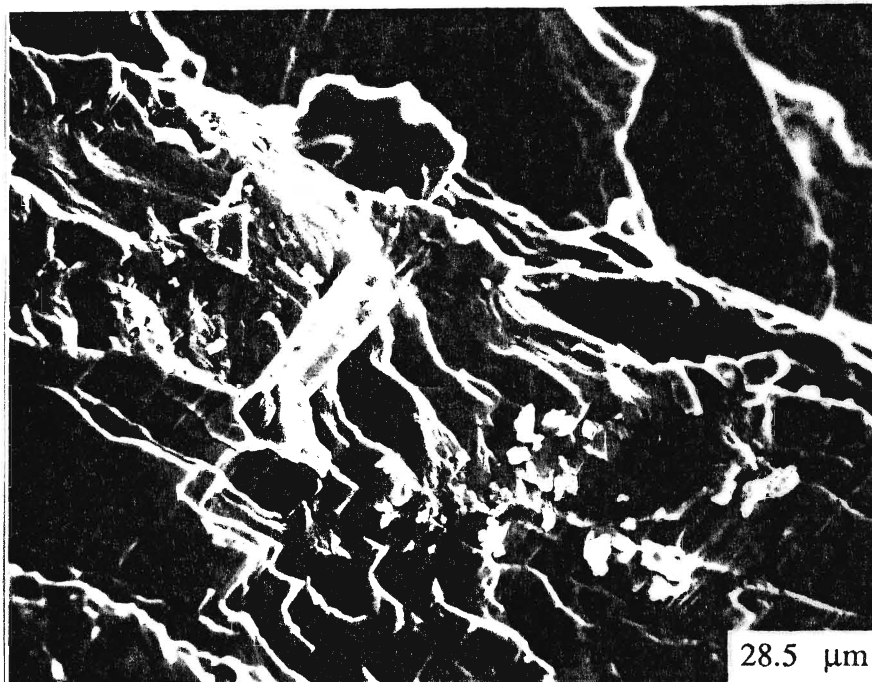
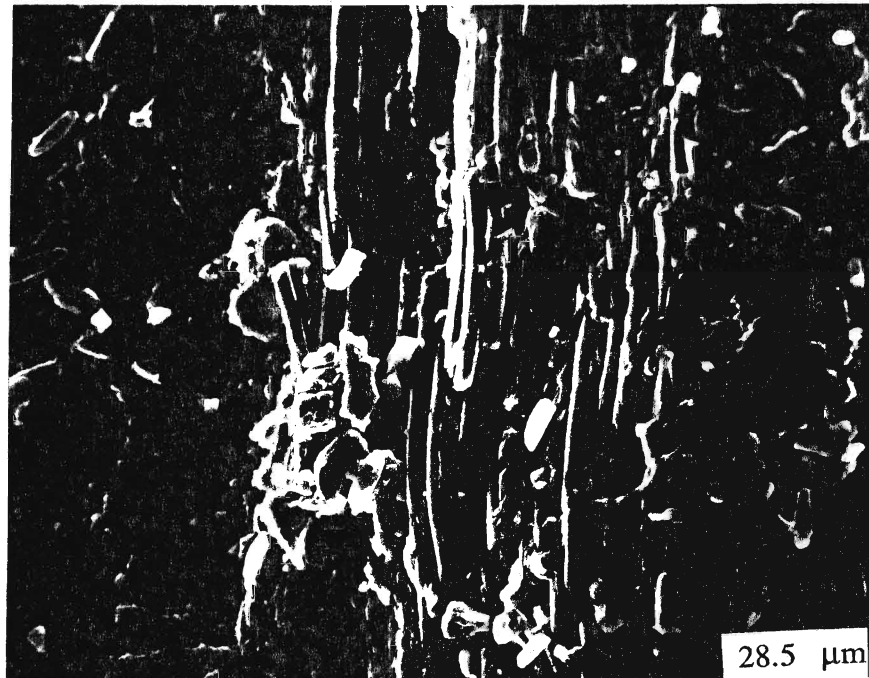
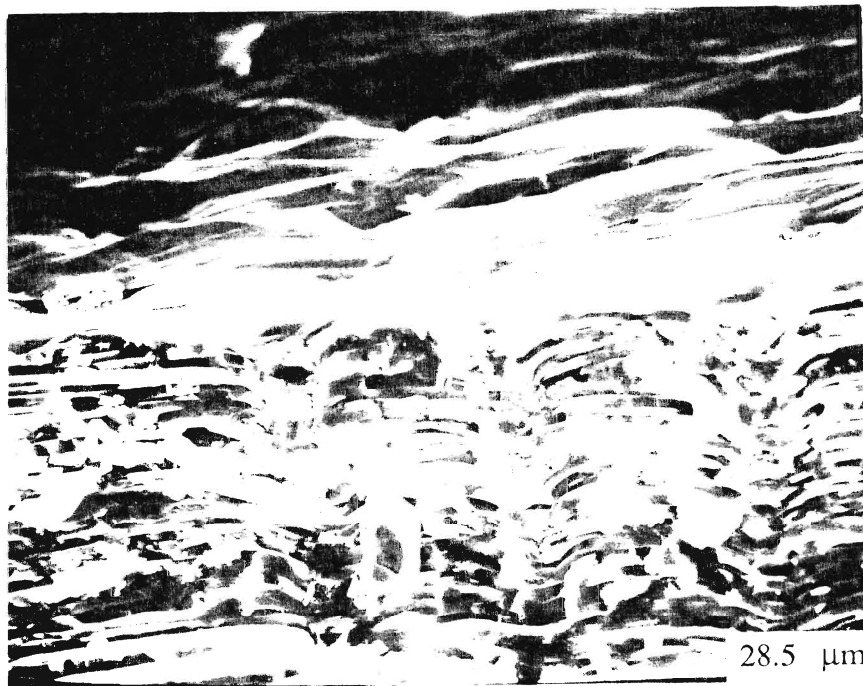
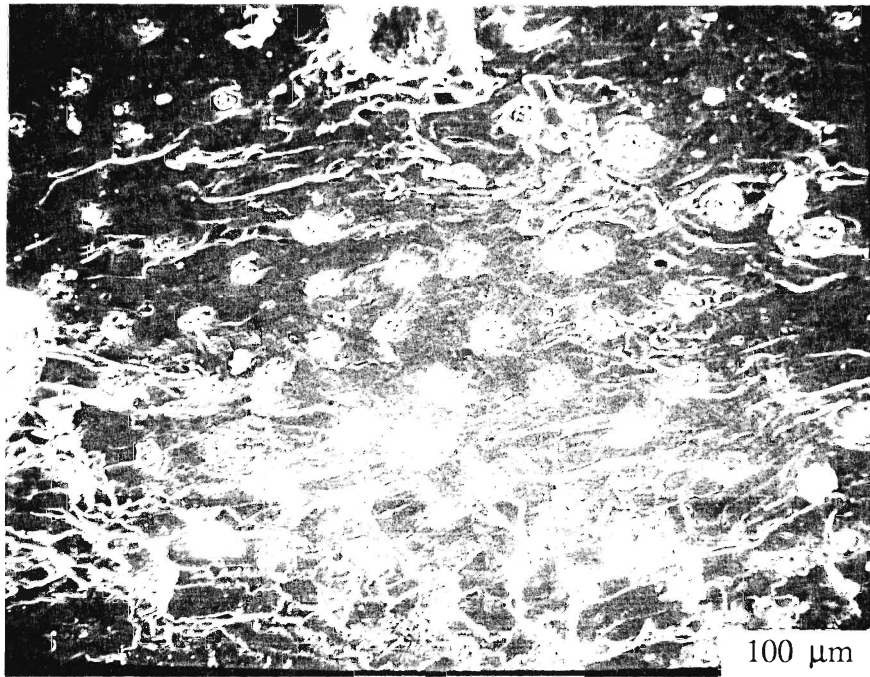


Figure 2.14. S.E.M. micrograph of the internal surface of an etched *Tropidoleptus carinatus* (#409, Wanakah Shale, New York State). Numerous punctae are evident on the inner brachial valve although not regularly spaced as in some modern species (Kemyzs, 1965). Shallow pits are evident surrounding punctal openings, while the small punctal pores (a few micrometres in diameter) are partially filled with cements.

Figure 2.15. S.E.M. micrograph cross section of the secondary shell layer of *Tropidoleptus carinatus* (#409, Wanakah Shale, New York State). Foliation of secondary layer fibrous calcite is penetrated by small undulating punctal pores that pass completely through. The punctae do not appear to be significantly filled with secondary calcites. The upper oblique view of the internal valve surface shows the depressions surrounding the punctal openings.



layer around each punctae is still visible and are comparable to those seen in modern brachiopods (compare Figs. 2.15 with 2.2). In specimens of *Rhipidomella vanuxemi* regularly spaced punctae are visible and the stacked fibrous calcites of the secondary layer meet the inner valve surface at a low angle (Fig. 2.16).

An etched outer surface of an *Eospirifer radiatus* (Rochester Shale; Middle Silurian) valve reveals minute pore openings (Fig. 2.17). These pores are about 1 μm in diameter, are not filled and do not penetrate into the fibrous layer. Their function is unknown but they could be part of shell micro-ornamentation.

Diagenetic structures

Although brachiopods are composed of low-Mg calcite and are relatively stable in the presence of diagenetic fluids, microstructural alteration does occur and varying states of preservation are recognized in Paleozoic specimens. Alteration of the fibrous layers ranges from slight dissolution between calcite rods (Fig. 2.18, 2.19) to almost complete obliteration of any structural features (Fig. 2.20). Slight dissolution and subsequent calcite cement filling between fibres is evident (e.g., *Athyris spiriferoides* valve; Fig. 2.18). Dissolution, reprecipitation and fusing of calcite fibres progressively obscures microstructural detail (Fig. 2.19). In rare cases, the microstructures of a few valves of *Rhipidomella vanuxemi*, *Athyris spiriferoides*, *Resserella elegantula* are almost completely obliterated and are replaced by fine grained secondary calcites. Valves of *Pentameroides* sp. are invariably completely recrystallized (Fig. 2.22).

Figure 2.16. S.E.M. micrograph of the internal valve surface of *Rhipidomella vanuxemi* (#412, Wanakah Shale, New York State) Stacked oblate and flattened fibrous calcites meet the internal surface at low angles. Pits and depression are evident surrounding punctal openings which are partially filled with secondary calcites.

Figure 2.17 S.E.M. micrograph of micropores on the internal valve surface of *Eospirifer radiatus* (#2195, Lewiston Member, New York).

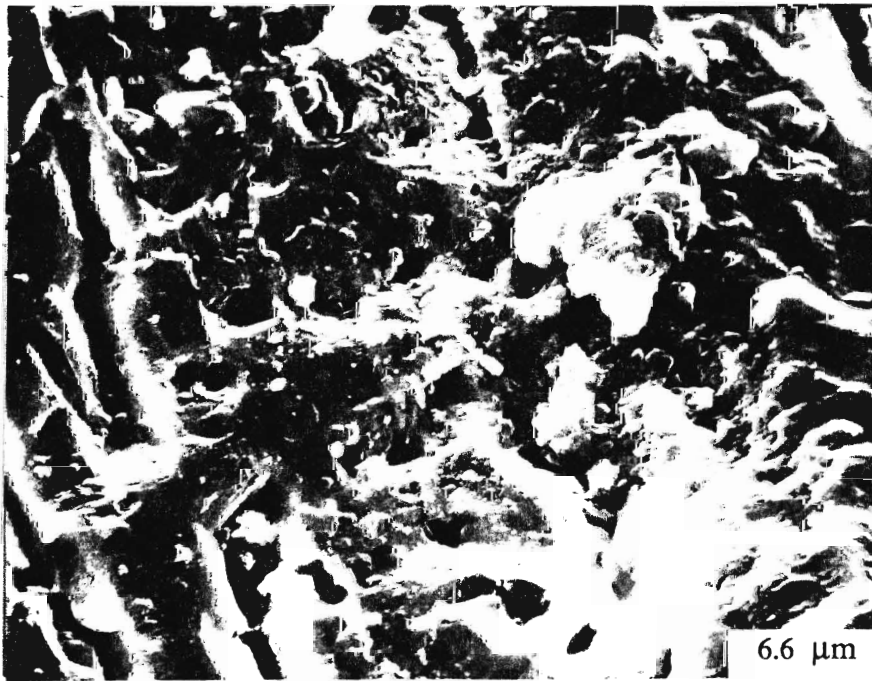
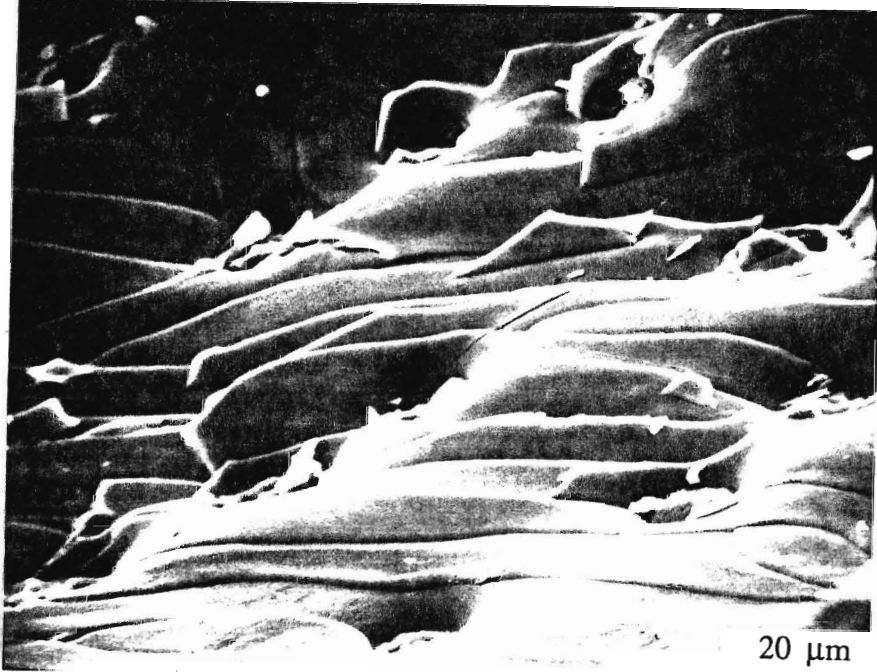


Figure 2.18. S.E.M. micrograph of the secondary fibrous shell layer of altered *Athyris spiriferoides* (#5, Wanakah Shale, Middle Devonian, New York). There is evidence of slight dissolution and fusing of fibres.

Figure 2.19. S.E.M. micrograph of the secondary fibrous shell layer of altered *Athyris spiriferoides* (#5, Wanakah Shale, Middle Devonian, New York). Progressed alteration has resulted in fusing and obscuring of secondary layer fibres and structure and significant dissolution and reprecipitation.

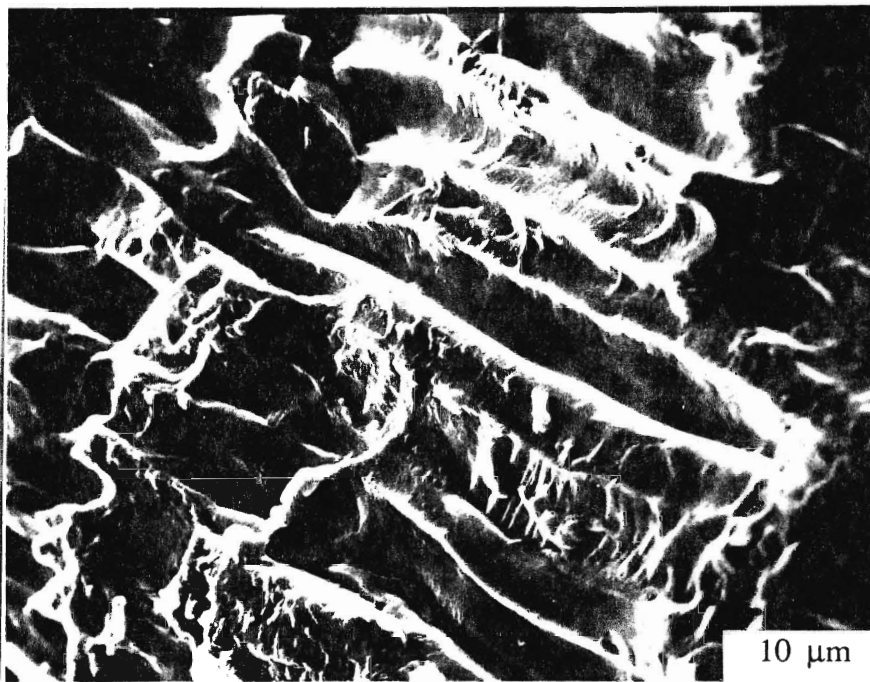
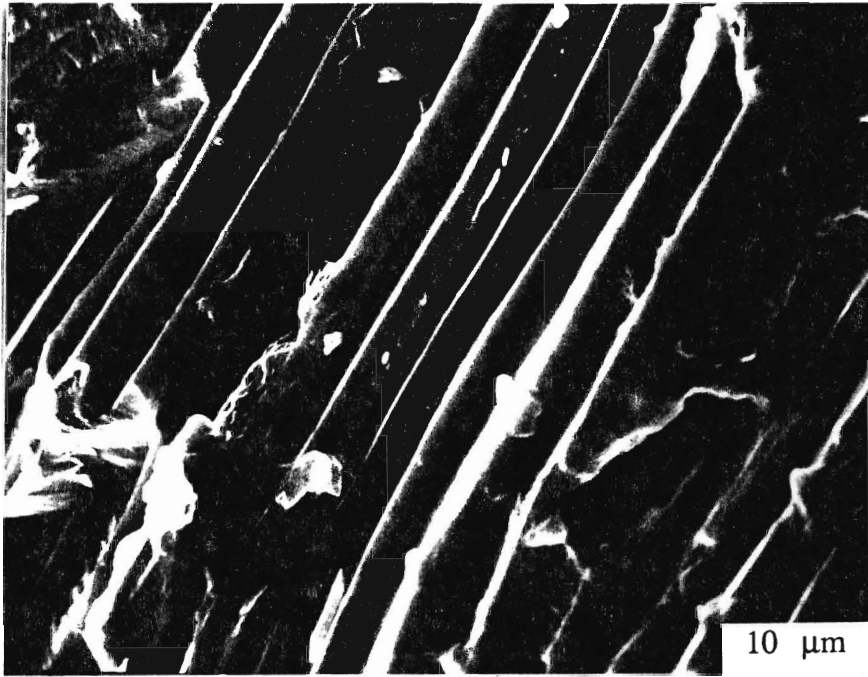
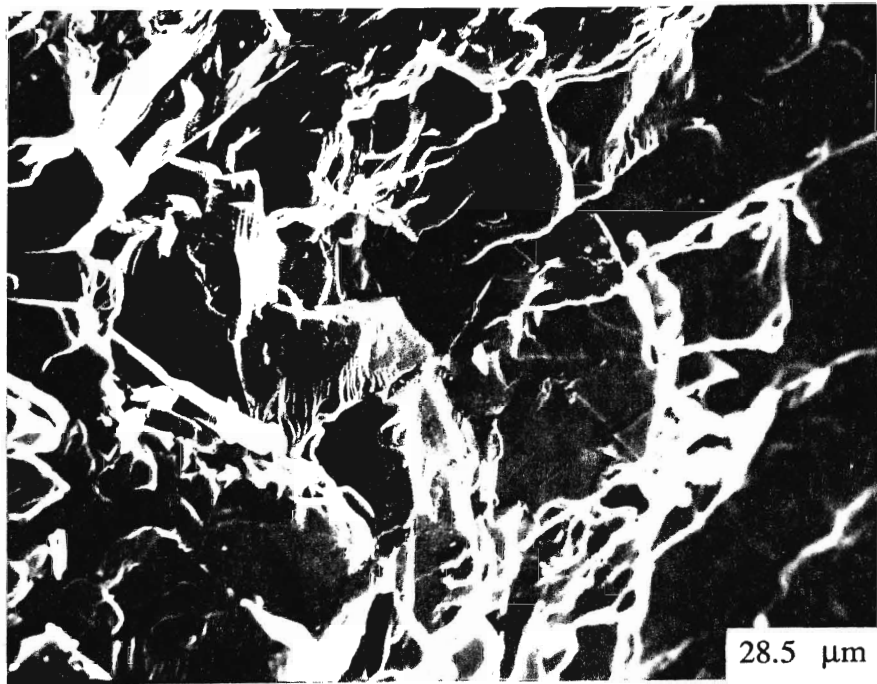


Figure 2.20. S.E.M. micrograph of recrystallized *Pentameroides* sp. from the Merritton Formation (#2007, Middle Silurian, Ontario). Recrystallization of primary or secondary shell layers is complete and original microstructures are replaced by calcite mosaic.

Figure 2.21. S.E.M. micrograph of laminar secondary shell structure of *Rafinesquina deltoidea* (#794, Verulam Formation, Ontario). The foliated secondary layer calcite laths are slightly fused.



Fused calcite laths apparently constitute the laminar shell layers of Strophomenids (Rowell and Grant, 1987), and as such makes it more difficult to identify pristine structure. The thin, flat valves of strophomenids *Sowerybella* sp., *Rafinesquina deltoidea* and *Coolinia subplana* are composed of fine laminar layers. Small calcite laths are recognized in some specimens (Fig. 2.21), but in most specimens the laminae appear fused (Fig. 2.22). It remains uncertain what degree of fusing can be ascribed to dissolution-reprecipitation events.

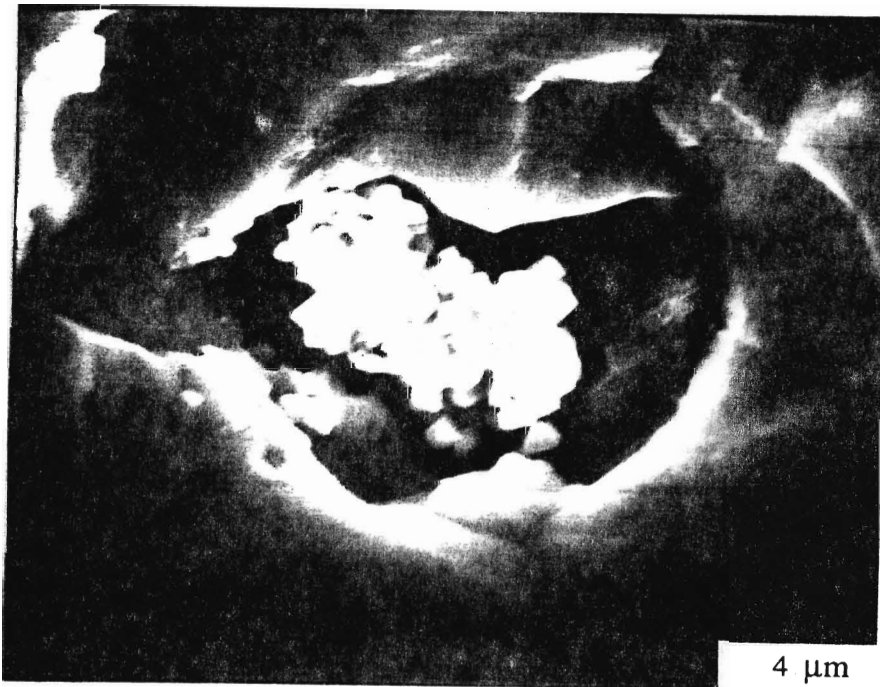
Although the punctae of *Tropidoleptus carinatus* and *Rhipidomella vanuxemi* are often open at the shell surface, the majority of punctal pores are partially filled with secondary calcites; many are filled with minute calcite cement rhombohedra (Fig. 2.23). The exposed face of an inner valve of *Tropidoleptus carinatus* reveals primary punctal pores but the openings are filled with pore cements (Fig. 2.14).

CONCLUSIONS

The results of S.E.M. study suggest that most brachiopod shell calcites of the Hamilton (Middle Devonian) and Clinton Groups (Middle Silurian) are essentially preserved in a pristine state. Brachiopod shell calcites from both these periods retain the original integrity of primary microstructural features, such as oblate calcite rod, shell foliation, and punctate structures. The termination of calcite fibres on internal surfaces of valves, here termed imbricate structure, is observed in modern and ancient specimens and indicative of the good degree of preservation.

Figure 2.22. S.E.M. micrograph of secondary shell structure of orthid *Dalmanella rogata* (#754, Verulam Formation, Ontario). The foliated calcite laths are slightly fused and there is some cement filling between laths.

Figure 2.23. S.E.M. micrograph of punctate brachiopod *Tropidoleptus carinatus* showing punctal filling cements (#409, Wanakah Shale, New York State).



Post-depositional alteration of some specimens is indicated by fusing of calcite rods, loss of integrity of the foliated layers, progressive obscuring of microstructure and precipitation of cements between fibres. Complete obliteration of shell structure is rare and recrystallization is restricted to Pentamerid specimens. Moreover, the punctal canals of *Tropidoleptus carinatus* and *Rhipidomella vanuxemi* are invariably cement filled, although surrounding foliation is preserved. A spectrum of microstructural alteration is evident in brachiopod shell calcites analysed from Trenton Group (Middle Ordovician) limestones and Georgian Bay Formation (Upper Ordovician) shales.

CHAPTER 3

Diagenetic and paleoenvironmental investigation of brachiopod shell calcite
from the Middle Devonian Hamilton Group;
New York State and Ontario.

INTRODUCTION

The elemental and isotopic composition of brachiopod shell calcite is potentially a record of the chemical environment within which the carbonate was precipitated. The analysis of preserved brachiopod calcite has led to the investigation of secular changes in the oceanic reservoirs of ^{18}O and ^{13}C and the establishment of carbon and oxygen isotopic curves for the Paleozoic (Popp et al., 1986; Veizer et al., 1986; Brand, 1989). However, it must be determined whether brachiopod low-Mg calcite has undergone chemical and microstructural changes with post-depositional alteration. Diagenetic alteration of calcite in either meteoric, marine or mixed settings will overprint primary elemental and isotopic compositions (Brand and Veizer, 1980, 1981; Baker et al., 1982; Al-aasm and Veizer, 1982; Veizer, 1983a, b). Manganese enriched contents of brachiopods (>100 ppm; Al-aasm and Veizer, 1982; Veizer et al., 1986) and the recognition of cathodoluminescent valves (Popp, 1981, 1986; Popp et al, 1986a, b; Adlis et al., 1989) have been used to eliminate altered brachiopods from geochemical interpretations. This approach is problematic, since Mn contents over 100 ppm may reflect primary compositions of shell calcite, rather than a diagenetic product (Brand, 1989a, b). It is assumed that brachiopods inhabited open marine, fully oxic conditions (Veizer et al., 1986) and as such, brachiopods of different ages, taxa and lithology are treated as a singularly uniform and chemically unvariable organism. However, recent studies suggest that ancient brachiopods had a wide range of environmental tolerances, especially of anoxia (Thayer, 1974, 1986a, b; Kammer et al., 1986; Thompson and Newton, 1987; Racki, 1989) and modern brachiopods are able to survive and function for prolonged periods with oxygen levels frequently below 0.1 mL^{-1} (Tunnicliffe and Wilson, 1988). Previous investigations of

secular isotopic changes have not taken into consideration possible inherent chemical variability within co-occurring brachiopod species, nor possible isotopic/elemental differences within single beds that reflect depth changes, organic carbon content and temperature variability. Shifts of 1-3‰ in $\delta^{18}\text{O}$ and $\delta^{13}\text{C}$ (Popp et al., 1986; Adlis et al., 1989) may not be overly significant if similar isotopic variability in one single shell bed can be explained as the response to a deepening basin and to local paleoenvironmental conditions.

During deposition of the Middle Devonian Hamilton Group in western New York State and southern Ontario, benthic habitats were occupied by diverse invertebrate fauna. These are the focus of recent paleoecologic and stratigraphic studies (e.g., Baird and Brett, 1981; Baird, 1983; 1985; Brett, 1986b; Brett and Cotrell, 1982; Brett and Baird, 1985; Brett et al., 1986; Dick and Brett, 1986; Savarese et al., 1986; Wygard, 1986; Baird and Brett, 1986; Brett et al., 1986a; Miller et al., 1988). Spatial distribution of brachiopods on the Hamilton Shelf can be defined within the context of idealized biofacies (Brett, et al., 1986b; Miller, 1986; Grasso, 1986), which represent groups of closely related intergrading fossil associations, the distribution of which are controlled by environmental parameters (e.g., depth, turbidity, oxic conditions; Fig. 3.1). Persistent brachiopod shell beds that deepen toward the basin centre can be traced across the shelf for tens of kilometers (Figure 3.2). These shell beds represent an ideal opportunity to investigate possible chemical and isotopic changes in brachiopod shell calcite reflecting taxonomic and environmental variability.

The purpose of this chapter is to investigate the diagenetic and depositional chemistries of brachiopods from Hamilton Group strata. Objectives are fourfold: i) to determine diagenetic trends within brachiopod calcite and select pristine specimens for further paleoenvironmental investigations; ii) to

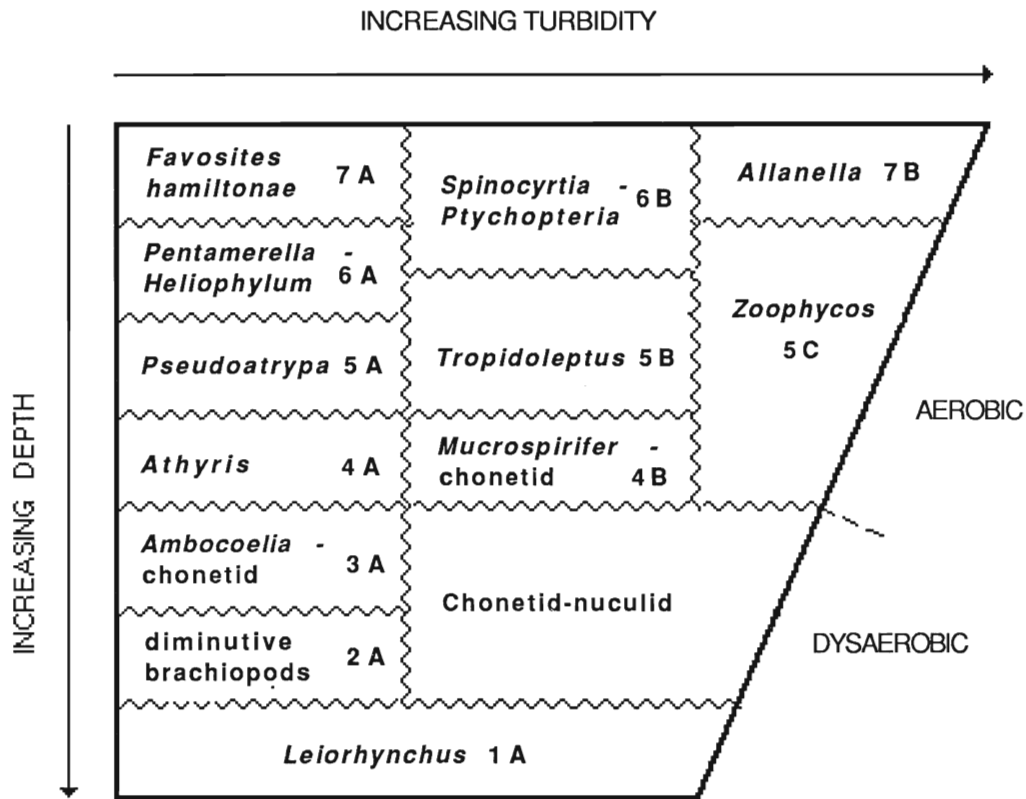
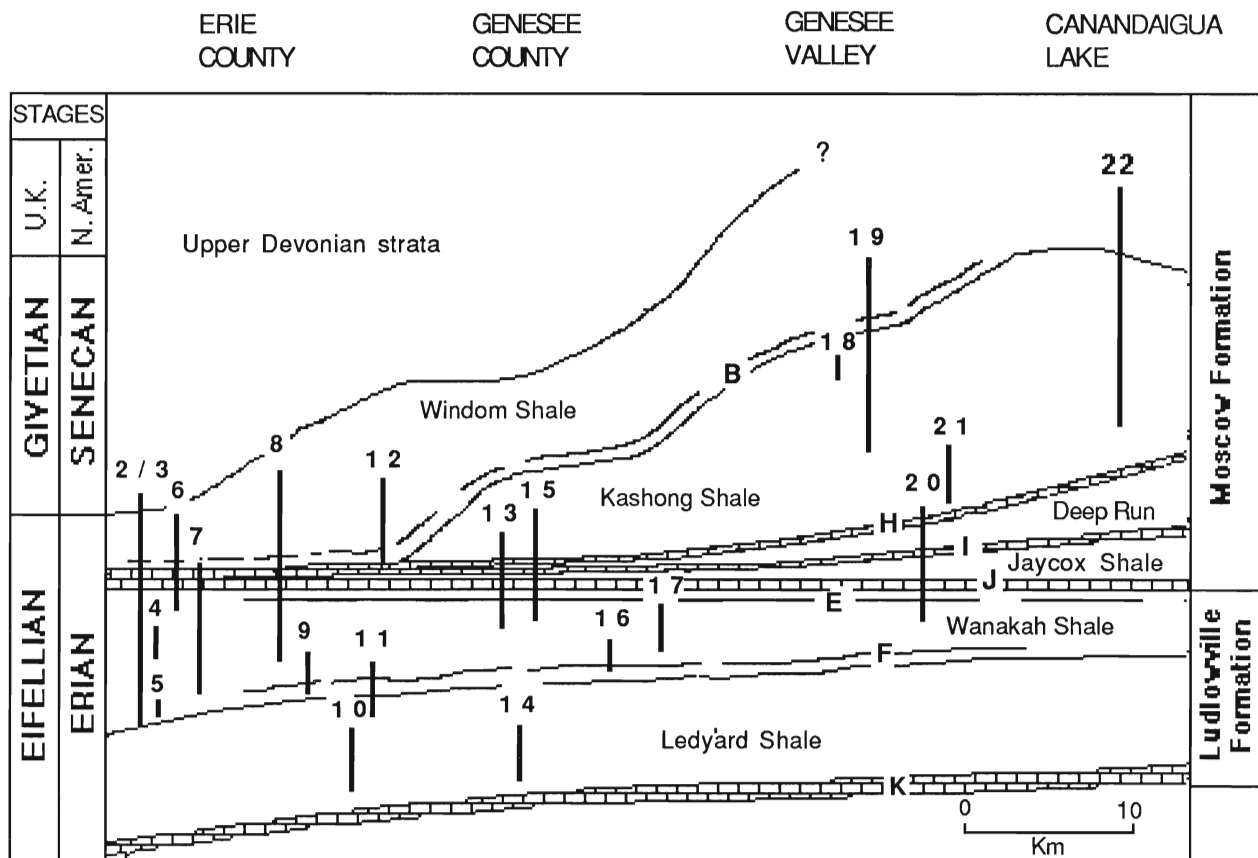


Figure 3.1. Generalized paleoecological model relating Hamilton Group biofacies to inferred gradients of depth-related parameters, turbidity and/or sedimentation rates and oxic conditions. From Brett et al. (1986).



- | | |
|--|---|
| <p>A Penn Dixie Pyrite Bed
 B Smoke Creek Trilobite Bed
 C Bay View Coral Bed
 D Tichenor Limestone
 E "Demissa" Bed
 F Murder Creek Trilobite Bed</p> | <p>G "Pleurodictyum" Bed
 H Menteth Limestone
 I Tichenor Limestone
 J Michenor Limestone
 K Centrefield Limestone</p> |
|--|---|

Figure 3.2. Diagrammatic cross-section of the Upper Hamilton Group (Middle Devonian) across western New York State. Vertical lines represent sections at sampling sites: numbers correspond to sampling localities listed in Appendix III. Lettering corresponds to prominent stratigraphic units and persistent shell beds. Modified from Baird (1979) and Brett and Cottrell (1982).

report the distinct chemical differences in shell carbonate between co-occurring brachiopod species; iii) evaluate the chemical and isotopic trends across a deepening basinwide shell bed, and; iv) investigate possible relationships between chemical and isotopic contents, biofacies and inferred paleoenvironmental conditions.

GENERAL GEOLOGY OF THE HAMILTON GROUP

During the Middle Devonian, reactivation of the Appalachian Basin and surrounding arches was initiated by the second tectonic phase of the Acadian Orogeny (Ettensohn, 1985a). Reconstruction of basin physiography suggests that a shallow tropical epicontinental sea occupied most of New York State and Pennsylvania (Fig. 3.3; Parsons et al., 1988). This semi-enclosed lobe of the Appalachian Basin lay south of the equator (Oliver, 1976; Heckel and Witzke, 1979; Kent, 1985; Miller, 1986; Vogel et al., 1987; Parsons et al., 1988) and, although basin waters were probably connected to the Rheic Ocean to the southwest, water exchange was apparently limited (Woodrow, 1985). Limestones and calcareous shales accumulated on the shallow shelf in the west (Fig. 3.2) whereas coarse siliciclastics, derived from the Acadian landmass, accumulated as the Catskill delta complex to the east (Woodrow, 1985; Parsons et al., 1988).

The Hamilton Group, which represents a time span of about 5-7 ($\pm 1-2$) million years (Harland et al., 1982; Brett, 1986a), is subdivided into four formations; the Marcellus, Skaneateles, Ludlowville and Moscow (Fig. 3.4). These units are separated by thin but persistent carbonate beds (e.g., Tichenor, Michenor, Menteth Limestones), which represent the culmination of large-scale transgressive-regressive sequences within each formation, and superimposed

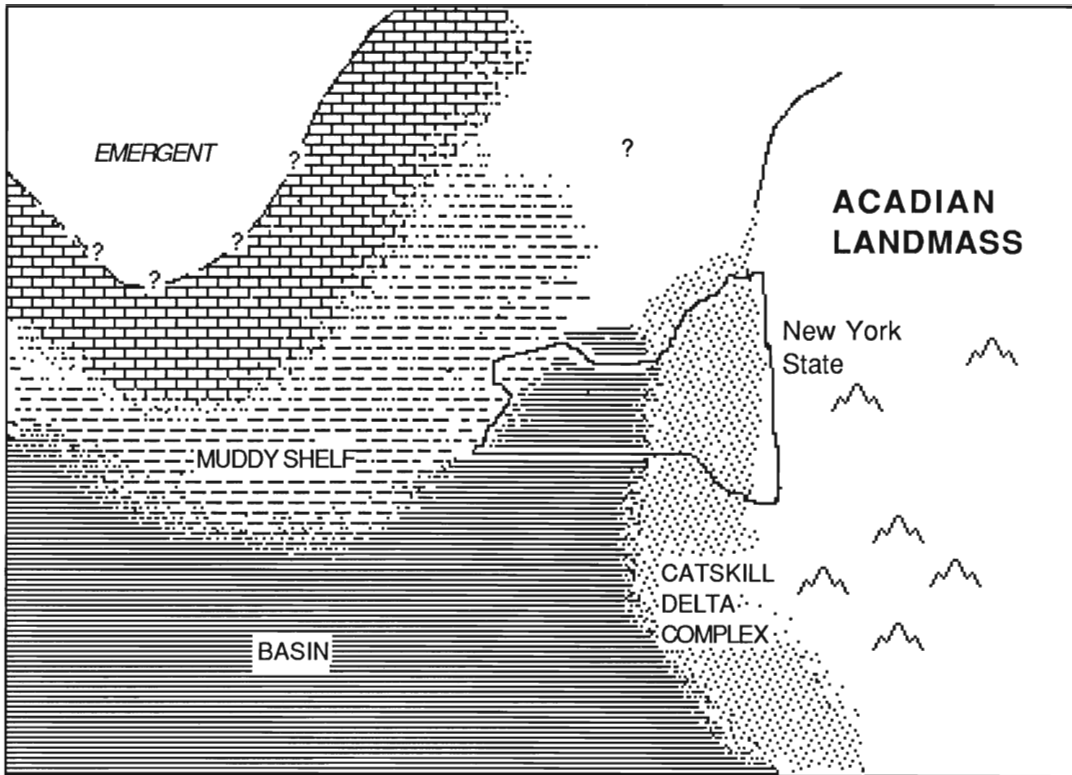


Figure 3.3. Paleogeographic reconstruction of the Appalachian Basin during deposition of the Middle Devonian Hamilton Group. Modified from Parsons et al. (1988).

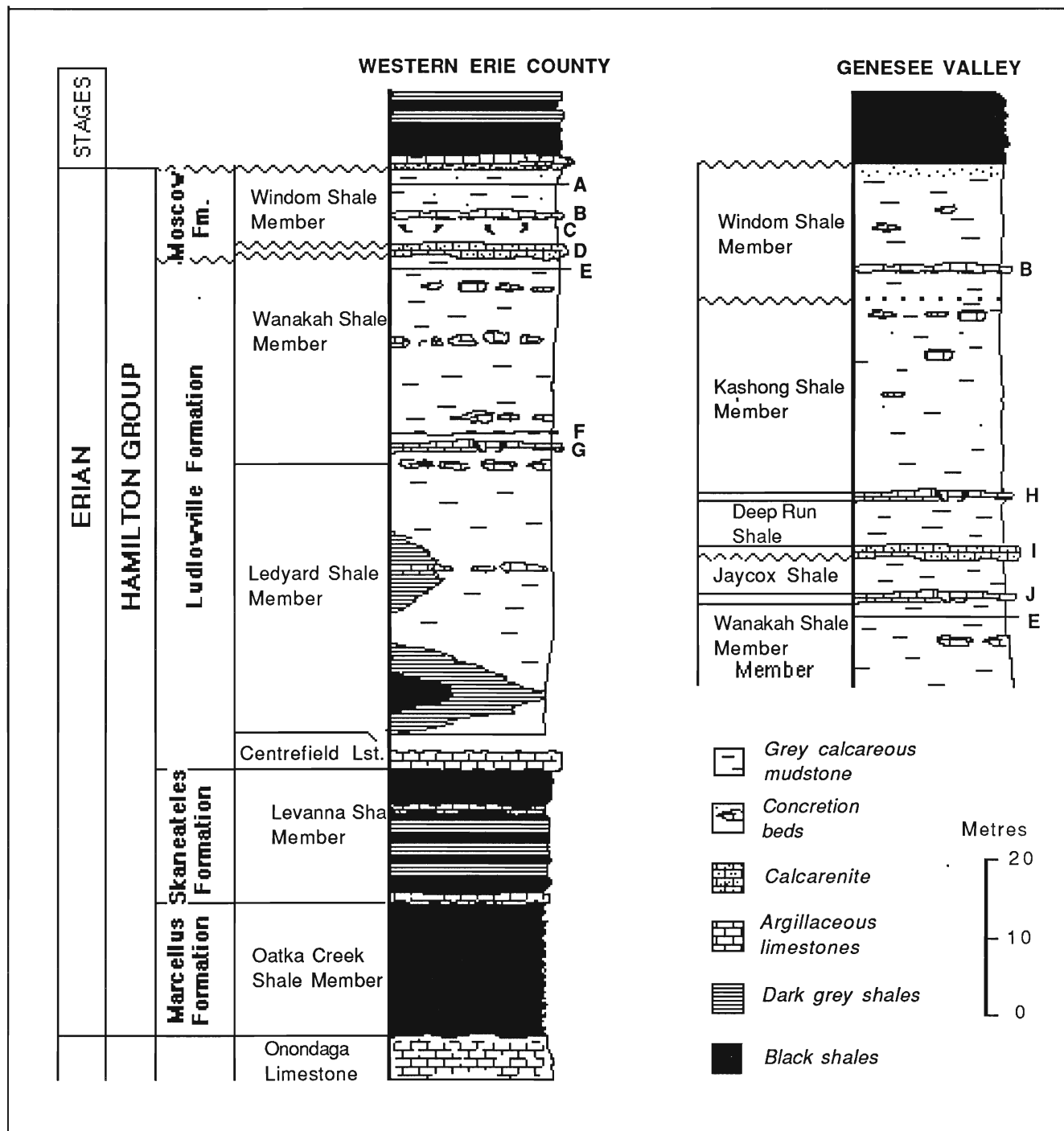


Figure 3.4. Generalized stratigraphic section of the Ludlowville and Moscow Formations of the Hamilton Group (Middle Devonian) in Erie County and Genesee Valley. Shell beds and thin limestones that are widely traceable across western New York State are designated by letters A to J (see Fig. 3.2. for explanation). Modified from Brett et al. (1986).

smaller transgressive-regressive cycles of 1-3m (Brett and Baird, 1985; Brett and Baird, 1986a, b; Savarese et al., 1986; Landing and Brett, 1987). This vertical sequence of sediment deposition in western New York was controlled by the lateral movement of facies belts in northward or southward directions as a result of transgressive-regressive events (Brett and Baird, 1982; Brett et al., 1986b). An actively subsiding trough was centred around the Seneca and Cayuga Lakes region and during deposition of the Ludlowville Formation, grey shales of the Ledyard and Wanakah Shale Members were transitional with black shales of the basin depocentre (Baird, 1981, Brett et al, 1986a, b). The basin axis slowly moved westward toward the Genesee Valley during subsequent deposition of the Moscow Formation Deep Run and Kashong Shale Members (Miller, 1986). The west and eastward thinning of the facies may be the result of condensation, non-deposition, and submarine erosion (Miller, 1986; Brett and Baird, 1986a, b).

RESULTS

Five co-occurring brachiopod species (i.e., impunctate spiriferids *Athyris spiriferoides spiriferoides*, *Mediospirifer audacula audacula* and *Mucrospirifer mucronatus mucronatus* and punctate *Rhipidomella vanuxemi vanuxemi* and *Tropidoleptus carinatus carinatus*) were chemically analysed from the Ludlowville and Moscow Formations of the Hamilton Group (Table 3.1). The ranges of their shell calcite chemical composition are similar to those reported for modern (e.g., Milliman, 1974; Morrison and Brand, 1986; Brand, 1989a) and ancient brachiopods (Brand and Veizer, 1980; Brand, 1983; Popp et al., 1986b; Veizer et al., 1986; Brand and Morrison, 1987). Elemental contents are variable (e.g. *Athyris spiriferoides* Mn; range 10-1645 ppm), reflecting the influence of

Table 3.1. Middle Devonian chemical data of all brachiopods and pristine brachiopods

Brachiopod species	Stat.	Ca	Mg	Sr	Mn	Na	Fe	Al	I.R.
ALL SPECIMENS									
<i>Athyris</i> (ALL; N=83)	Mean	372997	1339	863	211	1202	361	65	6.6
	Std. Dev	26520	270	88	223	212	376	70	
	min. max.	246830 437260	820 2175	560 1180	10 1645	680 1760	25 2480	0 270	
<i>Mucrospirifer</i> (ALL; N=74)	Mean	377044	1074	976	190	1437	389	72	6.5
	Std. Dev.	27525	376	117	126	218	290	77	
	min. max.	252720 416390	650 3495	695 1335	35 770	535 2000	100 1365	0 290	
<i>Mediospirifer</i> (ALL; N=59)	Mean	370850	868	918	160	1347	395	71	8.5
	Std. Dev.	36312	283	123	140	260	508	96	
	min. max.	211310 412910	340 1820	570 1100	10 1030	425 1900	65 3500	0 600	
<i>Tropidoleptus</i> (ALL; N=17)	Mean	377980	1556	876	527	1370	1087	87	9.9
	Std. Dev.	14995	446	76	274	213	687	75	
	min. max.	357690 405690	810 2340	750 1025	210 1080	870 1640	290 2480	1 316	
<i>Rhipidomella</i> (ALL; N=17)	Mean	348090	3118	887	381	1585	907	58	9.9
	Std. Dev.	40220	792	89	238	270	697	87	
	min. max.	268970 392720	1095 4300	635 1020	135 1030	1120 2195	200 2760	0 315	
.....									
PRISTINE CHEMISTRIES									
<i>Athyris</i> UNALTERED (N=70)	Mean	374024	1309	874	159	1216	241	53	6.3
	Std. Dev.	27294	258	85	99	195	120	63	
	min. max.	246830 437260	845 2175	735 1180	10 650	730 1760	25 580	0 260	
<i>Mucrospirifer</i> UNALTERED (N=62)	Mean	380277	1035	981	160	1440	284	65	6.0
	Std. Dev.	27233	373	116	80	216	128	73	
	min. max.	252720 416390	695 1335	695 1335	35 400	535 2000	100 715	0 290	
<i>Mediospirifer</i> UNALTERED (N=45)	Mean	372520	789	927	122	1354	229	53	8.5
	Std. Dev.	38301	206	119	67	178	65	61	
	min. max.	211310 410870	340 1285	610 1100	10 280	880 1670	65 545	0 210	

All elemental concentrations are in ppm.

two primary controls: 1) composition of the original precipitated shell calcite, regulated by the organism physiology and external chemical environment; and 2) the chemical changes associated with diagenetic re-equilibration of calcite in the presence of fluid(s).

Diagenetic Trends

The similarity of microstructure to modern brachiopods and the retention of the fabric integrity of most Hamilton Group brachiopod calcite indicates a high degree of chemical preservation (Figs. 2.6 to 2.8; 2.10). However, despite the stability of low-Mg calcite, a number of brachiopods were subjected to varying degrees of post-depositional alteration, resulting in textural changes (Figs. 2.18, 2.19) and the repartitioning of trace/minor elements into diagenetic low-Mg calcite. Microstructural alteration is evident in those specimens where calcite fibres show signs of fusing, dissolution and precipitation of cements between fibres. Moreover, complementary chemical changes are observed with diagenesis; similar chemical trends accompanying microstructural alteration are demonstrated in previous studies of molluscs, crinoids, trilobites and brachiopods (Brand and Veizer, 1980; Al-Aasm and Veizer, 1982; Morrison and Brand, 1987; McAllister, 1989; McAllister and Brand, 1989; Brand 1989a, b). A representative suite of Hamilton Group brachiopod specimens of different species are compiled in Table 3.2, with microstructural preservation listed against respective Mg, Mn, and Fe contents. These three elements were chosen because they are the most diagnostic of chemical alteration. It is apparent that there is a corresponding increase in the degree of fusing with progressive chemical diagenesis. Graphically, the direction of alteration is toward coeval matrix samples, which show the greatest effect of post-depositional alteration (Figure 3.5; 3.6), and follows theoretical considerations such as partition

Table 3.2. Comparison of microstructural preservation and chemical contents for selected brachiopods from the Middle Devonian Hamilton Group of western New York State and southern Ontario. Lithology symbols denote (S= dark grey shale).

Sample Number	Age	Lithology	Preservation State	Diagenetic features	Mg (ppm)	Mn (ppm)	Fe (ppm)	Figured Specimens
<i>A. spiriferoides</i>								
2	Dev.	S	Good	None	1030	200	110	
5	Dev.	S	Good	None	1185	150	380	2.18
6	Dev.	S	Fair	Slight dissolution	1545	225	370	
42	Dev.	S	Good	None	990	95	280	
60	Dev.	S	Fair	Slight dissolution	2175	100	200	
61	Dev.	S	Good	None	1450	120	275	2.19
64	Dev.	S	Poor	Dissolution	1440	250	700	
98	Dev.	S	Fair	Slight dissolution	1510	250	535	
99	Dev.	S	Good	None	1585	120	275	
104	Dev.	S	Good	None	1075	120	330	
170	Dev.	S	Poor	Recrystallization	540	1645	820	
172	Dev.	S	Good	None	1365	5	95	
253	Dev.	S	Good	None	1210	150	130	
254	Dev.	S	Good	None	1330	150	80	
401	Dev.	S	Good	None	1140	170	240	
402	Dev.	S	Fair	Slight dissolution	1215	385	825	
403	Dev.	S	Good	None	1420	170	275	2.10
428	Dev.	S	Good	None	1205	130	195	
444	Dev.	S	Good	None	1390	70	155	
445	Dev.	S	Good	None	1610	95	200	2.11
<i>M. audacula</i>								
18	Dev.	S	Fair	Slight dissolution	1000	220	555	
44	Dev.	S	Good	None	890	130	505	
71	Dev.	S	Good	Slight dissolution	725	110	140	2.12
126(1)	Dev.	S	Good	None	835	50	110	
126(2)	Dev.	S	Good	Slight dissolution	1025	135	265	
400	Dev.	S	Good	None	670	185	325	2.7
420	Dev.	S	Good	None	660	50	60	
422	Dev.	S	Good	None	340	50	70	
432	Dev.	S	Good	None	620	85	205	
<i>R. vanuxemi</i>								
41	Dev.	S	Poor	Dissolution	3720	620	2760	
83	Dev.	S	Good	None	3490	105	445	
84	Dev.	S	Good	None	3390	185	790	
113	Dev.	S	Poor	Dissolution	2855	360	445	
412	Dev.	S	Good	None	2975	340	850	2.16
<i>M. mucronatus</i>								
22	Dev.	S	Good	None	1250	140	530	
24	Dev.	S	Good	None	1060	140	475	
68	Dev.	S	Good	None	935	220	460	
89	Dev.	S	Good	None	850	110	375	
106	Dev.	S	Good	None	1065	130	310	
178	Dev.	S	Good	None	1075	90	370	2.8
415	Dev.	S	Good	None	770	130	195	
418	Dev.	S	Fair	Slight dissolution	2400	235	200	
<i>T. carinatus</i>								
129	Dev.	S	Poor	Dissolution	2340	520	710	
370	Dev.	S	Good	None	1350	820	2300	
371	Dev.	S	Good	None	1450	930	1495	
409	Dev.	S	Good	None	2200	225	420	2.23
410	Dev.	S	Good	None	2010	320	1230	

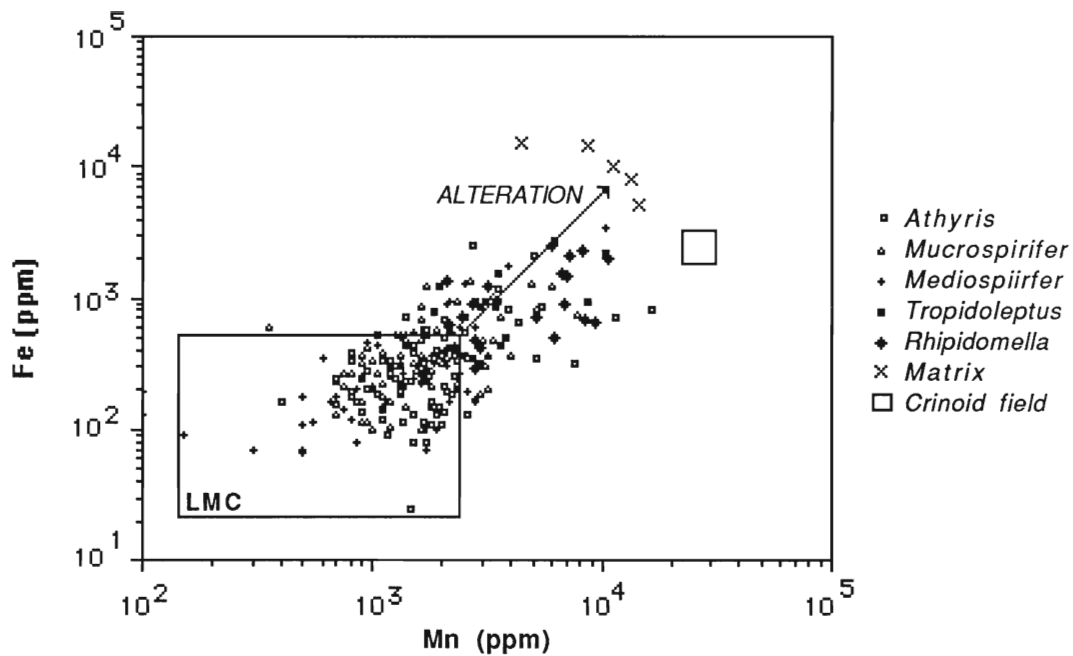


Figure 3.5. Scatter plot of Fe vs Mn for all Middle Devonian brachiopods. The LMC field represents the general categorization of microstructurally and chemically pristine brachiopods. The boundaries are loosely defined. A few *Tropidoleptus* specimens plot within this field but are deemed altered because of the presence of pore filling cements within punctae. Metastable high-Mg calcite crinoids from the Hamilton Group are extensively altered, plotting close to matrix values. The open meshwork structure, typical to crinoids (Bathurst, 1975; Brand and Morrison, 1987b; Brand, 1987) may have promoted fluid controlled reactions and multiple dissolution-precipitation events.

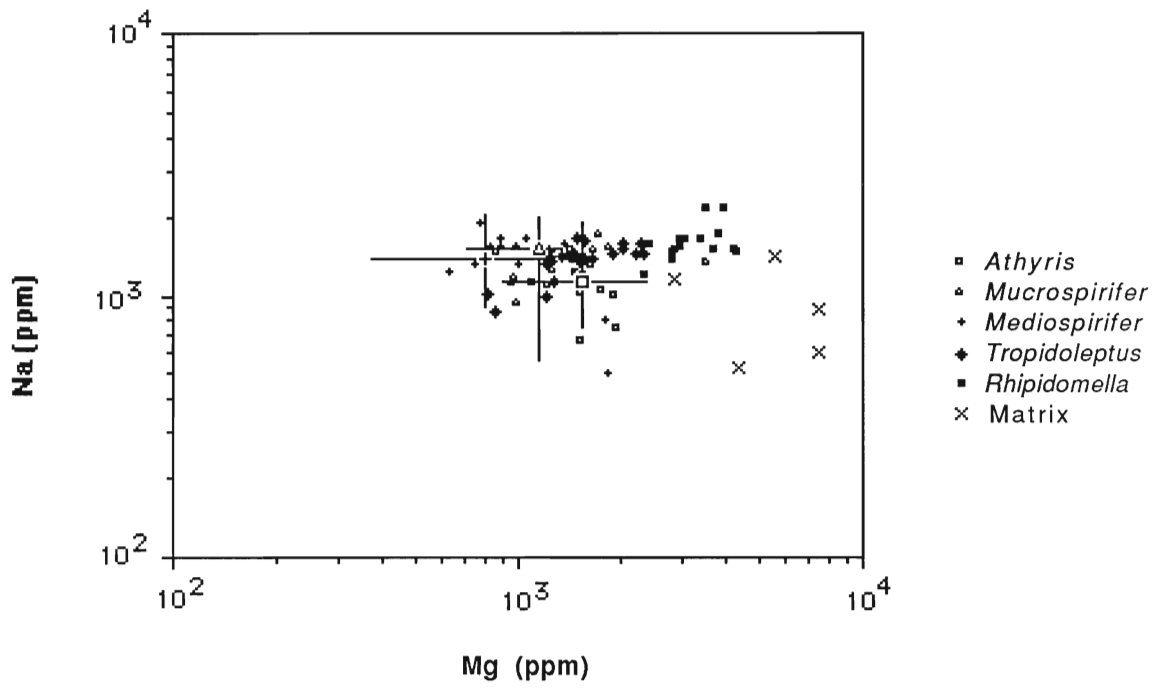


Figure 3.6. Scatter diagram of Na vs Mg for brachiopods and matrix of the Hamilton Group (Middle Devonian). The means and ranges of unaltered brachiopods are plotted amongst individual altered specimens.

coefficients, water chemistries and variable water-rock ratios (Brand and Veizer, 1980; Veizer, 1983a).

Factor analysis of chemical data supports the inference that diagenetic alteration can explain a significant percentage of variation observed in brachiopod calcite (Appendix IV, Tables A-1 to A-6.) and concurs with the observed chemical changes associated with diagenesis. Factor 1 is repeatedly loaded by Mg, Fe and Mn for brachiopods by species and by formation; similar confirmation of diagenetic trends is reported in other studies (e.g., Brand and Veizer, 1980; Al-Aasm and Veizer, 1982; 1986a, b; Veizer et al., 1986; Majid and Veizer, 1986; Brand 1989a, b).

The degree of brachiopod alteration is variable and reflects the composition of original shell calcite and diffusion or fluid controlled diagenesis (Veizer, 1983a; 1983b). The chemical equilibration process progresses by the dissolution of calcite fibres and subsequent reprecipitation of diagenetic low-Mg calcite cements into available pore spaces. Slightly altered specimens, which plot close to the pristine field (Fig. 3.5), have undergone diffusion controlled diagenesis and retain much of their original composition. Pore spaces between shell fibres are less than 1 μm wide (Figs. 2.7, 2.8), and as a consequence, alteration can be constrained by the minute dimensions of the reaction zone (Pingitore, 1976; 1978; Veizer, 1983, Brand, 1989).

The Mg, Fe and Mn contents of *Tropidoleptus carinatus* and *Rhipidomella vanuxemi* are significantly higher than co-occurring spirifers (Fig. 3.7, 3.8; Table 3.1) and reflects the presence of punctae in shell calcite. Although, the integrity of shell foliation is retained, the punctae are invariably filled with secondary calcite cements (Figs. 2.28, 2.30). The proportion of punctae may be small compared to the whole shell, but pore-filling cements

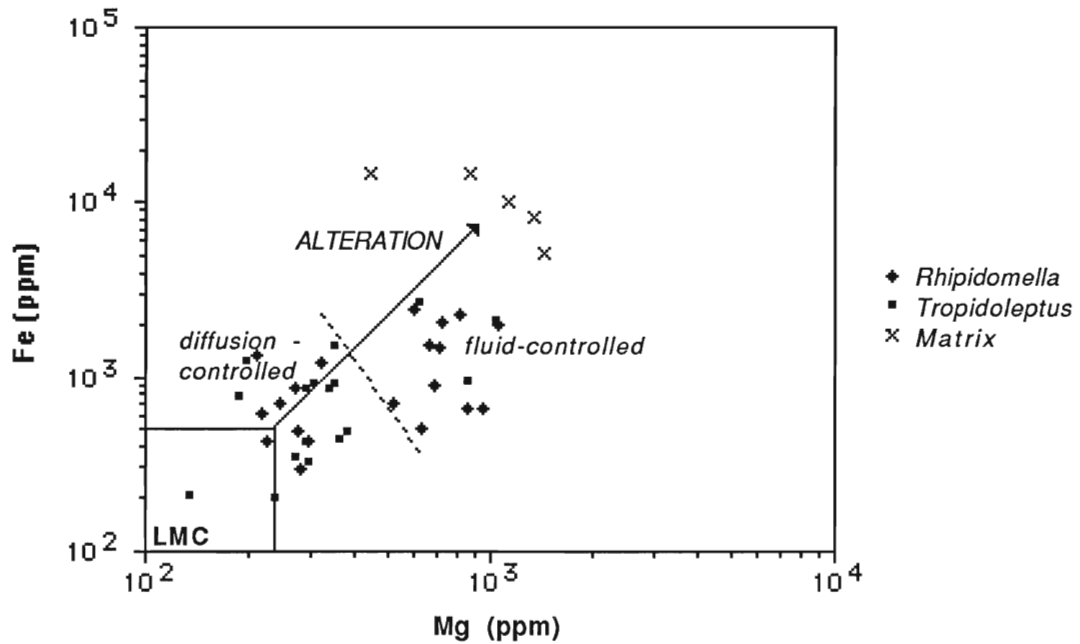


Figure 3.7. Scatter plot of Fe vs Mn for *Tropidoleptus* and *Rhipidomella* brachiopods from the Hamilton Group (Middle Devonian). The LMC field represents unaltered Hamilton Group brachiopods.

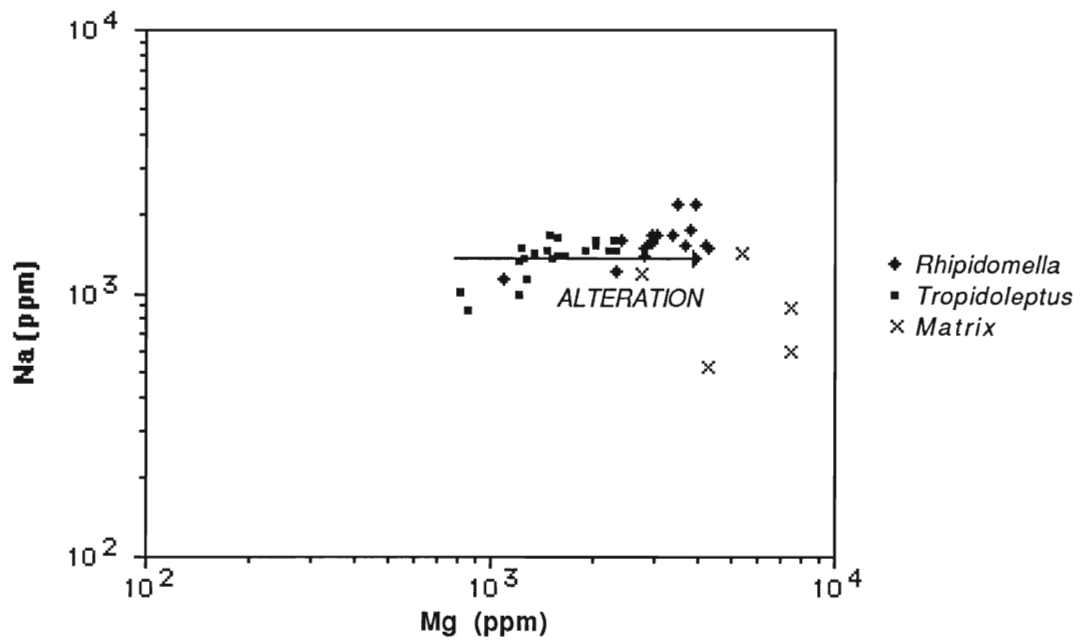


Figure 3.8. Scatter plot of Na vs Mg for *Tropidoleptus* and *Rhipidomella* of the Hamilton Group. Progressive enrichment in Mg may reflect increasing proportion of pore-filling cements within punctae.

contribute significantly to overall "averaged" calcite chemistry. Furthermore, the punctae may facilitate the passage of fluids through the shell calcite, and effectively increase the surface area available for diagenetic reaction. Magnesium contents reflect the extent of diagenetic re-equilibration and pore-filling cements. Altered *Tropidoleptus carinatus* specimens exhibit chemical ranges related to a whole spectrum of diffusion to fluid controlled alteration (Fig. 3.7). *Tropidoleptus carinatus* with low Mg contents reflect diffusion controlled reactions (Fig. 3.8), whereas those with higher Mg contents were altered in the presence of larger water volumes. The presence of pore-filling cements precludes the use of punctate brachiopods from paleoenvironmental investigation.

Diagenetic waters of the Hamilton Group

The alteration of Ludlowville and Moscow Formation brachiopod calcite resulted in progressive enrichment of Mg, Mn and Fe contents whereas Sr and Na contents were only slightly reduced. Retention of Sr and Na contents is not characteristic of meteoric diagenesis (Brand and Veizer, 1980; Veizer, 1983a, b), which suggests that the diagenetic fluids were essentially Mg, Sr and Na rich. The passage of marine- or mixed- waters is the most likely explanation, and it is possible that waters derived from the Upper Silurian Salina Group may have migrated through fracture planes; Salina Group fluids were probably highly ionic (O'Shea et al, 1988; Fritz et al, 1988). Alternately, *in situ* formation waters within this semi-enclosed basin may have been responsible for shell calcite alteration. The outcrop pattern in western New York State is essentially west to east and the passage direction of the diagenetic fluid(s) was impossible to decipher from this data set.

Selection of best preserved material

Previous workers have used trace and minor elemental compositions of brachiopod shell calcite to determine the best preserved material (e.g., Lowenstam, 1961; Brand and Veizer, 1980; Buchardt and Weiner, 1981; Al-Aasm and Veizer, 1982; Veizer et al., 1986; Brand, 1989). Low-Mg calcite precipitated in equilibrium with ambient seawater is expected to contain Mn contents averaging 5-50 ppm and Fe contents averaging 20-500 ppm (Brand and Veizer, 1980; Al-Aasm and Veizer, 1982; Morrison and Brand, 1987). Ordovician brachiopods from Anticosti Island with mean Mn contents of 150 ppm were deemed to be altered by as much as 20% by Al-Aasm and Veizer (1982) and Veizer et al. (1986). They suggested that shell calcites containing Mn contents over 70 ppm and Fe contents greater than 300 ppm are essentially altered.

In previous studies, brachiopods of different taxa and ages have been grouped together and deemed altered if they exceed a certain critical chemical value (i.e. >100 ppm Mn; <1200 ppm Na; <900 ppm Sr; Veizer et al., 1986). This oversimplification ignores the influence of inherent original variability of shell calcite between taxa, ionic regulation, and potentially different local chemical/physical environments. For example, although the Na and Mg chemical ranges of unaltered *Athyris spiriferoides*, *Mediospirifer audacula* and *Mucrospirifer mucronatus* overlap, there are distinct differences between species (Fig. 3.6; Table 3.1). Brachiopod shell calcite containing 1200 ppm Mg can be pristine or altered depending on whether it is an *Athyris spiriferoides* or a *Mediospirifer audacula*, the original composition controlling the chemistry of the diagenetic product. Therefore, careful evaluation of all elemental (i.e., Mn, Fe, Mg, Sr, Na, Al) and microstructural data must be used to establish pristine from altered specimens.

Similarly, cathodoluminescence in ancient brachiopods has been used by several workers to identify altered brachiopods (Popp, 1981; Popp et al., 1986a, 1986b; Adlis et al., 1989). For example, non-luminescing *Mucrospirifer mucronatus* valves from the Middle Devonian Hungry Hollow Formation were considered unaltered, whereas luminescent specimens from the Speeds and Beechwood Limestones were identified as altered (Popp, 1981; Popp et al., 1986b). In biogenic carbonates, cathodoluminescence results from the presence of Mn substituting for calcium within the crystal lattice (Meyers, 1974; Pierson, 1981; Frank and others., 1982), although other elements may serve as activators and sensitizers (Machel, 1985). The minimum Mn content required to produce luminescence ranges from 300 ppm (Frank et al., 1982) to as low as 15 ppm (Ten Have and Heijen, 1985) and is dependant on the presence or absence of other activators or quenchers; notably Fe acting as a quencher (Frank et al., 1982; Fairchild, 1983; Machel, 1985).

Both of these approaches to the selection of pristine shell calcite assume that brachiopods incorporated Mn and Fe in inorganic equilibrium with open marine seawaters. However, it is increasingly apparent that this may be an oversimplified assumption. Pristine, modern brachiopod calcite can contain as much as 300-450 ppm of Mn (Brand, 1989a), which is enough to activate luminescence. Similarly, ancient brachiopod calcite, by analogy, may reflect original compositions and the complexities of cation regulation by the organism and different chemical environments (e.g. redox conditions, temperature, salinity, precipitation rates). For example, Adlis et al. (1988) observed that the primary prismatic calcite shell-layer of a Pennsylvanian brachiopod *Crurithyris planoconvexa* are luminescent, whereas the secondary fibrous layers are non-luminescent. This may be related to the preferential alteration of the outer prismatic layer, but it may also represent inherent differences in the original

Mn/Fe compositions of both layers, which in turn may be partially related to such processes as biological fractionation and/or differential partitioning between the mineral morphologies.

The Fe and Mn chemistries of pristine Hamilton Group brachiopods are highly variable (5 to 200 ppm Mn and 70 to 650 ppm Fe) and many fall outside the compositional ranges observed in inorganic low-Mg calcite postulated to have precipitated in equilibrium with modern seawater (Table 3.1; Fig. 3.6). This divergence may be the result of a number of processes. The Mn and Fe contents of shell calcite may be partly controlled by soluble oxide coatings (Sherwood et al., 1987), or calcite metal fractions (Thomson et al., 1986), but these influences are generally restricted to deep water brachiopods (>1000 m). Alternately, the leaching of Mn and Fe from the aluminosilicate residue may contribute to chemical concentration in biogenic carbonates (Brand and Veizer, 1980; Boyle, 1981; Al-Aasm and Veizer, 1982; Veizer, 1983a). Significant leaching from the aluminosilicate fraction is indicated if factor analysis of data correlates Fe and Mn contents with I.R. and/or Al contents (Brand and Veizer, 1980; Al-aasm and Veizer, 1982; 1986a, b; Majid and Veizer, 1986; Veizer et al., 1986; Brand, 1989). However, the Mn, Fe and Mg contents of Hamilton Group brachiopod calcite do not correlate with I.R. or Al (Tables A-1 to A-6), which supports the assertion that they reflect primary chemical compositions. Moreover, Al contents are low (mean 40 ppm; range 0 to 330 ppm?), which is close to or below machine detection limits. Analytic methods and sample preparation apparently minimized contamination from alumnosilicates.

Alternately, the Mn compositions may reflect its active or passive incorporation into lattice or non-lattice positions within biogenic carbonates. Mn is apparently bound within pigments or is part of the mineralogical structure of carbonates (Rosenberg, 1980). Shen and Boyle (1988) observed that Mn, even

though ionically much smaller than calcium, is a chemical component of aragonite corals. They also suspect that reduction must take place in the coral ectoderm in order to incorporate Mn^{2+} into the aragonite lattice. Mn apparently substitutes for Ca in the aragonite lattice of *Mya arenaria* (White et al., 1977) and within the calcite lattice of *Mytilus edulis* (Blanchard and Chasteen, 1976). Boyle (1983) observed that the Mn/Ca ratios of Foraminifera tests increase significantly below the manganese redox boundary. The amount of Mn incorporated into calcite decreases with increasing precipitation rates (Lorens, 1981; Major et al., 1988; Mucci, 1988; Pingitore et al., 1988). Since brachiopod metabolism and secretion rates are slow (Rosenberg et al., 1988), this may promote the incorporation of Mn. Furthermore, the presence of minute organic-rich fluid inclusions (Bruni and Wenk, 1985; Gaffey, 1988) may have contributed to the overall chemical composition of shell calcite.

A number of previous authors have demonstrated that Mn and Fe contents in biogenic carbonates are related to facies controls and redox conditions (e.g., Veizer and Demovic, 1974; Veizer, 1977; Brand, 1987a, b; 1988; 1989; Morrison and Brand, 1988). Brand (1987) concluded that high Mn and Fe contents of Carboniferous brachiopods are a response to redox conditions and/or high detrital inputs. Moreover, the limited data of Recent brachiopods indicates that Mn and Fe chemistries are extremely variable (Mn, 5-460 ppm; Fe, 20-610 ppm) within a range of depths, salinities and temperatures (Brand, 1989a). Most Hamilton Group brachiopods have pristine microstructure and it is probable that the incorporation of these elements was controlled in part by oxygen and redox conditions within their external chemical environment.

BRACHIOPOD SHELL CALCITE CHEMISTRY

Generic Trends

Evaluation of chemically pristine brachiopod calcite from the Ludlowville and Moscow Formations suggests that there are inherent chemical differences in shell calcite compositions (Table 3.1). Significant differences are observed in the Mg, Sr and Na contents of the species *Mediospirifer audacula*, *Athyris spiriferoides* and *Mucrospirifer mucronatus* (Table 3.3; t-test, $p < 0.05$). This chemical pattern is repeated in systematic analysis of single shell beds within formations. Taxonomic differentiation and biological fractionation may be explained by each species physiological control of trace and minor element incorporation into shell calcite.

Fractionation of Mg

The three co-occurring spiriferid species of this study selectively discriminated against the incorporation of Mg into shell calcite when compared with Mg contents of inorganically precipitated calcite. Moreover, it is apparent that there are distinct taxonomic differences in the fractionation of Mg into shell calcite. The mean Mg contents of *Mediospirifer audacula* (789 ppm), *Mucrospirifer mucronatus* (1035 ppm) and *Athyris spiriferoides* (1309 ppm) are significantly different (Table 3.1, 3.3; Fig. 3.9) and this hierarchical pattern is always present within each shell bed or horizon sampled. The taxonomic control of Mg by Hamilton Group spirifers may be explained by a number of processes. Molecular and cation transport occurs across the epithelial cell membranes of modern brachiopods (Doherty, 1981) and divalent ions readily replace Ca^{2+} within Ca pumps (Rega, 1987). Substitute cations are delivered to the extracellular fluid which serves as the medium for carbonate secretion at

Table 3.3. T-test: Upper Hamilton Group unaltered brachiopods

		<i>Mucrospirifer</i>		<i>Mediospirifer</i>	
	Element	Signif.	T-stat	Signif.	T-stat
<i>Athyris</i>	Ca	$p < 0.05$	1.315	$p < 0.05$	0.246
	Mg	$p > 0.05$	4.950	$p > 0.05$	11.371
	Sr	$p > 0.05$	6.129	$p > 0.05$	2.796
	Mn	$p < 0.05$	0.070	$p > 0.05$	2.183
	Na	$p > 0.05$	6.253	$p > 0.05$	3.844
	Fe	$p > 0.05$	1.990	$p < 0.05$	0.485
	D.O.F.		(130)		(113)
<i>Mediospirifer</i>	Ca	$p < 0.05$	1.225		
	Mg	$p > 0.05$	3.984		
	Sr	$p > 0.05$	2.369		
	Mn	$p > 0.05$	2.572		
	Na	$p > 0.05$	2.182		
	Fe	$p > 0.05$	2.138		
	D.O.F.		(105)		

Table 3.4. T-test: Dimissa Bed (Wanakah Shale) unaltered brachiopods

		<i>Mucrospirifer</i>		<i>Mediospirifer</i>	
	Element	Signif.	T-stat	Signif.	T-stat
<i>Athyris</i>	Ca	$p < 0.05$	0.074	$p < 0.05$	0.482
	Mg	$p > 0.05$	3.694	$p > 0.05$	4.340
	Sr	$p > 0.05$	6.045	$p < 0.05$	0.797
	Mn	$p < 0.05$	1.057	$p < 0.05$	0.688
	Na	$p > 0.05$	3.696	$p < 0.05$	1.601
	Fe	$p > 0.05$	1.468	$p < 0.05$	1.473
	D.O.F.		(32)		(29)
<i>Mediospirifer</i>	Ca	$p < 0.05$	0.452		
	Mg	$p > 0.05$	1.771		
	Sr	$p > 0.05$	3.016		
	Mn	$p < 0.05$	0.134		
	Na	$p < 0.05$	2.045		
	Fe	$p < 0.05$	0.453		
	D.O.F.		(23)		

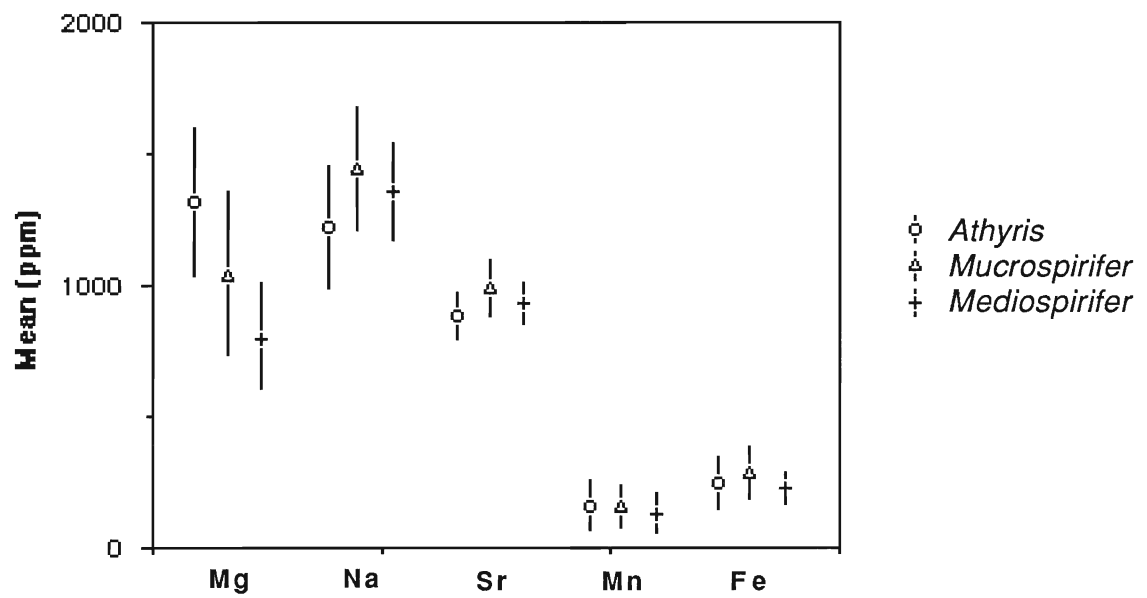


Figure 3.9. The mean and standard deviations of unaltered elemental chemistries of three Hamilton Group brachiopod genera.

nucleation sites (Fig. 3.10; Simkiss, 1976; McConnaughey, 1989b). Slightly different physiological systems may have directly controlled Mg contents in extracellular fluids which in turn may influence the amount of Mg incorporated into shell calcite. Alternately, differential brachiopod growth rates, in association with changing partition coefficients of Mg, could conceivably have controlled the resultant incorporation of Mg from extracellular fluids.

Fractionation of Sr.

Inorganic low-Mg calcite precipitated in equilibrium with ambient seawater is postulated to contain about 1000ppm of Sr (Veizer, 1983a). Hamilton Group spirifers contain Sr contents close to apparent equilibrium conditions (means 850-980ppm Sr; Table 3.1), but there are significant differences between species. *Mucrospirifer mucronatus* incorporates more Sr compared to *Athyris spiriferoides* and *Mediospirifer audacula*. Consequently, this suggests there are taxonomic differences in the physiological or secretory regimes controlling Sr composition. Sr fractionation may be influenced by relative precipitation rates since the partition coefficient (**D**) of Sr increases with precipitation rates. Furthermore, there appears to be competition between Sr²⁺ and Mn²⁺ for lattice and non-lattice sites (Mucci, 1988). The Sr and Mn contents of Hamilton Group spirifers are inversely related which suggests that there is a fractionation relationship between these elements. Similar trends were seen in the chemistries of some aragonitic molluscs (Fig. 7; p. 152; Rosenberg, 1980). This has implications for the evaluation of Mn chemistries of any ancient brachiopod shell calcite. If Mn is preferentially fractionated by the organism for the purpose of incorporation as a structural component of shell calcite, Mn concentrations may not therefore, singularly represent redox conditions of the environment, diagenetic compositions or the presence of soluble iron oxides.

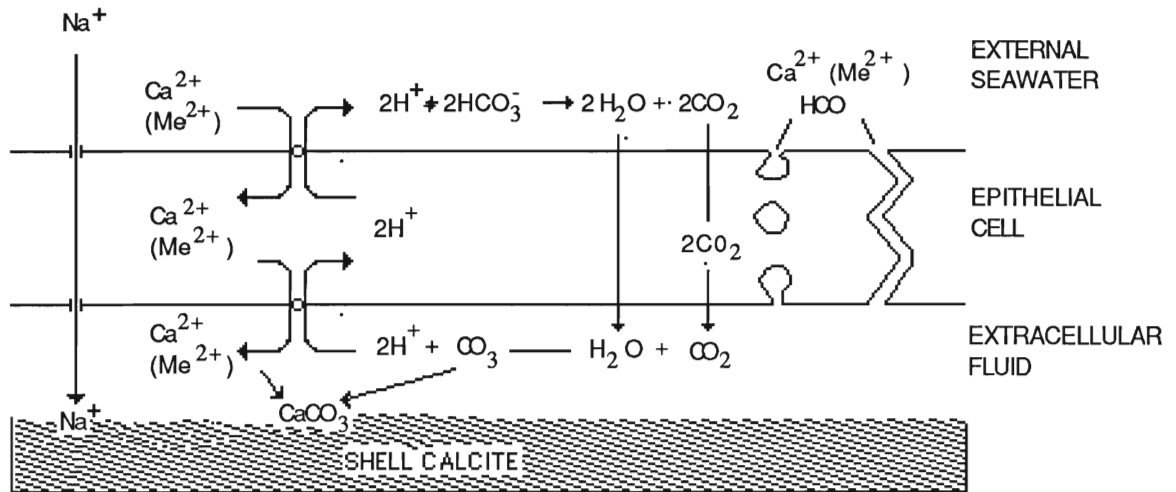


Figure 3.10. Routes of elemental transport from the external environment toward the site of carbonate secretion. The flux of Ca and minor/trace elements is controlled by a calcium pump in the epithelial membrane and the enzyme Calcium ATPase (Alberts et al., 1983; Rega, 1987). Na is osmo-regulatorily controlled by Na-K pumps, and Na incorporation into shell calcite is partly dependant on amount of crystal lattice defects present. Modified from McConnaughey (1989b).

Fractionation of Na

Sodium contents of inorganic low-Mg calcite, precipitated in equilibrium with ambient seawater, range from 100-300ppm (Milliman, 1974), whereas Na contents in modern brachiopods, range from 500 to 3600ppm (Brand, 1989a; Morrison and Brand, 1987). Mean Na contents of Hamilton Group brachiopods range from 1250ppm to 1560ppm, which is indicative of preferential incorporation of Na into brachiopod calcite. This concurs with the Brand and Veizer (1980) observation of biological Na fractionation in fossil brachiopods.

Taxonomic differences of Na content are evident in Hamilton Group brachiopods (Tables 3.1; 3.3; Fig. 3.9). Na incorporation into biogenic carbonates may be a function of either solid solution with the calcite lattice (Fritz and Katz, 1972; Land and Hopps, 1973; White, 1977); leaching from the aluminosilicate fraction; or in fluid inclusions (Al-Aasm and Veizer, 1986). Na contents in artificial calcites were smaller by factors of 20 than for biogenic calcites (White, 1978). The presence of organics may be responsible for the higher levels in biogenic carbonates (White, 1978) but Isikawa and Ishikuni (1984) report similar Na levels between synthetic and biogenic calcites. However, the amount of Na may be dependant on the number of defects in the calcite lattice (Busenberg and Plummer, 1985). The number of defects increase with precipitation rate resulting from the substitution of Ca^{2+} by other cations (Mucci, 1988). Skeletal carbonates contain minute fluid inclusions in amounts that range from a few tenths of a percent to 2-3% by weight (Gaffey, 1985). The number of fluid inclusions is higher in aragonite nacreous layers than the prismatic low-Mg calcite layers of molluscs (Towe and Thompson, 1972), and may partly explain the higher Na contents of aragonitic carbonate.

Although sodium pumps in epithelial membranes probably regulated Na contents in extracellular fluids (Fig. 3.10), taxonomic controls of Na may not

necessarily be a reflection of different extracellular fluid compositions between species. Differential growth rates, thus calcite precipitation rates, may have controlled the amounts of Na within shell calcite of Hamilton Group brachiopods. Higher growth rates may increase Na incorporation into shell calcite by increasing lattice defects.

Relationship of shell chemistry to biofacies and environmental parameters

Evaluation of pristine brachiopod calcites from the Wanakah Shale Member (Ludlowville Formation) in western Erie County (New York State) suggests that there may be a relationship between depth and the incorporation of Mg, Sr and Na into shell calcites (Fig. 3.11). The spatial distribution of Ludlowville Formation brachiopods and idealized biofacies can be related to environmental parameters such as relative depth and turbidity (Fig. 3.1; Brett and Baird, 1986). Several distinct brachiopod associations were sampled throughout the Wanakah Shale Member, representative of the various offshore (deepest) to nearshore (shallowest) biofacies. Among the horizons and shell beds sampled, brachiopods were analysed from the deepest *Ambocoelia* association (3A), the *Athyris spiriferoides* (4A) and *Mucrospirifer mucronatus*-chonetid (4B) associations and from the shallowest winnowed shell beds, containing a high diversity of brachiopods species belonging to the *Pseudoatrypa* (5A) or *Tropidoleptus carinatus* (5B) brachiopod associations.

Taxonomic differentiation of elemental fractionation is observed within single shell bed analysis of *Athyris spiriferoides*, *Mucrospirifer mucronatus* and *Mediospirifer audacula* calcites (Fig. 3.11), confirming earlier statements. Overprinting this taxonomic control is an environmental control on shell calcite composition. Chemically, *Athyris spiriferoides* calcite, from the shallow

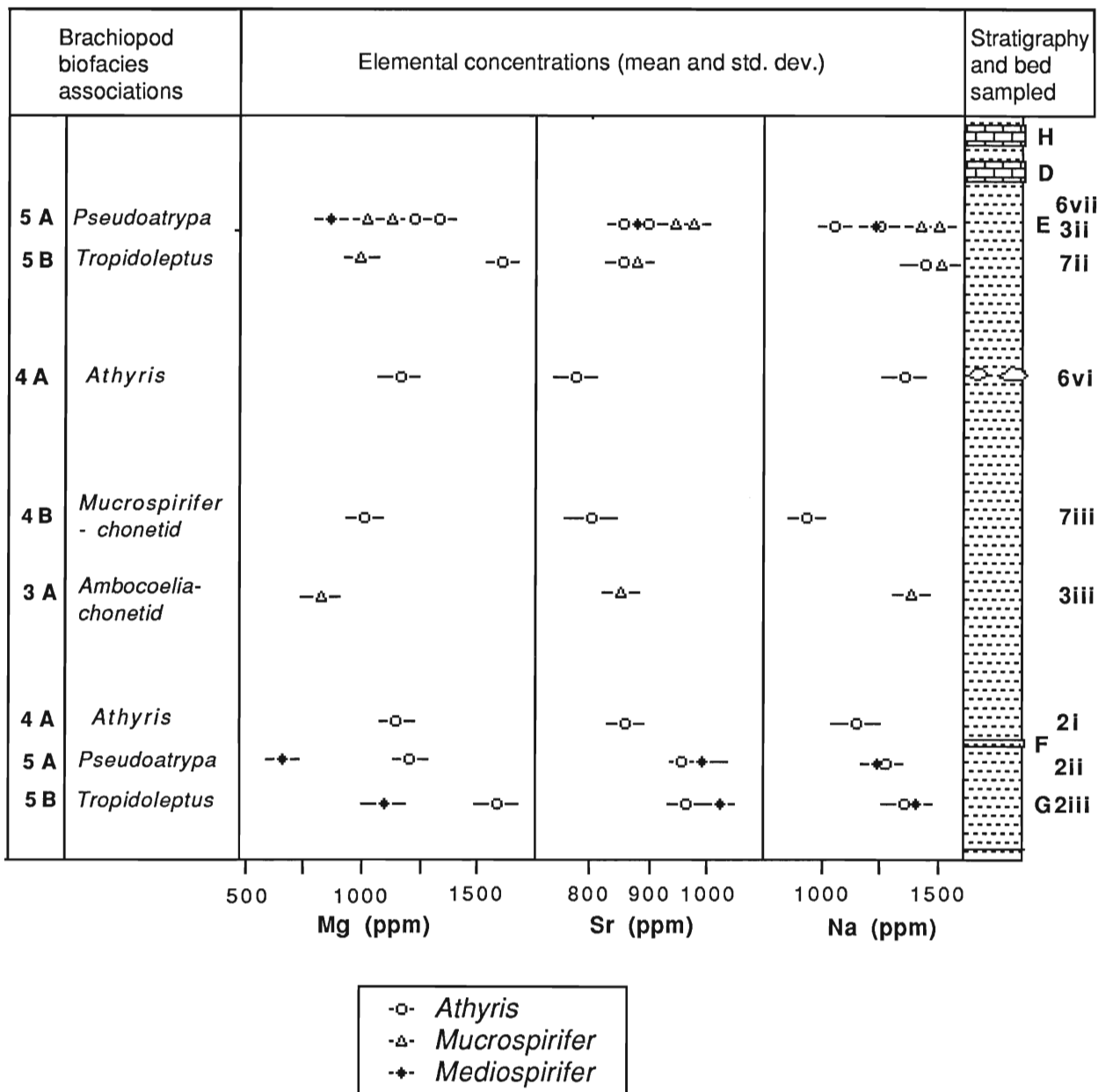


Figure 3.11. Mean and standard deviations of unaltered brachiopod elemental chemistries related to brachiopod biofacies and depth (Brett et al., 1986). Brachiopods are sampled from the Wanakah Shale (Hamilton Group) of Erie County, New York State. Specific beds are listed in Fig. 3.4 and Appendix I whereas the relationship of biofacies associations to environmental parameters are identified in Fig. 3.1.

Tropidoleptus carinatus association (5B) contains significantly higher Mg, Sr and Na contents than *Athyris spiriferoides* calcites from the deeper *Athyris spiriferoides* association (4A), which in turn are higher than those from the deepest *Ambocoelia* -chonetid association (3A). This chemical trend is repeated for *Mucrospirifer mucronatus* and *Mediospirifer audacula*. Thus, the incorporation of Mg, Sr and Na into brachiopod calcite appears to be in part dependant upon depth. The cause of this relationship is difficult to determine, since there is no empirical data on chemical variations with depth within modern brachiopod populations. It may conceivably be a function of: different secretory regimes; the relationship between functional morphology, structural requirements and mineral morphology of the shell structure within any given habitat; growth and maturation rates; and physiological needs of the organism. Slower growth rates, for example, whether caused by a combination of depth, less particulate matter, cooler temperatures or oxic conditions, could result in reduced incorporation of Sr (D_{Sr} increases with precipitation rates; Lorens, 1981; Mucci 1988). Moreover, there may have been more time for the organism to actively discriminate against Mg, either at nucleation sites or within the extracellular fluids. Furthermore, reduced precipitation rates of calcite may have decreased the percentage of lattice defects and, as a consequence, Na contents would presumably be lower. Tunnicliffe and Wilson (1988) report that populations of the modern brachiopod *Terebratulina*, in depths of over 80m and within a marginally aerobic environment, are significantly smaller than shallower populations (this presumably is the result of reduced metabolism and slower growth rates). Despite the uncertainty of its cause, this chemical relationship has implications for the use of brachiopod calcite in paleoenvironmental investigation, since it may be possible to predict relative depths from shell calcite chemistry. Further chemical and isotopic testing of

brachiopods within these beds and associations is required to confirm this scenario.

Isotopic Trends

The control of elemental contents in Hamilton Group spirifers may be related to growth rates. Similarly, growth rates may also influence the isotopic compositions of brachiopods, since "kinetic" disequilibrium is dependant on growth/calcification rates (McConnaughey, 1989a). There appears to be no significant difference between the isotopic values of pristine *Mediospirifer audacula* and *Athyris spiriferoides* shell calcites of the Hamilton Group (t-test, $p > 0.05$, $f = 22$). However, factor analysis correlates Mg, which is taxonomically controlled, with $\delta^{18}\text{O}$ and $\delta^{13}\text{C}$ (Factor 2; Table A-15), although this is not evident in the unrotated correlation matrix and may be an analytic artifact.

A potential vital effect of 4-5‰ was observed in $\delta^{13}\text{C}$ for three specimens of a modern brachiopod *Argyrotheca bermudana* from the Bermuda Platform (Wefer, 1985). The analysed brachiopods were collected from Walsingham Pond and are isotopically light (-0.41‰, $\delta^{13}\text{C}$; p. 70) compared to waters and substrate (+1.9-2.1‰, $\delta^{13}\text{C}$ and +3.6-4.4‰, $\delta^{13}\text{C}$; p. 18; Wefer, 1985). However, the water and substrate isotopic analyses come from Harrington Sound, Bermuda and these two inshore water settings are very different (for discussion of substrate, salinities, temperature see Morris et al., 1977; Barnes and Bodungen, 1978; Bodungen et al., 1982). Harrington Sound is an enclosed marine lagoon with a water residence time of about 150 days and coarse carbonate eolianite substrates. Seasonal temperature, oxygen and density stratifications occur annually (Morris et al., 1977). In contrast, Walsingham Pond, is an enclosed mangrove swamp, connected to Castle Harbour lagoon by only a small boat cut (Logan, 1975; pers. obs. 1986). The

Argyrotheca community is a relict population existing marginally within the land locked Walsingham pond. Isotopically-light organic muds derived from mangrove decomposition, may explain the light $\delta^{13}\text{C}$ values observed in shell calcite by Wefer (1985). Isotopic analysis of coeval waters, substrate and brachiopods from Walsingham Pond, needs to be done to confirm this assertion. Moreover, in small brachiopods (< 5-7mm), 70-80% of the total organic matter is located within the shell (Peck et al., 1987) and the organic matrix may have significantly contributed to isotopic analysis of the diminutive *Argyrotheca* (<2mm; Logan, 1975; Sterrer, 1986).

Modern brachiopods appear to be oxygen minimal organisms (Thayer, 1981) which metabolize very slowly (Rosenberg et al., 1988). The calcification process is essentially a "kinetic" disequilibrium process. However, slow precipitation rates reduce the isotopic displacement due to kinetic disequilibrium since isotopic exchange can quickly equilibrate internal extracellular DIC with external DIC prior to calcification (McConnaughey, 1989a; 1989b). Assuming slow metabolic and precipitation rates for ancient brachiopods, it is likely that brachiopod shell-calcite was secreted in isotopic equilibrium with ambient conditions. Therefore, if altered specimens are eliminated from the analysis, shell calcite should reflect ambient physical and chemical parameters, such as temperature, salinity and composition of oceanic isotopic reservoir. The following discussion will assume that brachiopods incorporated isotopes essentially in equilibrium with ambient conditions.

CHEMICAL TRENDS WITHIN THE "DEMISSA" BED

Shell beds are recognized in the Hamilton Group and many are persistent across western New York State for tens of kilometres (Figs. 3.2, 3.4).

Detailed taphonomic analysis of these mudstone beds suggest they are the result of storm winnowing and episodically blanketed by rapid deposition of muds (Parsons et al., 1988). The shell beds may represent accumulations of long duration (10-1000 years) and many of these beds have complex internal geometries (e.g., Smoke Creek Bed, lower Windom Shale Member; Speyer and Brett, 1985). The "*Demissa*" Bed, an upper Wanakah shell bed, is recognized across western New York, from the Lake Erie to the Genesee Valley, a distance of 120-130 km. This complex shell bed (10-15cm thick) is an amalgamation of lenticular, simple shell beds separated by thin, grey bioturbated peloidal mudstones (Brett et al., 1986).

In Erie County, the bed contains a diverse brachiopod fauna (e.g., epibenthic spirifers *Mediospirifer audacula*, *Mucrospirifer mucronatus*, *Athyris spiriferoides*; *Ambocoelia umbonata*, *Devonochonetes*, *Pseudoatrypa*; *Stropheodonta*, reclining orthids *Tropidoleptus carinatus*, *Rhipidomella vanuxemi*) which correspond to the relatively shallow *Pseudoatrypa* association (5A; Fig. 3.1) of Brett and Baird (1986). Articulation ratios are high but variable between species. Many brachiopods are closed and show few signs of abrasion or corrosion. In the Genesee Valley, the bed is less fossiliferous and is dominated by *Athyris spiriferoides* and *Mediospirifer audacula*, comprising a deeper water assemblage (*Athyris*, 4A). Articulation ratios remain high and many individuals are found in life position. This bed may represent brachiopod patch communities across the shelf, which were episodically winnowed and buried by muds. The fact that articulation ratios are high, implies that there has been little or no transport within the "*Demissa*" Bed. This bed fits the criteria for an autochthonous (in place assemblage) or parautochthonous (*sensu* Aigner 1985) winnowed coquinite (Brett et al., 1986; Parsons et al., 1988). The depositional setting of this bed deepens west to east

towards the basin depocentre, which is centred around Seneca and Cayuga Lakes. As such, it provides a time correlative model for testing elemental and isotopic trends across a deepening shelf.

Chemical trends

Pristine brachiopods of the "*Demissa*" Bed illustrate several inherent taxonomic and environmental differences. The Mg contents of shell calcite within this bed are taxonomically controlled (Table 3.4, 3.5; Fig. 3.12). Although Mg varies within this shell bed, *Athyris spiriferoides* shell calcite always contains more Mg than *Mucrospirifer mucronatus* calcite, which in turn contains more than *Mediospirifer audacula*. Similarly, *Mucrospirifer mucronatus* shell calcite always contains more Na and Sr than co-occurring *Athyris spiriferoides* calcite. The Na contents of *Mucrospirifer mucronatus* across the shelf are significantly greater than either *Athyris spiriferoides* or *Mediospirifer audacula*. It is apparent that *Mucrospirifer mucronatus* selectively incorporated Na when compared to other co-occurring species. However, it is difficult to ascertain whether this is related to either different physiological systems controlling the composition of the extracellular fluid, the mineral morphology and percentage of lattice defects or if Na is involved as structural component of shell calcite.

Previously, it was observed that the decreasing Mg, Sr and Na contents of *Athyris spiriferoides*, *Mediospirifer audacula* and *Mucrospirifer mucronatus* are related to increasing depth. The "*Demissa*" bed is essentially autochthonous and brachiopod shell calcite should reflect a significant deepening across the shelf. However, the Sr, Fe and Mn contents remain fairly constant across the shelf, while brachiopods from the deepest locality (20) are not depleted in Na or Mg. If we assume that the relationship of depth and incorporation of Mg, Sr and Na can be applied to this situation, the lack of

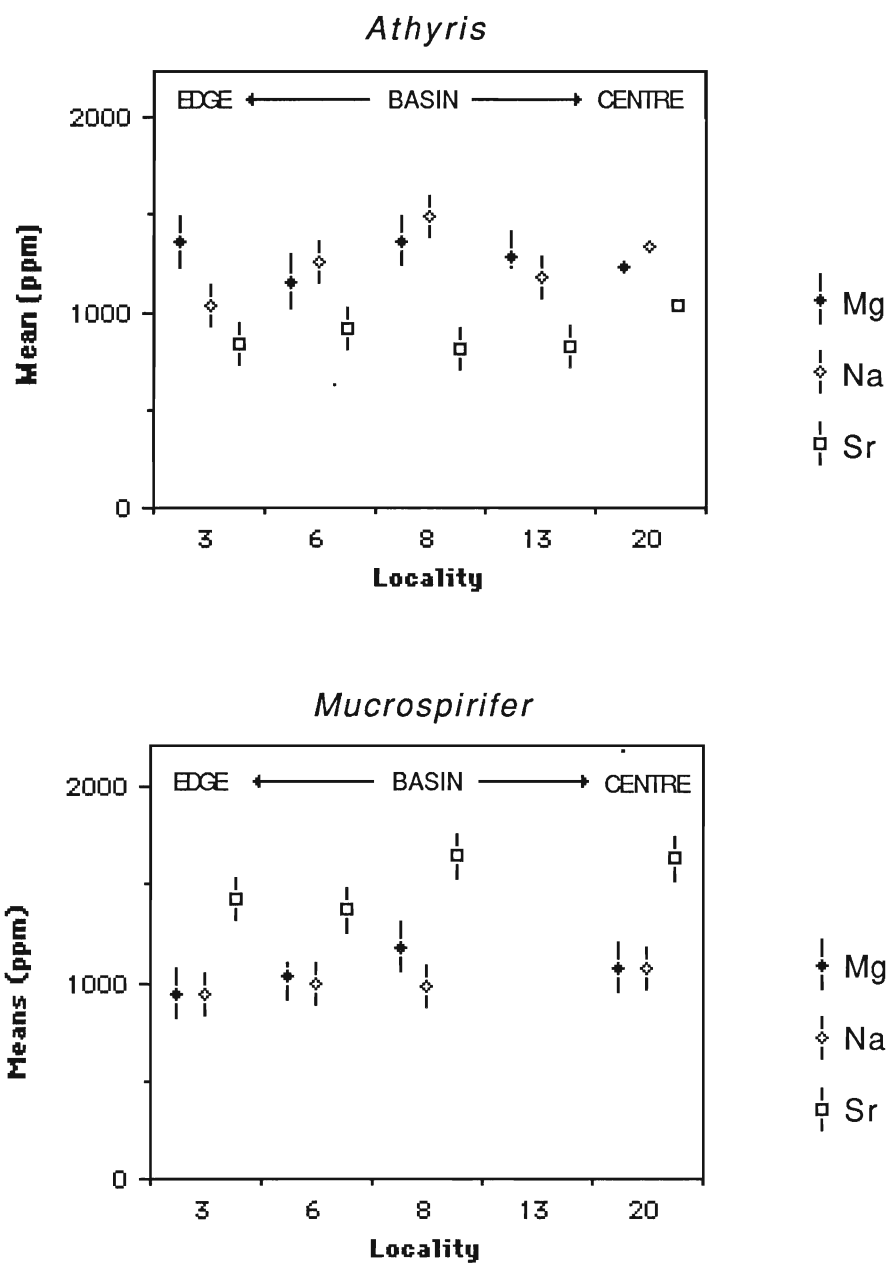


Figure 3.12. Mean and standard deviation of unaltered chemistries; *Athyris* and *Mucrospirifer* from the "Demissa" Bed across the Hamilton Group shelf. Locality data in Appendix III.

Table 3.5. Dimissa Bed (Upper Wanakah Shale) unaltered brachiopod chemical data

Brachiopod species	Stat.	Ca	Mg	Sr	Mn	Na	Fe
<i>Athyris</i> UNALTERED	Mean	370278	1321	850	171	1258	262
	Std. Dev.	41755	238	65	45	216	170
	(N=20)						
	min	246830	845	770	80	840	25
	max	437260	1820	1035	250	1600	690
<i>Mucrospirifer</i> UNALTERED	Mean	371471	1058	988	155	1560	338
	Std. Dev.	52505	136	67	35	260	110
	(N=14)						
	min	215280	805	910	100	1215	210
	max	411700	1290	1100	230	2000	525
<i>Mediospirifer</i> UNALTERED	Mean	362846	832	876	158	1377	350
	Std. Dev.	39694	213	117	56	160	140
	(N=9)						
	min	265360	650	610	50	1150	110
	max	401140	1250	1100	240	1630	555

All elemental concentrations are in ppm.

significant elemental trends suggests that either the depth changes were not great, or that there are other unrecognized contributing factors. The chemical changes recognized within the vertical Wanakah Shale sequence were related to transitions from the deeper *Mucrospirifer* association (3A) to the shallow *Tropidoleptus carinatus* association (5B). Within the "Demissa" Bed, the environmental conditions controlling the distribution of the *Pseudoatrypa* (5A) and *Athyris spiriferoides* (4A) associations may not be significantly different. The chemical variation observed in "Demissa" bed brachiopods may reflect slight changes in a number of inter-related factors such as temperature, salinity, seawater composition, growth/calcification rates and inherent chemical variability of a population.

The chemical variation observed within the shell bed may reflect a slight salinity, temperature and ambient seawater elemental compositions may be slightly different between sites. The Mg contents of Paleozoic brachiopods have been attributed to different seawater chemistries (Brower, 1978). In molluscan carbonate the incorporation of Sr and Mg is dependant on temperature (see Rosenberg, 1980), while Sr contents of shell calcite may be directly controlled by concentrations within external seawater (Rosenberg, 1980; Morrison and Brand, 1986, 1988).

Isotopic trends

An apparent deepening across the Hamilton shelf is reflected in the isotopic values (Fig. 3.13). "Demissa" bed brachiopods close to the basin depocentre (Genesee Valley) are heavy for carbon (+4.8‰, $\delta^{13}\text{C}$) and oxygen (-3.0‰, $\delta^{18}\text{O}$) compared to those in the west (Erie County; +2.4-3.0‰, $\delta^{13}\text{C}$; -3.5-4.6‰, $\delta^{18}\text{O}$). The isotopic depositional trends between depocentre and shallower reaches of the basin are repeated for Jaycox, Deep Run and

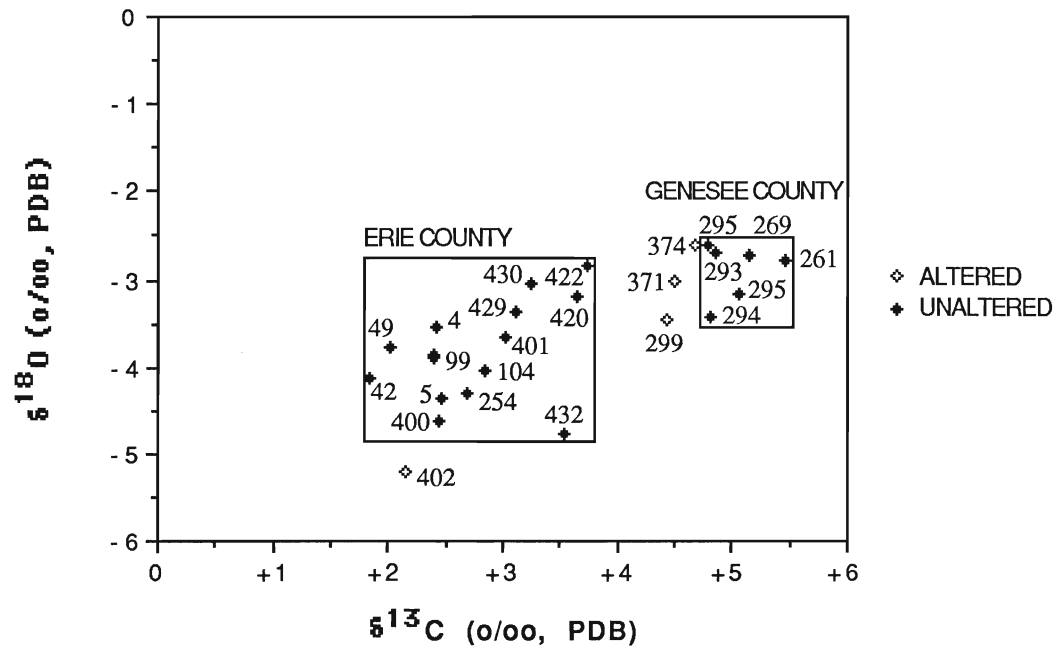


Figure 3.13. Isotopic compositions of *Athyris* and *Mediospirifer* brachiopods from the Hamilton Group. Sample numbers are listed in Appendix III.

Kashong brachiopods (Fig. 3.13) and during deposition of these units the basin depocentre was located in the Genesee Valley region. If we assume there were no salinity changes across the shelf, this isotopic trend may indicate that the bottom waters were cooler and depleted in organic matter toward the basin centre (Genesee Valley) during the deposition of the shell bed. The "*Demissa*" bed bottom waters to the west were apparently warmer and contained more light carbon. Alternately, this isotopic trend may be related to other environmental conditions such as density, oxygen or temperature stratification of the basin waters. Transition of facies from grey to black shales toward the basin axis suggests that this semi-restricted basin may have been subject to temperature, salinity and oxygen stratification. There is evidently a large variation in isotopic values within the same bed (about 1.5-2.5‰, $\delta^{13}\text{C}$; and 0.5-1.5‰, $\delta^{18}\text{O}$). This has significant implications for interpretations of secular changes in Paleozoic oxygen and carbon reservoirs since many trends are based on smaller isotopic shifts (e.g., Adlis et al., 1988). If isotopic analyses are not constrained by sedimentological and paleoecological parameters, secular trends may only represent onshore-offshore isotopic trends. Isotopic variability throughout geologic time, must therefore, be evaluated with extreme care.

PALEOENVIRONMENTAL ANALYSIS OF THE LOWER WINDOM SHALE

Windom Shale brachiopods were sampled from the lowest two metres at Eighteen Mile Creek and Penn Dixie Quarry (localities 3, 6). At Eighteen Mile Creek, a thin sequence of dark-grey, *Ambocoelia*. dominated shales overlie the calcarenite Tichenor Member. Associated with these pavements are small, juvenile, closed and articulated *Mucrospirifer mucronatus* and *Athyris*

spiriferoides . Overlying these beds are the bioturbated coral-rich Bay View Bed mudstones. Suprajacent shale beds correspond to a general deepening transition from the shallow coral-rich Bay View Bed, to calcareous shales of a complex shell bed (Smoke Creek Bed) to deeper dark-grey ambocoeliid-chonetid dominated shales of the Middle Windom Member (Speyer and Brett, 1985). Laterally this sequence is restricted between Lake Erie and Cazenovia Creek, whereas the Smoke Creek Bed outcrops across western New York as far as Fall Brook Falls, Geneseo (Locality 19).

Chemical trends

Three separate fields of chemically pristine brachiopods, corresponding to different horizons, can be observed (Fig. 3.14) and may reflect potentially oxygen depleted, reducing conditions. Brachiopods from the ambocoeliid dominated, dark shale plot with significantly higher Fe and Mn contents than those from the Bay View and Smoke Creek Beds (Fig. 3.14). These ambocoeliid pavements are interpreted by Brett and co-workers to belong to a deeper and potentially more dysaerobic brachiopod biofacies (*Ambocoelia-chonetid*; 3A; Fig. 3.1; Brett et al., 1986; Miller, 1986; Grasso, 1986). The bioturbated Bay View Bed with a diverse association of brachiopods and corals represents a much shallower biofacies association (Fig. 3.1; *Pseudoatrypa* : 5A). The majority of *Mediospirifer audacula* and *Pseudoatrypa* are disarticulated, whereas *Rhipidomella vanuxemi* are commonly articulated. The Smoke Creek bed is a complex shell bed that may represent a rapid depositional event (Speyer and Brett, 1985; Parsons et al., 1988) and analysed brachiopods from subunit C are predominantly articulated and non-splayed. Chemically, the brachiopods reflect the apparent shallowing facies transition from lowest Windom dark ambocoeliid shales into the Bay View Bed. Although these

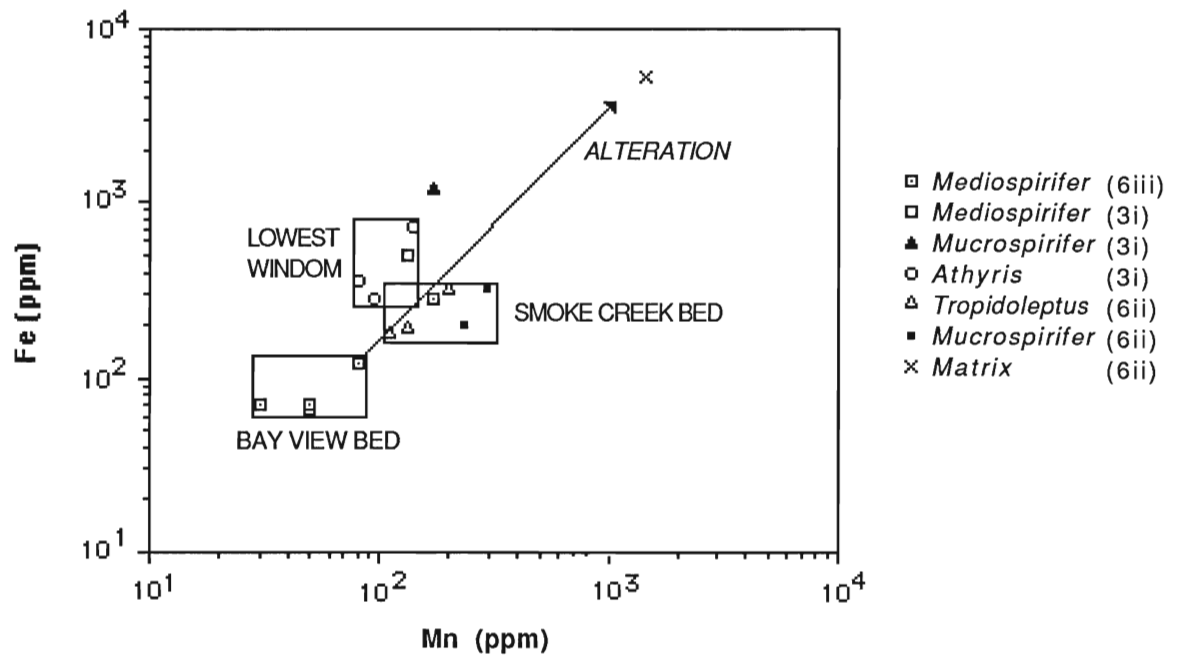


Figure 3.14. Scatter plot of Fe vs Mn for Lower Windom brachiopods from western New York State.

brachiopod biofacies are generalized and transitional (Brett et al., 1986), the Mn and Fe chemical data supports the paleoecological inferences, particularly of brachiopod associations in potentially more oxygen depleted environments.

Isotope trends of the Lower Windom Shale

Brachiopods from the Bay View Bed are isotopically enriched in ^{13}C (+3.70‰ $\delta^{13}\text{C}$) relative to those from the ambocoeliid pavements which are isotopically lighter (+1.93‰ $\delta^{13}\text{C}$). Strict interpretation of biofacies would suggest that the ambocoeliid dominated beds were probably deeper, cooler, and within bottom waters tending to dysaerobia. However, isotopic analysis suggests the opposite. Lighter carbon values in the ambocoeliid bed indicate that these beds were more organically rich, and organic content usually declines with depth (Fürsich and Hurst, 1980). Oxygen isotopic data is more negative in the ambocoeliid beds ($\delta^{18}\text{O}$; -3.97‰) than the Bay View Bed ($\delta^{18}\text{O}$; -3.01‰) and paleotemperature analysis suggests that the Bay View Bed waters (25-30°C) were much cooler than the ambocoeliid layer waters (30-35°C) and thus potentially deeper. This contradicts the physical parameters inferred from biofacies associations. Conceivably, the ambocoeliid brachiopod community at this site, may represent a shallower, warmer water association. However, the presence of oxygen depleted bottom waters may have allowed only the colonization of slight dysaerobia-tolerant brachiopods such as *Ambocoelia*, and limited growth of small spiriferids. Subsequently, cooler and less organic rich, but more aerobic bottom waters, may have promoted the colonization of a diverse faunal association found in Bay View Bed. The dysaerobic *Leiorhynchus* brachiopod communities recognized in the Middle Devonian sediments of New York State (Kammer et al., 1986; Thompson and Newton, 1986), may not be depth dependant *sensu strictu*, but anoxia bottom

water dependant. More study is required into the isotopic composition of brachiopods and the redox, depth relationships of ambient seawater.

PALEOENVIRONMENTAL ANALYSIS OF THE KASHONG SHALE

Two stratigraphic horizons within the Kashong Shale (Moscow Formation) were sampled to investigate possible chemical difference between them. Sparsely fossiliferous dark-grey fissile shales and thin wackestones of the Lower Kashong Shale are exposed at Eleven Mile Creek (Fig. 3.2; locality 13A) and are dominated by *Mediospirifer audacula* brachiopods in association with *Athyris spiriferoides*, *Ambocoelia* and *Strophomena* (4A biofacies; Fig. 3.1). Closed, unabraded brachiopods and articulated crinoid stems and trilobites (e.g., *Phacops rana*) attest to the quiet water habitat, minimal disturbance and autochthoneity of this fauna. Upper Kashong Shales outcrop at Retsof (Brett and Cottrell, 1982; locality 18) and consist of light grey shales with diverse crinoid, trilobite and brachiopod faunas dominated by *Tropidoleptus carinatus*. Articulation ratios are low and many valves show evidence of abrasion which suggests that they may have been transported. This brachiopod assemblage corresponds to a shallow water *Tropidoleptus carinatus* biofacies (5B; Fig. 3.1).

Elemental contents of biogenic calcites from the Kashong Shale are variable reflecting a range of chemically unaltered to altered specimens. Metastable high-Mg calcite crinoids are extensively altered and chemically similar to matrix compositions (Fig. 3.15). The open meshwork structure, typical to crinoids (Bathurst, 1975; Brand and Morrison, 1987b; Brand 1987), may have promoted fluid controlled reactions and extensive dissolution-reprecipitation events. The chemistry of altered brachiopods is variable and may be related to lithological availability of Fe and Mn in diagenetic waters, redox conditions of the diagenetic fluids and the pore geometry of the host lithology and shell.

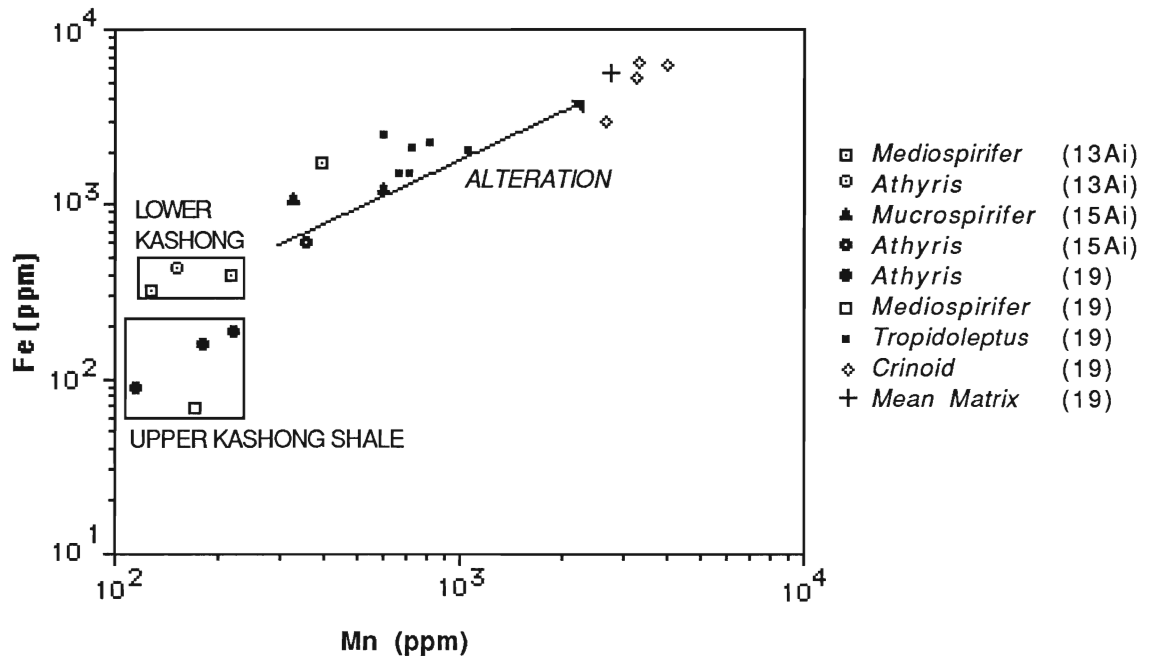


Figure 3.15. Scatter diagram of Fe vs Mn contents of upper and lower Kashong Shale Member brachiopods (upper Hamilton Group). Each field represents pristine brachiopod compositions

Punctae within the shell calcite of *Tropidoleptus carinatus* probably facilitated pore filling and chemical alteration.

Despite the similarity of Na and Mg chemistries within pristine brachiopod calcites, there are significant differences in Fe and Mn contents (Fig. 3.15). An apparent relationship is recognized between the depth controlled biofacies associations and concentrations of Fe and Mn. Enriched Mn and Fe contents of the Lower Kashong brachiopod calcite can be explained if there was increased availability of Fe and Mn for incorporation into shell calcite. These elements are redox controlled and potentially oxygen depleted bottom waters may have partially controlled shell calcite compositions. The semi-restricted Appalachian Basin was centred around the Genesee Valley area during deposition of the Kashong Shale. Marginally placed brachiopod communities, close to the oxycline-pycnocline, may have been periodically exposed to oxygen depleted waters. In contrast, the Fe and Mn contents of brachiopod shell calcites from the shallow, turbulent *Tropidoleptus carinatus* association (Upper Kashong) appear to reflect fully aerobic conditions.

HUNGRY HOLLOW, WIDDER AND ARKONA FORMATIONS

Mucrospirifer mucronatus were collected from the Hungry Hollow section at Arkona, southern Ontario (locality 1) and show clear alteration trends towards the chemistries of matrix and cement samples (Fig. 3.16). Samples within the general field represent Fe and Mn compositions of unaltered brachiopods. This data encompasses brachiopods collected from dark grey shales of the Arkona, Hungry Hollow and Widder Formation (Appendix I). Chemical evaluation of the unaltered field suggests that redox conditions may have controlled Fe and Mn distribution in *Mucrospirifer mucronatus*. Specimens from the light grey calcareous shales of the Widder Formation plot with the lowest Fe and Mn

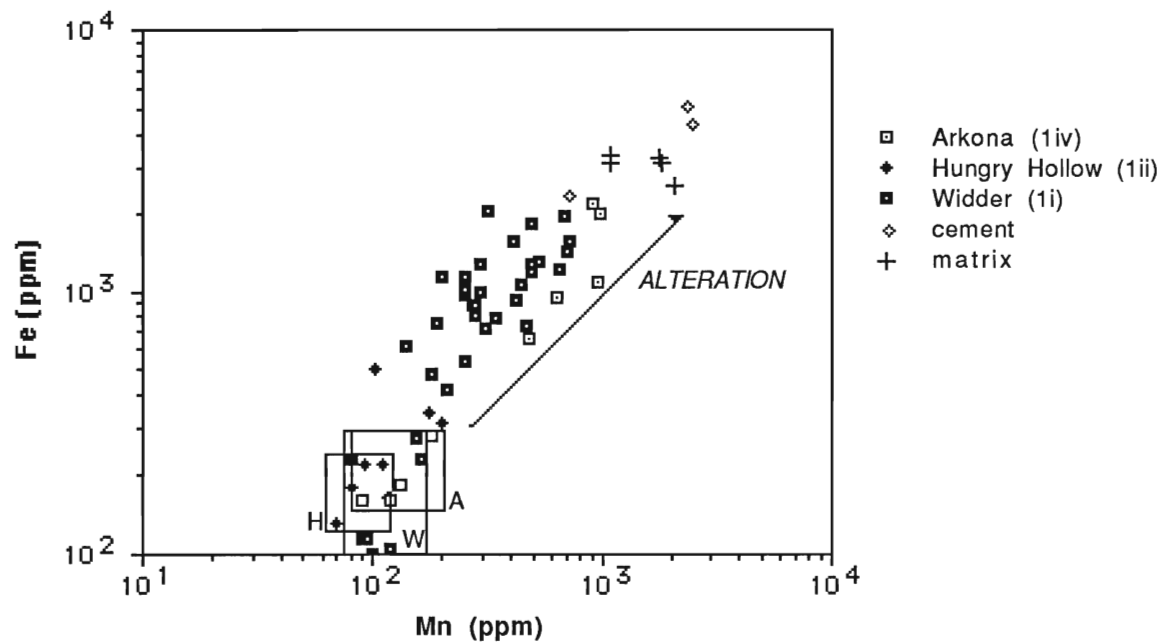


Figure 3.16. Scatter plot of Fe vs Mn for *Mucrospirifer* brachiopods from the Arkona, Hungry Hollow and Widder Formations (Middle Devonian). Unaltered *Mucrospirifer* fields are denoted by A (Arkona Fm.); H (Hungry Hollow Fm.); and W (Widder Fm.). *Mucrospirifer* plotting outside these fields, show evidence of minor dissolution and reprecipitation of cements. Alteration of brachiopods becomes progressively more fluid-controlled toward matrix and cement chemistries. Additional data from Popp et al., (1986b) and L. Wassenaar (1986; unpublished data)

contents, whereas brachiopods from the grey shales of the Hungry Hollow and Arkona Formations have higher Fe contents. The upper Arkona Formation is interpreted as a marginally aerobic to dysaerobic setting (Landing and Brett, 1987) because of the presence of syngenetic pyrite and the lateral transition of the Arkona grey claystones into the dark grey/black shales of the Appalachian Basin. At Hungry Hollow, *Mucrospirifer mucronatus* are predominantly articulated perhaps indicative of quiet, deeper soft substrates of the Upper Arkona. The divergence of Fe and Mn chemistry in *Mucrospirifer mucronatus* may reflect the Eh of the depositional waters.

Individual specimens of *Mucrospirifer mucronatus* falling just outside this unaltered field have slightly elevated Mn and Fe contents although their Sr, Mg and Na chemistries are not concurrently depleted (Figure 3.16, 3.17). Shell calcites may have either undergone slight alteration, contain soluble iron oxide coatings or the Fe/Mn compositions reflect depositional conditions. *Mucrospirifer mucronatus* sampled from a thin skeletal-packstone limestone bed, of the lower Arkona Formation, have significantly different chemistries compared with *Mucrospirifer mucronatus* sampled from shales. Brachiopods in these thin, episodic tempestites (Landing and Brett, 1987) are monotypically *Mucrospirifer mucronatus*, disarticulate and abraded. The magnitude of re-equilibration and reaction toward cement and matrix chemistry indicates a fluid-controlled diagenetic regime. Therefore, grain size and pore geometry (see discussion Pingitore, 1976, 1982) has significantly influenced the potential of brachiopod LMC to resist alteration.

Brachiopods and lower oxygen conditions

Recent studies of modern brachiopod metabolism, secretory mechanisms and environmental tolerances (Doherty, 1981; Curry, 1982;

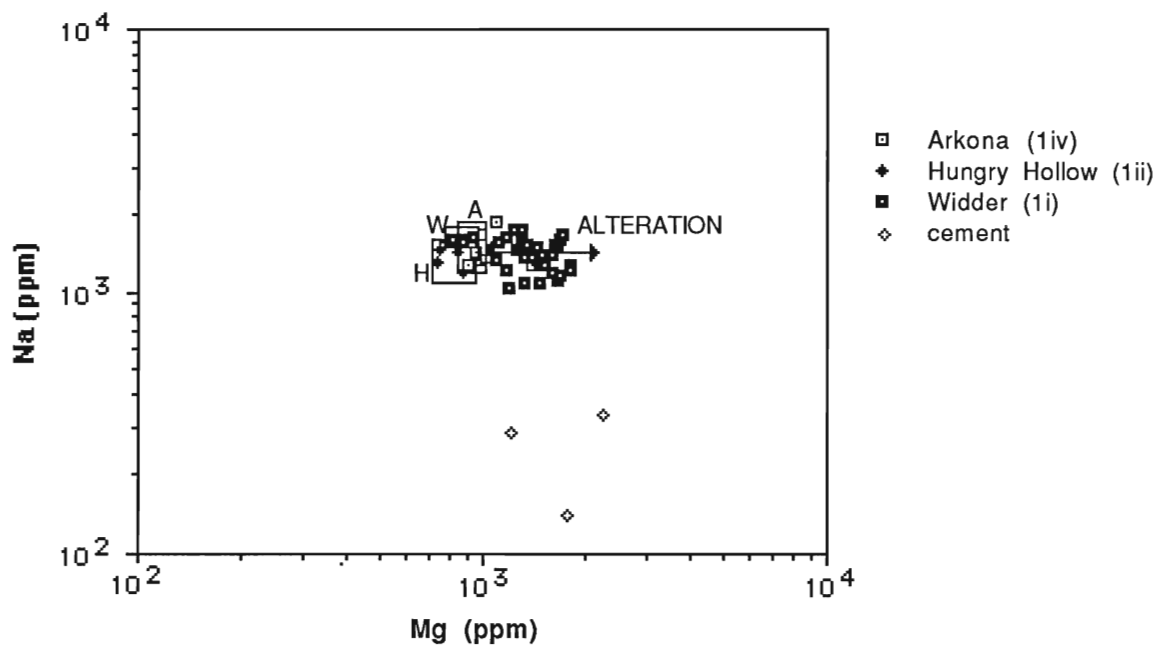


Figure 3.17. Scatter plot of Na vs Mg for *Mucrospirifer* brachiopods from the Arkona, Hungry Hollow and Widder Formations (Middle Devonian). Unaltered *Mucrospirifer* fields are denoted by A (Arkona Fm.); H (Hungry Hollow Fm.); and W (Widder Fm.). *Mucrospirifer* plotting outside these fields, show evidence of minor dissolution and reprecipitation of cements. Additional data from L. Wassenaar (1986; unpublished data)

Shumway, 1982; Thayer, 1986a, b; Peck et al., 1987; Rosenberg et al., 1988; Hiller, 1988) augment our understanding of chemical and isotopic trends observed in ancient brachiopod shell calcite. The increased Mn and Fe contents of Hamilton Group shell calcites from the deeper parts of the basin may reflect periodic oxygen-deficient conditions in the Appalachian Basin.

Brachiopods have very low rates of oxygen extraction ($0.76\text{mL}\cdot\text{h}^{-1}$) when compared to bivalves (Doherty, 1981). They have a low pumping ability but are either oriented toward or can actively orient themselves toward currents (LeBarbera, 1977; 1978; 1981b; Richardson, 1981c). Furthermore, some modern species are capable of anaerobic metabolism (Hammen, 1977; Peck et al., 1989) and can function with depressed metabolic rates for considerable lengths of time (Shumway, 1982). Moreover, several modern brachiopod species thrive in areas where dissolved oxygen levels are periodically below $0.1\text{ mL}\cdot\text{L}^{-1}$ (Saanich Inlet; Tunnicliffe and Wilson, 1988) and under potentially reduced water conditions (Nissenbaum et al., 1972; Presley et al., 1972). Thus these species are able to survive within dysaerobic environments as defined by Rhoads and Morse (1971) and modified by Thompson et al. (1985). In the Appalachian Basin, during deposition of the Hamilton Group, a number of species (e.g. *Leoirhynchus* and *Ambocoelia*) inhabited relatively shallow (50-100m depth; Brett and Baird, 1986a) dysaerobic black shale environments (Thompson and Newton, 1986; Kammer et al., 1986; Miller, 1986). Many of the deeper brachiopod biofacies are transitional with these permanent dysaerobic communities. The presence of black shales and semi-restricted circulation suggests that the basin waters were probably stratified (Kammer et al., 1986; Witzke, 1987). The development of a relatively shallow oxycline/pycnocline, as the result of organic decay (anoxia can develop within depths of only 10-15 metres; Devils Hole; Morris et al., 1977) and/or surface biological productivity

(Demaison and Moore, 1980) is indicated. Many of the brachiopod communities were marginally placed to these oxygen-depleted waters and it is conceivable that fluctuation of the oxycline may have periodically pushed low-oxygen waters into shallower habitats. As with modern brachiopod populations (Tunncliffe and Wilson, 1988), the community structure and depth patterns of Hamilton Group brachiopods (evidenced by the vertical and lateral faunal successions of *Leiorhynchus* to *Ambocoelia* to *Mucrospirifer mucronatus* dominated associations etc.) may have changed in response to longer-term shifts in oxic conditions.

The chemical composition of shell calcite is 'time-averaged' and as such encompasses potentially variable external conditions within a lifespan of 5-10 years (Paine, 1969). If we assume that Mn and Fe contents in shell calcites reflect "time-averaged" redox conditions, brachiopod calcite will reflect episodes of oxygen-deficiency, despite the lack of permanent anoxic conditions. Brachiopods would have continued to metabolize during low oxygen conditions and transport divalent ions (e.g. reduced Mn and Fe) across epithelial membranes to nucleation sites of shell calcite. Further study of modern brachiopods within marginally dysaerobic environments (e.g., *Terebratulina*, Saanich Inlet) and of ancient faunal successions in black shales (e.g., *Leiorhynchus* in Genesee Shale, central New York State) is required to confirm a redox and low oxygen control of Mn and Fe contents in shell calcite.

CONCLUSIONS

The majority of brachiopod shell calcites of the Hamilton Group are microstructurally and chemically well preserved. A few altered specimens re-equilibrated in the presence of meteoric-mixed waters. Analysis of pristine calcites from three co-occurring spiriferid species suggests that Mg, Na, Sr

contents were fractionated into shell calcite. Moreover, an inherent taxonomic difference in Mg contents is observed between *Athyris spiriferoides*, *Mucrospirifer mucronatus* and *Mediospirifer audacula*. This hierarchical differentiation of elemental contents into shell calcite is repeated in each shell bed or mudstone horizon studied. Similarly, a taxonomic control of Sr and Na is observed and may reflect complexities of slightly different physiological systems, secretory mechanisms and mineral morphologies. Furthermore, analysis of these brachiopods from different biofacies associations in the Wanakah Shale indicates that there is an inverse relationship of Mg, Sr and Na incorporation into shell calcite with relative depth of the brachiopod habitat. This chemical relationship is potentially related to slower calcification rates in deeper waters promoting the active discrimination against Mg and Sr and reducing Na incorporation into lattice defects.

Analysis of *Athyris spiriferoides* and *Mediospirifer audacula* from a persistent Wanakah Shale shell bed indicates that there is large variation in isotopic values within a single bed. Isotopic values from deeper basinal brachiopod calcites are more positive by 1.5-2.5‰ $d^{18}O$ and 0.5-1.5‰ $d^{13}C$ than calcites of shallower brachiopods. Similarly, shifts in isotopic values of brachiopods from the Lower Windom Shale also reflects changes in environmental conditions between suprajacent depth controlled brachiopod associations. A significant proportion of secular variation of ^{18}O and ^{13}C isotopes through time may reflect unrecognized depth-controlled onshore-offshore trends.

Analysis of pristine brachiopods from the Windom, Kashong, Widder, Arkona and Hungry Hollow Formations indicates that Mn and Fe contents are not a result of diagenetic alteration but a reflection of possible fractionation and complex chemical environments. Brachiopod calcites analysed from deeper

and apparently dysaerobia-tolerant communities contain elevated Mn and Fe contents compared to brachiopods in shallower habitats. Fluctuation of the oxycline and incursions of low oxygen waters in the semi-restricted stratified basin may have influenced marginally positioned communities, controlling faunal succession and the incorporation of redox controlled elements.

CHAPTER 4

Diagenetic and paleoenvironmental study of brachiopod calcite
from the Clinton Group (Middle Silurian);
western New York State and southern Ontario.

INTRODUCTION

Ancient brachiopods are assumed to have incorporated oxygen and carbon isotopes into shell calcite in equilibrium with ambient external conditions (Lowenstam, 1963; Veizer et al., 1986; Popp et al., 1986a; Brand, 1989a). Moreover, since the fractionation of oxygen isotopes into biogenic carbonates is reported to be temperature and salinity dependant (Epstein et al., 1953; Faure, 1983), chemically pristine shell calcite can potentially be used to retrieve information about salinity, temperature and depth changes within specific environments. Recently, brachiopod calcite of *Crurithyris* was analysed from two Pennsylvanian cyclothems in the Midland Basin, Texas, and isotopic shifts were suggested by Adlis et al. (1988) to be the result of relative depth changes of approximately 70m. Similar changes within recognized transgressive-regressive cycles should be recorded in other brachiopod shell calcite.

In Middle Silurian strata of western New York State and Ontario, a transgressive-regressive cycle is sedimentologically and paleoecologically reported in the Lewiston Member of the Rochester Shale Formation (Brett, 1983a). The Rochester Shale contains some of the best taphonomically preserved fossils in North America (Brett, 1983) and the abundance of brachiopods (notably *Eospirifer radiatus*) throughout the section allows the study of elemental and isotopic changes within this vertical sequence. Furthermore, previous studies have indicated that the Silurian oceans were depleted in ^{18}O by about 5.5‰ (Brand and Veizer, 1981; Veizer et al., 1986; O'Shea et al., 1988). Therefore isotopic analysis of *Eospirifer radiatus* and other brachiopods will verify possible secular variation of oceanic ^{18}O during the Middle Silurian.

The purpose of this chapter is to investigate: i) the diagenetic and depositional chemistries of brachiopod shell calcite from Clinton Group (Middle Silurian) sediments in western New York State and southern Ontario; ii) the isotopic and elemental trends within brachiopod calcites collected from a transgressive-regressive cycle.

GENERAL GEOLOGY

During the Wenlockian, Clinton Group strata accumulated within the shallow northern Appalachian Basin and intervening arch/platform areas (Brett, 1983a; Droste and Shaver, 1987). Paleogeographic reconstructions of the Middle Silurian in North America suggest that the basin, extending across Ontario, New York State and Pennsylvania, was close to the equator (Zeigler et al., 1977). Clinton Group siliciclastic and carbonate deposition was probably controlled by movements of the Algonquin Arch to the northwest (Sanford et al., 1985; Johnson, 1987) and uplift of a Taconic landmass to the southeast (Brett, 1983a). In southern Ontario and western New York State, a sequence of shallow marine limestones and shales of the Merritton, Neagha and Reynales Formations (Fig. 4.1; Grasso, 1983; Liebe and Grasso, 1986) accumulated on a Upper Ordovician to early Middle Silurian clastic wedge (Queenston, Grimsby and Thorold Formations; Grasso, 1983; Fail, 1985). Between the Reynales and Irondequoit Formations, a non-depositional erosional surface of several million years is present in Ontario (Brett, pers. comm. 1988), whereas in western New York State, these units are separated by the Sodus Shale and Williamson Shale Formations (Liebe and Grasso, 1986). Crinoidal biosparites and biomicrites of the Irondequoit Formation were deposited within crinoidal shoal banks on the platform areas overlying the Algonquin-Findlay Arch. Presumed

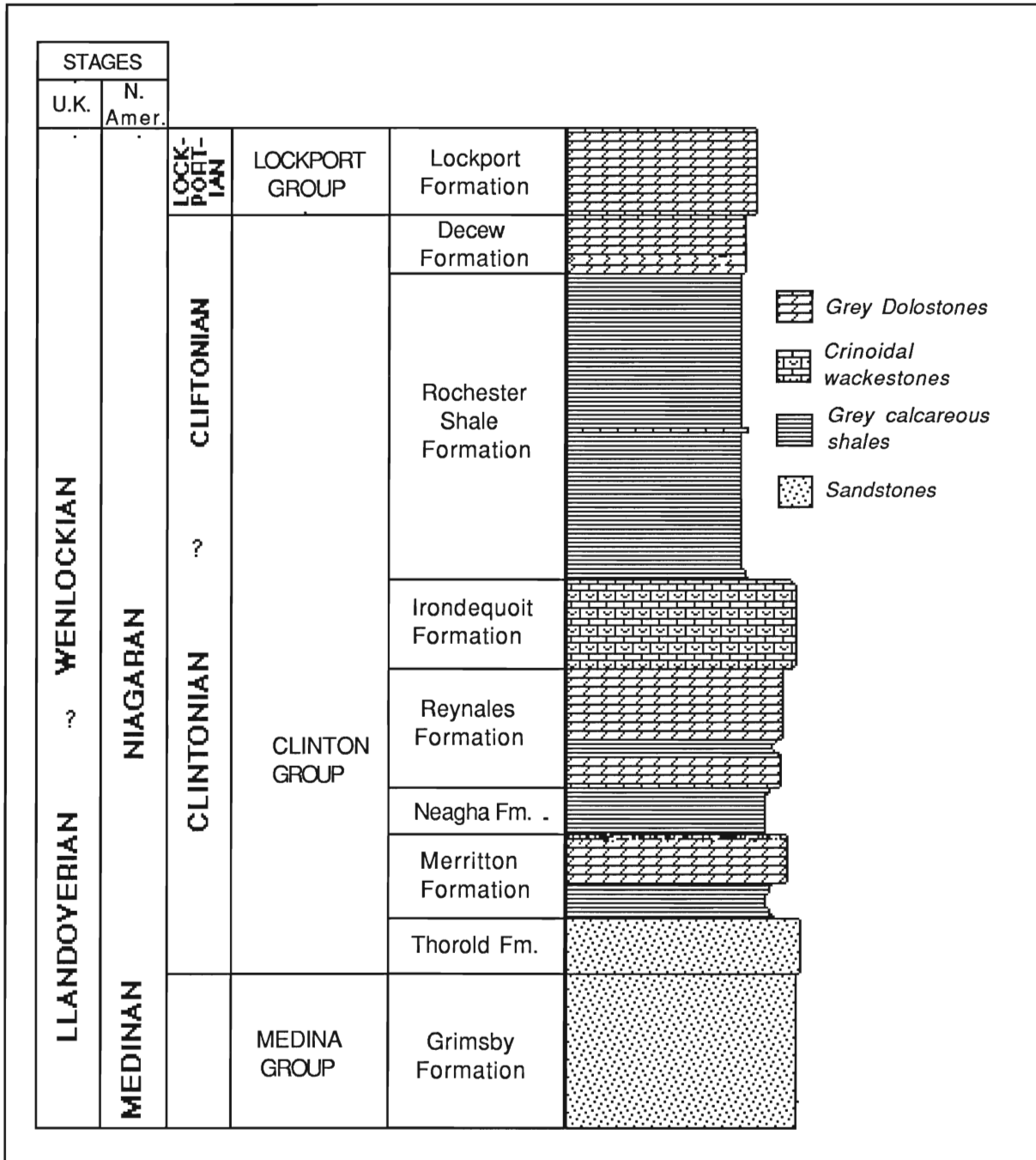


Figure 4.1. Middle Silurian stratigraphy of southern Ontario and New York State. The Williamson and Sodus Shales are present between the Reynales and Irondequoit Formation in western New York State. Sources and ages from Telford, 1978; Grasso, 1983; Brett, 1983a, b; Liebe and Grasso, 1986.

deepening of the basin and arch, resulted in accumulation of grey calcareous mudstones of the Rochester Shale Formation, where complex lithofacies and faunal distributions have been attributed to the north-south migration of facies belts (Brett, 1983a). Toward the northwest, the Rochester Shale thins and merges with the platform carbonate sediments of the Warton-Amabel Group and to the south, thickens towards the Appalachian Trough in central New York State and Pennsylvania (Brett, 1983a). Brachiopods were collected from these Middle Silurian formations (localities listed in Appendix I and Fig. 1.2). Recent research on the stratigraphical, sedimentological and paleoecological aspects of the Clinton Group (Thusu, 1972; Brett, 1983a, 1983b, 1989; Grasso, 1983; Liebe and Grasso, 1986) provides a framework for evaluating the diagenetic and depositional chemical trends within these units.

RESULTS AND DISCUSSIONS

Chemical trends

The trace and minor element data of Clinton Group brachiopods (Table 4.1) are comparable to the chemical ranges of other Paleozoic brachiopods (Brand and Veizer, 1980; Al-Aasm and Veizer, 1982; Veizer et al., 1986; Brand and Morrison, 1987). Chemical and microstructural evaluation of shell calcite indicates that the majority of specimens are pristine (e.g. Figs. 2.9, 2.13), although post-depositional alteration of some brachiopod calcite has occurred (e.g. Fig. 2.20). The valves of *Eospirifer radiatus*, *Atrypa reticularis* and *Whitfieldella* which show signs of dissolution and calcite layer fusion, are also significantly enriched in Mn, Fe and Mg (Fig. 4.2; Table 4.2); indicating that a significant degree of diagenetic alteration has taken place. Further confirmation of this diagenetic trend is provided by factor analysis of the data (Tables A-7 to

Table 4.1. Summary of chemical data for all Clinton Group brachiopods and for pristine specimens.

Brachiopod species	Stat.	Ca	Mg	Sr	Mn	Na	Fe	Al	I.R.
<i>Eospirifer</i> (ALL; N=31)	Mean	380759	3146	1322	130	1202	272	65	6.6
	Std. Dev.	27420	270	88	223	212	376	70	
	min	246830	820	560	10	680	25	0	
	max	437260	2175	1180	1645	1760	2480	270	
<i>Whitfieldella</i> (ALL; N=48)	Mean	378698	3573	1189	153	1017	288	87	6.0
	Std. Dev.	32040	2770	139	187	220	282	54	
	min.	283730	1160	830	1	740	50	0	
	max	441070	15520	1625	930	1500	1280	260	
<i>Atrypa</i> (ALL; N=59)	Mean	386529	4038	1206	237	1439	363	96	7.3
	Std. Dev.	34412	2762	133	211	187	293	50	
	min	282990	1150	855	35	905	70	0	
	max	446840	22020	1560	1390	1830	2230	190	

All elemental concentrations are in ppm.

Table 4.2. Comparison of microstructural preservation and chemistry for selected brachiopods, representing different species, and lithologies. Lithology symbols denote (S= dark grey shale; CM= calcareous mudstones; ML= micritic limestones; W= wackestones; P= packstones; CG= crinoidal grainstones)

Sample Number specimens	Species	Age ology	Lith-State	Preservation features	Diagenetic	Mg (ppm)	Mn (ppm)	Fe (ppm)	Figured
2602	Pentameroides	Rey.	CG	Poor	Recrystallized	3900	370	1235	2.20
2007	Pentameroides	Mer.	ML	Poor	Recrystallized	12330	300	870	
2193	<i>A. reticularis</i>	Lew.	CM	Good	None	2970	115	225	2.13
2308	<i>A. reticularis</i>	Lew.	CM	Poor	Dissolution	3975	220	320	
2306	<i>A. reticularis</i>	Lew.	CM	Fair	Slight diss.	5160	215	375	
2108	<i>W. nitida</i>	Lew.	CG	Good	None	2120	75	230	2.17
2190	<i>W. nitida</i>	Lew.	CM	Good	None	1320	80	90	
2132	<i>W. nitida</i>	Iro.	CG	Good	None	4050	220	385	
2182	<i>W. nitida</i>	Lew.	CM	Poor	Recrystallized	15520	930	1280	
2100	<i>E. radiatus</i>	Lew.	CG	Good	None	1090	20	130	2.9
2301	<i>E. radiatus</i>	Lew.	CM	Good	None	3240	90	150	
2195	<i>E. radiatus</i>	Lew.	CM	Good	None	2860	120	210	2.17
2193	<i>E. radiatus</i>	Lew.	CM	Good	None	2970	115	225	
2104	<i>E. radiatus</i>	Lew.	CG	Good	None	3060	165	295	
3018	<i>Dalejina</i>	BH.	CM	Good	None	3390	120	660	2.17
3011	<i>Dalejina</i>	BH.	CM	Good	None	3610	180	470	
3025	<i>Dalejina</i>	BH.	CM	Good	None	4410	130	720	
3036	<i>Dalejina</i>	BH.	CM	Good	None	3170	180	695	
3014	<i>R. elegantula</i>	BH.	CM	Good	None	4960	175	610	2.17
3016	<i>R. elegantula</i>	BH.	CM	Good	None	5400	190	790	
3015	<i>R. elegantula</i>	BH.	CM	Poor	Recrystallized	8470	265	930	

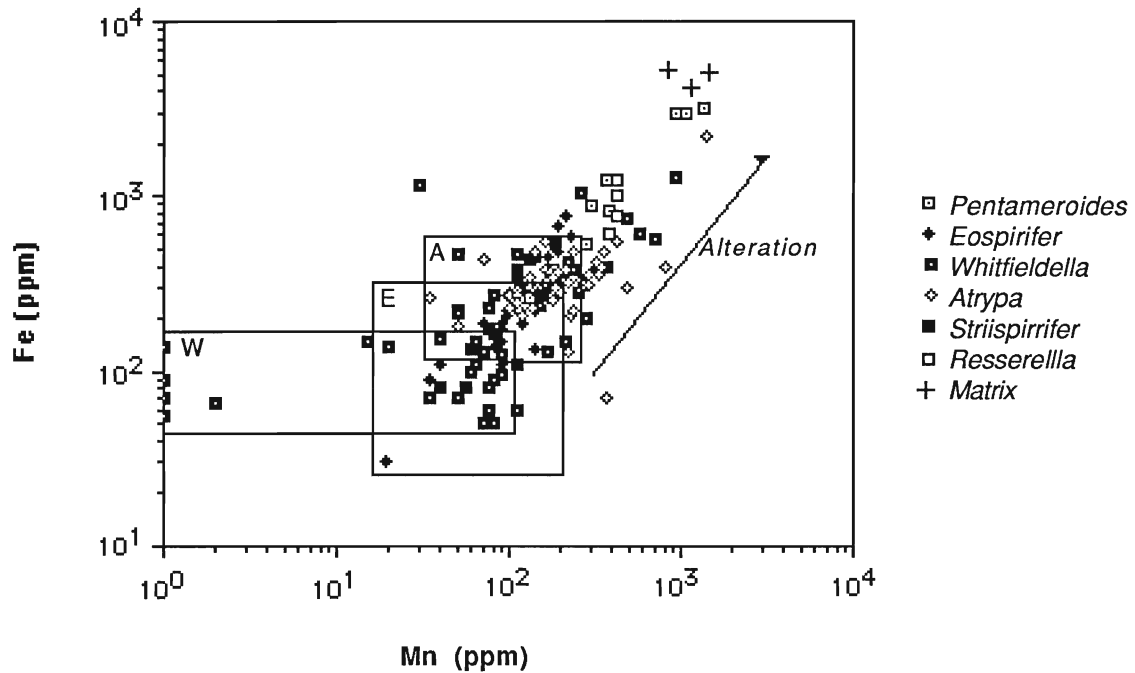


Figure 4.2. Scatter plot of Fe vs Mn for all genera from the Middle Silurian Clinton Group (Wenlockian). The diagenetic trend shows an increase of Mn and Fe contents with progressive diagenesis. The dashed fields define the approximate unaltered brachiopod of each species. W denotes pristine *Whitfieldella*; E denotes pristine *Eospirifer* and A denotes pristine *Atrypa*.

A-10). Diagenetic re-equilibration has not significantly depleted Na and Sr contents of shell calcite, which suggests that Na and Sr rich fluids were involved in the alteration process.

Elemental fractionation and taxonomic trends

Ancient brachiopods fractionate Mg and Na (Brand and Veizer, 1980; Morrison and Brand, 1987) when compared to low-Mg calcites precipitated in inorganic equilibrium with ambient conditions. Chemical data of pristine Clinton Group shell calcites suggests that these brachiopods also fractionated Mg and Na. They discriminated against Mg and preferentially incorporated Na into shell calcite. Furthermore, comparisons between three co-occurring species *Whitfieldella nitida*, *Eospirifer radiatus* and *Atrypa reticularis*, indicates that the incorporation of Na and to a lesser extent Mg, Mn, and Fe, was taxonomically controlled (Table 4.1). *Atrypa reticularis* calcite contains significantly higher Na and Mg contents than co-occurring *Whitfieldella nitida* and *Eospirifer radiatus* calcite (Table 4.3; unpaired t-test, $p > 0.05$, $f > 66$). Taxonomic differentiation is likely to be determined by physiological factors, dissimilar growth rates (calcification rates) and/or the mineral morphology/structural requirements of their shells. Sr appears to be randomly distributed between the studied species.

Isotopic trends

The majority of brachiopod calcite analysed from the Irondequoit and Rochester Shale Formations represent pristine isotopic compositions. In several specimens isotopic re-equilibration of shell calcite with diagenetic waters is indicated by the fact that increasing Mn, Fe and Mg contents correspond with more negative $\delta^{18}\text{O}$ and $\delta^{13}\text{C}$ values (Fig. 4.3). Valves of *Pentameroides* from the Reynales and Merriton Formations are chemically and microstructurally the

Table 4.3a. Summary of pristine brachiopods calcites from the Rochester Shale and Irondequoit Formations.

Brachiopod species	Stat.	Ca	Mg	Sr	Mn	Na	Fe	Al	I.R.
<i>Eospirifer</i> (n=23)	Mean	377550	2406	1230	103	1311	192	91	6.9
	Std. Dev.	26400	670	72	41	99	69	50	
	min	318340	1090	1070	19	1140	30	0	
	max	416460	3800	1360	190	1545	295	190	
<i>Whitfieldella</i> (n=31)	Mean	388034	2061	1215	64	1027	133	77	5.5
	Std. Dev.	32574	513	121	48	214	80	53	
	min	283730	1160	830	1	750	50	0	
	max	441070	3605	1625	215	1500	385	260	
<i>Atrypa</i> (n=45)	Mean	387567	3545	1222	181	1466	305	97	7.1
	Std. Dev.	35613	205	128	79	187	92	51	
	min	282990	1150	855	35	905	70	0	
	max	446840	4020	1560	370	1830	560	190	

All elemental concentrations are in ppm.

Table 4.3b. Unpaired T-test: pristine brachiopod chemistry (Clinton Group).

	Element	<i>Whitfieldella</i>	<i>Atrypa</i>
<i>Eospirifer</i>	Ca	t (53) = 1.115, $p < 0.05$	t (66) = 1.315, $p < 0.05$
	Mg	t (53) = 0.957, $p < 0.05$	<u>t (66) = 5.698, $p > 0.05$</u>
	Sr	t (53) = 1.831, $p < 0.05$	t (66) = 0.087, $p < 0.05$
	Mn	t (53) = 1.067, $p < 0.05$	<u>t (66) = 4.109, $p > 0.05$</u>
	Na	<u>t (53) = 6.849, $p > 0.05$</u>	<u>t (66) = 4.040, $p > 0.05$</u>
	Fe	t (53) = 0.622, $p < 0.05$	<u>t (66) = 5.191, $p > 0.05$</u>
<i>Atrypa</i>	Ca	t (75) = 0.255, $p < 0.05$	
	Mg	t (75) = 1.392, $p < 0.05$	
	Sr	t (75) = 1.806, $p < 0.05$	
	Mn	t (75) = 0.772, $p < 0.05$	
	Na	<u>t (75) = 10.979, $p > 0.05$</u>	
	Fe	<u>t (75) = 2.042, $p > 0.05$</u>	

n.b. Populations which are significantly different at the 95% confidence level are underlined

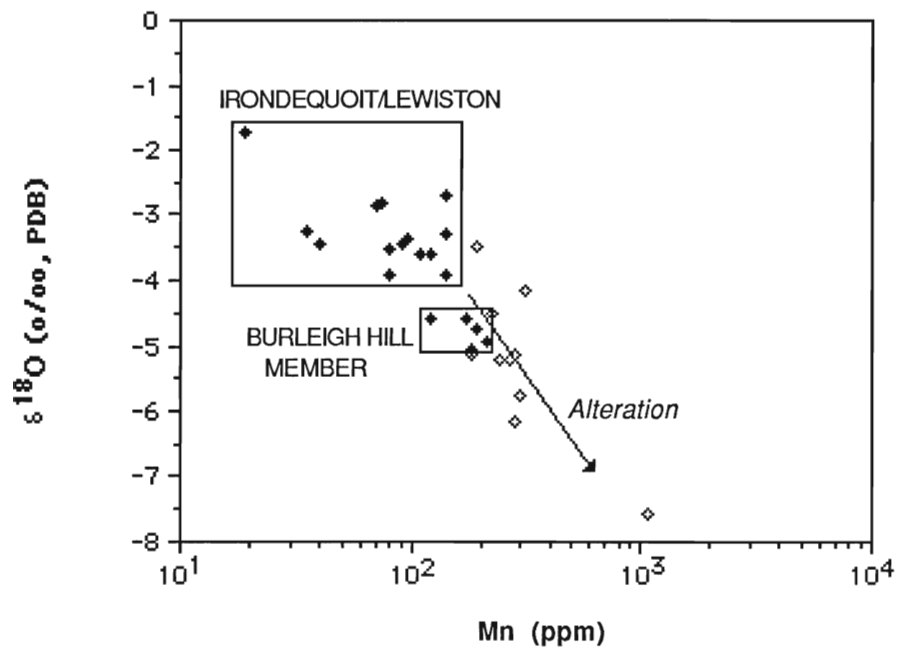


Figure 4.3. Diagenetic trend of isotopic composition of Middle Silurian Clinton Group brachiopods. ◇ denotes altered; ♦ denotes unaltered

most altered and show considerable diagenetic displacement of isotopic compositions.

In addition, significant differences of oxygen and carbon isotopes are evident between Irondequoit/Lewiston Member and Burleigh Hill Member pristine brachiopods (t-test, $p > 0.05$, $f = 24$; Fig. 4.4). Oxygen isotopic differences may be attributed to changes in salinity, temperature, paleodepth, and oceanic $\delta^{18}\text{O}$ composition, whereas carbon is influenced by the $\delta^{13}\text{C}$ of ambient dissolved inorganic carbon (DIC) of the seawater (Anderson and Scholle, 1983).

DIAGENETIC EVALUATION OF CLINTON GROUP BRACHIOPODS

Merritton Formation

Large, disarticulated *Pentameroides* brachiopods were collected from the dense green-grey calcareous mudstones of the Merritton Formation (Lower Clinton Group). The upper surface (3-4 cm deep) of this unit is a heavily phosphatized, pyritized hardground. Specimens from the hardground and underlying micrites were physically abraded and corroded, with little retention of original shell microstructure. Chemically, these brachiopods have high Mn, Fe and Mg contents, which are indicative of extensive dissolution and recrystallization (Fig. 4.2); Sr and Na contents are also retained in the diagenetic product. Meteoric diagenesis tends to significantly deplete Sr and Na (Brand and Veizer, 1980), therefore Merritton Formation diagenetic waters must have contained higher Sr and Na contents than surficially-derived meteoric waters. The hardground may represent an omission surface produced by a slowdown in sedimentation rates and during submarine lithification and early cementation, marine-derived waters may have contributed to the post-

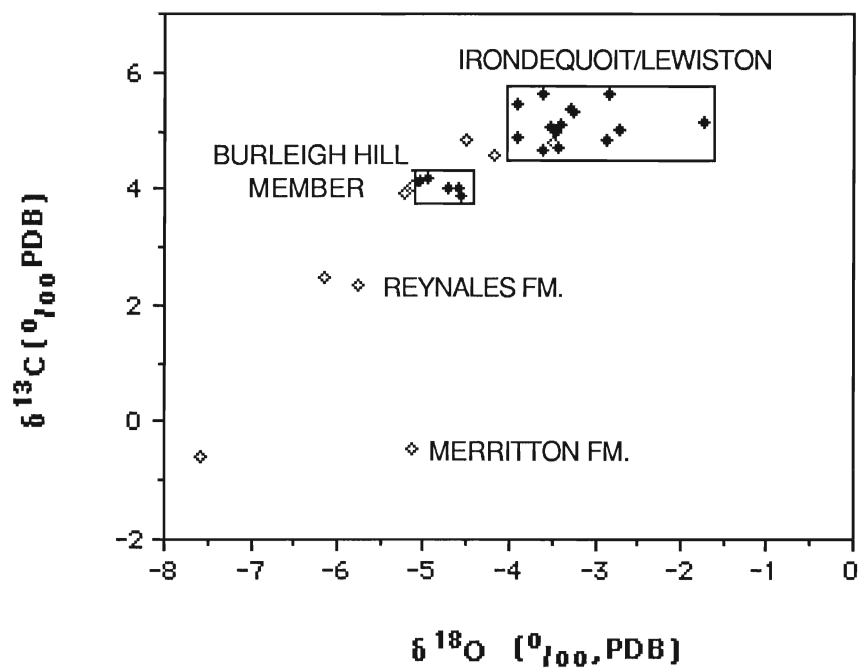


Figure 4.4. Isotopic compositions of *Eospirifer* from Irondequoit, Rochester, Reynales and Merritton Formations of the Middle Silurian Clinton Group. ◇ denotes altered; + denotes unaltered

depositional alteration of *Pentameroides* calcite. However, there are no chemical distinctions between shell calcite from the hardground or the micrites beneath. The micritic limestone matrix is partially dolomitized which suggests the post-depositional passage of mixed waters, since dolomitization is restricted to the matrix and probably postdates brachiopod alteration.

Reynales Formation

The Reynales Formation consists of 6m of grey, crystalline limestones and dolomitic limestones with thin shaly partings (Liebe and Grasso, 1986). In the Genesee river gorge at Rochester (Locality 44), *Pentameroides* sp. were collected from biostrome beds of the Wallington sub-member of the Reynales Formation, which was deposited in shallow shoal to subtidal marine settings (Grasso, 1983). Although the matrix is predominantly calcitic biomicrite, fine euhedral rhombs of dolomite have replaced about 5-15% of the matrix. *Pentameroides* sp. shell valves exhibit physical evidence of extensive corrosion and dissolution, and poor microstructural preservation is complemented by chemical alteration. Dissolution and reprecipitation steps toward equilibration with diagenetic waters is suggested by enrichments of Fe, Mn and Mg and significant depletion of Sr and Na (Fig. 4.2); similar trends are exhibited in other studies of brachiopod diagenesis (Brand and Veizer, 1980). By comparison to the Merritton Formation, this chemical trend suggests that meteoric-derived waters were responsible for alteration of brachiopod calcite. Dolomitization of the matrix has left the brachiopod specimens unaffected, indicating that the passage of Mg-rich fluids probably postdates equilibration of shell calcite.

Irondequoit and Rochester Shale Formation diagenetic waters

Enrichments of Mg with alteration in Irondequoit and Lewiston brachiopods are significant but, by contrast, there is no significant depletion of Sr and Na contents with alteration (Fig. 4.5). Thus despite alteration of Irondequoit and Lewiston brachiopods, Sr and Na contents have been retained at similar values to original unaltered compositions, suggesting the influence of relatively marine-dominated waters in the diagenetic process. There are taxonomic and environmental controls of original chemistries and resultant diagenetic reaction directions are constrained by these initial compositions. Many *Eospirifer radiatus*, *Atrypa reticularis*, *Striispirifer niagarensis* and *Resserella elegantula* from the Irondequoit and Rochester Formations show progressive increases of Mg with alteration, the direction of which is constrained by their original elemental contents (Trend A; Fig. 4.5). The average Na contents of pristine *Eospirifer radiatus* and *Atrypa reticularis* are about 1300-1400 ppm which is retained in altered specimens. In contrast, pristine *Whitfieldella nitida* contain Na compositions of 850-1000 ppm and the alteration direction is similarly constrained by original shell calcite composition (Trend B; Fig. 4.5). The Irondequoit crinoidal biosparite is pervasively dolomitized, which has selectively replaced the matrix but left brachiopods unaffected. Alteration appears to be diffusion controlled because the diagenetic product retains much of the original chemistry; only two specimens appear to be partially dolomitized. Similarly, dolomitization of the Lewiston and Burleigh Hill members is quite pervasive. The grey mudstone, calcisiltite and calcarenite beds are partially dolomitized; replaced by fine-grained euhedral dolomite rhombs. The brachiopods are unaffected by the dolomitization process. At least two phases of diagenetic alteration are suggested by these observations. The

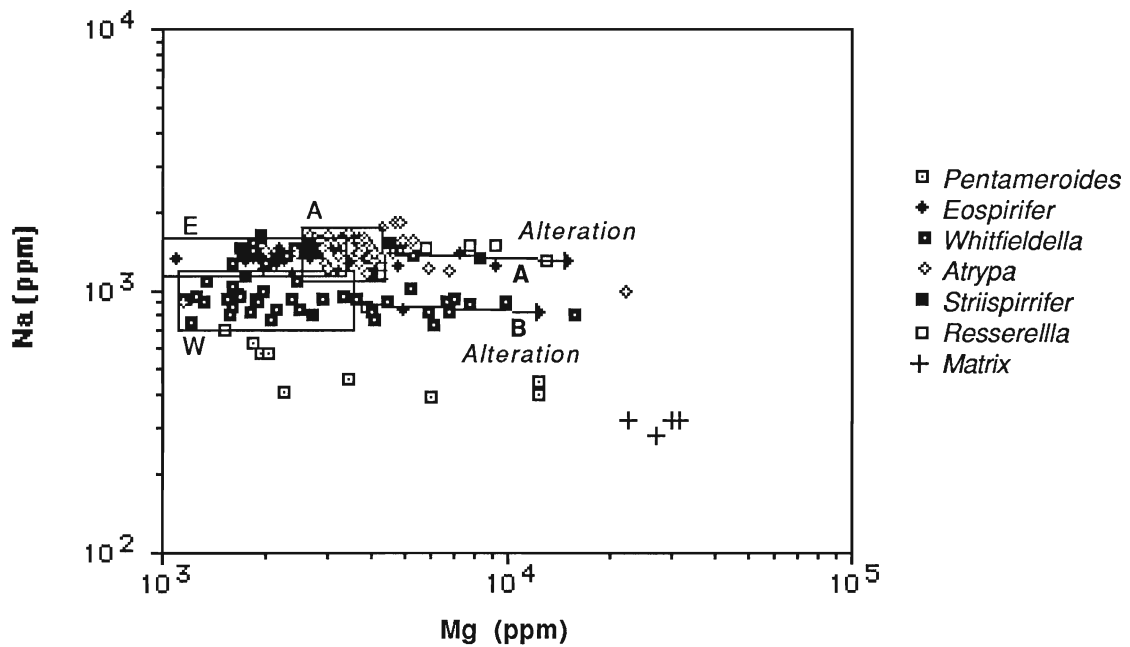


Figure 4.5. Scatter plot of Na vs Mg for all species from the Middle Silurian Clinton Group (Wenlockian). The diagenetic trend shows an increase of Mg contents with progressive diagenesis. The dashed fields define the approximate unaltered brachiopod of each species. W denotes pristine *Whitfieldella* ; E denotes pristine *Eospirifer* and A denotes pristine *Atrypa* .

first was a post-depositional alteration of brachiopods (and matrix?) in the presence of relatively marine dominated mixed waters followed by the passage of the dolomitizing fluids. Marine formation waters may have been the brachiopod-altering diagenetic fluids. The origin of the Mg rich fluids may be related to mixed water processes (Brand, pers. comm. 1989).

PALEOENVIRONMENTAL ANALYSIS OF THE IRONDEQUOIT FORMATION

The Irondequoit Formation varies from dolomitic grainstones in the east (Lockport, N.Y.) to dolosparites in the west (Hamilton, Ontario) and represents a crinoidal bank facies deposited under normal, open marine conditions (Brett, 1983a). Between St. Catharines, Ontario and Lewiston, New York State, the Irondequoit is less pervasively dolomitized and brachiopods are commonly preserved. In the Niagara Gorge (locality 40), the lower and middle Irondequoit consists of thick-bedded crinoidal grainstones which possess a low diversity brachiopod fauna dominated by *Whitfieldella nitida*. Most bioclasts are comminuted and disarticulated valves of *Whitfieldella nitida* are abraded and corroded, suggesting prolonged exposure and erosion. Winnowing of fines from these biosparites suggest these brachiopods occupied a moderate to high energy environment within the shallowest part of the crinoid shoal. The upper 20cm of the Irondequoit Formation is dominated by large brachiopods such as *Leptaena rhomboidalis*, *Atrypa reticularis*, *Whitfieldella nitida* and *Eospirifer radiatus* in varying states of disarticulation. The presence of micrite in these crinoidal biosparites suggests a reduction in the winnowing of fines or the influx of muddy siliciclastics prior to the deepening of the basin. Both faunal

associations are assigned by Brett (1989) to a shallow-water *Atrypa reticularis* - *Whitfieldella nitida* brachiopod association (Fig. 4.6).

Several chemical trends are evident from the data. The generally low Fe and Mn contents of pristine brachiopod calcite suggests that the shallow-waters of these Irondequoit crinoidal bank were well oxygenated, supporting the paleoecological and taphonomic assertions (Brett, 1983a; 1989). Differences between species in re-equilibration with diagenetic waters are evident in Fe and Mn plots of Irondequoit brachiopod data (Fig. 4.7). Pristine *Whitfieldella nitida* has significantly lower Mn and Fe contents than unaltered *Atrypa reticularis* and *Eospirifer radiatus* (Table 4.1; Fig. 4.2). The variable enrichments in Mn and Fe are a response to re-equilibration with diagenetic waters controlled by diffusion- or fluid- reactions; increasing enrichments representing increased control by fluids on the chemistry of the alteration product (Fig. 4.7). Diagenetic trends are also constrained by the original shell calcite composition. *Eospirifer radiatus* and *Atrypa reticularis* preferentially incorporate more Na compared to *Whitfieldella*, and the enrichment trend of Mg is dependant on this phenomena (Fig. 4.8). Although there is no change in lithology, the Na and Mg chemistries of pristine *Whitfieldella nitida* specimens are significantly higher in the upper Irondequoit than in the lower and middle. This may be due to shallower more turbulent conditions and fresh waters introduced by storms may have created slightly brackish conditions thereby reducing Na and Mg incorporation into shell calcite. Alternately, if the relationship between depth and Mg, Na contents observed in the Hamilton Group (this study) is applicable to these brachiopods, this may indicate slightly deeper waters within the upper biosparites of the Irondequoit Formation. The presence of large, thickened shells within the uppermost Irondequoit may be a

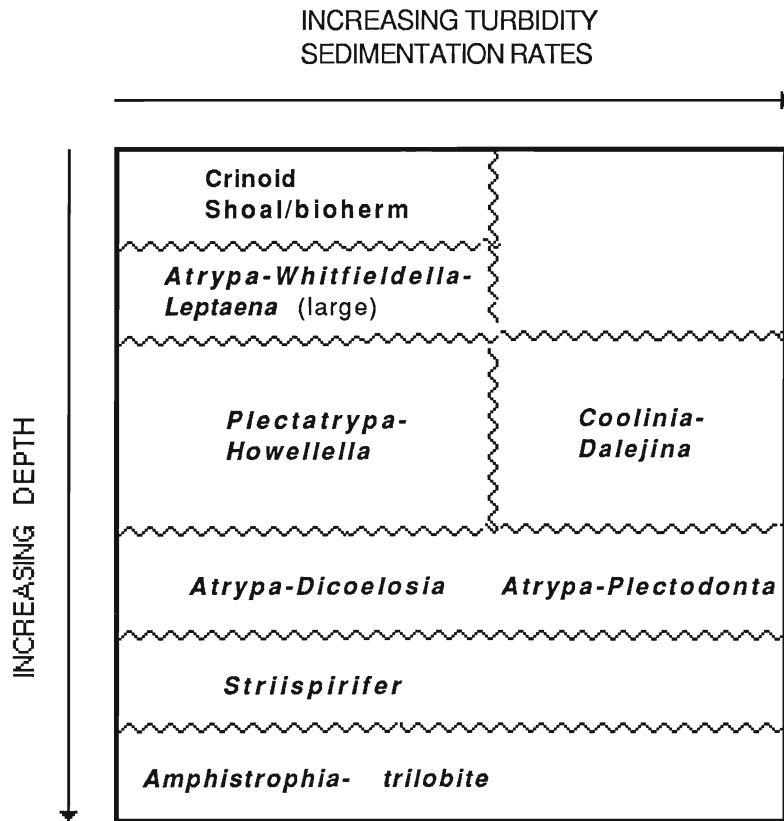


Figure 4.6. Rochester Shale/ Irondequoit Formation brachiopods associations with reference to inferred gradients of depth-related parameters and turbidity and/or sedimentation rates. Source from Brett (1989).

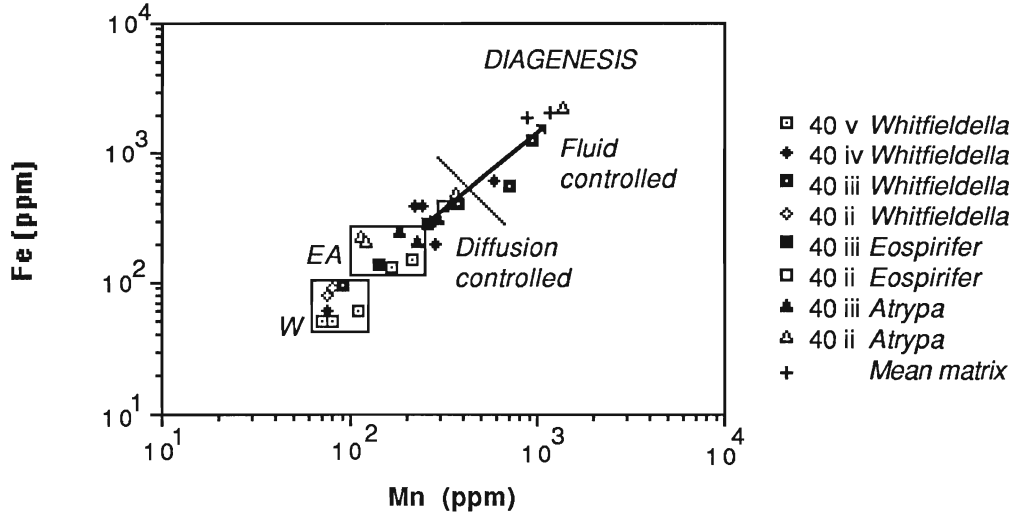


Figure 4.7. Diagenetic trend of Irondequoit Formation brachiopods (Middle Silurian). Field W is unaltered *Whitfieldella* specimens and field EA represents unaltered *Eospirifer* and *Atrypa*. Matrix data from Milinkovich (1986).

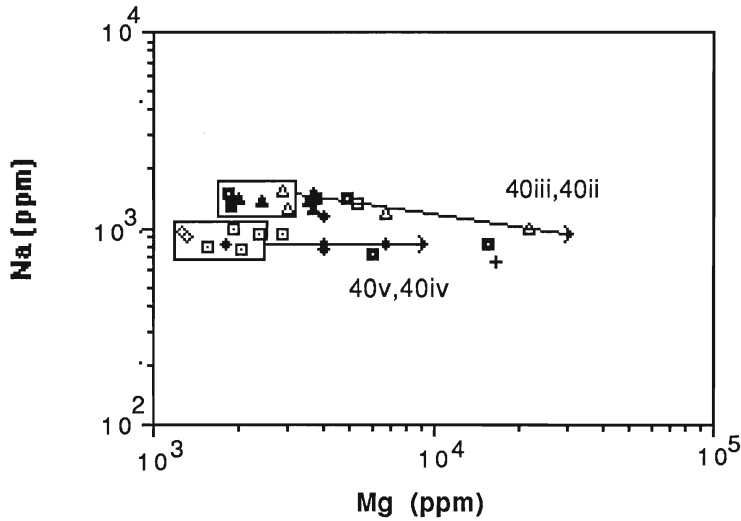


Figure 4.8. Scatter plot of Na vs Mg contents of Irondequoit brachiopods illustrates two diagenetic trends. Lower trend is from middle Irondequoit Formation (localities 40v, 40iv) and upper trend are brachiopods from upper 20cm of the Irondequoit (localities 40iii, 40ii). Key as in Figure 4.6. Matrix data from Milinkovich (1986).

morphological adaptation to a more turbulent (and presumably shallower?) environment (Fursich and Hurst, 1974).

PALEOENVIRONMENTAL ANALYSIS OF THE ROCHESTER SHALE FORMATION

Introduction

Medium to dark grey calcareous mudstones and thin limestones of the Rochester Shale conformably overlie the crinoidal Irondequoit Formation and are in turn overlain gradationally by the dolostones of the Lockport Formation (Thusu, 1972; Brett, 1983b). The Rochester Shale can be subdivided into the lower Lewiston Member and the upper Burleigh Hill Member between Brockport, New York State, and Grimsby, Ontario; to the east, the formation becomes undifferentiated (Brett, 1983a). West of Grimsby, the Burleigh Hill member grades into argillaceous dolostones of the Stoney Creek Member, which northwest of Hamilton Ontario, quickly pinch out. Brachiopods were collected from Lewiston Member type locality in the Niagara Gorge, New York , the Burleigh Hill Member type locality in St. Catharines, Ontario (Fig. 4.9), and from several additional localities in western New York and the Niagara peninsula (Fig. 1.2).

Stratigraphic setting of the Lewiston Member

Several recent studies have defined recurring and cyclical faunal associations within the Rochester Shale (Brett, 1983a; 1989). Sedimentologically and paleoecologically the entire Rochester Shale Formation has been interpreted as a transgressive-regressive cycle (Brett, 1983a; 1989; Tetrault, 1987) which is a result of the migration of facies belts in a

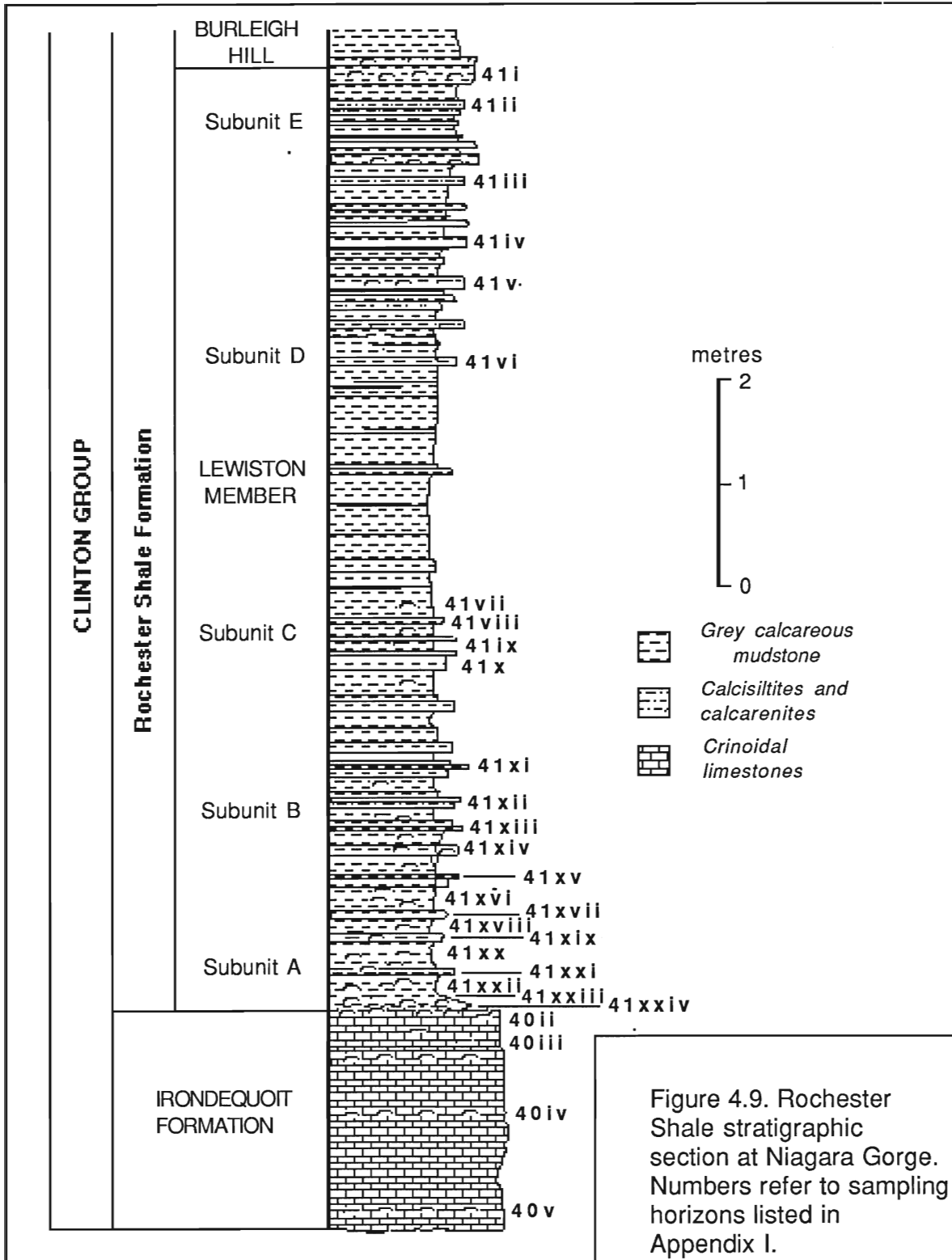


Figure 4.9. Rochester Shale stratigraphic section at Niagara Gorge. Numbers refer to sampling horizons listed in Appendix I.

north-south direction (Fig. 4.10). Superimposed upon this, the Lewiston Member, divided into 5 subunits (Brett, 1983b), records a smaller scale deepening (subunits A to C) and shallowing subcycle (subunits C to E). The sub-unit A is a brachiopod-dominated, argillaceous grey mudstone sequence which has a gradational contact with the Irondequoit Formation. In the Niagara Gorge, a large bryozoan bioherm at the Irondequoit/Rochester Shale contact interfingers with and extends into the subunit A. The uppermost Irondequoit Formation and lowest 20-30 cm of the subunit A is characterized by an association of large disarticulated brachiopods (*Leptaena rhomboidalis rhomboidalis*, *Atrypa reticularis reticularis*, *Whitfieldella nitida nitida*, *Eospirifer radiatus radiatus*, *Dicoelosia biloba*) which have been assigned to a *Atrypa reticularis* - *Whitfieldella nitida* community by Brett (1989) and may represent shallow, turbulent waters within crinoidal banks (Fig. 4.6). The middle and upper parts of subunit A are characterized by a diversity of brachiopod species (*Dicoelosia biloba*, *Atrypa reticularis reticularis*, *Whitfieldella nitida nitida*, *Leptaena rhomboidalis rhomboidalis*, *Coolinia subplana subplana*, *Plectodonta transversa*, *Eospirifer radiatus radiatus*, *Howellella crispa*) that have been assigned to the deeper *Atrypa reticularis*-*Leptaena rhomboidalis* community (Brett, 1989). This sequence of thin graded calcarenite and calcisiltite beds (2-6cm thick), interbedded with grey mudstones, contain an abundance of articulated brachiopods.

Subunit B consists of light grey mudstones interbedded with thin fossiliferous calcisiltites and calcarenites which have been interpreted as medial and distal storm deposits (Brett, 1983a). Subunit C consists of a sequences of grey mudstones interbedded with thin fossiliferous shales and calcisiltite beds (distal storm deposits). The presence of fossiliferous horizons with articulate crinoids, complete trilobites and graptolites suggests these beds

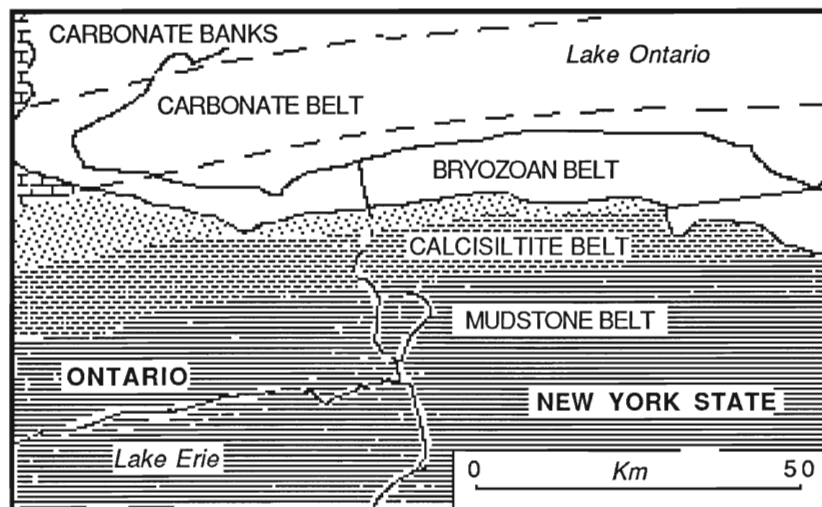


Figure 4.10. Facies map of the Rochester Shale across southern Ontario and western New York State. North/south migrations of facies belts produced transgressive-regressive sequence in Lewiston Member. Modified from Brett (1983a).

were quickly blanketed by muds and deposited in low-energy settings (Brett and Eckert, 1982). The brachiopod fauna, including *Striispirifer niagarenseniagarensis*, *Eospirifer radiatus* and *Atrypa reticularis*, which are commonly articulate and in life position, has been assigned to the *Striispirifer niagarensis* community and has been interpreted by Brett (1983a; 1989) as having occupied quiet, deeper shelf environments, that were episodically disturbed by storms.

Subunit D, of the Lewiston Member, resembles the subunit B lithologically and paleoecologically. The frequency of calcisite and calcarenite beds increases from subunits C to E and represents a general shallowing upward sequence, culminating in the shallow bryozoan communities of the upper subunit E. There are abundant brachiopod faunas in association with these subunit E bryozoa beds (*Howellella*, *Atrypa reticularis*, *Whitfieldella nitida*, *Resserella*, *Dicoelosia*, *Plectodonta* are common) assigned to a *PlectAtrypa reticularis*-*Howellella*-fenestrate bryozoan community by Brett (1989). Overlying subunit E are barren dark grey shales of the Burleigh Hill Member. A disconformity between the Lewiston subunit E and the Burleigh Hill Member is represented by a thin heavily pyritized hardground (Fig. 4.8, locality 41). The Burleigh Hill Member records a shallowing upwards sequence (Brett, 1983a), and may represent a punctuated aggradational cycle of Goodwin and Anderson (1985).

Chemical trends

Most shell beds of the Lewiston Member are essentially autochthonous and transport, if any, was minimal. Therefore, the elemental and isotopic trends reflect depositional conditions at this locality during the transgressive-regressive cycle. The majority of brachiopods from the Lewiston Member are

microstructurally and chemically well preserved, but a few altered specimens were significantly enriched in Mg, Mn and Fe (Fig. 4.11) while retaining their Sr and Na contents (Fig. 4.12). Although brachiopods were analysed from a variety of lithofacies such as grey mudstones, calcisiltites and graded calcarenites, there was no systematic variation in brachiopod alteration between these beds. Specimens of *Resserella elegantula* from the uppermost pyritized hardground of the E subunit contain much higher Mg contents (5750-12860 ppm) than brachiopods in underlying Lewiston beds which may be a reflection of hardground cementation.

Once these altered specimens were eliminated from the data set, investigation of systematic changes in trace and minor element chemistries could continue. Within the transgressive-regressive cycle of the Lewiston Member, redox-controlled elements such as Mn and Fe varied between 10 and 180ppm but there was no significant difference between shallow (subunits A, E) and deeper facies (subunit C). Bottom waters of the Lewiston sea may therefore have alternated between aerobic and slightly dysaerobic conditions but this is not related to stratigraphic trends (Fig. 4.13).

Mg incorporation into brachiopod calcite was observed by Lowenstam (1961) to be dependant on salinity and related to the effect of greater ion concentrations on the physiology of the organism. Similarly, Na contents in biogenic carbonates have been used to determine paleosalinities (Veizer and Demovic, 1974; Veizer et al., 1978), but Ishikawa and Ichikuni (1984) suggest that Na contents in biogenic carbonates are not proportional to salinities over 10 ppt. Analysis of pristine brachiopods from the Hamilton Group suggests that Mg, Na and Sr contents are inversely proportional to depth (cf. Chapter 3) but analysis of Lewiston Member brachiopod calcites cannot confirm this finding. The concentrations of Sr and Na within shell calcite remains fairly constant

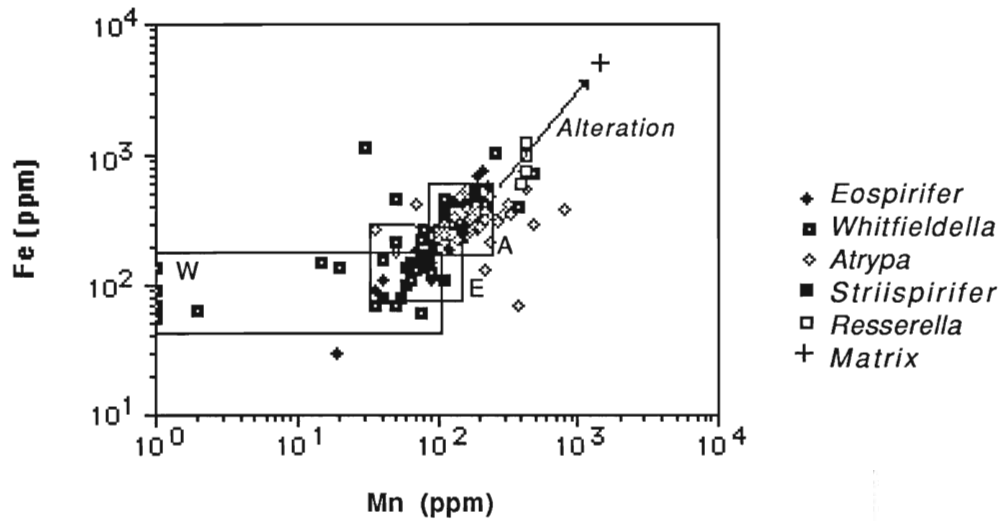


Figure 4.11. Scatter plot of Fe vs Mn for all species from the Lewiston Member of the Rochester Shale Formation. The diagenetic trend shows an increase of Mn and Fe contents with progressive diagenesis. The fields define the approximate unaltered brachiopod of each species. W denotes *Whitfieldella*, E denotes *Eospirifer*; and A denote *Atrypa*.

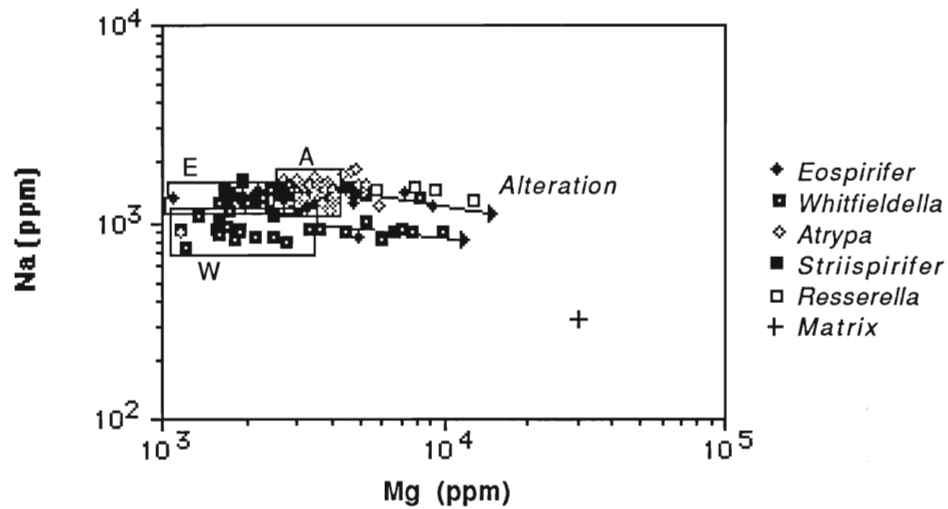


Figure 4.12. Na vs Mg scatter plot of Lewiston Member brachiopods. The fields define approximate unaltered chemistries of each species; W denotes *Whitfieldella*; E denotes *Eospirifer*; and A denote *Atrypa*. In general the Na contents of *Eospirifer* and *Atrypa* are higher than *Whitfieldella*; Mg contents are significantly higher in *Atrypa* than *Eospirifer* and *Whitfieldella*.

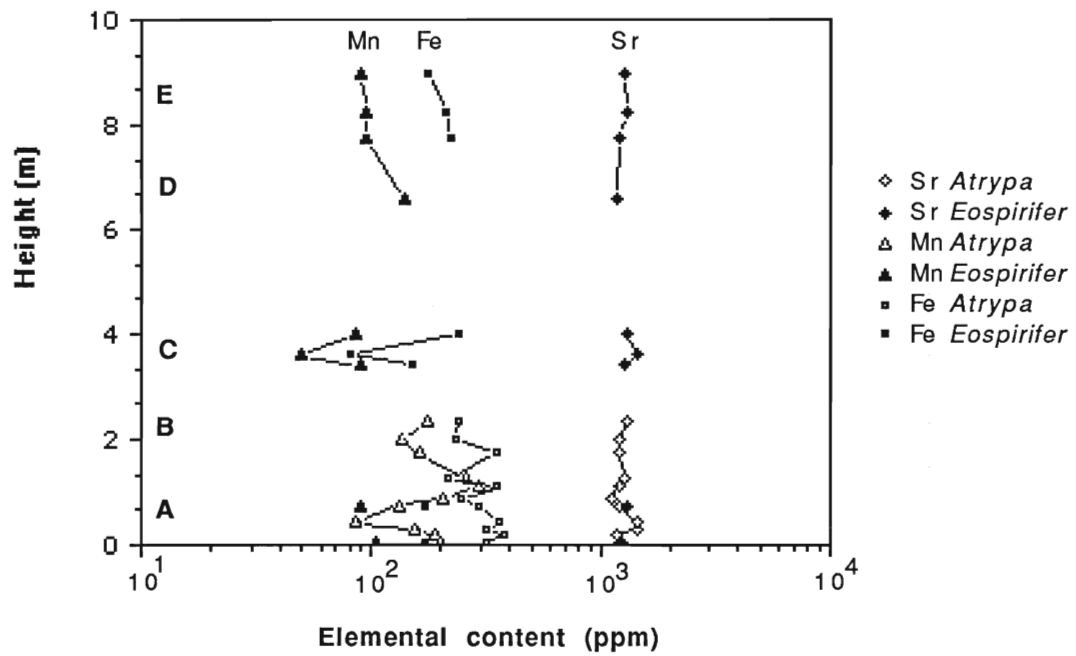


Figure 4.13. Plot of mean Sr, Mn and Fe contents of *Atrypa* and *Eospirifer* against height within Lewiston Member section.

throughout the section (Sr 1050-1200 ppm; Fig. 4.13: Na 1200-1600 ppm; Fig. 4.14), and there are significant differences between shallow and deep facies of the Lewiston Member (Fig. 4.14, 4.15). Mg contents of *Atrypa reticularis* calcite do decrease from the base of the Lewiston to the middle of subunit B, but whether this is related to depth cannot be confirmed because the Mg contents of *Atrypa reticularis* in subunits C to E reflect chemically altered calcites.

Rochester Shale *Eospirifer radiatus*, *Atrypa reticularis* and *Whitfieldella nitida* biologically fractionated Mg and Na, discriminating against Mg and preferentially incorporating Na (Tables 4.1, 4.3). This fractionation is also taxonomically controlled because each species has significantly different Mg and Na contents. This phenomena is complicated by the fact that *Atrypa reticularis* incorporates Mg and Na differently from bed to bed in proportion, presumably, to concentrations determined by an environmental or physiological control. Analysis of pristine *Atrypa reticularis* from a number of horizons in subunits A and B, suggests that Mg and Na incorporation is inversely related; higher Mg contents correspond to lower Na contents and vice versa (Fig. 4.15). Growth rates may determine the amount of Na incorporated into shell calcite as a substitute for Mg and this may be determined by slight variation in environmental conditions such as salinity and temperature. This Na/Mg relationship does not correlate with the apparent transgressive-regressive cycle. Furthermore, *Atrypa reticularis* may have preferentially fractionated Mn and Fe, when compared to *Eospirifer radiatus* and *Whitfieldella nitida* (Table 4.1 and 4.3).

Isotope trends

Oxygen and carbon isotopes can reflect deepening events associated with trasgressive-regressive processes. A 5°C decrease in water temperature

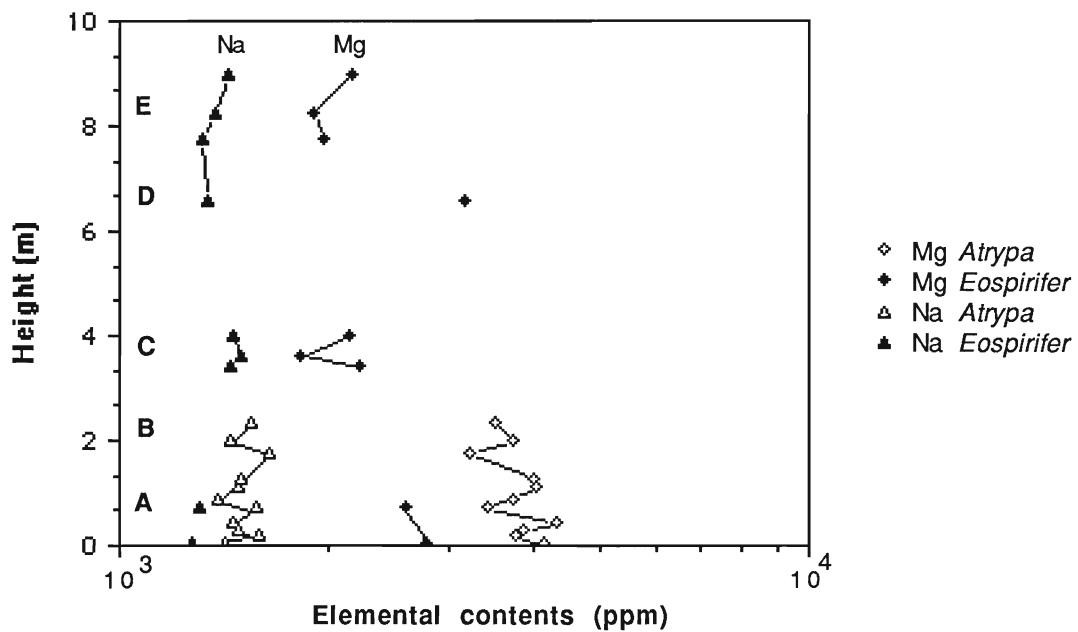


Figure 4.14. Plot of mean Mg and Na contents of pristine *Atrypa* and *Eospirifer* against height within Lewiston Member section.

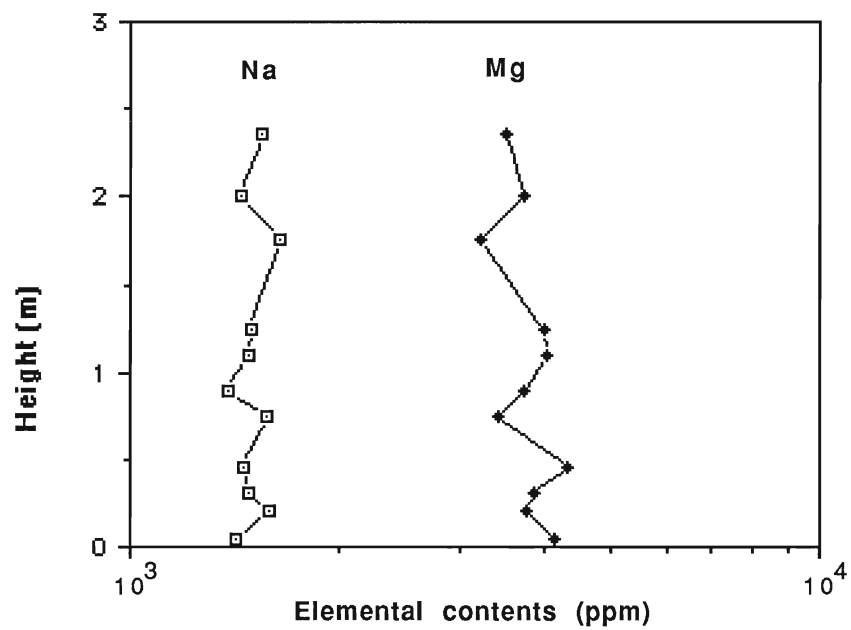


Figure 4.15. Plot of mean Na and Mg contents of pristine *Atrypa* from the Lewiston Member subunits A and B. Incorporation of Na and Mg into shell calcite is inversely related.

can cause a 1‰ increase in $\delta^{18}\text{O}$ (Epstein et al., 1953; Rye and Sommer, 1980). Adlis et al. (1989) have attributed slight shifts in $\delta^{13}\text{C}$ and $\delta^{18}\text{O}$ within the brachiopod shell calcite of *Planoconvexa crurithyris* to deepening within a Pennsylvanian cyclothem sequence. A $\delta^{18}\text{O}$ increase of 0.6‰ has been ascribed to a cooling and depth change of 70m, associated with marine transgression and glacial dilution of the Pennsylvanian $\delta^{18}\text{O}$ oceanic reservoir (Adlis et al., 1989). Similarly, changes in the $\delta^{13}\text{C}$ have been attributed to deepening below the photic zone, stagnation, and increased influence of pore-water carbon derived from organic matter (Adlis et al., 1988). These authors assume no salinity effects associated with the transition from shallow marine limestones to deeper marine phosphatized gondolellid shales. Furthermore, these cyclothem were deposited in the semi-enclosed Midland basin, and isotopic variation caused by changing patterns of fresh water influx and salinity during transgression-regression may have contributed to the slight shifts in $\delta^{18}\text{O}$.

Specimens of *Eospirifer radiatus* were analysed isotopically through the Lewiston Member sequence, because they are present in many horizons. The analysis of a single species eliminated any potential isotopic differences between species and *Eospirifer radiatus* was assumed to incorporate isotopes in equilibrium with ambient conditions. Although only a limited number were analysed, several distinct observations can be made. Average $\delta^{13}\text{C}$ composition of the brachiopods was +5.0‰ (+4.6‰ to +5.7‰), which suggests that the ambient bottom waters were relatively enriched in ^{13}C . Average shell calcite $\delta^{18}\text{O}$ composition was -3.2‰ (range -1.7‰ to -3.9‰). This corresponds to paleotemperatures of 26-31°C if the Wenlockian seas had the same $\delta^{18}\text{O}$ composition as the modern ocean (Broecker, 1974). These time-averaged (brachiopod life span) temperatures are reasonable, considering that

southern Ontario was within 10-15° south of the paleoequator during the Middle Silurian (Scotese et al., 1979). This finding does not support the assertion that Silurian oceans were depleted in ^{18}O by 5-6‰ (Brand and Veizer, 1981; Veizer et al., 1986). Indeed, no correction of isotopic data from this study is necessary and it is therefore pre-emptive to assume that throughout the Silurian, mean oceanic $\delta^{18}\text{O}$ compositions were depleted by 5.5‰ (O'Shea et al., 1988). Conditions within the Michigan basin during deposition of the Upper Silurian Salina Group may indeed reflect depletion of ^{18}O at that particular time within a restricted basin (O'Shea et al., 1988). The previously reported brachiopod isotopic data on brachiopod calcite may simply reflect the influence of postdepositional alteration, salinity and temperature effects, glacial dilution, local environmental conditions and physiography of epicontinental oceans.

The isotope stratigraphy of the Lewiston Member is illustrated for the Niagara Gorge section in Fig. 4.16. There appears to be no significant trends in $\delta^{13}\text{C}$ and $\delta^{18}\text{O}$ in relation to the apparent deepening and subsequent shallowing observed within the Lewiston Member. Lowenstam (1961) observed that Mg contents in brachiopods were related to temperature and $\delta^{18}\text{O}$ values; increasing $\delta^{18}\text{O}$ is related to cooling associated with deepening. However, within the Lewiston sequence, there is no correlation between Mg and $\delta^{18}\text{O}$ values (Fig. 4.17; hence temperature). Isotopically, *Eospirifer radiatus* from the deepest Lewiston C beds (*Striispirifer* community) are similar to those from the shallowest Lewiston A and E subunits. Furthermore, *Eospirifer radiatus* from the shallow crinoidal banks of the underlying Irondequoit Formation are not significantly different from *Eospirifer radiatus* in the Lewiston Member. The variation of $\delta^{18}\text{O}$ is about 0.5‰ (~3°C) and $\delta^{13}\text{C}$ is approximately 0.7‰. The more negative $\delta^{18}\text{O}$ values and hence slightly warmer paleotemperatures (~2-3°C) occur in the deeper Lewiston subunits B and C Members; contradictory to

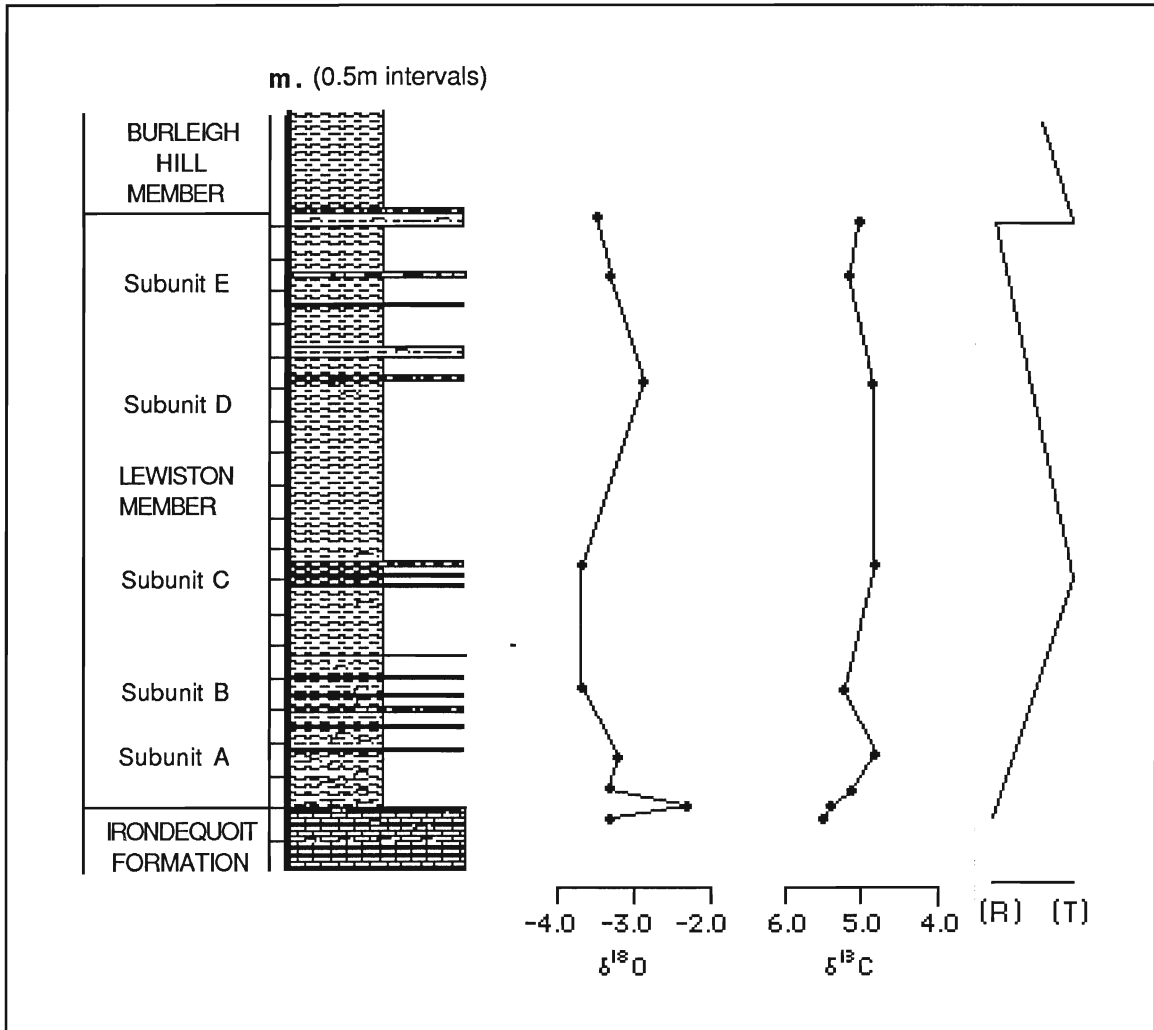


Figure 4.16. Mean isotopic composition (in per mil; PDB) of pristine *Eospirifer* from the Irondequoit Formation and Lewiston Member of western New York State (Clinton Group; Middle Silurian). Interpretation of transgressive-regressive cycle from Brett (1983a).

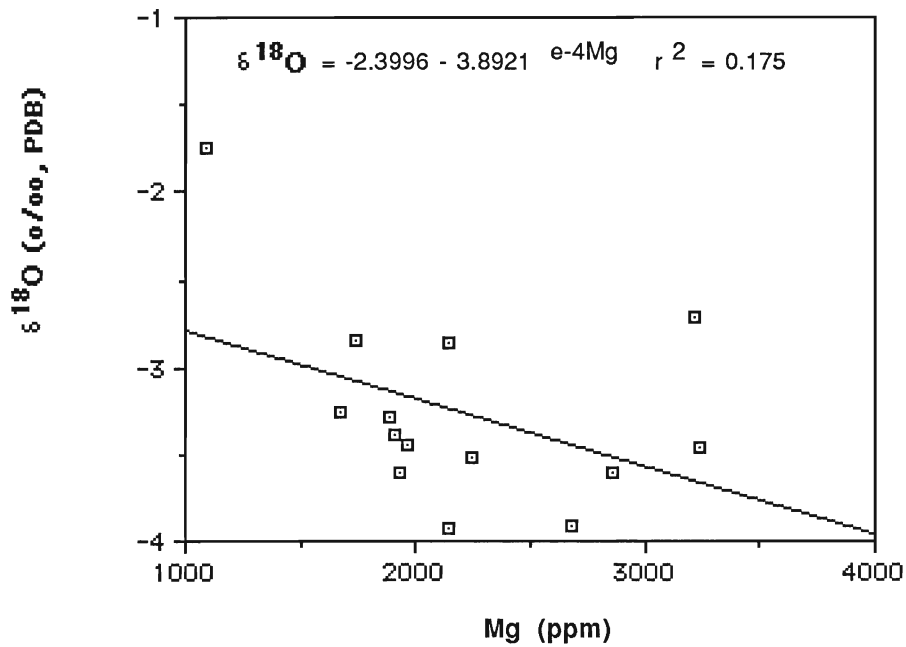


Figure 4.17. Plot of oxygen isotopes versus Mg contents within pristine *Eospirifer* calcites from the Irondequoit Formation and Lewiston Member (Clinton Group, Middle Silurian).

paleoecologic interpretation (Brett, 1983a; 1989). There may be several possible explanations for these observations. Transgressions associated with glacio-eustatic changes, may decrease mean oceanic $\delta^{18}\text{O}$ composition by 1‰ (Shackleton, 1967; 1974; Adlis et al., 1989). If the Lewiston cycle is assumed to be the result of glacio-eustatic changes, then the slightly more negative $\delta^{18}\text{O}$ values from the middle Lewiston may be explained by changes in the mean oceanic $\delta^{18}\text{O}$ composition. Alternately, salinity changes associated with cyclonic depressions that swept across the region may explain the slight $\delta^{18}\text{O}$ variations observed for this sequence. In tropical latitudes, seawater $\delta^{18}\text{O}$ can decrease by 0.1‰ per ‰ salinity change (Craig and Gordon, 1965).

The Lewiston Member isotopic and elemental data does not support any temperature gradient associated with depth changes in this transgressive-regressive cycle. There may be a number of explanations for this. The cycle may not have involved major fluctuations in relative seawater and bottom water conditions may not have changed significantly. Depth changes need not have been great to produce significant lateral movements of facies and faunal associations. The slight differences observed in $\delta^{13}\text{C}$, $\delta^{18}\text{O}$ and elemental contents may represent the natural variations inherent to shell biomineralization and small fluctuations in the temperature, salinity, redox conditions, dissolved inorganic carbon, mean oceanic and localized oxygen compositions (Fig. 4.11).

Geochemistry of brachiopods from the Burleigh Hill Member

The lowest 6m of the Burleigh Hill Member consist of dark grey shales punctuated by a few thin but persistent calcisiltite lenses (Fig. 4.18). Few macrofossils are present (notably *Coolinia subplana*). About 5.7 m above the basal contact with the subunit E is a shell bed, informally termed the "*Coolinia subplana*" Bed, which contains abundant disarticulated and fragmented

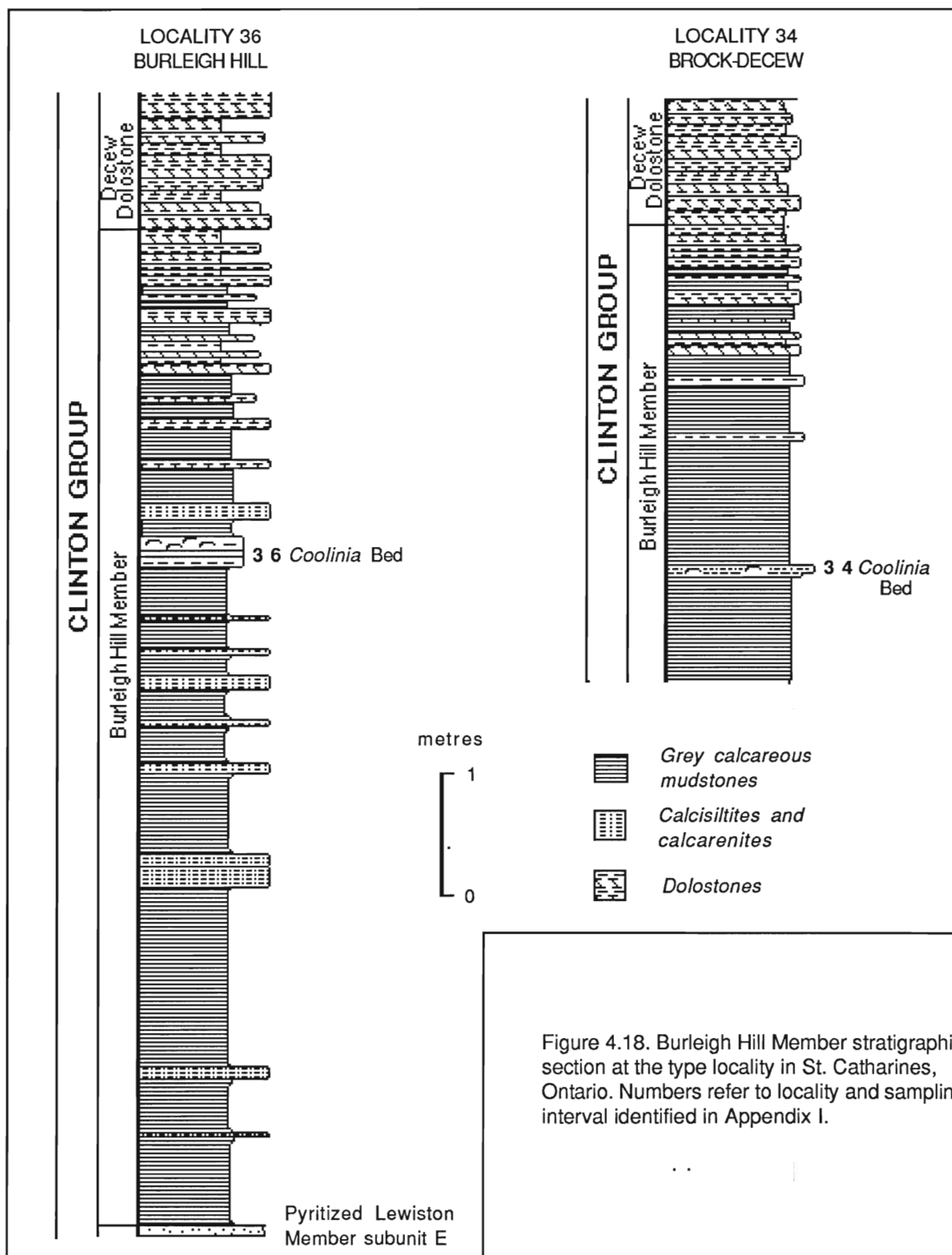


Figure 4.18. Burleigh Hill Member stratigraphic section at the type locality in St. Catharines, Ontario. Numbers refer to locality and sampling interval identified in Appendix I.

brachiopods, including *Dalejina*, *Resserella elegantula*, *Leptaena rhomboidalis* and *Coolinia subplana* and trilobites *Dalmanites limulurus* and *Trimerus* sp. In the type section at Burleigh Hill (locality 36), this shell bed consists of several thin (5-7 cm) discrete calcisiltite beds, whereas westward, at Decew Falls, this shell bed is present as a thin amalgamated bed about 10 cm thick. The "*Coolinia subplana*" bed may represent winnowed distal storm beds deposited well below the fair weather wave base and below all but the deepest storm waves (Brett, 1989). The fauna within this bed can be assigned to the *Coolinia subplana*-*Dalejina* community of Brett (1983a; 1989) occupying higher energy environments.

Four brachiopod species were analysed from the *Coolinia subplana* Bed; *Resserella elegantula elegantula*, *Coolinia subplana subplana*, *Leptaena rhomboidalis rhomboidalis* and *Dalejina*. Microstructurally, most brachiopod calcite appear to be in a good preservation state, although post-depositional alteration is evident in the remaining specimens (Fig. 4.19; 4.20). There are significant difference in brachiopod calcite compositions between the Rochester and Irondequoit Formations (Tables 4.2 and 4.4). The Mn and Fe contents are significantly higher in the Burleigh Hill brachiopods than those from the Lewiston Member or the Irondequoit Formation. This could be the result of significant leaching of Fe and Mn from aluminosilicates. However, these brachiopods may simply have precipitated shell calcite in depleted oxygen conditions that facilitated the incorporation of Mn and Fe. Differences between Mn/Fe contents are seen between the strophomenids *Coolinia subplana* /*Leptaena rhomboidalis* and the orthids *Resserella elegantula* and *Dalejina*. The higher Mn/Fe contents of the strophomenids may, in part, be a function of laminar secondary-layer calcite secretion.

Table 4.4. Unaltered brachiopod chemistries from locality 36 (Burleigh Hill Member)

Brachiopod species	Stat.	Ca	Mg	Sr	Mn	Na	Fe	Sr/Ca 1000
<i>Atrypa</i>	mean	348597	3920	2111	122	1526	639	5.98
	S. Dev.	17533	370	670	35	247	83	1.46
	min	288792	3390	1165	70	1075	470	3.85
	max	422530	4410	2900	180	1860	720	8.22
<i>Resserella</i>	mean	358316	5028	2368	192	1451	752	6.53
	S. Dev.	36873	820	616	39	118	141	1.33
	min	285087	3980	1255	110	1325	535	3.88
	max	415023	6360	2975	250	1610	915	8.04
<i>Leptaena</i>	mean	344161	5485	2555	190	1403	902	7.14
	S. Dev.	59361	1987	1300	50	157	245	2.86
	min	275644	3765	1170	140	1280	620	4.24
	max	380111	7660	3750	240	1580	1060	9.95
<i>Coolinia</i>	mean	380941	6725	2462	272	1452	1309	6.58
	S. Dev.	27564	2792	695	52	97	263	2.21
	min	380941	3420	1755	210	1335	890	4.34
	max	407550	10080	3315	360	1600	1605	9.23
<i>Whitfieldella</i> sp.		351754	5790	2510	205	1450	864	7.14

All elemental concentrations are in ppm

Table 4.5. Unaltered brachiopod chemistries from locality 34 (Burleigh Hill Member)

Brachiopod species	Stat.	Ca	Mg	Sr	Mn	Na	Fe	Sr/Ca 1000
<i>Atrypa</i>	mean	358373	4930	1998	308	1459	744	5.55
	Std. Dev.	11490	1546	467	114	119	135	1.14
	min	342014	3170	1610	160	1310	570	4.53
	max	376040	6810	2600	415	1595	930	6.92
<i>Resserella</i>	mean	352849	5490	1892	244	1431	825	5.35
	Std. Dev.	32085	2398	439	83	84	210	1.00
	min	304150	2940	1315	140	1340	620	3.77
	max	392850	8470	2665	390	1565	1160	6.78

All elemental concentrations are in ppm

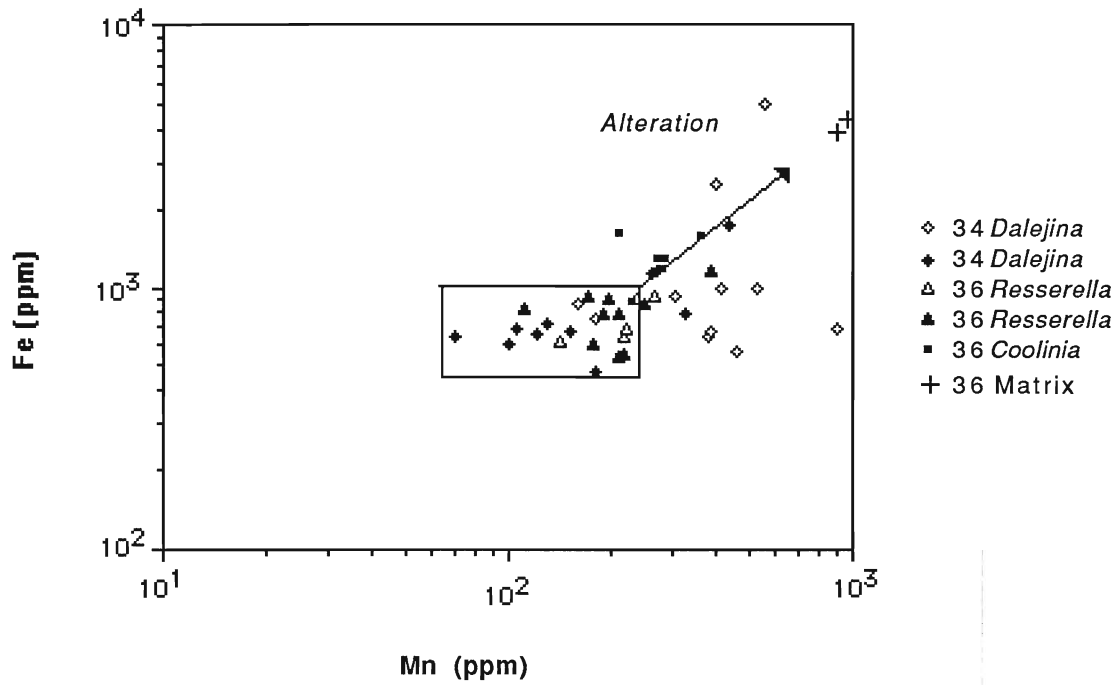


Figure 4.19. Scatter plot of Fe vs Mn for all species from the Burleigh Hill Member (Clinton Group). The diagenetic trend shows an increase of Mn and Fe contents with progressive diagenesis. The field represents pristine brachiopods

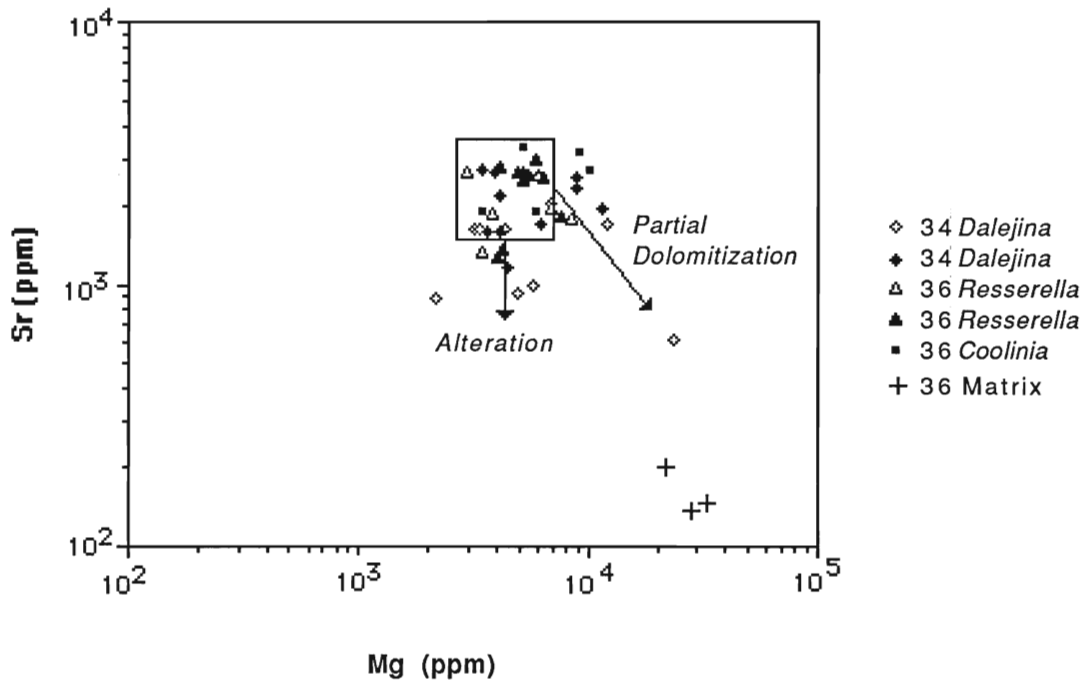


Figure 4.20. Scatter plot of Sr vs Mg for all brachiopod species of the Burleigh Hill Member (Clinton Group). The diagenetic trend shows an decrease of Sr with progressive alteration and an increase in Mg contents with partial dolomitization. The field represents pristine brachiopods.

Sr contents are unusually high for all four species, falling well outside the range of chemistries recorded in this study and other Silurian brachiopods previously (Brand and Morrison, 1987). It is uncertain whether this is a physiological phenomena or a reflection of originally high Sr content of the local depositional waters. Sr contents in brachiopods from the Lewiston Member (~1200 ppm) and the overlying Burleigh Hill Member (~2300 ppm) are significantly different. This twofold increase in Sr contents occurs in *Resserella elegantula*, *Atrypa reticularis* and *Whitfieldella nitida*. The concentration of Sr in modern oceans is quite uniform, and mean oceanic Sr composition has apparently remained fairly constant throughout the Phanerozoic (Holland, 1978, 1984; Brand and Morrison, 1987; Brand, 1988). Consequently, this observed increase may represent a regional influx of Sr-rich waters; the source of which is difficult to determine. Strontium derived from weathering of the Appalachian landmass to the east may explain the lateral east-west decline of Sr contents in the "*Coolinia subplana*" Bed.

Conclusions

Articulate brachiopods collected from the Middle Silurian Clinton Group are in general chemically and microstructurally well preserved. However, post-depositional alteration of some brachiopod shell calcite has resulted in Mg, Mn and Fe enrichments while the retention of Na and Sr contents suggests that the diagenetic waters were probably of marine- or mixed-water derivation. Subsequent, Mg-rich dolomitizing fluids selectively replaced matrices leaving brachiopods generally unaffected.

Clinton Group brachiopods apparently fractionated Mg and Na, which has been demonstrated previously in studies of other Paleozoic brachiopods (Brand and Veizer, 1980; Popp et al., 1986b; this study). The incorporation of

Mg and Na into the shell calcites of *Atrypa reticularis*, *Eospirifer radiatus* and *Whitfieldella nitida* was apparently taxonomically controlled. In contrast, Sr contents in brachiopod shell calcite were largely determined by the ambient concentrations of Sr in seawater. No significant isotopic and elemental trends were observed corresponding to a transgressive-regressive cycle is recognized in the Lewiston Member. This cycle may be illusory because the seawater conditions remained fairly constant during this vertical sequence. Slight variations in elemental contents and isotopic values may have been determined by inherent physiological variability and random temperature, salinity and growth rate fluctuations. Minor depth changes may have caused the migration of facies belts, explaining the lithological and paleoecological changes. Isotopic analysis of *Eospirifer radiatus* and other brachiopods from the Rochester and Irondequoit Formations averaged -3.3‰ for $\delta^{18}\text{O}$. Paleotemperatures calculated from pristine shell calcites ranged from 18°C - 32°C , which is in accordance with a postulated equatorial position of their habitats. The mid-Wenlockian ocean situated within the northern Appalachian Basin had oceanic $\delta^{18}\text{O}$ values similar to that observed in modern oceans. Uncorrected $\delta^{18}\text{O}$ contents of brachiopod calcite from this study do not support the assertion that Silurian oceans were depleted in $\delta^{18}\text{O}$ by 5‰ - 6‰ (Brand and Veizer, 1981; Veizer et al., 1986; O'Shea et al., 1988).

CHAPTER 5

Diagenetic and paleoenvironmental study of brachiopod calcite
from the Middle and Upper Ordovician;
southern Ontario and Manitoulin Island.

INTRODUCTION

Marine sediments of the Middle and Upper Ordovician of Ontario were deposited in apparently warm water, shallow-marine seas close to the equatorial belt (Scotese et al., 1979; Brookfield and Brett, 1988) and contain a diverse fauna including brachiopods, corallgal colonies, nautiloids, crinoids and trilobites. Brachiopods are common to the complex limestone facies of the Trenton Group which represents a carbonate sequence deposited on a transgressed shelf (Brookfield and Brett, 1988). Similarly, brachiopods are also present within basal sections of the Collingwood Formation (Whitby Formation) black shales which were deposited within a shallow anoxic epicontinental sea (Johnson and Rong, 1989)

The purpose of this chapter is to evaluate the degree of chemical preservation of three commonly occurring brachiopods within shales and limestones of the Middle and Upper Ordovician. If brachiopod calcites are unaltered, investigation of elemental and isotopic trends in shell calcites, associated with transgressed carbonate facies and anoxic environments, will proceed.

GENERAL GEOLOGY

Paleozoic sedimentary accumulation within southern Ontario and New York State was probably controlled by plate motions and orogenic processes affecting the stable Precambrian North American craton (Sanford et al., 1985). Sedimentary deposition was constrained by the relative uplift or subsidence of two depositional basins, the Michigan and Appalachian, and the arch that separated them (Algonquin-Findlay). Uplift during the Lower Ordovician,

resulted in the subaerial exposure of strata in southern Ontario (Telford, 1978; Sanford et al., 1985). By early Middle Ordovician, the regional subsidence of the arch, associated with the Taconic Orogeny (Rodgers, 1971), created a broad ramp that extended across southern Ontario, into New York State and as far as West Virginia and Maryland (Titus 1986; Carter et al., 1988; Brookfield and Brett, 1988). The ramp deepened to the west and a shelf break was present in central New York State (Cisne et al., 1982). The resultant transgression of the shelf spanned in age the mid-Blackriveran to earliest Maysvillian (Barnes et al., 1978; Ludvigsen, 1978) and resulted in the sequential deposition of supratidal/tidal flat clastics and carbonates (Gull River Formation), lagoonal/shoal bar carbonates (Bobcaygeon Formation), and shallow to deep shelf carbonates (Verulam and Cobourg Formations), in southern Ontario (Fig. 5.1). The ramp and basin were influenced by gentle crustal upwarping (Titus and Cameron, 1976; Titus, 1986) and facies distribution was controlled by emergent carbonate shoals and Precambrian Shield islands (Brookfield and Brett, 1988). Marine sedimentation on a Precambrian (Lorraine Quartzite) rocky shore occurred in the Manitoulin Island area (Johnson and Rong, 1989) where the Basal Beds were succeeded by the Swift Current, Cloche Island, Verulam and Cobourg Formations (Fig. 5.2).

At the beginning of the Upper Ordovician, subsidence of the Appalachian basin associated with the Taconic Orogeny, buried the carbonate sediments of southern Ontario with grey/black shales of the Whitby Formation. Trenton Group limestones in Virginia and West Maryland were similarly replaced by clastics of the Martinsburg and Reedsville Shales (Kreisa, 1981; Carter et al., 1988). Suprajacent calcareous shales and carbonates of the Georgian Bay Formation are deposited in southern Ontario. In Manitoulin Island, rapid transgression resulted in the deposition of Collingwood Formation (Whitby Formation) black

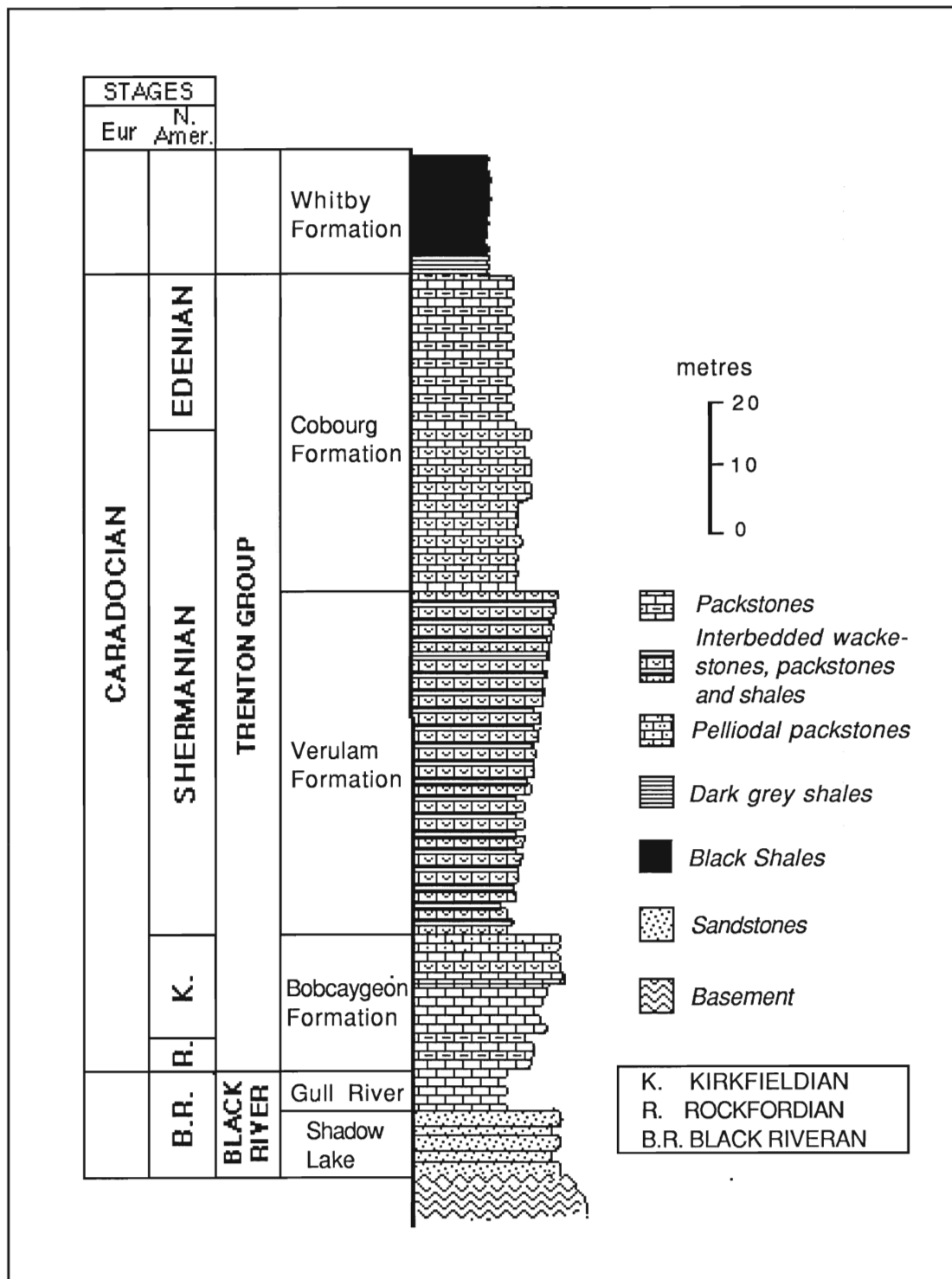


Figure 5.1. Generalized stratigraphic section of southern central Ontario. Ages from Rickard (1975); Sweet and Bergstrom (1976); Ludvigsen and Odin (1978); Brookfield and Brett (1988).

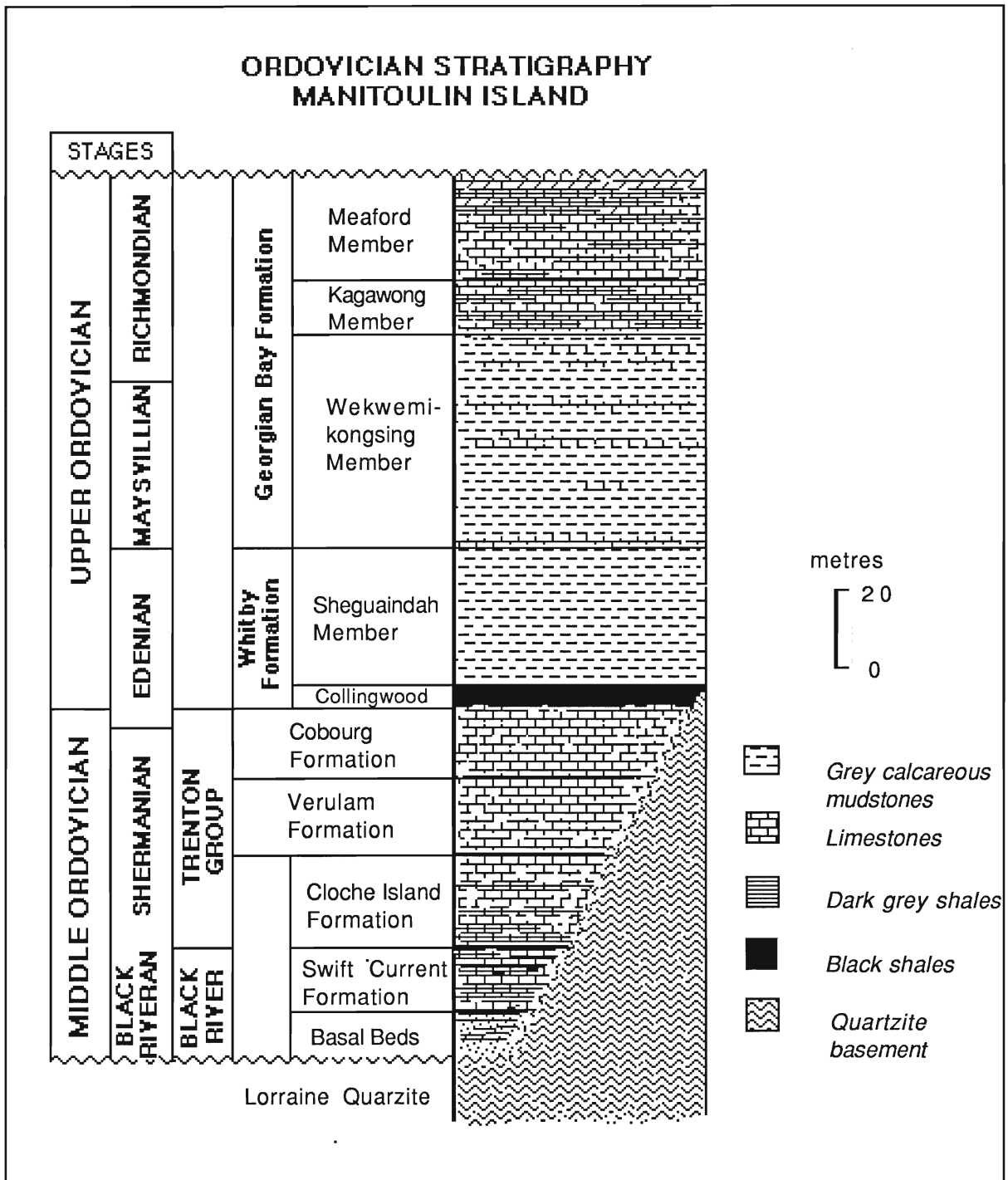


Figure 5.2. Middle and Upper Ordovician stratigraphy of Manitoulin Island. Stratigraphic information and ages are from Barnes et al., 1978; Telford (1978), Sanford and Mosher, (1978), Telford et al. (1981), Johnson and Rong (1989).

shales, which were succeeded by shales of the Sheguiandah Member (Whitby Formation), and deposition of the Wekwemikongsing, Meaford and Kagawong Formations (Georgian Bay Formation; Sanford and Mosher, 1978; Johnson and Rong, 1989; Fig. 5.2).

RESULTS AND DISCUSSIONS

Chemical trends

Three brachiopod species, *Dalmanella rogata*, *Rafinesquina eltoidea* and *Sowerybella* sp., were analysed from shale and limestone units of southern Ontario and Manitoulin Island (Table 5.1). SEM analysis of shell calcites from these species indicates that preservation states are variable. Good microstructure is observed in a number of specimens primarily from the Trenton Group and Whitby Formation. However, the majority of shell calcites appear to have undergone some degree of postdepositional alteration. Although primary foliation is generally retained, there is considerable fusing of calcite laths/rods and minor reprecipitation of cements between fibres. Correspondingly, chemical alteration is apparent in a greater number of shell calcites (Table 5.2). Many specimens contain elevated Mn and Fe contents, and are reciprocally depleted in Sr and Na, which is diagnostic of partial re-equilibration of brachiopod calcite with diagenetic waters (Fig. 5.3; Brand and Veizer, 1980; Al-Aasm and Veizer, 1982; Brand, 1989). Furthermore, factor analysis supports this observation because Fe and Mn are significantly loaded together (Factor 1, Tables A-15 to A-18).

Table 5.1. Geochemical data of Middle and Upper Ordovician brachiopods from southern Ontario and Manitoulin Island.

Brachiopod species	Stat.	Ca	Mg	Sr	Mn	Na	Fe	Al	I.R.
<i>Dalmanella</i> (ALL; N=45)	Mean	377217	5847	754	222	1046	1561	137	11.8
	S. Dev.	55589	5079	249	178	247	588	147	
	min	215150	1135	370	70	345	90	0	
	max	621040	19670	1395	610	3565	6700	740	
<i>Rafinesquina</i> (ALL; N=64)	Mean	377249	4137	965	260	1143	640	118	7.6
	S. Dev.	19906	1558	222	243	456	380	185	
	min	317000	2490	490	45	215	135	0	
	max	440450	11100	1485	1160	2370	2300	1300	
<i>Sowerybella</i> (ALL; N=21)	Mean	386786	3069	792	118	1108	402	154	7.3
	S. Dev.	24265	646	206	61	340	238	96	
	min	303810	1510	310	40	100	50	55	
	max	413690	4850	1100	270	1525	790	420	
.....									
<i>Dalmanella</i> Unaltered (VERULAM) (N=9)	Mean	384387	3132	835	100	973	149	105	5.4
	S. Dev.	16498	551	138	28	320	49	77	
	min	360090	1935	685	35	540	90	30	
	max	403820	3675	1135	135	1620	230	290	
<i>Rafinesquina</i> Unaltered (VERULAM) (N=17)	Mean	358731	3470	1073	94	1244	456	110	4.3
	S. Dev.	10385	580	104	39	216	119	112	
	min	346390	2740	955	70	955	335	5	
	max	376400	4560	1270	160	1580	620	260	
<i>Sowerybella</i> Unaltered (VERULAM) (N=16)	Mean	388634	3050	843	106	1189	387	156	7.1
	S. Dev.	25063	400	150	458	179	241	99	
	min	303810	2435	650	40	850	50	55	
	max	413690	4270	1100	205	1525	790	420	

All elemental concentrations are in ppm.

Table 5.2. Comparison of microstructural preservation and chemistry for selected brachiopods, representing different species, and lithologies. Lithology symbols denote (S= dark grey shale; CM= calcareous mudstones; ML= micritic limestones; W= wackestones; P= packstones; CG= crinoidal grainstones)

Sample Number Specimens	Species	Age	Lithology	Preservation State	Diagenetic features	Mg (ppm)	Mn (ppm)	Fe (ppm)	Figured
835	<i>Sowerybella</i>	Ver.	W	Good	No	2975	40	50	
798	<i>Sowerybella</i>	Ver..	W	Fair	Slight diss.	3240	100	310	
797	<i>Sowerybella</i>	Ver.	P	Fair	Slight diss.	3570	160	400	
765	<i>Sowerybella</i>	Ver..	P	Fair	Slight diss.	4270	205	680	
773	<i>Dalmanella</i>	Ver..	CG	Good	Slight diss.	3185	130	120	2.22
736	<i>Dalmanella</i>	G.B..	S	Poor	Dissolution	13030	510	3900	
776	<i>Dalmanella</i>	Ver.	CP	Good	Slight diss.	3990	150	130	
839	<i>Dalmanella</i>	Ver.	CG	Good	Slight diss.	3350	110	90	
899	<i>Dalmanella</i>	Whit.	S	Good	Slight diss.	4810	70	550	
794	<i>Rafinesquina</i>	Ver.	P	Good	None	3790	115	665	
825	<i>Rafinesquina</i>	Ver..	CG	Poor	Yes	4295	300	700	
764	<i>Rafinesquina</i>	Ver..	P	Poor	Yes	3810	160	520	2.21
827	<i>Rafinesquina</i>	Ver..	CG	Poor	Yes	3945	255	430	
822	<i>Rafinesquina</i>	Ver..	P	Good	No	3160	50	495	

All elemental values are in ppm.

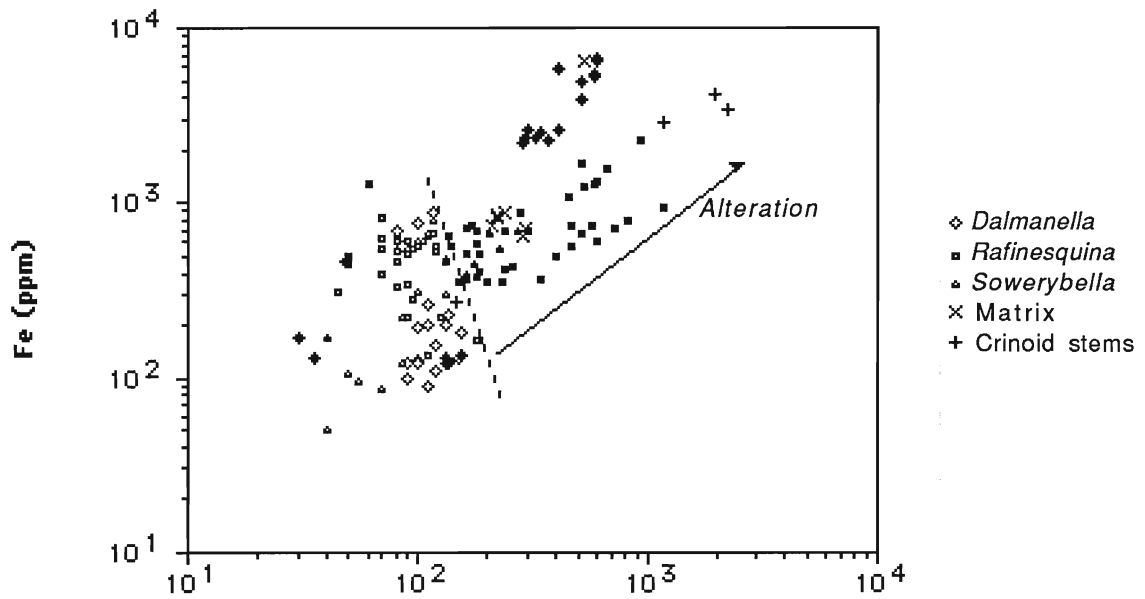


Figure. 5.3. Scatter plot of Fe vs Mn for all brachiopods from the Middle and Upper Ordovician of southern Ontario and Manitoulin Island. Open symbols denote unaltered specimens and closed symbols denote altered material. Altered specimens that plot with low Mn contents (~40-75ppm) are partially silicified.

Isotopic trends

Covariances of $\delta^{13}\text{C}$ and $\delta^{18}\text{O}$ contents with diagenetic re-equilibration of shell calcite is observed in specimens from the Middle and Upper Ordovician Ontario. For example, Mn and $\delta^{18}\text{O}$ contents of brachiopods show complementary diagenetic trends (Figure 5.4) and altered brachiopods are significantly more negative in $\delta^{13}\text{C}$ and $\delta^{18}\text{O}$ (Figure 5.5). The best preserved brachiopod shell calcites of *Dalmanella rogata* and *Rafinesquina deltoidea* have an average $\delta^{13}\text{C}$ of $+1.2\text{‰}$ (range 0.5‰ to 1.7‰) and contain an average value $\delta^{18}\text{O}$ of -5.7‰ (range -6.8‰ to -4.5‰). In contrast, altered calcite have a more negative average $\delta^{13}\text{C}$ of -0.2‰ (range -0.8‰ to 0.6‰) and $\delta^{18}\text{O}$ of -5.7‰ (range -6.8‰ to -4.5‰). It is apparent that all the Upper Ordovician brachiopods analysed are post-depositionally altered, whereas Trenton Group shell calcites are the least altered.

Lithology and preservation potential

Lithologic control of chemical alteration of carbonates is reported by Pingitore (1978, 1982). In this study, the preservation of brachiopod low-Mg calcite appears also to be directly dependant upon lithology and pore geometries. Brachiopods analysed from limestone facies (i.e. wackestones) have divergent diagenetic trends to those analysed from shale facies (Figure 5.6). The relative enrichment or depletions of elemental contents is dependant on a number of factors. The Mn and Fe contents of a diagenetic product will depend upon fluid compositions and the Eh of the diagenetic microenvironment. Meteorically-derived fluids are compositionally enriched in Mn and Fe relative to marine waters (Drever, 1982) only if they exist in lower oxidation states within a reducing phreatic zone (James and Choquette, 1984); reduced divalent ions are more readily available for incorporation into

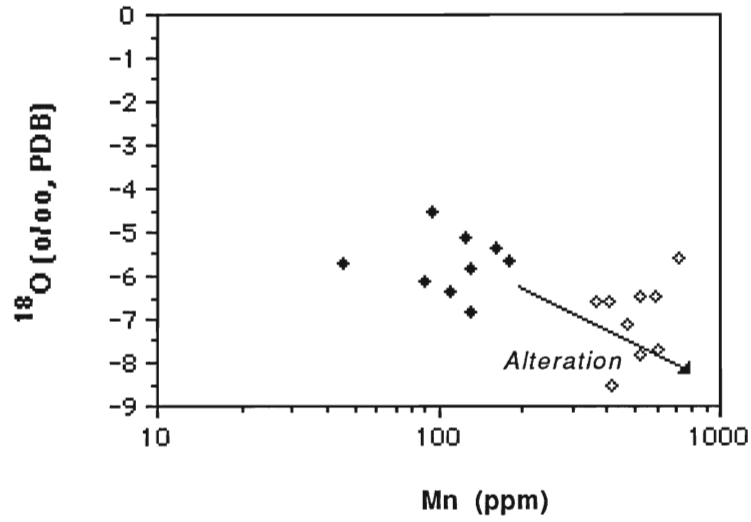


Figure 5.3. Diagenetic trend of oxygen isotopic composition for Middle and Upper Ordovician *Dalmanella* and *Rafinesquina* brachiopods of southern Ontario. Symbols denote; \diamond altered, \blacklozenge least-altered.

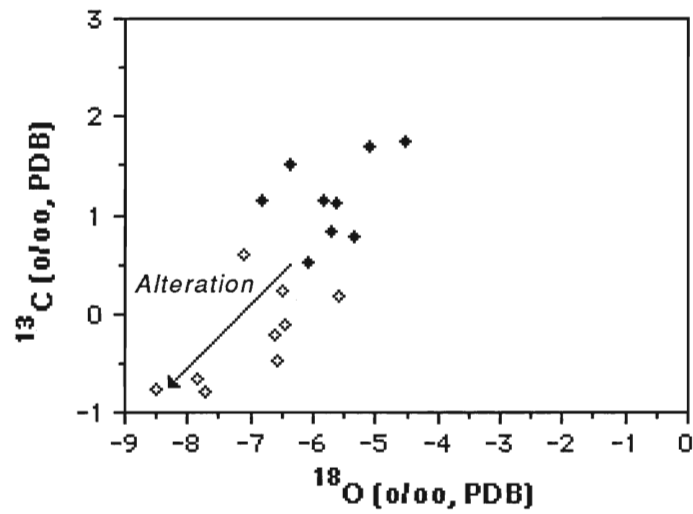


Figure 5.5. Diagenetic trend of isotopic compositions of *Dalmanella* and *Rafinesquina* brachiopods from the Middle and Upper Ordovician of southern Ontario and Manitoulin Island. Symbols as in Figure 5.4.

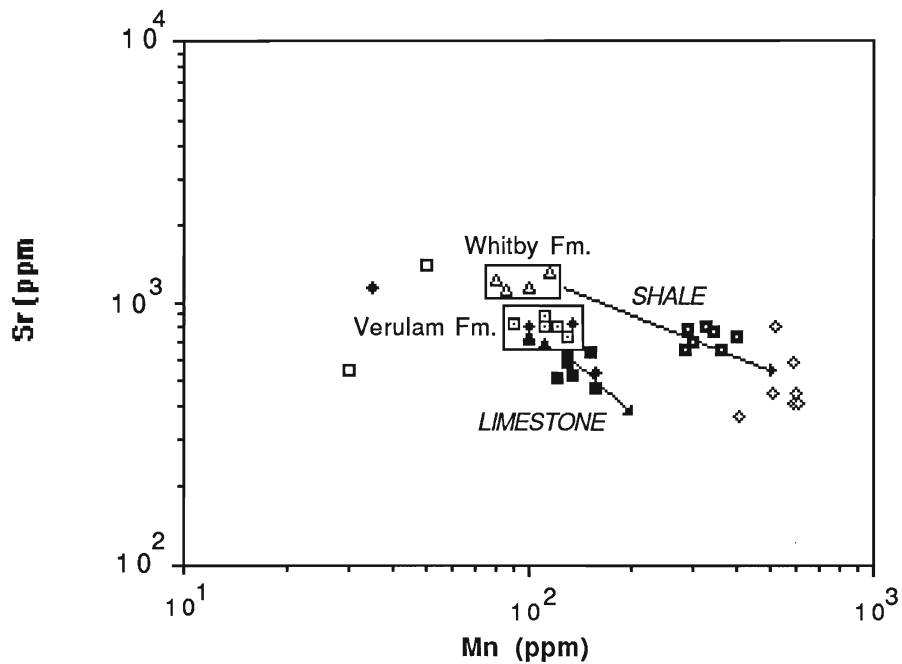


Figure 5.6. Scatter plot of Sr vs Mn for shell calcites of *Dalmanella rogate*. Fields define range of pristine brachiopods and arrows depict direction of alteration for brachiopod calcite in shales and limestones. □ Verulam (locality 63i); ♦ Verulam (63ii); ■ Wekwemikongsing (51); ◇ Sheguiandah (50); ■ Verulam (65); □ Bobcaygeon (66A); ▲ Verulam (66B); △ Collingwood beds; Whitby Fm. (59i). *Dalmanella* in the Verulam Formation are from mudstones and wackestones with the exception of locality 66B. *Dalmanella* calcites from the uppermost metre of cross laminated and bedded skeletal grainstone and packstone beds at Kirkfield Quarry (locality 65) are the most altered. Bioclasts are predominantly well sorted coarse crinoid columnals with brachiopod, bivalves and gastropods. Pore filling equant sparite is common. Thus pore geometries may have constrained diagenetic alteration and preservation potential.

diagenetic low-Mg calcite. The divergence of diagenetic trends observed here can be directly attributed to the lithological availability of Fe and Mn in shales compared to limestones. In addition, altered brachiopod calcites reflect the more "open", fluid controlled diagenesis of wackestone/packstone lithologies compared to diffusion controlled reactions in shale.

The control of lithology on potential preservation and magnitude of elemental repartitioning is also evident within brachiopod calcites of *Dalmanella rogata* and *Sowerybella* (Figure 5.7). The Na, Sr and Mg contents of *Dalmanella rogata* from the Verulam Formation are not significantly different between localities with the exception of those from the crinoidal grainstones at the Kirkfield road cut (locality 66B). Mn contents are elevated (Figure 5.6) and Na and Sr contents are significantly lower. Similarly, shell calcites of *Sowerybella* from a Verulam Formation wackestone bed from the County Road 6 Kirkfield exposure (locality 66b) are the least altered (Fig. 5.7). Specimens from skeletal packstones at Lakefield Quarry (locality 75) are increasingly altered, while those calcites from crinoidal grainstones (skeletal biosparites from localities 78, 79, 68) show the greatest effect of post-depositional alteration (Fig. 5.7). These crinoidal grainstones are pore filled with equant sparite cement. A spectrum of diffusion to fluid controlled diagenetic alteration appears to be directly controlled by lithology and pore geometries.

Diagenetic waters of the Middle and Upper Ordovician

Brachiopods altered in an essentially meteoric environment usually show a depletion of Sr and Na in association with Mn and Fe enrichments (Brand and Veizer, 1980; Al-Aasm and Veizer, 1982; Veizer 1983a) whereas the magnitudes of trace element diagenetic shifts are dampened in the presence of diagenetic waters of marine parentage (Veizer, 1983a). The concentration of

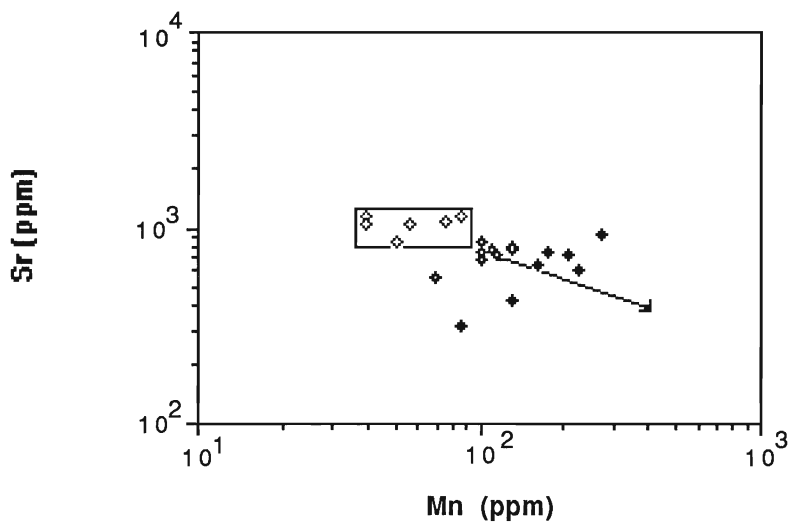


Figure 5.7. Scatter plot of Sr vs Mn for *Sowerybella* sp. Symbols denote lithology; \diamond wackestones (locality 66B), \blacklozenge packstones (localities 78i); and \blackstar grainstones (68, 77, 78i, 80). *Sowerybella* specimens show varying degrees of alteration which is controlled by lithology and pore geometry. A few of the crinoidal grainstone beds were graded and *Sowerybella* were in varying states of taphonomic preservation.

ionic species is that much greater (i.e. Na, Sr and Mg contents; Drever, 1982) and altered shell calcites retain high Sr and Na contents and enriched $\delta^{13}\text{C}$ and $\delta^{18}\text{O}$ compositions. Furthermore, Mg-depleted biogenic carbonates can gain Mg during recrystallization with marine derived waters (Baker et al., 1982).

Examination of chemical data for Trenton Group and Whitby Formation brachiopods of southern Ontario and Manitoulin Island suggests that there are different diagenetic fluids involved in brachiopod alteration (Figure 5.8). A plot of Na vs Mg for all brachiopods clearly illustrates these trends. Those brachiopods collected from southern Ontario show depletion of Na and Sr (not shown) with diagenesis, while Mg contents remain close to their original compositions. This chemical trend is characteristic of meteoric diagenesis described by previous authors (Brand and Veizer, 1980; Al-Aasm and Veizer, 1982; Veizer, 1983a; 1983b). In contrast, brachiopods analysed from the shales and carbonates of Manitoulin Island become progressively enriched in Mg with chemical alteration and do not show characteristic co-variant depletions of Sr and Na. The retention of Na, Sr and the enrichment of Mg suggests that the diagenetic waters responsible for alteration of shell calcites had significant ionic strength and were of marine parentage (Veizer, 1983a, b). These divergent diagenetic trends were observed in shell calcites of *Dalmanella rogata*, *Sowerybella*, *Rafinesquina deltoidea* and small rhynchonellids (*Rhynchotrema* sp.) from the Trenton and Whitby Formations. Moreover, analysis of brachiopods just from the Verulam Formation also revealed a similar diagenetic divergence between southern Ontario and Manitoulin Island, despite the fact that the lithologies of both areas are very similar; thin to medium (4-15 cm thick), irregularly bedded skeletal packstones and grainstones interbedded with thin grey green shales (Sanford and Mosher, 1978).

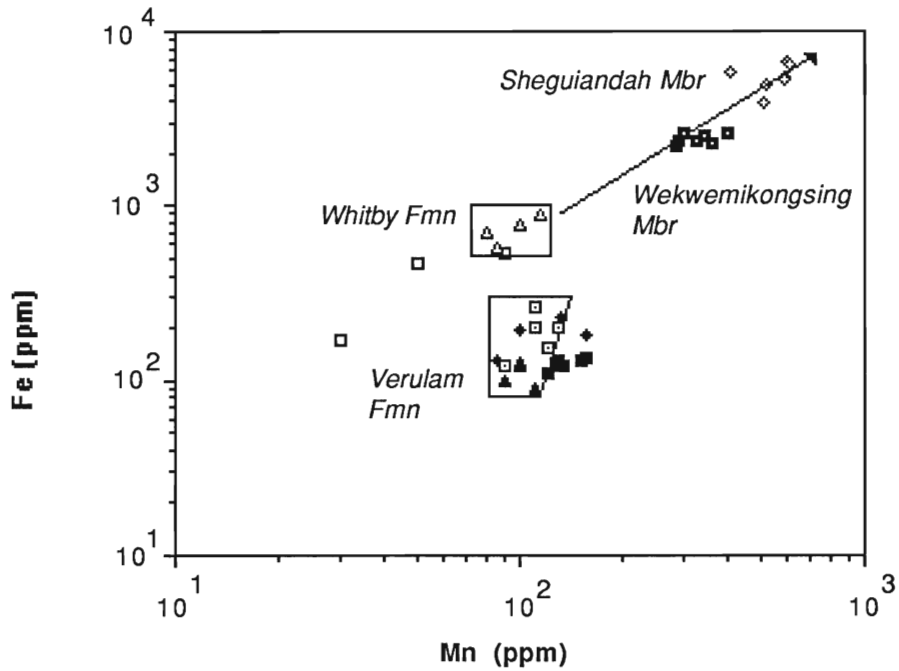


Figure 5.8. Scatter plot of Mn vs Fe for *Dalmanella rogata*. Symbols denote □ Verulam (locality 63i); ♦ Verulam (63ii); ■ Wekwemikongsing (51); ◇ Sheguiandah (50); ■ Verulam (65); □ Bobcaygeon (66A); ▲ Verulam (66B); • Collingwood beds; Whitby Fm. (59i). Fields represent chemically pristine brachiopods. Brachiopods from the Bobcaygeon Formation are partially silicified. *Dalmanella* brachiopods were collected from a shell pavement (6-8cm) within the upper sequence of grey shales belonging to the Sheguiandah Member in Manitoulin Island (Whitby Formation). This bed was composed exclusively of articulate *Dalmanella* coated with limonite. Their shell calcites are chemically altered, with elevated Mn, Fe and Mg contents (Fig. 5.?) and reciprocal depletion of Sr, Na, d13C and d18O contents. Similarly, *Dalmanella* collected from grey shales of the Wekwemikongsing Member in Manitoulin are also extensively altered.

The chemistries of the diagenetic fluids responsible for alteration can be estimated from the chemical contents and appropriate partition coefficients (Veizer 1983a, b; Brand, 1989b). Calculated molar ratios of the diagenetic fluids from southern Ontario suggests that the fluids were close to surface water compositions i.e. meteorically-derived. Furthermore, calculation of diagenetic waters from Manitoulin Island suggests that marine or marine-derived fluids were responsible for brachiopod alteration. However, experimental partition coefficients are variable and altered brachiopod calcite may not have fully equilibrated with diagenetic fluids. The limited isotopic data cannot confirm these diagenetic trends. Shell calcites from southern Ontario and those from Manitoulin Island show depletions of $\delta^{13}\text{C}$ and $\delta^{18}\text{O}$ with alteration, characteristic of meteoric derived waters (Veizer, 1983a; 1983b). Additional isotopic testing of brachiopods, cements and matrix from Manitoulin Island may help determine the waters involved in brachiopod alteration.

An explanation for these divergent diagenetic waters of the Trenton Group is at best speculative. The Algonquin Arch trending through southern Ontario was rejuvenated during Middle Ordovician times (Sanford et al., 1985) and the carbonate platform may have been emergent during Trentonian times (Telford, 1978; Sanford et al., 1985; Brookfield and Brett, 1988). Trenton carbonate deposition is often around Precambrian inliers (Liberty, 1969; Brookfield and Brett, 1988) and hardgrounds may or may not be evidence of aerial exposure of the platform (Brett and Brookfield, 1984). Dolomitization is widespread in the Middle Ordovician carbonates deposited basinward on the Findlay Arch. Sanford et al., (1985) suggests that dolomitizing fluids were either derived from Cambrian sandstones or from meteoric waters during a hiatus at the close of the Middle Ordovician. Conceivably, exposure of Trenton Group carbonates in southern Ontario may have resulted in the build-up of surficially

derived meteoric waters that were responsible for brachiopod alteration. In this scenario, brachiopods would have been close to the presumed recharge zone on the Algonquin Arch high and undergone alteration in gradients driven by these surficially derived fluids. In Manitoulin Island, there was an apparent hiatus before rapid transgression and deposition of the Upper Ordovician Collingwood Formation (Copper, 1978). Since this region was on the flank of the arch, there may not have been exposure of Trenton carbonates and alteration of brachiopod calcite could have proceeded within a phreatic mixing zone or marine phreatic zone.

PALEOENVIRONMENTAL ANALYSIS OF MIDDLE TO UPPER ORDOVICIAN

The least altered brachiopods were selected by evaluating elemental concentrations of Fe, Mn, Mg, Sr and Na in combination with microstructural preservation. Unaltered brachiopod calcites were recognized primarily from the Verulam and Collingwood Formations. As a preliminary caveat to further discussions, it must be stated that strict interpretations about *Sowerybella* and *Rafinesquina deltoidea* chemistry are constrained by the fact that the slightly fused nature of these strophomenid shell calcites, recognized as a primary structure by other authors (Rowell and Grant, 1987), may indeed be a diagenetic structure. Despite this, covariances of elemental contents will give a good indication of degree of chemical alteration and altered specimens are eliminated from further discussion. A number of potentially environmentally controlled chemical trends are evident in the best preserved material.

Taxonomic differences in shell calcite composition

Within the best preserved material of the Verulam Formation, there appears to be a significant difference in Fe contents between the strophomenids *Rafinesquina deltoidea* and *Sowerybella* with the orthid *Dalmanella rogata* (Table 5.3; t-test, $p < 0.05$, $f=31$). This may reflect either unrecognized diagenetic alteration, the Eh and potential reducing conditions of the depositional setting or a physiological/mineralogical difference between these species. Alternately it may be due to differences in habitat/substrate preference between each species.

Relationship of depth to Mg, Sr and Na compositions of brachiopod calcite

In a previous chapter, a possible relationship between Mg, Sr, Na contents and environmental factors (i.e., depth) was observed in Hamilton Group brachiopod species. A similar relationship is observed between the three species analysed from the Verulam Formation. Lithofacies distribution of Verulam sediments deposited on the Trenton platform range from shallow high energy shoal-bar facies to quieter, potentially deeper shoal margin and open marine facies (Brett and Brookfield, 1984). In general, distribution of brachiopods is restricted to various lithotypes and presumed energy environments (Brookfield and Brett, 1988). *Dalmanella rogata* and *Sowerybella* were collected from mudstone and wackestone sequences that may represent quiet-water, low to moderate energy environments whereas *Rafinesquina deltoidea* were sampled from presumably shallower, shoal-bar crinoidal grainstones and packstones. Mg, Sr and Na contents of *Rafinesquina deltoidea* shell calcite are correspondingly higher compared to *Dalmanella rogata* and *Sowerybella* (Fig. 5.9). Although there is the potential for diagenetic bias, this

Table 5.3. T-test: Verulam Formation

		<i>Rafinesquina</i>		<i>Sowerybella</i>	
	Element	Signif.	T-stat	Signif.	T-stat
<i>Dalmanella</i>	Ca	$p > 0.05$	0.127	$p > 0.05$	0.459
	Mg	$p < 0.05$	<u>2.860</u>	$p > 0.05$	0.444
	Sr	$p > 0.05$	1.085	$p > 0.05$	0.139
	Mn	$p > 0.05$	0.333	$p > 0.05$	0.674
	Na	$p > 0.05$	2.258	$p > 0.05$	1.544
	Fe	$p < 0.05$	<u>2.902</u>	$p < 0.05$	<u>5.862</u>
	D.O.F.		(25)		(24)
<i>Sowerybella</i>	Ca	$p > 0.05$	0.386		
	Mg	$p < 0.05$	<u>3.131</u>		
	Sr	$p > 0.05$	1.106		
	Mn	$p > 0.05$	0.404		
	Na	$p > 0.05$	0.904		
	Fe	$p > 0.05$	1.340		
	D.O.F.		(33)		

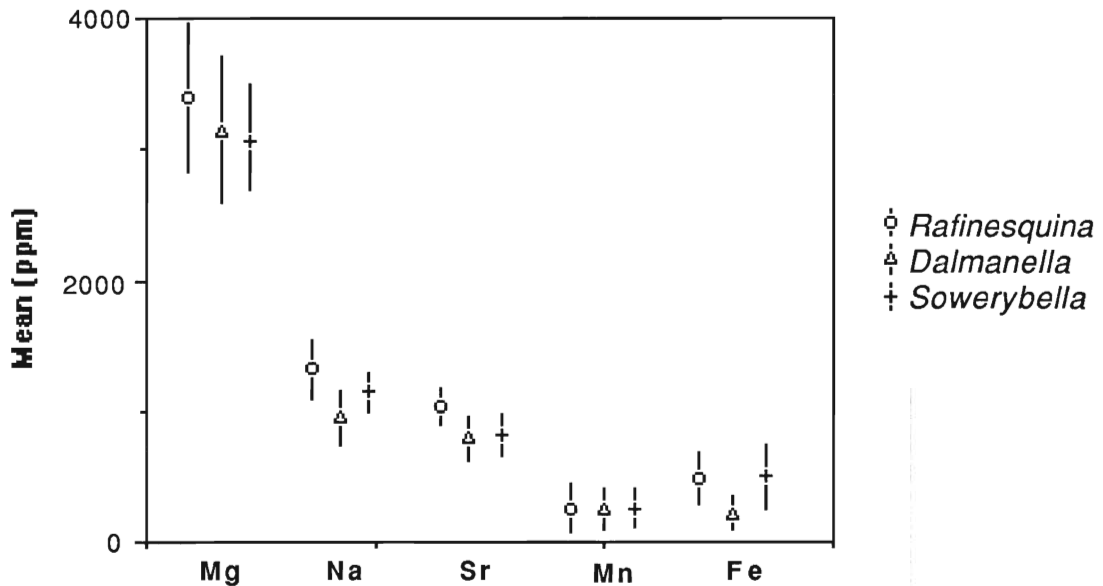


Figure 5.9. Mean and standard deviation of unaltered chemistries of *Dalmanella*, *Rafinesquina* and *Sowerybella* from the Verulam Formation. There are differences in Mg, Sr and Na chemistries between the shallow water *Rafinesquina* and slightly deeper *Dalmanella* and *Sowerybella*. *Sowerybella* and *Dalmanella* were collected from sequences of thin nodular wackestones and mudstones. *Sowerybella* brachiopods were often found in shell pavements on the upper surfaces of medium bedded, nodular mudstones and wackestones. Taphonomic preservation was good, with articulated valves and lack of fragmentation common. *Dalmanella* were present within thin (3-5cm thick) irregular, hummocky mudstones and wackestones, interbedded with occasional packstones (crinoidal biosparites) and thin partings of dark grey claystones. Their shells were commonly articulated and there was little evidence of abrasion, encrustation or fragmentation of valves. This suggests that there was minimal reworking and transport of these brachiopods. They may have inhabited deeper parts of the shoal margins or depressions, close to the storm wavebase (Brookfield and Brett 1988).

Disarticulated *Rafinesquina deltoidea* were collected from thin to thick (5cm-25cm thick) planar or irregular bedded, graded packstone and grainstone beds. These grainstones often contain low-angle cross lamination and are composed of well rounded crinoidal stems and other bioclasts with *Rafinesquina* as the dominant brachiopod. Graded grainstone beds often contain disarticulate and abraded *Rafinesquina* in lower part of bed and articulated *Sowerybella* on the upper surface (e.g., Lakefield quarry; Trenton). It is uncertain if this represents ecologic succession within the bed or size sorting of storm beds (Westrop, 1986). *Rafinesquina* collected from these low-angle cross-laminated grainstones are interpreted by Brett and Brookfield (1984) as representing sediments deposited on a shallow shoal bar facies, within the fairweather wavebase.

chemical relationship may reflect environmental/physical conditions (i.e., depth, turbidity and energy of environment) and substrate preferences which controlled precipitation rates and shell calcite compositions.

Brachiopod calcite and low oxygen conditions

Articulated *Dalmanella rogata* were analysed from the dark grey shales of the lower Whitby Formation, which overlies the Cobourg Formation (locality 59). The lowest couple of metres of the Whitby is composed of a sequence of dark grey shales separated by thin shell pavement beds (0.5-1.5cm thick). *Dalmanella rogata* brachiopods are the dominant fauna within these winnowed shell beds. Preservation is variable, with a spectrum of articulated valves to disarticulated, abraded and fragmented specimens. Significant reworking, and postmortem transport indicate a position above storm wave base. Overlying these basal beds are black fissile shales that contain abundant *Pseudogygites* trilobites in varying states of articulation. The lack of bioturbation, petroliferous nature of the dark shales, and presence of abundant pyrite suggests a high input of organics and a potentially anoxic/reducing environment.

Whitby Formation *Dalmanella rogata* are microstructurally preserved and have Mn contents similar to *Dalmanella rogata* from mudstones and wackestones of the Verulam Formation. However, Fe contents are significantly higher (Fe; 575-880ppm; Fig. 5.10) which is possibly explained by a difference in redox conditions between the shallow turbid shoal-margin facies of the Verulam and the black shale facies of the Whitby Formation. In Manitoulin Island, the black shale facies of the Collingwood Formation has been interpreted to be the result of a thermocline, developed just below the normal wavebase (Johnson and Rong, 1989). Emplacement of the thermocline is modelled on the periodic influx of brackish waters into an epicontinental sea

(Witzke, 1987). The presence of an oxycline/pycnocline close to shallow marginally placed *Dalmanella rogate* populations may have caused the periodic impingement of dysaerobic and potentially more reducing water conditions into bottom waters surrounding *Dalmanella rogate*. As previously discussed, these ancient brachiopods probably could survive periods of dysaerobia and as such will reflect time-averaged incorporation of redox controlled elements.

The chemical compositions of *Dalmanella rogate* brachiopods from the Verulam Formation appear to be related to type of facies. *Dalmanella rogate* from the distal shoal margin mudstones and wackestones at the Bolsover roadcut (locality 63iii; Figure 5.10) have generally higher Mn and Fe contents than *Dalmanella rogate* from the shoal bar facies (locality 66B; Figure 5.10). Slight differences in oxic conditions between these environments may have similarly affected the availability of Fe and Mn for incorporation into *Dalmanella rogate* shell calcite.

Depositional waters

Previous authors have used elemental compositions of ancient pristine molluscan carbonate and experimentally derived partition coefficients to determine the chemistry of depositional waters (Brand, 1986, 1987, 1989b). This study has indicated that there is fractionation of Mg, Sr, Na and possibly Mn by varying degrees within brachiopod species of the Hamilton Group (Middle Devonian) and Clinton Group (Middle Silurian). Trenton Group brachiopod shell calcite appears to reflect a complex interaction of taxonomic regulation and possible environmental controls. Partition coefficients are derived from inorganic calcites, and biological regulation of shell calcite

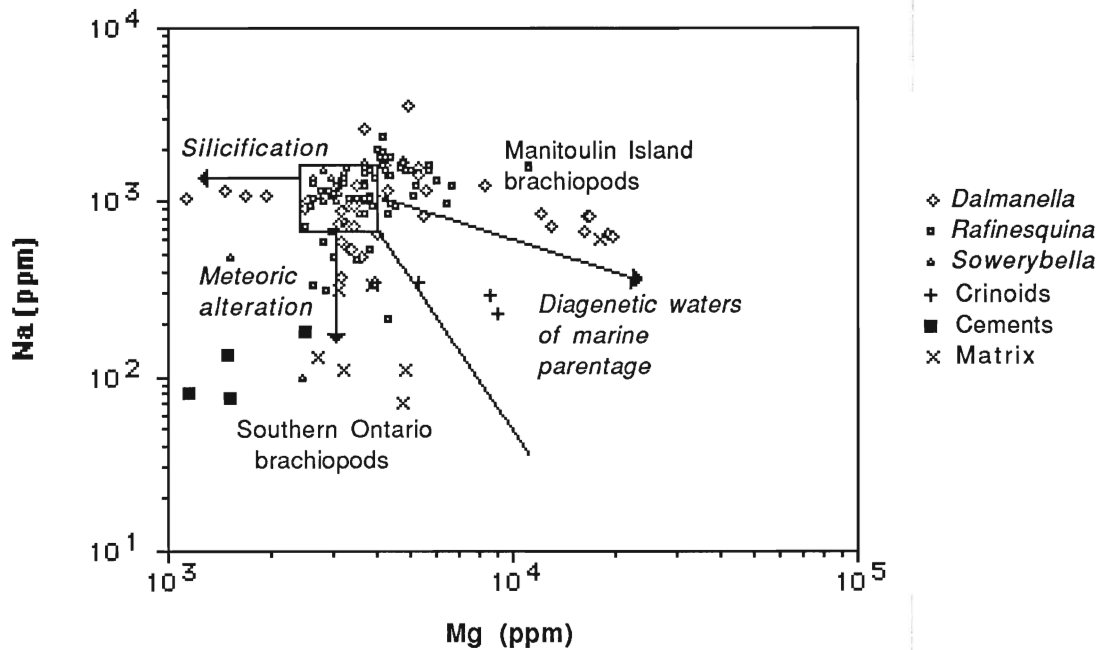


Figure 5.10. Scatter diagram of Na vs Mg for brachiopods from Manitoulin Island and from southern Ontario. Specimens collected from the Trenton Group, Sheguiandah and Wekwemikongsing Members in Manitoulin Island were altered in the presence of Sr, Mg and Na rich water (i.e. of marine derivation). Brachiopods from the Trenton Group in southern Ontario were altered in the presence of meteoric type waters. These divergent diagenetic trends are observed for *Rafinesquina*, *Dalmanella* and *Sowerybella* brachiopods. Field indicates ranges of unaltered specimens. Silicification trend occurs in Bobcaygeon Formation brachiopods.

composition does not allow the unequivocal retrieval of information about original depositional waters from brachiopod calcites.

Isotope trends

Paleogeographic reconstructions of the Trenton platform suggests that carbonates were precipitated from warm, shallow-marine waters within the equatorial belt (Scotese et al., 1984; Brookfield and Brett, 1988). Salinities were probably within normal ranges and disturbed only by episodic climatic depressions contributing fresh waters to surficial marine environments. Changes in the isotopic compositions of brachiopod shell calcites, associated with the marine transgression in Ontario, are not evident with data from this study. Slight differences in the $\delta^{18}\text{O}$ contents of pristine brachiopods calcites may be related to natural isotopic variability of shell calcite, localized water temperature and salinity changes or unrecognized diagenetic effects. The $\delta^{13}\text{C}$ contents of Trenton Group brachiopods become more negative by 1‰ (PDB) from the Bobcaygeon to Cobourg Formations, although the isotopic data is limited. Brachiopods from the shallow shoal facies are the most positive in $\delta^{13}\text{C}$ whereas those specimens from the deeper shoal margin proximal facies are slightly enriched in ^{12}C . Further isotopic testing needs to be done to confirm whether there is significance to this trend.

CONCLUSIONS

Many of the brachiopod shell calcites analysed from limestones and shales of the Middle and Upper Ordovician are chemically altered and a relationship between the degree of chemical alteration and lithology is observed. Divergent diagenetic trends are apparent between altered

brachiopods analysed from southern Ontario and those from Manitoulin Island. Brachiopod calcites analysed from southern Ontario appear to have altered in meteorically derived waters which may have resulted from exposure of Trenton carbonates at the end of the Middle Ordovician. In contrast, brachiopod calcites in Manitoulin Island altered in the presence of diagenetic fluids of marine parentage.

Verulam Formation *Rafinesquina deltoidea*, analysed from shallow shoal bar facies, are elevated in Mg, Sr and Na contents compared to *Sowerybella* and *Dalmanella rogata rogata*, which inhabited deeper shoal margin environments. This trend confirms a previous relationship of brachiopod calcite composition with depth observed for Hamilton Group brachiopods (this study). The Fe chemistry of unaltered *Dalmanella rogata* calcite appears to be related to ancient seawater conditions. Marginally positioned *Dalmanella rogata* populations, which presumably lived above a thermocline developed during deposition of the Collingwood Formation, may reflect periodic incursions of oxygen deficient waters into shallower areas of the shelf.

CHAPTER 6

Secular trends of oxygen and carbon isotopes

INTRODUCTION

Marine sediments have provided a means for investigating the isotopic and elemental changes in ocean-atmosphere chemistry during the Phanerozoic (e.g., Holland, 1978, 1984; Veizer, 1985). Modelling of the long term changes in carbon, atmospheric O₂ and CO₂ levels, and climate have been focused on the isotopic compositions of marine carbonates (Kump, 1988; 1989a, b; Kasting, 1989; Popp et al., 1989; Lasaga, 1989). Furthermore, analysis of chemical sediments has provided a means of isotopically resolving stratigraphic correlations and investigating anoxic ocean events (e.g., Arthur et al., 1985a, b; Holser et al., 1986; Magaritz et al., 1986; Aharon et al., 1987; Arthur et al., 1989; Brasier and Magaritz, 1989). However, the vulnerability of chemical sediments to post-depositional alteration has led to the increasing use of biogenic carbonates for paleochemical investigation (e.g., Holser, 1984; Veizer et al., 1986; Popp et al., 1986; Holser et al., 1989; Gruszczynski et al., 1989; Brand, 1989a, c), since chemical trends derived from matrix carbonate will tend to reflect polymineralic compositions and varying degrees of diagenetic re-equilibration (Popp et al., 1986). Thus brachiopods, composed of low-Mg calcite which is stable in most diagenetic settings, can be used since they record the ambient isotopic compositions of their depositional environment. Kinetic fractionation in biogenic carbonates is dependant on calcification rates; the faster growth rates the greater the apparent isotopic disequilibria (McConnaughey, 1989a). Since brachiopod metabolism is slow, it is likely that ¹³C and ¹⁸O were indeed in equilibrium with ambient conditions. Moreover, brachiopod calcites and preserved aragonitic molluscs from the Boggy and other Carboniferous formations have similar δ¹³C values, reflecting depositional conditions rather than isotopic fractionation (Brand, 1987, 1989).

Carbon isotopes

The variation in $^{13}\text{C}_{\text{carb}}$ during the Paleozoic has been interpreted in terms of changes in the geochemical cycles of sulphur and carbon (Berner et al., 1983; Lasaga et al., 1985; Kump and Garrells, 1986; Berner, 1987) and changes in sedimentation and burial rates of organic and inorganic carbon (Berner, 1989; Berner and Canfield, 1989). Positive shifts in $\delta^{13}\text{C}$ are related to increased burial rates of organic carbon (Brand, 1988; Delaney, 1989). The distribution of carbon between carbonate and ^{13}C depleted organic carbon sedimentary reservoirs controls the average oceanic carbon isotopic ratio and a change in the balance of these geological cycles by increased or reduced rates of Corg. burial will result in complementary changes in mean oceanic $\delta^{13}\text{C}$ values (Delaney, 1989). Similarly, carbon isotopes can reflect oceanic primary productivity such that a increase in $\delta^{13}\text{C}$ may correspond to a reduction in primary productivity and enrichment in the dissolved inorganic carbon of deep bottom waters. Gruszczynski et al., (1989) report a positive carbon isotopic spike recorded in brachiopod calcite close to the Permo-Trias boundary, which they attribute to increased oxidation of organic carbon. This is suggested to have drastically affected oceanic nutrients and atmosphere oxygen levels sufficiently to result in mass extinctions of fauna.

A number of previous authors have reported gradual increases in $\delta^{13}\text{C}_{\text{carb}}$ spanning the Ordovician to Permian (Veizer et al., 1980; Holser, 1984; Popp et al., 1986; Veizer et al., 1986; Popp et al, 1989). A positive shift in brachiopod $\delta^{13}\text{C}$ from Middle Devonian to Permian, has been attributed to a greater burial of organic carbon and the expansion of the terrestrial biomass during the late Devonian (Brand, 1989a, c). The secular variation of $\delta^{13}\text{C}_{\text{carb}}$ during the Paleozoic has been inversely correlated with variation of $\delta^{34}\text{S}$ values

in sulphate minerals (Veizer et al., 1986). This isotopic relationship of sulphur and carbon has been attributed to the redox balance of oxygen and carbon exogenic cycles (Berner et al., 1983; Veizer et al., 1986). The coupling of carbon and sulphur was modelled by Garrels and Lerman (1981) to predict changes in $\delta^{13}\text{C}_{\text{carb.}}$ during the Devonian, and they suggest that the $\delta^{13}\text{C}$ of seawater should have been heavier in Middle Devonian ($> +1\text{‰}$) compared to Early and Late Devonian ($< -1\text{‰}$). However, Veizer et al. (1986) reported that the $\delta^{13}\text{C}$ compositions of Devonian brachiopods averaged about -1‰ and they postulated that the lack of correlation with the Garrels and Lerman (1981) model was due to deterioration of the carbon-sulphur coupling.

Isotopic analyses of brachiopod calcites from this study indicate that the $\delta^{13}\text{C}$ composition of shell calcite is much heavier ($+2.5\text{‰}$ to $+6.0\text{‰}$; Fig. 6.1) than previously reported for brachiopods of Devonian or Silurian age ($\sim -1\text{‰}$ to $+1\text{‰}$; Popp et al., 1986a, b; Veizer et al., 1986; Brand, 1989a). The $\delta^{13}\text{C}$ composition of Devonian brachiopods is reported to vary between -1‰ to $+1\text{‰}$ (Popp et al., 1986a; Veizer et al. 1986). Similarly, the $\delta^{13}\text{C}$ compositions of late Silurian brachiopod calcites vary between -1.0‰ and $+2.8\text{‰}$ (Popp et al., 1986a; Veizer et al. 1986). In contrast, the isotopic compositions of pristine Hamilton Group (Middle Devonian) brachiopod calcite shifts range between $\sim +2.0\text{‰}$ to $\sim +5.5\text{‰}$ while the $\delta^{13}\text{C}$ values of Middle Silurian shell calcites range between $+4.5\text{‰}$ and $+6.0\text{‰}$. Furthermore, isotopic variation within a single shell bed is observed to be $2\text{--}2.5\text{‰}$ and reflects changes in depositional waters with deepening toward the basin centre. These heavy $\delta^{13}\text{C}$ values may reflect greater burial rates and fluctuations in the marine biomass during these times. The absence of vascular plants prior to the Late Silurian (Niklas et al., 1985; Knoll and James, 1986; Berner, 1989) negates a terrestrial influence of carbon. Comparison of these new isotopic data to sulphate curves in Holland

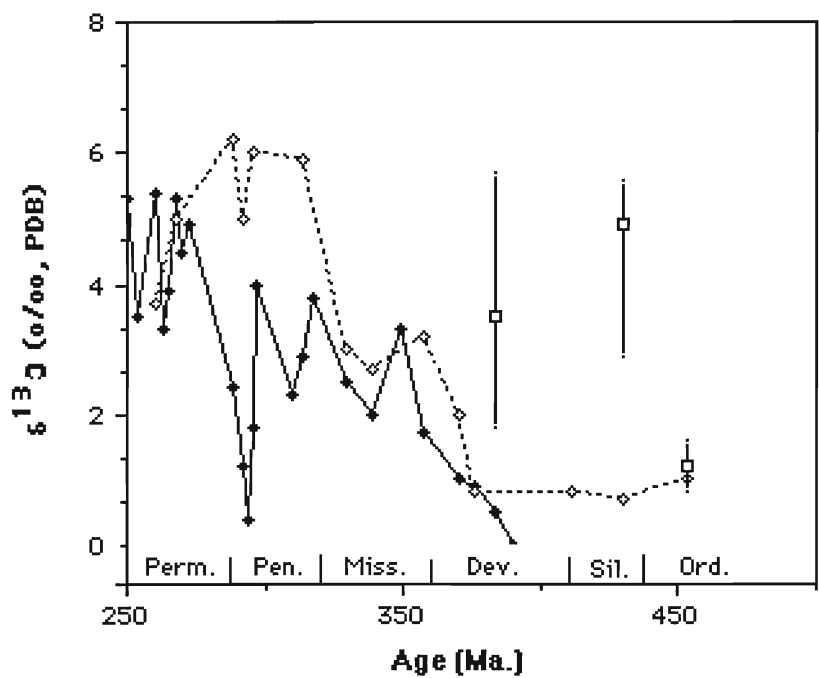


Figure 6.1. Secular variation curve of carbonate carbon isotopes with geologic age. Curves from Popp et al. (1986); open diamond; and Brand (1988); closed diamond. Data from this study is plotted as the mean and range of unaltered brachiopod material (open square). Approximate ages are from Harland et al. (1982).

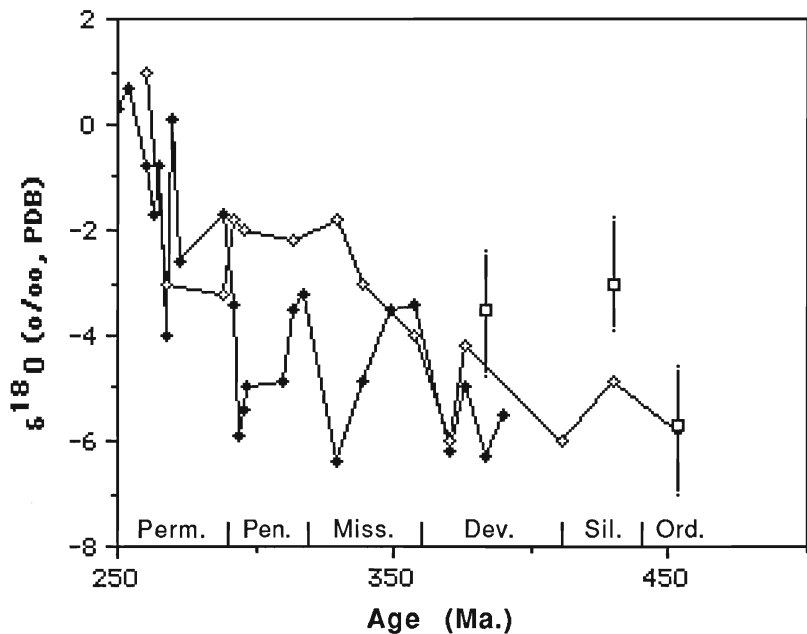


Figure 6.2. Secular variation curve of carbonate oxygen isotopes with geologic age. Curves from Popp et al. (1986); open diamond; and Brand (1988); closed diamond. Data from this study is plotted as the mean and range of unaltered brachiopod material (open square). Approximate ages are from Harland et al. (1982).

(1984; Fig. 9.12, source Claypool et al. 1980), Veizer et al. (1986) and Kump, (1989a) suggests that the carbon isotopic compositions of brachiopods from the Middle Devonian and Middle Silurian are in accordance with the postulated values modelled by the C-S coupling during the Paleozoic (Garrels and Lerman, 1981; Veizer et al., 1986). However, extrapolation of these isotopic data to secular variation of $\delta^{13}\text{C}$ is problematic. The stratigraphic resolution and intervals of sampling is limited. Therefore the significance of trends within the basin is difficult to relate to global cycling of oxygen, carbon and sulphur during the Middle Devonian and Middle Silurian and requires further isotopic testing. Furthermore, the isotopic compositions of brachiopod calcites are only specifically pertinent to depositional waters of the Appalachian Basin reflecting environmental controls within the basin of $\delta^{13}\text{C}$. Similarly, all the $\delta^{13}\text{C}$ carbonate values reported previously are from epicontinental basins (Veizer et al., 1986; Popp et al., 1986; Brand, 1989a). If we assume that epicontinental basin waters are uniform with mean ocean compositions then a direct extrapolation of data is possible. However, variation of 2.5-3.0‰ $\delta^{13}\text{C}$ within the *Demissa* bed illustrates the potential of the depositional environment to control shell calcite composition.

Oxygen Isotopes

A trend of decreasing $\delta^{18}\text{O}$ values with increasing age has been recognized in marine chemical sediments (e.g., Perry and Tan, 1972; Knauth and Epstein, 1976; Veizer and Hoefs, 1976). Similarly, a shift in $\delta^{18}\text{O}$ values of brachiopod calcites in the late Paleozoic has been reported (Veizer et al., 1986; Popp et al., 1986a; Brand 1989a). This trend has been attributed to either the post-depositional equilibration of brachiopod calcite, higher Paleozoic temperatures, or changes in the oxygen isotopic composition of seawater over

time (Veizer et al., 1986). Veizer et al. (1986) reported that the most positive ^{18}O values for Ordovician to Devonian brachiopod samples were -4‰ PDB; Ordovician samples ($n=21$) averaging -4.5‰ to -5.5‰ ; Silurian-Devonian samples ($n=54$; $n=178$) ranging from -5‰ to -7‰ . Paleothermometry of these isotopic values suggests that marine temperatures, if brachiopods are assumed to incorporate ^{18}O in equilibrium with ambient conditions, were well over 40°C in Paleozoic tropical oceans. Veizer et al (1986), and Brand (1989a) suggest that these temperature ranges were greater than the thermal tolerances of marine metazoans, although the precise upper limit is debatable (38°C - 50°C ; Brock, 1985; Valentine, 1985). As an alternative, Veizer et al., (1986) propose that the isotopic composition of Paleozoic oceans has changed during geologic time. The cause of an enrichment in mean oceanic ^{18}O compositions is suggested by Veizer et al. (1986) to be due to "a substantial enhancement in the rate of high temperature oxygen isotopic exchange (plutonism, deep ocean ridge circulation, etc.) relative to low-temperature processes (e.g., shallow ridge circulation, submarine weathering)". Again this argument is unequivocal, since fluid inclusion analyses report $\delta^{18}\text{O}$ values similar to present day $\delta^{18}\text{O}$ values as far back as the Silurian (Knauth, 1985 et al; Knauth and Beeunas, 1986). Furthermore, the alteration of oceanic metabasalts with seawater and the buffering of $\delta^{18}\text{O}$ at 0‰ by reaction with silicates of oceanic crust (Muehlenbachs and Clayton, 1976) may have maintained Paleozoic ocean $\delta^{18}\text{O}$ isotopic compositions close to 0‰ (SMOW) (Veizer et al., 1986).

Isotopic analysis of brachiopods from this study indicate that Middle Ordovician isotopic values range from -4.5‰ to -6.0‰ , which is in agreement with previous studies (Fig. 6.2). However, Middle Silurian and Middle Devonian brachiopod isotope values are considerably heavier than previously reported (Popp et al., 1986a; Veizer et al., 1986; Brand, 1989a). Middle Silurian values

range from 1.8‰ to -3.6‰ and Middle Devonian range from -2.5‰ to -4.0‰. Uncorrected paleotemperatures (assuming normal salinity, 0‰ SMOW and no fractionation effects) derived from these isotopic values suggest that the Clinton sea temperature (Middle Silurian) ranged from 18°C to 28°C and Hamilton seas (Middle Devonian) ranged between 24°C and 29°C. If a non-glacial correction of -1‰ SMOW is applied to the data, the temperatures decrease by 4-5°C (Berger, 1979). Paleogeographical reconstructions place these respective seas close to the equator (within 5-15°), whereby the paleotemperatures are well within the climatic ranges expected. Clearly, these temperatures cannot be reconciled with high Paleozoic ocean temperatures, which have been suggested by a number of authors (Knauth and Epstein, 1976; Karhu and Epstein, 1986), or reconciled with the general shift in $\delta^{18}\text{O}$ during the late Paleozoic (Fig. 6.2; Popp et al., 1986a; Veizer et al., 1986; Brand, 1989a). These isotopic values suggest that Hamilton and Clinton Group waters were probably compositionally close to 0‰ (SMOW). A unidirectional trend in mean oceanic ^{18}O composition may not be an unequivocal explanation for isotopic shifts.

Diagenetic alteration of biogenic carbonate tends to result in more negative oxygen isotopes (Veizer and Fritz, 1976; Brand and Veizer, 1981) which reflect interactions with isotopically-light surficial and meteoric waters (Siegenthaler, 1979). Unrecognized post-depositional alteration may provide an explanation for the more negative values, reported by the other authors. Alternately, the scatter in isotopic values may represent brachiopod calcites sampling from a wide spectrum of different depositional and environmental settings. Significant variation in circulation patterns, glacio-eustatic conditions, temperature, salinity, fresh water input to the shelf and basin stratification may have controlled brachiopod calcite isotopic compositions. Hamilton and Clinton

Group brachiopods reflect conditions within an epicontinental sea that occupied the Appalachian Basin during the Middle Devonian and Middle Silurian. Similarly, the majority of brachiopod isotopic data reported elsewhere reflect the composition of waters within specific epicontinental basins (Brand and Veizer, 1981; Brand, 1981, 1983; Veizer et al., 1986; Popp et al., 1986a; Brand 1989a). Processes controlling isotopic compositions within these epicontinental seas may have been more manifold and complicated than previously realized. Thus, the variation in isotopic values of brachiopods shell calcites may reflect significantly different localized conditions and not per se, mean oceanic isotopic compositions. Isotopic trends may therefore have to be constrained by deep/shallow trends and environmental conditions within each sampled bed. Extrapolation of isotopic data into secular shifts may be pre-emptive, since the stratigraphic resolution and spatial distribution of sampling is so limited. However, it may ultimately be possible to relate isotopic changes to flux or perturbations in atmospheric O₂ (Kump and Garells, 1984) as outlined in Brand (1989a), or to tectonically controlled cycles of oxygen exchange between seawater and the silicate crust (Veizer, 1985; Veizer et al., 1986).

CONCLUSIONS

The $\delta^{13}\text{C}$ and $\delta^{18}\text{O}$ compositions of brachiopod calcites from the Middle Devonian and Middle Silurian of New York State and Ontario are enriched relative to values previously reported. Variability of isotopic compositions within beds suggests that the isotopic compositions of brachiopod calcite are strongly influenced by the depositional conditions. Therefore the significance of secular isotopic shifts has to be interpreted in relation to environmental controls (i.e., basin type, depth) and within the context and confines of available paleoecologic, stratigraphic, and sedimentologic information.

Acknowledgements

I would like to thank my graduate advisor, Dr. Uwe Brand, for his continual encouragement, financial support and geochemical training. His demand for excellence and dedication to research inspired me to the fulfillment of this thesis.

Special thanks to Drs. Steve Westrop, and Rick Cheel, for their constant encouragement, many hours of discussion and help in the preparation of this thesis. I also thank Dr. J. Terasmae who introduced me to paleoecology.

Many thanks go to my fellow student, John McAllister, for his company in the field and during laboratory work, discussion of ideas and continual encouragement. My gratitude goes to D. Tetreault, of the University of Rochester, who first introduced me to the Rochester Shale Formation and for providing me with sample material from central New York. I further extend my thanks to Dr. C. Brett, for his advice on Silurian stratigraphy.

My gratitude goes to H. Melville, who assisted me with S.E.M. photos and I thank Ian Colquhoun and Danny Soo for their friendship, discussions and support.

Finally, I extend my thanks to Margaret Best, without whom this thesis could not exist and for her assistance in collecting samples, preparation of material, and during laboratory work. Without her understanding, patience and love, this task would have been impossible.

References

- Adlis, D.S., Grossman, E.L., Yancey, T.E., and McLerran, R.D., 1988, Isotope stratigraphy and paleodepth changes of Pennsylvanian cyclical sedimentary deposits: *Palaeis*, v.4, p.
- Aharon, P., Schidlowski, M., and Singh, I.B., 1987, Chronostratigraphic markers in the end-Precambrian carbon isotope record of the Lesser Himalaya. *Nature*, v. **327**, p. 699-702.
- Aigner, T., 1985, Storm depositional dynamics: Dynamic Stratigraphy in Modern and Ancient Shallow Marine Sequences: Lecture Notes In Earth Sciences, v. **3**, Springer Verlag, Berlin, Heidelberg, 174p.
- Al-Aasm, I., and Veizer, J., 1982, Chemical stabilization of low-Mg calcite: an example of brachiopods: *Journal of Sedimentary Petrology*, v. **52**, p. 1101-1109.
- _____, 1986a, Diagenetic stabilization of aragonite and low-Mg calcite: I Trace elements in Rudists: *Journal of Sedimentary Petrology*, v. **56**, p. 138-152.
- _____, 1986b, Diagenetic stabilization of aragonite and low-Mg calcite: II Stable isotopes in Rudists: *Journal of Sedimentary Petrology*, v. **56**, p. 763-770.
- Alexander, R.R., 1975, Phenotypic lability of the brachiopod *Rafinesquina alternata* (Ordovician) and its correlation with the sedimentologic regime: *Journal of Paleontology*, v. **49**, p. 607-618.
- _____, 1984, Comparative hydrodynamic stability of brachiopod shells on current-scoured arenaceous substrates: *Lethaia*, v. **17**, p. 17-32.
- _____, 1986, Life orientations and post mortem reorientation of Chesterian brachiopod shells by paleocurrents: *Palaeis*, v. **1**, p. 303-311.
- Aldridge, A.E., 1981, Intraspecific variation of shape and size in subtidal populations of two Recent New Zealand articulate brachiopods: *New Zealand Journal of Zoology*, v. **8**, p. 169-174.
- Anderson, T.F., and Arthur, M.A., 1983, Stable isotopes of oxygen and carbon and their application to sedimentologic and paleoenvironmental problems. in *Stable Isotopes, S.E.P.M., Short Course* v. **10**, p. 1-151.
- Anonymous, 1972, Limestone industries of Ontario: O.D.M. Industrial Mineral Report 39.
- Arthur, M.A., Dean, W.E., and Sclanger, S.O., 1985, Variations in the global carbon cycle during the Cretaceous related to climate, volcanism, and changes in atmospheric CO₂. in Sundquist, E.T., and Broecker, W.S.,

- (eds.). Carbon cycle and atmospheric CO₂: Natural variations Archean to present. Geophysical Monograph, v. **32**, p. 504-530.
- Arthur, M.A., Dean, W.E., and Pratt, L.M., 1989, Geochemical and climatic effects of increased marine organic carbon burial at the Cenomanian/Turonian boundary. *Nature*, v. **337**, p. 714-717.
- Baird, G.C., 1979, Sedimentary relationships of Portland Point and associated Middle Devonian rocks: in central and western New York. *New York State Museum Bulletin*, v. **433**, 24p.
- _____, 1981, Submarine erosion on a gentle paleoslope. A study of two discontinuities in the New York Devonian: *Lethaia*, v. **14**, p. 105-122.
- Baird, G.C., and Brett, C.E., 1981, Submarine discontinuities and sedimentary condensation in the Upper Hamilton Group (Middle Devonian): Examination of marine shelf and paleoslope deposits in the Cayuga Valley: *in* Enos, P., (ed.), *New York State Geological Association, 53th Annual Meeting Field Trip Guidebook*, Cornell University, N.Y., p. 115-145.
- _____, 1983, Regional variation and paleontology of two coral beds in the Middle Devonian Hamilton Group of Western New York: *Journal of Paleontology*, v. **57**, p. 417-446.
- _____, 1986, Submarine erosion on the dysaerobic seafloor: Middle Devonian corrasional disconformities in the Cayuga Valley: *in* *New York State Geological Association, 58th Annual Meeting Field Trip Guidebook*, Cornell University, N.Y., p. 23-80.
- Baker, P.A., Gieskes, J.M., and Elderfield, H., 1982, Diagenesis of carbonates in deep-sea sediments - evidence from Sr/Ca ratios and interstitial dissolved Sr²⁺ data: *Journal of Sedimentary Petrology*, v. **52**, p. 71-82.
- Barnes, C.R., Telford, P.G., and Tarrant, G.A., 1981, Ordovician and Silurian conodont biostratigraphy, Manitoulin Island and Bruce Peninsula, Ontario: *in* *Geology of the Manitoulin Area: Michigan Basin Geological Society Special Paper No. 3*.
- Barnes, J.A., and Bodungen, B.V., 1978, The Bermuda marine environment: volume II; Bermuda Biological Station Special Publication No. 17, 189p.
- Bathurst, R.G.C., 1975, Carbonate sediments and their diagenesis: Elsevier, Amsterdam, 2nd edition, 658p.
- Berger, W., 1979, Stable isotopes in foraminifera. S.E.P.M. Short Course Notes **6**, p. 156-198.

- Berner, R.A., 1987, Models for carbon and sulphur cycles and atmospheric oxygen: Application to Paleozoic geologic history. *American Journal of Science*, v. **287**, p. 177-196.
- _____, 1989, Biogeochemical cycles of carbon and sulfur and their effect on atmospheric oxygen over Phanerozoic time. *Palaeogeography, Palaeoclimatology, Palaeoecology (Global and Planetary Change Section)*, v. **75**, p. 97-122.
- Berner, R.A., and Canfield, D.E., 1989, A new model for atmospheric oxygen over Phanerozoic time. *American Journal of Science*, v.**289**, p. 333-361.
- Berner, R.A., Lasaga, A.C., and Garrells, R.M., 1983, The carbonate-silicate geochemical cycle and its effect on atmospheric carbon dioxide over the past 100 million years: *American Journal of Science*, v. **283**, p. 641-683.
- Blanchard, S.C., and Chasteen, N.D., 1976, Electron paramagnetic resonance spectrum of a seashell. *Journal of Physical Chemistry*, v. **80**, p. 1362-1367.
- Bodungen, B. von., Jickells, T.D., Smith, S.R., Ward, J.A.D., and Hillier, G.B., 1982, The Bermuda marine environment: The final report of the Bermuda inshore waters investigations 1975-1980: Bermuda Biological Station Special Publication No. 18, 123p.
- Bolton, T.E., 1965, Illustration of Canadian fossils: Silurian faunas of Ontario: Geological Survey of Canada, Dept. of Mines and Technical Surveys, Paper **66-5**.
- _____, 1975, Pre-Guelph, Silurian Formations of the Niagara Peninsula, Ontario: *in* Telford P.G., (ed.), G.A.C. Field Guide Book, Waterloo 1975, p. 54-80.
- Bordine, M.W., Holland, H.D., and Borczik, M., 1965, Coprecipitation of manganese and strontium with calcite: in *Problems of Postmagmatic Ore Deposition, Proceedings Symposium, Prague*, v. **2**, p. 401-406.
- Boucot, A.J., 1981, Principles of benthic marine paleoecology. Academic Press. 467p.
- Boyle, E.A., 1981, Cadmium, zinc, copper and barium in foraminiferal tests. *Earth Planetary Science Letters*, v. **53**, p. 11-35.
- _____, 1983, Manganese carbonate overgrowths on foraminiferal tests. *Geochimica et Cosmochimica Acta*, v. **47**, p. 1815-1819.
- Brand, U., 1981a, Mineralogy and chemistry of the Lower Pennsylvanian Kendrick fauna, eastern Kentucky, 1. Trace elements: *Chemical Geology*, v. **32**, p. 1-16.

- _____, 1981b, Mineralogy and chemistry of the Lower Pennsylvanian Kendrick fauna, eastern Kentucky, 2. Stable isotopes: *Chemical Geology*, v. **32**, p. 17-28.
- _____, 1982, The oxygen and carbon isotopic composition of Carboniferous fossil components: *Sedimentology*, v. **29**, p. 139-147.
- _____, 1983, Mineralogy and chemistry of the Lower Pennsylvanian Kendrick fauna, eastern Kentucky, 3. Diagenetic and paleo-environmental analysis: *Chemical Geology*, v. **40**, p. 167-181.
- _____, 1986, Paleoenvironmental analysis of Middle Jurassic (Callovian) ammonoids from Poland: Trace elements and stable isotopes: *Journal of Paleontology*, v. **60**, p. 293-301.
- _____, 1987, Depositional analysis of the Breathitt Formation's marine horizons, Kentucky, U.S.A.: Trace elements and stable isotopes: *Chemical Geology*, v. **65**, p. 117-136.
- _____, 1989a, Biogeochemistry of Late Paleozoic North American brachiopods and secular variation of seawater composition: *Biogeochemistry*.
- _____, 1989b, Aragonite-calcite transformation based on Pennsylvanian molluscs: *Geological Society of America Bulletin*, v. **101**, p. 377-390.
- _____, 1989c, Late Devonian biotic crisis: Stable isotope biogeochemistry of North American and European brachiopods. 28th Int. Geol. Cong., Washington, v. **1**, p. 191.
- Brand, U., and Veizer, J., 1980, Chemical diagenesis of a multicomponent carbonate system 1. Trace elements: *Journal of Sedimentary Petrology*, v. **50**, p. 1219-1236.
- _____, 1981, Chemical diagenesis of a multicomponent carbonate system 2. Stable isotopes: *Journal of Sedimentary Petrology*, v. **51**, p. 987-997.
- _____, 1983, Origin of coated grains: Trace element constraints, *in* Peryt, T., (ed.), *Coated Grains*: Springer Verlag, Berlin, Heidelberg, New York and Tokyo, p. 18-29.
- Brand, U., and Morrison, J.O., 1987a, Paleoscene #6. Biogeochemistry of fossil marine invertebrates: *Geoscience Canada*, v. **14**, p. 85-107.
- _____, 1987b, Diagenesis and pyritization of crinoid ossicles: *Canadian Journal of Earth Sciences*, v. **24**, p. 2486-2496.

- Brand, U., Morrison, J.O., Brand, N., and Brand, E., 1987, Isotopic variation in the shells of Recent marine invertebrates from the Canadian Pacific coast. *Chemical Geology*, v. **65**, p. 137-145.
- Brasier, M.D., and Magaritz, M., 1989, Toward an integrated carbon isotope-small shelly fossil stratigraphy for the Precambrian-Cambrian boundary. 28th Int. Geol. Cong., Washington D.C., v. **1**, p.195-196.
- Brett, C.E., 1983a, Sedimentology, facies and depositional environments of the Rochester Shale (Silurian; Wenlockian) in western New York and Ontario: *Journal of Sedimentary Petrology*, v. **53**, p. 947-971.
- _____, 1983b, Stratigraphy and facies relationships of the Silurian Rochester Shale (Wenlockian: Clinton Group) in New York State and Ontario: *in* Centennial Colloquium Issue: Geology of the Genesee Region of New York State since Fairchild, *Proc. Roch. Acad. Sci.*, v. **15**, no. 2, p. 118-144.
- _____, 1986, The Middle Devonian Hamilton Group of New York: An overview: *in* Brett, C.E., (ed.), *Dynamic stratigraphy and depositional environments of the Hamilton Group (Middle Devonian) in New York State, Part 1*. New York State Museum Bulletin, Nos. **457**, p. 1-4.
- _____, 1989 (in press), Wenlockian fossil communities in New York: *Paleontology and paleoecology*.
- Brett, C.E., and Baird, G.C., 1982, The Genesee-Moscow contact in western New York: evidence for regional erosive bevelling during the late Middle Devonian: *in* New York State Geological Association Guidebook, 54th Annual Meeting, p. 19-53.
- Brett, C.E., and Baird, G.C., 1985, Carbonate-shale cycles in the Middle Devonian of New York: An evaluation of models for the origin of limestones in terrigenous shelf sequences: *Geology*, v. **13**, p. 324-327.
- _____, 1986a, Comparative taphonomy: A key to paleoenvironmental interpretation based on fossil preservation: *Palaios*, v. **1**, p. 207-227.
- _____, 1986b, Symmetrical and upward shallowing cycles in the Middle Devonian of New York State and their implications for the punctuated aggradational cycle hypothesis: *Paleoceanography*, v. **1**, p. 431-445.
- Brett, C.E., and Brookfield, M.E., 1984, Morphology, faunas and genesis of Ordovician hardgrounds from southern Ontario, Canada. *Palaeogeography, Palaeoecology, Palaeoclimatology*, v. **46**, p. 233-290.
- Brett, C.E., and Cottrell, J.F., 1982, Substrate specificity in the Devonian Tabulate coral *Pleurodictyum* : *Lethaia*, v. **15**, p. 247-262.

- Brett, C.E., and Eckert, J.D., 1982, Paleoeecology of a well-preserved crinoid colony from the Silurian Rochester Shale in Ontario. *Royal Ontario Life Sci. Contrib.*, v. **131**, p. 1-20.
- Brett, C.E., Speyer, S.E., and Baird, G.C., 1986a, Storm-generated sedimentary units: Tempestite proximity and event stratification in the Middle Devonian Hamilton Group of New York: *in* Brett, C.E., (ed.), *Dynamic stratigraphy and depositional environments of the Hamilton Group (Middle Devonian) in New York State, Part 1*. New York State Museum Bulletin, Nos. **457**, p. 129-156.
- Brett, C.E., Baird, G.C., and Miller, K.B., 1986b, Sedimentary cycles and lateral facies gradients across a Middle Devonian shelf-to-basin ramp, Ludlowville Formation, Cayuga Basin: *in* Enos, P., (ed.), *New York State Geological Association, 53th Annual Meeting Field Trip Guidebook*, Cornell University, N.Y., p. 81-127.
- Brock., T.D., 1985, Life at high temperatures: *Science*, v. **230**, p. 132-138.
- Broecker, W.S., 1974, *Chemical oceanography*: New York, Harcourt, Brace and Jovanovitch, 214p.
- Brookfield, M.E., and Brett, C.E., 1988, Paleoenvironments of the Mid-Ordovician (Upper Caradocian) Trenton limestones of southern Ontario, Canada: Storm sedimentation on a shoal-basin model: *Sedimentary Geology*, v. **57**, p. 75-105.
- Bruni, S.F., and Wenk, H.R., 1985, Replacement of aragonite by calcite in sediments from the San Cassiano Formation (Italy): *Journal of Sedimentary Petrology*, v. **55**, p. 159-170.
- Buchardt, B., and Weiner, S., 1981, Diagenesis of aragonite from Upper Cretaceous ammonites: A geochemical case study: *Sedimentology*, v. **28**, p. 423-438.
- Busenberg, E., and Plummer, L.N., 1985, Kinetic and thermodynamic factors controlling the distribution of SO_4^{2-} and Na^+ in calcites and selected aragonites: *Geochimica et Cosmochimica Acta*, v. **49**, p. 713-725.
- Campbell, H.J., and Fleming, C.A., 1981, Brachiopoda from Fiordland, New Zealand, collected during the New Golden Hind expedition, 1946: *New Zealand Journal of Zoology*, v. **8**, p. 145-155.
- Carter, B., Miller, P., and Smosna, R., 1988, Environmental aspects of Middle Ordovician limestones in the Central Appalachians: *Sedimentary Geology*, v. **58**, p. 23-36.
- Carter, J.G., 1980, Environmental and biological controls of bivalve shell mineralogy and microstructure: *in* *Skeletal Growth of Aquatic Organisms*;

- (eds.) Rhoads, D.C., and Lutz, R.A.); Plenum Press, New York, London, p. 69-114.
- Chapman and Richardson, J.R., 1981, Recent species of *Neothyris* (Brachiopoda: Terebratellinae): *New Zealand Journal of Zoology*, v. **8**, p. 157-161.
- Chave, K., 1954, Aspects of the biogeochemistry of magnesium - I. Calcareous marine organisms: *Journal of Geology*, v. **62**, p. 266-283.
- Child, D., 1973, *The essentials of factor analysis*. Holt, Rinehart and Winston, 107p.
- Cisne, J.L., Karig, D.E., Rabe, B.D., and Hay, B.J., 1982, Topography and tectonics of the Taconic Outer Trench Slope as revealed through gradient analysis of fossil assemblages: *Lethaia*, v. **15**, p. 229-246.
- Claypool, G.E., Holser, W.T., Kaplan, I.R., Sakai, H., and Zak, I., 1980, The age curves of sulfur and oxygen isotopes in marine sulphate and their mutual interpretation. *Chemical Geology*, v. **28**, p. 199-260.
- Cocks, L.R.M., 1967, Depth patterns in Silurian marine communities: *Marine Geology*, v. **5**, p. 379-382.
- Cocks, L.R.M., and Fortey, R.A., 1982, Faunal evidence for the oceanic separations in the Paleozoic of Britain: *Journal of Geological Society London*, v. **139**, p. 465-478.
- Copper, P., 1978, Paleoenvironments and paleocommunities in the Ordovician-Silurian sequence of Manitoulin Island. *in* Sanford, J.T., and Mosher, R.E., (eds.). *Geology of the Manitoulin Area*. Michigan Basin Geological Society, Special Paper **3**, p. 47-61.
- Craig, H., 1957, Isotopic standards for carbon and oxygen and corrections factors for mass spectrometric analysis of carbon dioxide: *Geochimica et Cosmochimica Acta*, v. **12**, p. 133-149.
- Craig, H. and Gordon, L.I., 1965, Deuterium and oxygen 18 variation in the ocean and the marine atmosphere. *in* Torgiorgi, E., (ed.), *Stable isotopes in oceanographic studies and paleotemperatures*, spoletto, Cons. Naz. Ric., p. 9-130.
- Crenshaw, M.A., 1980, Mechanisms of shell formation and dissolution: *in* *Skeletal Growth of Aquatic Organisms*; (eds.) Rhoads, D.C., and Lutz, R.A.; Plenum Press, New York, London, p. 115-132.
- Curry, G.B., 1982, Ecology and population structure of the Recent brachiopod *Terebratulina* from Scotland: *Paleontology*, v. **6**, p. 227-246.

- _____, 1983a, Microborings in Recent brachiopods and the functions of caeca: *Lethaia*, v. **16**, p. 119-127.
- _____, 1983b, Brachiopod caeca - a respiratory role: *Lethaia*, v. **16**, p. 311-312.
- Delaney, M.L., 1989, Extinctions and carbon cycling: *Nature*, v. **337**, p. 18-19.
- Demaison, G.J., and Moore, G.T., 1980, Anoxic environments and oil source bed genesis: *American Association of Petroleum Geologists Bulletin*, v. **64**, p. 1179-1209.
- Dick, V.B., and Brett, C.E., 1986, Petrology, taphonomy and sedimentary environments of pyritic fossil beds from the Hamilton Group (Middle Devonian) of Western New York: *in* Brett, C.E., (ed.), *Dynamic stratigraphy and depositional environments of the Hamilton Group (Middle Devonian) in New York State, Part 1*. New York State Museum Bulletin, Nos. **457**, p. 102-128.
- Doherty, P.J., 1981, The contribution of dissolved amino acids to the nutrition of articulate brachiopods: *New Zealand Journal of Zoology*, v. **8**, p. 183-188.
- Drever, J.I., 1982, *The geochemistry of natural waters*: Prentice Hall, Englewood Cliffs, N.J., 388p.
- Droste, J.B., and Shaver, R.H., 1987, Paleooceanography of Silurian seaways in the midwestern basins and arches region; *Paleooceanography*, v. **2**, no. 2, p.213-227.
- Dunham, R.J., 1962, Classification of carbonate rocks according to depositional texture. *in* Ham, W.E., (ed.), *Classification of carbonate rocks*. A.A.P.G. Memoir 1, p. 108-121.
- Elderfield, H., Baker, P.A., Gieskes, J. M., Oldfield, R.K., Hawksworth, C.J., and Millar, R., 1982, $^{87}\text{Sr}/^{86}\text{Sr}$ and $^{18}\text{O}/^{16}\text{O}$ ratios, interstitial water chemistry and diagenesis in deep-sea carbonate sediments of the Ontong Java Plateau. *Geochimica et Cosmochimica Acta*, v. **46**, p. 2259-2268.
- Epstein, S., Buchbaum, R., Lowenstam, H.A., and Urey, H.C., 1953, Revised carbonate-water isotopic scale: *Geological Society of America Bulletin*, v. **64**, p. 1315-1325.
- Ettensohn, F.R., 1985a, The Catskill Delta complex and the Acadian Orogeny: A model: *in* *The Catskill Delta* (eds. Woodrow, D.L., and Sevon, W.D.): *Geological Society of America Special Paper*, v. **201**, p. 39-50.
- _____, 1985b, Controls on development of Catskill Delta Complex basin-facies: *in* *The Catskill Delta* (eds. Woodrow, D.L., and Sevon, W.D.): *Geological Society of America Special Paper*, v. **201**, p. 65-78.

- Fail, R.T., 1985, The Acadian Orogeny and the Catskill Delta: *in* The Catskill Delta (eds. Woodrow, D.L., and Sevon, W.D.): Geological Society of America Special Paper, v. **201**, p. 15-38.
- Fairchild, I.J., 1983, Chemical controls of cathodoluminescence of natural dolomites and calcites: New data and review: *Sedimentology*, v. **30**, p. 579-583.
- Faure, G., 1986, Principles of isotope geology: John Wiley and Sons, New York, 589p.
- Folk, R.L., 1962, Spectral subdivision of limestone types. *in* Ham, W.E., (ed.), Classification of carbonate rocks. American Association of Petroleum Geologists Memoir 1, p. 62-84.
- Foster, M.W., 1974, Recent antarctic and subantarctic brachiopods: Antarctic Research Series (American Geophysics Union) Geo. W. King, Baltimore 189p.
- _____, 1989, Brachiopods from the extreme South Pacific and adjacent waters. *Journal of Paleontology*, v. **63**, no. 3, p. 268-300.
- Frank, J.R., Carpenter, A.B., and Oglesby, T.W., 1982, Cathodoluminescence and composition of calcite cement in the Taum Sauk Limestone (Upper Cambrian), S.E. Missouri: *Journal of Sedimentary Petrology*, v. **52**, p. 631-638.
- Fritz, P., and Katz, A., 1972, The sodium distribution of dolomite crystals: *Chemical Geology*, v. **72**, p. 170-194.
- Fritz, P., Lapcevic, P.A., Miles, M., Frape, S.K., Lawson, D.E., and O'Shea, K.J., 1988, Stable isotopes in sulphate minerals from the Salina Formation in southwestern Ontario. *Canadian Journal of Earth Sciences*, v. **25**, p. 195-205.
- Fursich, F.T., and Hurst, J.M., 1974, Environmental factors determining the distribution of brachiopods: *Palaeontology*, v. **17**, p. 879-900.
- _____, 1980, Euryhalinity of Palaeozoic articulate brachiopods: *Lethaia*, v. **13**, p. 303-312.
- Gaffey, S.J., 1985, Reflectance spectroscopy in the visible and infrared (0.35-2.55 microns): applications in carbonate petrology. *Geology*, v. **13**, p. 270-273.
- _____, 1988, Water in skeletal carbonates: *Journal of Sedimentary Petrology*, v. **58**, p. 397-414.

- Garrels, R.M., and Lerman, A., 1981, Phanerozoic cycles of sedimentary sulfur and carbon. *Proc. Nat. Acad. Sci.*, v. **78**, p. 4652-4656.
- Gonzalez, L.A., and Lohmann, K.C., 1985, Carbon and oxygen isotopic composition of Holocene reefal carbonates. *Geology*, v. **13**, p. 811-814.
- Goodwin, P.W., and Anderson, E.J., 1985, Punctuated aggradational cycles: A general hypothesis of episodic stratigraphic accumulation: *Journal of Geology*, v. **93**, no. 5, p. 515-533.
- Gordon, L., Salutsky, M.L., and Willard, H.H., 1959., *Precipitation from homogenous solution*: Wiley, New York, 289p.
- Gorjansky, W, J., and Popov, L.Y., 1986, On the origin and systematic position of the calcareous-shelled inarticulate brachiopods: *Lethaia*, v. **19**, p. 233-240.
- Graf, D.L., 1960, *Geochemistry of carbonate sediments and sedimentary carbonates*, 1-4: Illinois State Geological Circular, v. 297, 298, 301 and 388, 250p.
- Grasso, T.X., 1983, Silurian and Devonian history of the Genesee Valley: A synopsis: *Proceedings Rochester Academy Science*, p. 99-117.
- _____, 1986, Redefinition, stratigraphy and depositional environments of the Mottville Member (Hamilton Group) in central and Eastern New York. *in* Brett, C.E., (ed.), *Dynamic stratigraphy and depositional environments of the Hamilton Group (Middle Devonian) in New York State, Part 1*. New York State Museum Bulletin, Nos. **457**, p. 5-31.
- Grasso, T.X., Harrington, J.W., and Kirshgasser, W.T., 1986, Stratigraphy and paleontology - around Cayuga Lake once again; in *New York State Geological Association, 58th Annual Meeting Fieldtrip Guidebook*, p. 167-197.
- Grossman, E.L., 1984, Stable isotope fractionation in live benthic foraminifera from the southern California borderland: *Palaeogeography, Palaeoclimatology, Palaeo-ecology*, v. **47**, p. 301-327.
- _____, 1987, Stable isotopes in modern benthic foraminifera: A study of vital effect: *Journal of Foraminiferal Research*, v. **17**, p. 48-61.
- Grossman, E.L., Betzer, P.R., Dudley, W.C., and Dunbar, R.B., 1986, Stable isotopic variation inpteropods and atlanysids from North Pacific sediment traps: *Marine Micropaleontology*, v. **10**, p. 9-22.
- Gruszczynski, M., Halas, S., Hoffman, A., and Malkowski, K., 1989, A brachiopod calcite record of the oceanic carbon and oxygen isotope shifts at the Permian/Triassic transition: *Nature*, v. **337**, p. 64-68.

- Hammen, C.S., 1977, Brachiopod metabolism and enzymes: *American Zoologist*, v. **17**, p. 141-147.
- Hancock, N.J., Hurst, J.M., and Fursich, F.T., 1974, The depths inhabited by Silurian brachiopod communities: *Journal of Geological Society London*, v. **130**, p. 151-156.
- Harland, W.B., Cox, A.V., Llewellyn, P.G., Pickton, C.A.G., Smith, A.G., and Walters, R., 1982, *A geologic time scale*. Cambridge University press, Cambridge, p. 54.
- Heckel, P.H., and Witzke, B.J., 1979, Devonian world paleogeography determined from distribution of carbonates and related lithic paleoclimatic indicators. *The Devonian System: The Palaeontological Association (London) Special Papers in Palaeontology*, v. **23**, p. 99-123.
- Hiller, N., 1988, The development of growth lines on articulate brachiopods: *Lethaia*, v. **21**, p. 177-188.
- Holland, H.D., 1978, *The chemistry of the atmosphere and oceans*: Wiley-Intersciences.
- _____, 1984, *The chemical evolution of the atmosphere and oceans*: Princeton Press.
- Holser, W.T., 1984, Gradual and abrupt shifts in ocean chemistry during Phanerozoic time: *in* Holland, H.D., and Trendall, A.F., (eds.) *Patterns of change in earth evolution*, p. 123-143.
- Holser, W.T., Magaritz, M., and Clark, D.L., 1986, Carbon-isotope stratigraphic correlations in the late Permian. *American Journal of Science*, v. **286**, p.390-402.
- _____, 1989, Carbon isotopes across a continuous marine sequence of the Permo-Trias, Austrian Alps. *Nature*, v. **337**, p. 39-44.
- Hughes, W.W., Rosenberg, G.D., and Tkachuck, R.D., 1989, Growth increments in the shell of the living brachiopod *Terebratalia transversa* : *Marine Biology*, v. **27**, p.
- Ishikawa, M., and Ichikuni, M., 1984, Uptake of sodium and potassium by calcite: *Chemical Geology*, v. **42**, p. 137-146.
- Jaanusson, V., 1966, Fossil brachiopods with probable aragonitic shell: *Geol. Foren. Stockholm Forhandl*, v. **88**, p. 279-281.

- James, N.P., and Choquette, P.C., 1984, Diagenesis 9: Limestones - the meteoric diagenetic environment. *Geoscience Canada*, v. **11**, no. 4., p. 161-194.
- Johnson, M.E., 1987, Extent and bathymetry of North American platform in the early Silurian. *Paleoceanography*, v. **2**, no. 2, p. 185-211.
- Johnson, M.E., and Rong, J.Y., 1989, Middle to Late Ordovician rocky bottoms and rocky shores from the Manitoulin Island are, Ontario. *Canadian Journal of Earth Sciences*, v. **26**, p. 642-653.
- Jones, B., 1982, Paleobiology of the Upper Silurian brachiopod *Atrypoides*: *Journal of Paleontology*, v. **56**, p. 912-923.
- _____, 1983, Analysis of growth patterns in brachiopods and its potential use for the identification of species: *Journal of Paleontology*, v. **57**, p. 662-685.
- Jones, B., and Narbonne, G.M., 1984, Environmental controls on the distribution of *Atrypoides* species in the Upper Silurian strata of Arctic Canada: *Canadian Journal of Earth Sciences*, v. **21**, p. 131-144.
- Jones, S.J., 1985, Growth increments and geochemical variations in the molluscan shell: *in* Broadhead, T.W., (ed.), *Mollusks: Notes for a Short Course*, University of Tennessee, Dept. of Geological Sciences, *Studies in Geology*, p. 72-81.
- Kahru, J., and Epstein, S., 1986, The implications of the oxygen isotope records in coexisting cherts and phosphates: *Geochimica et Cosmochimica Acta*, v. **40**, p. 1095-1108.
- Kammer, T.W., Brett, C.E., Boardman, D.R., and Mapes, R.H., 1986, Ecological stability of the dysaerobic biofacies during the late Paleozoic: *Lethaia*, v. **19**, p. 109-121.
- [Kanip, J., 1986, Fossil and facies geochemistry of the Middle Devonian Kashong Shale (Upper Hamilton Group), Western New York: unpublished B.Sc. thesis, Brock University, 71p.]
- Kasting, J.F., 1989, Long-term stability of the Earth's climate: *Palaeogeography, Palaeoclimatology, Palaeoecology (Global and Planetary Change Section)*, v. **75**, p. 83-95.
- Kemezys, K.J., 1965, Significance of punctae and pustules in brachiopods: *Geological Magazine*, v. **102**, p. 315-324.
- Kent, D.V., 1985, Palecontinental setting for the Catskill Delta: *in* The Catskill Delta (eds. Woodrow, D.L., and Sevon, W.D.): *Geological Society of America Special Paper*, v. **201**, p. 9-14.

- Kinsman, D.J.J., 1969, Interpretation of Sr²⁺ concentrations in carbonate minerals and rocks: *Journal of Sedimentary Petrology*, v. **39**, p. 486-508.
- Knauth, P.A., and Epstein, S., 1976, Hydrogen and oxygen isotope ratios in nodular and bedded cherts: *Geochimica et Cosmochimica Acta*, v. **40**, p. 1095-1108.
- Knauth, P.A., and Beunas, M.A., 1986, Isotope geochemistry in fluid inclusions in Permian halite with implications for the isotopic history of ocean water and the origin of saline formation waters. *Geochimica et Cosmochimica Acta*, v. **50**, p. 419-433.
- Knauth, P.A., Kealy, S., and Larimer, S., 1985, Isotopic composition of Silurian seawater. *Geol. Soc. Amer. Ann. Meet. Abs.*, p. 630.
- Knoll, M.A., and James, W.C., 1987, Effect of the advent and diversification of vascular landplants on mineral weathering through geologic time: *Geology*, v. **15**, p. 1099-1102.
- Kramer, J.W., and Friedman, G.M., 1986, Centerfield limestone and its clastic correlations (Middle Devonian, New York): A sedimentological approach: *Northeastern Geology*, v. **8**, p. 61-90.
- Krantz, D.E., Williams, D.F., and Jones, D.S., 1987, Ecological and paleoenvironmental information using stable isotope profiles from living and fossil molluscs: *Palaeogeography, Palaeoclimatology, Palaeoecology*, v. **58**, p. 249-266.
- Krantz, D.E., Kornick, A.T., and Williams, D.F., A model for interpreting continental-shelf hydrographic processes from the stable isotope and cadmium:calcium profiles of scallop shells: *Palaeogeography, Palaeoclimatology, Palaeoecology*, v. **64**, p. 123-140.
- Kreisa, R.D., 1981, Storm-generated structures insubtidal marine facies with examples from the Middle and Upper Ordovician of southwestern Virginia: *Journal of Sedimentary Petrology*, v. **51**, p. 823-848.
- Kump, L.R., 1988, Terrestrial feedback in atmospheric oxygen regulation by fire and phosphorus: *Nature*, v. **335**, p. 152-154.
- _____, 1989a, Chemical stability of the atmosphere and ocean: *Palaeogeography, Palaeoclimatology, Palaeoecology* (Global and Planetary Change Section), v. **75**, p. 123-136.
- _____, 1989b, Alternative modelling approaches to the geochemical cycles of carbon, sulphur and strontium isotopes. *American Journal of Science*, v. **289**, p. 390-410.

- Kump, L.R., and Garrels, R.M., 1986, Modelling atmospheric O₂ in the global sedimentary redox cycle. *American Journal of Science*, v. **286**, p. 337-360.
- LaBarbera, M., 1977, Brachiopod orientation to water movement 1. Theory, laboratory behaviour and field orientations: *Paleobiology*, v. **3**, p. 270-287.
- _____, 1978, Brachiopod orientation to water movement: functional morphology: *Lethaia*, v. **11**, p. 67-79.
- _____, 1981a, The ecology of Mesozoic *Gryphaea*, *Exogyra*, and *Ilymatogyra* (Bivalvia: Mollusca) in a modern ocean: *Paleobiology*, v. **7**, no. 4., p. 510-526.
- _____, 1981b, Water flow patterns in and around three species of articulate brachiopods; *Journal of Experimental Marine Biology and Ecology*, v. **55**, p. 185-206.
- Land, L.S., Lang, J.C., and Barnes, D.J., 1975, Extension rate: A primary control on the isotopic composition of West Indian (Jamaican) scleractinian reef coral skeletons. *Marine Biology*, v. **33**, p. 221-233.
- Landing, E., and Brett, C.E., 1987, Trace fossils and regional significance of a Middle Devonian (Givetian) disconformity in Southwestern Ontario: *Journal of Paleontology*, v. **61**, p. 205-230.
- Lasaga, A.C., 1989, A new approach to isotopic modeling of the variation of atmospheric oxygen through the Phanerozoic. *American Journal of Science*, v. **289**, p. 411-435.
- Lasaga, A.C., Berner, R.A., and Garrels, R.M., 1985, An improved geochemical model of atmospheric CO₂ fluctuations over the past 100 million years. in Sundquist, E.T., and Broecker, W.S., (eds.). *The carbon cycle and atmospheric CO₂: Natural variations Archean to present*. American Geophysical Union Monograph, **32**, p. 397-411.
- Laverack, M.S., 1987, *Invertebrates; Lecture notes on invertebrate zoology*: Blackwell Scientific Publications, p. 166-168.
- Liberty, B.A., 1969, Paleozoic geology of the Lake Simcoe area, Ontario: Geological Survey of Canada Memoir **355**, 210p.
- _____, 1975, Upper Ordovician Stratigraphy of the Toronto Area: in Telford P.G., (ed.), *G.A.C. Field Guide Book*, Waterloo 1975, p. 43-53.
- Liberty, B.A., and Bolton, T.E., 1971, Paleozoic geology of the Bruce Peninsula area, Ontario: Geological Survey of Canada Memoir **360**, 163p.

- Liebe, R.M., and Grasso, T.X., 1988, Geology of the Rochester Gorge, Rochester, New York: *Northeastern Geology*, v. **10**, no.1, p. 13-18.
- Lindholm, R.C., and Finkelman, R.B., 1972, Calcite staining: semiquantative determinations of ferrous iron. *Journal of Sedimentary Petrology*, v. **42**, p. 239-242.
- Lockley, M.G., 1983, A review of brachiopod dominated palaeocommunities from the type Ordovician: *Palaeontology*, v. **26**, p. 111-145.
- Logan, A., 1975, Ecological observations on the Recent articulate brachiopod *Argyrotheca bermudana* (Dall) from the Bermuda Platform: *Bulletin of Marine Science*, v. **25**, no. 2, p. 186-204.
- Lorens, R.B., 1981, Sr, Cd, Mn and Co distribution coefficients in calcite as a function of calcite precipitation rate: *Geochimica et Cosmochimica Acta*, v. **45**, p. 553-561.
- Lowenstam, H.A., 1961, Mineralogy, $^{18}\text{O}/^{16}\text{O}$ ratios, and strontium contents of Recent and fossil brachiopods and their bearing on the history of the oceans: *Journal of Sedimentary Petrology*, v. **69**, p. 241-260.
- _____, 1963, Biologic problems relating to the composition and diagenesis of sediments: *in* Donnelly, T.W., (ed.), *The Earth Sciences: Problems and progress in current research*: University of Chicago Press, Chicago, p. 137-195.
- Ludvigsen, R., 1978, Towards an Ordovician trilobite biostratigraphy of southern Ontario. *in* Sanford, J.T., and Mosher, R.E., (eds.). *Geology of the Manitoulin Area*. Michigan Basin Geological Society, Special Paper **3**, p. 43-45.
- Lutz, R.A., and Rhoads D.C., 1977, Anaerobiosis and a theory of growth line formation: *Science*, v. **198**, p. 1222-1227.
- Machel, H.G., 1985, Cathodoluminescence in calcite and dolomite and its chemical interpretation: *Geoscience Canada*, v. **12**, p. 134-147.
- Majid, A.H., and Veizer, J., 1986, Deposition and chemical diagenesis of Tertiary carbonates, Kirkuk Oil field, Iraq. *A.A.P.G. Bulletin*, v. **70**, p. 898-913.
- Major, R.P., Halley, R.B., and Lucas, K.J., 1988, Cathodoluminescent bimineralic ooids from the Pleistocene of the Florida continental shelf: *Sedimentology*, v. **35**, p. 843-855.
- Maliva, R.G., and Siever, R., 1988, Mechanism and controls of silicification of fossils in limestones: *Journal of Geology*, v. **96**, p. 387-398.

- [McAllister, J.M., 1987, Trace element geochemistry of Ordovician and Devonian trilobite cuticles, Ontario and New York State. Unpublished B.Sc. thesis, Brock University, 79p.]
- [_____, 1989, Paleozoic trilobite biogeochemistry of North America. unpublished M.Sc. thesis, Brock University, ?p.]
- McAllister, J.M., and Brand, U., 1989, Primary and diagenetic microstructures in trilobites. *Lethaia*, v. **22**, p. 101-111.
- McConnaughey, 1989a, ^{13}C and ^{18}O isotopic disequilibrium in biological carbonates: I. Patterns: *Geochimica et Cosmochimica Acta*, v. **53**, p. 151-162.
- _____, 1989b, ^{13}C and ^{18}O isotopic disequilibrium in biological carbonates: II. *In vitro* simulation of kinetic isotope effects: *Geochimica et Cosmochimica Acta*, v. **53**, p. 163-171.
- McIntire, W.L., 1963, Trace element partition coefficients - a review of theory applications to geology: *Geochimica et Cosmochimica Acta*, v. **27**, p. 1209-1264.
- Meyers, W.J., 1974, Carbonate cement stratigraphy of the Lake Valley Formation (Mississippian), Sacramento Mountains, New Mexico. *Journal of Sedimentary Petrology*, v. **44**, p. 837-861.
- [Milinkovich, T., 1984, Dolomitization and luminescence stratigraphy of the Irondequoit Formation, Ontario and New York. Unpublished B.Sc. thesis, Brock University, St. Catharines, 88p.]
- Miller, K.B., 1986, Depositional environments and sequences, "Pleurodictyum zone", Ludlowville Formation of Western New York: *in* Brett, C.E., (ed.), *Dynamic stratigraphy and depositional environments of the Hamilton Group (Middle Devonian) in New York State, Part 1*. New York State Museum Bulletin, Nos. **457**, p. 57-77.
- Miller, K.B., Brett, C.E., and Parsons, K.M., 1988, The paleoecologic significance of storm generated disturbance within a Middle Devonian muddy epeiric sea: *Palaios*, v. **3**, p. 35-52.
- Milliman, J.D., 1974, *Marine carbonates*. Springer Verlag, Berlin, 375p.
- Mook, W.G., 1971, Paleotemperatures and chlorinities from stable carbon and oxygen isotopes in shell carbonate: *Palaeogeography, Palaeoclimatology, Paleoecology*, v. **9**, p. 245-263.
- Moran, S.B., and Moore, R.M., 1988, Evidence from mesocosm studies for biological removal of dissolved aluminium from sea water: *Nature*, v. **335**, p. 706-708.

- Morris, B., Barnes, J., Brown, F., and Markham, J., 1977, The Bermuda marine environment: A report of the Bermuda inshore waters investigations 1976-1977: Bermuda Biological Station Special Publication No. 15, 118p.
- [Morrison, J.O., 1986, Molluscan carbonate geochemistry and paleoceanography of the late Cretaceous Western Interior Seaway of North America. Unpublished M.Sc. thesis, Brock University, St. Catharines, 214p.]
- Morrison, J.O., and Brand, U., 1984, Secular and environmental of seawater: an example of brachiopod chemistry. Geol. Assoc. Can., Ann. Meet., Prog. Abst. v. **10**, p. 91.
- _____, 1986, Geochemistry of Recent marine invertebrates: Geoscience Canada, v. **13**, p. 237-254
- _____, 1988, An evaluation of diagenesis and chemostratigraphy of Upper Cretaceous molluscs from the Canadian Interior Seaway: Chemical Geology (Isotope Geoscience Section), v. **72**, p. 235-248.
- Morrison, J.O., Brand, U., and Rollins, H.B., 1985, Paleoenvironmental analysis of the Pennsylvanian Brush Creek Fossil Allochems, Pennsylvania, U.S.A. C.R., 10th Int. Cong. on Carboniferous Stratigraphy and Geology, v. **2**, p. 271-280.
- Mucci, A., and Morse, J.W., 1983, The incorporation of Mg²⁺ and Sr²⁺ into calcite overgrowths: influences of growth rate and solution composition: Geochimica et Cosmochimica Acta, v. **47**, p. 217-233.
- Mucci, A., 1988, Manganese uptake during calcite precipitation from seawater: conditions leading to the formation of a pseudokutnahorite: Geochimica et Cosmochimica Acta, v. **52**, p. 1859-1868.
- Muehlenbachs, K., and Clayton, R.N., 1976, Oxygen isotope composition of the oceanic crust and its bearing on seawater. Journal of Geophysical Research, v. **81**, p. 4365-4369.
- Nie, H.H., Hull, C.H., Jenkins, J.G., Steinbrenner, K., and Bent, D.H., 1975, Statistical package for the Social Sciences: McGraw-Hill.
- Niklas, K.J., Tiffney, B.H., and Knoll, A.H., 1985, Patterns in vascular land plant diversification: an analysis at the species level: *in* Phanerozoic Diversity Patterns (ed. Valentine, J.W.), p. 97-128.
- Nissenbaum, A., Presley, B.J., and Kaplan, I.R., 1972, Early diagenesis in a reducing fjord, Sasnich Inlet, British Columbia, 1. Chemical and isotopic

- changes in major components of interstitial water: *Geochimica et Cosmochimica Acta*, v. **36**, p. 1007-1027.
- O'Shea, K.J., Miles, M.C., Fritz, P., Frapce, S.K., and Lawson, D.E., 1988, Oxygen-18 and carbon-13 in the carbonates of the Salina formation of southwestern Ontario. *Canadian Journal of Earth Sciences*, v. **25**, p. 182-194.
- Oliver, W.A., 1976, Biogeography of Devonian Rugose corals: *Journal of Paleontology*, v. **50**, p. 365-373.
- Okumura, M., and Kitano, Y., 1986, Coprecipitation of alkali metal ions with CaCO_3 : *Geochimica et Cosmochimica Acta*, v. **50**, p. 49-58.
- Paine, R.T., 1969, Growth and size distribution of the brachiopod *Terebratalia transversa* Sowerby. *Pacific Science*, v. **23**, p. 337-343.
- Parsons, K.M., Brett, C.E., and Miller, K.B., 1988, Taphonomy and depositional dynamics of Devonian shell-rich mudstones: *Palaeogeography, palaeoecology, palaeo-climatology*, v. **63**, p. 109-139.
- Peck, L.S., Morris, D.J., and Clarke, A., 1986, The caeca of punctate brachiopods: a respiring tissue not a respiratory organ: *Lethaia*, v. **19**, p. 232.
- _____, 1989, Oxygen consumption and the role of caeca in the Recent Antarctic brachiopod *Liothyrella uva notorcadensis* (Jackson, 1912); in Emig, C.C., and Rachebouef, P.R., (eds.); *Proceedings of the 1st International Congress on brachiopods*, Brest, France. *Biostratigraphie du Paleozoique*, v. **5**.
- Peck, L.S., Clarke, A., and Holmes, L.J., 1987, Size, shape and the distribution of organic matter in the Recent Antarctic brachiopod *Liothyrella uva*: *Lethaia*, v. **20**, p. 33-40.
- Perry, E.C., and Tan, F.C., 1972, Significance of oxygen and carbon isotope variations in Early Precambrian cherts and carbonate rocks of southern Africa: *Geological Society of America Bulletin*, v. **83**, p. 647-664.
- Pierson, B.J., 1981, The control of cathodoluminescence in dolomite by iron and manganese. *Sedimentology*, v. **28**, p. 601-610.
- Plummer, L.N., and Busenberg, E., 1982, The solubilities of calcite, aragonite and vaterite in CO_2 - H_2O solutions between 0° and 90°C and an evaluation of the aqueous model for the system CaCO_3 - CO_2 - H_2O : *Geochimica et Cosmochimica Acta*, v. **46**, p. 1011-1040.

- Pingitore, N.J., 1976, Vadose and phreatic diagenesis: processes, products and their recognition in corals: *Journal of Sedimentary Petrology*, v. **46**, p. 985-1006.
- _____, 1978, The behaviour of Zn^{2+} and Mn^{2+} during carbonate diagenesis: theory and applications: *Journal of Sedimentary Petrology*, v. **48**, p. 799-814.
- _____, 1982, The role of diffusion of diffusion during carbonate diagenesis: *Journal of Sedimentary Petrology*, v. **52**, p. 27-39.
- Pingitore, N.J., and Eastman, M.P., 1985, The co-precipitation of Sr^{2+} with calcite at 25°C and 1 atm.: *Geochimica et Cosmochimica Acta*, v. **50**, p. 2195-2203.
- Pingitore, N.J., Eastman, M.P., Snadige, M., Oden, K., and Freiha, B., 1988, The co-precipitation of manganese (II) with calcite: an experimental study. *Marine Chemistry*, v. **23**,
- [Popp, B.N., 1981, Coordinated textural, isotopic and elemental analyses of constituents in some middle Devonian limestones: Unpublished M.Sc. thesis, Urbana, University of Illinois, 136p.]
- [_____, 1986, The record of carbon, oxygen, sulfur, and strontium isotopes among constituents in late Paleozoic brachiopods: Unpublished Ph.D. thesis, Urbana, Illinois, University of Illinois, 199p.]
- Popp, B.N., Anderson, T.F., and Sandberg, P.A., 1986a, Brachiopods as indicators of original isotopic compositions in some Paleozoic limestones: *Geological Society of America Bulletin*, v. **97**, p. 1262-1269.
- _____, 1986b, Textural, elemental and isotopic variation among constituents in Middle Devonian Limestones, North America: *Journal of Sedimentary Petrology*, v. **56**, p. 715-727.
- Popp, B.N., Takigiku, R., Hayes, J.M., Louda, J.W., and Baker, E.W., 1989, The post-Paleozoic chronology and mechanism of ^{13}C depletion in rprimary marine organic matter. *American Journal of Science*, v. **289**, p. 436-454.
- Presley, B.J., Kolodny, Y., Nissebaum, A., and Kaplan, I.R., 1972, Early diagenesis in a reducing fjord, Sasnich Inlet, British Columbia, II. Trace element distribution in interstitial water and sediment: *Geochimica et Cosmochimica Acta*, v. **36**, p. 1073-1090.
- Quinlan, G.M., and Beaumont, C., 1984, Appalachian thrusting, lithospheric flexure and the Paleozoic stratigraphy of the eastern interior of North America: *Canadian Journal of Earth Sciences*, v. **21**, p. 973-996.

- Racki, G., 1989, Articulate brachiopods and Late Paleozoic dysaerobic biofacies: *Lethaia*, v. **22**, p. 148.
- Reeder, R.J., 1983, Crystal chemistry of the rhombohedral carbonates: *in* Reeder, R.J., (ed.) *Carbonates: Mineralogy and Chemistry*, Reviews in Mineralogy, v. **11**, Washington D.C., Mineralogical Society of America, p. 1-48.
- Reeder, R.J., and Grams, J.C., 1987, Sector zoning in calcite cement crystals: Implications for trace element distributions in carbonates: *Geochimica et Cosmochimica Acta*, v. **51**, p. 187-194.
- Rega, A.F., 1987, *The Ca²⁺ pump of plasma membranes*: CRC Press, Inc., p. 91.
- Rhoads, D.C., and Morse, J.W., 1971, Evolutionary and ecologic significance of oxygen-deficient marine basins. *Lethaia*, v. **4**, p. 413-428.
- Rickard, L.V., 1981, The Devonian System of New York State: *in* Oliver, W.A., and Klapper, G., (eds.), *Devonian Biostratigraphy of New York, Part 1: International Union of Geological Sciences, Subcommision on Devonian Stratigraphy*, Washington, D.C., p. 5-22.
- Richardson, J.R., 1981a, Brachiopods and pedicles: *Paleobiology*, v. **7**, p. 87-95.
- _____, 1981b, Brachiopods in mud: resolution of a dilemma: *Science*, v. **211**, p. 1161-1163.
- _____, 1981c, Distribution and orientation of six brachiopod species from New Zealand, *New Zealand Journal of Zoology*, v. **8**, p. 189-196.
- Richardson, J.R., and Mineur, R.J., 1981, Differentiation of species of *Terebratella* (Brachiopoda: Terebratellinae): *New Zealand Journal of Zoology*, v. **8**, p. 163-167.
- Rollins, H.B., Sandweiss, D.H., Brand, U., and Rollins, J.C., 1987, Growth increment and stable isotope analysis of marine bivalves: Implications for the geochronological record of El Niño. *Geochronology*, v. **2**, no. 3,
- Rodgers, J., 1971, The Taconic Orogeny: *Geological Society of America Bulletin*, v. **82**, p. 1141-1178.
- Rosenberg, G.D., 1980, An ontogenetic approach to the environmental significance of bivalve shell chemistry: *in* *Skeletal Growth of Aquatic Organisms*; (eds.) Rhoads, D.C., and Lutz, R.A.); Plenum Press, New York, London, p. 133-168.

- Rosenberg, G.D., Hughes, W.W., and Tkachuck, R.D., 1988, Intermediary metabolism and shell growth in the brachiopod *Terebratalia transversa*: *Lethaia*, v. **21**, p. 219-230.
- Ross, R.J., and others, 1982, The Ordovician system in the United States. International Union of Geological Sciences, Publication **12**.
- Rowell, A.J., and Grant, R.E., 1987, Phylum Brachiopoda: *in* Fossil Invertebrates (eds.) Boardman, R.S., Cheetham, A.H., and Rowell, A.J.; Blackwell Scientific Publications, p. 445-496.
- Rudwick, M.J.S., 1970, Living and Fossil Brachiopods: London, Hutchinson and Company, 179p.
- Russell, D.J., and Telford, P.G., 1983, Revisions to the stratigraphy of the Upper Ordovician Collingwood beds of Ontario- A potential oil shale: *Canadian Journal of Earth Sciences*, v. **20**, p. 1780-1790.
- Rye, D.M., and Sommer, M.A., 1980, Reconstructing paleotemperature and paleosalinity regimes with oxygen isotopes. *in* Skeletal Growth of Aquatic Organisms; (eds.) Rhoads, D.C., and Lutz, R.A.; Plenum Press, New York, London, p. 169-203.
- Sanford, J., and Mosher, R.E., 1978, Geology of the Manitoulin Area: Michigan Basin Geological Society Special Paper No. 3.
- Sanford, B.V., Thompson, F.J., and McFall, G.H., 1985, Plate tectonics - A possible controlling mechanism in the development of hydrocarbon traps in southwestern Ontario: *Bulletin of Canadian Petroleum Geology*, v. **33**, p. 52-71.
- Savarese, M., Gray, L.M., and Brett, C.E., 1986, Faunal and lithologic cyclicity in the Centerfield Member (Middle Devonian: Hamilton Group) of Western New York: A reinterpretation of depth history: *in* Brett, C.E., (ed.), Dynamic stratigraphy and depositional environments of the Hamilton Group (Middle Devonian) in New York State, Part 1. *New York State Museum Bulletin*, Nos. **457**, p. 1-4.
- Scotese, C.R., Bambach, R.K., Barton, C., Van Der Voo, R., and Zeigler, A.M., 1979, Paleozoic base maps: *Journal of Geology*, v. **87**, p. 217-277.]
- Shackleton, N.J., 1974, Oxygen isotope analyses and Pleistocene temperatures re-assessed: *Nature*, v. **215**, p. 15-17.
- _____, 1977, Oxygen isotope and paleomagnetic evidence for early northern hemisphere glaciation: *Nature*, v. **268**, p. 618-620.

- Shen, G.T., and Boyle, E.A., 1988, Determination of lead, cadmium and other trace metals in annually-banded corals: *Chemical Geology* v. **67**, p. 47-62.
- Sherwood, B.A., Sager, S.L., and Holland, H.D., 1987, Phosphorus in foraminiferal sediments from North Atlantic Ridge cores and impure limestones: *Geochimica et Cosmochimica Acta*, v. **51**, p. 1861-1866.
- Shumway, S.E., 1982, Oxygen consumption in brachiopods and the possible role of punctae. *Journal of Experimental Marine Biology and Ecology*, v. **58**, p. 207-220.
- Shimer, H.W., and Shrock, R.R., 1972, *Index fossils of North America*: The M.I.T. Press, Cambridge, Mass., 837p.
- Siegenthaler, U., 1979, Stable hydrogen and oxygen isotopes in the water cycle. in Jager, E., and Hunziker, J.C., (eds.). *Lectures in isotope geology*. Springer, Berlin, p. 264-273.
- Simkiss, K., 1976, Cellular aspects of calcification: *in* Watabe, N., and Wilbur, K.M. (eds.) *The mechanisms of calcification in invertebrates*; University of South Carolina Press, p. 1-31.
- Sinclair, G.W., 1975, Some Ordovician fossils from Central Ontario: *in* Telford P.G., (ed.), *G.A.C. Field Guide Book*, Waterloo 1975, p. 33-42.
- Sinclair, G.W., Copeland, M.J., and Bolton, M.E., 1984, Ordovician fossils from Lakefield Quarry: *G.A.C. Field Meeting Guidebook*, Toronto, 1984, p. 24-29.
- Speyer, S.E., and Brett, C.E., 1985, Clustered trilobite assemblages in the Middle Devonian Hamilton Group: *Lethaia*, v. **18**, p. 85-103.
- _____, 1986, Trilobite taphonomy and Middle Devonian taphofacies: *Palaeo*, v. **1**, p. 312-327.
- _____, 1988, Taphofacies models for epeiric sea environments: Middle Paleozoic examples: *Palaeogeography, Palaeoclimatology, Palaeoecology*, v. **63**, p. 225-262.
- Sterreri, W., 1986, The fauna of Bermuda. Bermuda Biological Station report, p. 517-519.
- Stewart, I.R., 1981, Population structure of articulate brachiopod species from soft and hard substrates. *New Zealand Journal of Zoology*, v. **8**, p. 197-207.

- Stricker, S.A., and Reed, C.G., 1985, The protegulum and juvenile shell of a recent articulate brachiopod: pattern of growth and chemical composition: *Lethaia*, v. **18**, p. 295-303.
- Swart, P.K., 1983, carbon and oxygen isotope fractionation in scleractinian corals: a review: *Earth Science Review*, v. 19, p. 51-80.
- Tarutani, T., Clayton, R.N., and Mayeda, T.K., (1969), The effect of polymorphism and magnesium substitution on oxygen isotope fractionation between calcium carbonate and water: *Geochimica et Cosmochimica Acta*, v. **33**, p. 987-996.
- Tasch, P., 1973, *Paleobiology of the Invertebrates*: John Wiley and Sons, Inc, New York, London, Sydney, Toronto, 946p.
- Telford, P.G., 1978, Silurian stratigraphy of the Niagara Escarpment, Niagara Falls to the Bruce Peninsula: *Geological Association of Canada Field Guide Book*, Toronto 1978, p. 28-48.
- Telford, P.G., Johnson, M.E., and Verma, H., 1981, Manitoulin Island: Field Trip Guidebook: *Canadian Paleontology and Biostratigraphy Seminar*, Ontario Geological Survey.
- Temple, J.T., 1978, The use of factor analysis in geology, *Mathematical geology*, v. **10**, no. 4, 379-387.
- Ten Have, K.M., and Heijnen, W., 1985, Cathodoluminescence activation and zonation in carbonate rocks: an experimental approach. *Geologie Mijnb.*, v. **64**, p. 297-310.
- Tetrault, D.K., 1987, Silurian (Wenlockian) trilobite associations of western New York and Southern Ontario: *Geological Society of America, Northeastern Section Meeting, Pittsburgh, Abs. with Program*, v. **19**, no. 1, p. 61.
- Thayer, C.W., 1974, Salinity tolerances of articulate brachiopods: *Geological Society of America, Northeastern Section, 9th Ann. Meet., Abs. with Programs*, p. 80-81.
- _____, 1979, Biological bulldozers and the evolution of marine benthic communities: *Science*, v. **203**, p. 458-461.
- _____, 1983, Sediment-mediated biological disturbance and the evolution of marine benthos: *in* Tevesz, M.J.S., and McCall, P.L., (eds.), *Biotic interactions in Recent and Fossil Benthic Communities. Topics in Geobiology 3*, Plenum Press, New York, p. 479-625.
- _____, 1986a, Are brachiopods better than bivalves? Mechanisms of turbidity tolerance and their interaction with feeding in articulates: *Paleobiology*, v. **12**, p. 161-174.

- _____, 1986b, Respiration and the function of brachiopod punctae: *Lethaia*, v.19, p. 23-31.
- Thompson, J., Mullins, H.T., Newton, C.R., and Vercootere, T.L., 1985, Alternative biofacies model for dysaerobic communities. *Lethaia*, v. 18, p. 167-179.
- Thompson, J., and Newton, C.R., 1987, Ecological reinterpretation of the dysaerobic "*Leiorhynchus* fauna": Upper Devonian Genesee Black Shale, Central New York: *Palaeis*, v.2, p. 274-281.
- Thomson, J., Higgs, N.G., Jarvis, I., Hydes, S.D. Jr., Colley, S., and Wilson, T.R.S., 1986, The behaviour of manganese in Atlantic carbonate sediments: *Geochimica et Cosmochimica Acta*, v. 50, p. 1807-1818.
- Thusu, B., 1972, Depositional environment of the Rochester Formation (Middle Silurian) in Southern Ontario: *Journal of Sedimentary Petrology*, v. 42, p. 130-134.
- Tipper, J.C., 1975, Lower Silurian animal communities- Three case histories: *Lethaia*, v. 8, p. 287-299.
- Titus, R., 1986, Fossil communities of the Upper Trenton Group (Ordovician) of New York State: *Journal of Paleontology*, v. 60, no. 4, p. 805-824.
- Titus, R., and Cameron, B., 1976, Fossil communities of the lower Trenton Group (Middle Ordovician) of central and northwestern New York State: *Journal of Paleontology*, v. 50, p. 1209-1225.
- Towe, K.M., and Thompson, G.R., 1972, The structure of some bivalve shell carbonates prepared by ion-beam thinning. *Calc. Tissue Research*, v. 10, p. 38-48.
- Tunncliffe, V., and Wilson, K., 1988, Brachiopod populations: distribution in fjords of British Columbia and tolerance of low oxygen concentrations: *Marine Ecology Progress Series*, v. 47, p. 117-128.
- Urey, H.C., Lowenstam, H.A., Epstein, S., and McKinney, C.R., 1951, Measurements of paleotemperatures and temperatures of the Upper Cretaceous of England, Denmark and the southeastern United States. *Geological Society of America Bulletin*, v. 62, p. 399-416.
- Valentine, J.W., 1985, Are interpretations of ancient marine temperatures constrained by the presence of ancient marine organisms: *in* : The CO₂ cycle

- Veizer, J., 1977a, Geochemistry of lithographic limestone and dark marls from the Jurassic of southern Germany: *Neues Jahrbuch, Geol. Palaont., Abh.*, v. **153**, p. 129-146.
- _____, 1977b, Diagenesis of pre-Quaternary carbonates as indicated by tracer studies: *Journal of Sedimentary Petrology*, v. **47**, p. 561-581.
- _____, 1983a, Chemical diagenesis of carbonates: theory and application of trace element techniques. *in* *Stable Isotopes in sedimentary Geology: S.E.P.M., Short Course No. 10*, p. 3.1-3.100.
- _____, 1983b, Trace element and stable isotopes in sedimentary carbonates, *in* Reeder, R.J., (ed.) *Carbonates: mineralogy and chemistry: Reviews in Mineralogy*, v. **11**, p. 265-299.
- _____, 1985, Carbonates and ancient oceans: isotopic and chemical record on time scales of 10^7 - 10^9 years in Sundquist, E.T., and Broecker, W.S., (eds.) *Carbon cycle and atmospheric CO₂: Natural variations Archean to present. Geophysical Monograph 32*, p. 595-601.
- Veizer, J., and Demovic, R., 1974, Strontium as a tool in facies analysis: *Journal of Sedimentary Petrology*, v. **44**, p. 93-115.
- Veizer, J., and Fritz, P., 1976, Possible control of post-depositional alteration in oxygen paleotemperature determinations: *Earth and Planetary Science Letters*, v. **33**, p. 255-260.
- Veizer, J., and Hoefs, 1976, The nature of $^{18}O/^{16}O$ and C^{13}/C^{12} secular trends in sedimentary carbonate rocks: *Geochimica et Cosmochimica Acta*, v. **40**, p. 1387-1395.
- Veizer, J., Lemieux, J., Jones, B., Gibling, M.R., and Savelle, J., 1978, Paleosalinity and dolomitization of a Lower Paleozoic carbonate sequence, Somerset and Prince of Wales Islands. *Canadian Journal of Earth Science*, v. **15**, p. 1448-1461.
- Veizer, J., Holser, W.T., and Wilgus, C.K., 1980, Correlation of $^{13}C/^{12}C$ and $^{34}S/^{32}S$ secular variations: *Geochimica et Cosmochimica Acta*, v. **44**, p. 579-587.
- Veizer, J., Fritz, P., and Jones, B., 1986, Geochemistry of brachiopods: Oxygen and carbon isotopic records of Paleozoic oceans: *Geochimica et Cosmochimica Acta*, v. **50**, p. 1679-1696
- Vogel, K.K., Golubic, S., and Brett, C.E., 1987, Endolithic associations and their relation to facies distributions in the Middle Devonian of New York State: *Lethaia*, v. **20**, p. 263-290.

- Walker, K.R., and Laporte, L.F., 1970, Congruent fossil communities from Ordovician and Devonian carbonates of New York: *Journal of Paleontology*, v. **44**, p. 928-944.
- Walker, K.R., and Bambach, R.K., 1974, Feeding by benthic invertebrates: Classification and terminology for paleoecological analysis: *Lethaia*, v. **7**, p. 67-78.
- [Waasenaar, L.N., 1986, A geochemical and paleoceanographic investigation using marine molluscs of the late Quaternary marine submergences Quebec, Ontario, British Columbia. Unpublished M.Sc. thesis, Brock University, St. Catharines, 174p.]
- Watkins, R., and Boucot, A.J., 1975, Evolution of Silurian brachiopod communities along the southeastern coast of Acadia: *Geological Society of America Bulletin*, v. **86**, p. 243-254.
- Wefer, G., 1983, Die Verteilung stabiler Sauerstoff und Kohlenstoff-isotopen in Kalkschalen mariner organismen: Grundlage einer Isotopischen Palokologie: *Habitationschrift, Universitat Kiel*, 151p.
- _____, 1985, Die Vertelung stabiler isotope in Kalkschalen mariner organismen: *Geologisches Jahrbuch, A*. **82**, 3-111.
- Westrop, S.R., 1986, Taphonomic versus ecologic controls on taxonomic relative abundance patterns in tempestites: *Lethaia*, v. **19**, p. 123-132.
- White, A.F., 1977, Sodium and potassium coprecipitation in aragonite; *Geochimica et Cosmochimica Acta*, v. **42**, p. 1896-1904.
- _____, 1978, Sodium co-precipitation in calcite and dolomite: *Chemical Geology*, v. **23**, p. 65-76.
- White, L.K., Szabo, A., Carkner, P., and Chasteen, N.D., 1977, An electron paramagnetic study of Mn II in the aragonite lattice of a clam shell, *Mya arenaria*. *Journal of Physical Chemistry*, v. **81**, p. 1420-1424.
- Williams, A., 1966, Growth and structure of the shell of living articulate brachiopods: *Nature*, v. **211**, p. 1146-1148.
- _____, 1968a, Evolution of the shell structure of articulate brachiopods: *Palaeontological Association of London Special Papers in Palaeontology*, No.2, 55p.
- _____, 1968b, A history of skeletal secretion among articulate brachiopods: *Lethaia*, v. **1**, p. 268-287.

- _____, 1971, Scanning electron microscopy of the calcareous skeleton of fossil and living brachiopods: *in* Heywood (ed.) Scanning Electron Microscopy: Systematics and evolutionary applications, Academic Press.
- Williams, A., and Rowell, A.J., 1965, Morphology: *in* Moore, R., (ed.); Treatise on Invertebrate Paleontology, Brachiopoda, Part H, H57-H138. Geological Society of America and University of Kansas Press, Lawrence.
- Wilson, M.V.H., 1982, Origin of brachiopod-bryozoan assemblages in an Upper Carboniferous limestone: importance of physical and ecological controls: *Lethaia*, v. 15, p. 263-273.
- Witman, J.D., and Cooper, R.A., 1983, Disturbance and contrasting patterns of population structure in the brachiopod *Terebratulina septentrionalis* (Couthoy) from two subtidal habitats: *Journal of Experimental Marine Biology and Ecology*, v. 73, p. 57-79.
- Witkze, B.J., 1987, Models for circulation patterns in epicontinental seas applied to Paleozoic facies of the North American craton, *Paleoceanography*, v. 2, no. 2, p. 229-248.
- Woodrow, D.L., 1985, Paleogeography, paleoclimate, and the sedimentary processes of the Late Devonian Catskill Delta: *in* The Catskill Delta (eds. Woodrow, D.L., and Sevon, W.D.): Geological Society of America Special Paper, v. 201, p. 51-64.
- Worsley, D., and Broadhurst, F.M., 1975, An environmental study of Silurian atrypid communities from southern Norway: *Lethaia*, v.8, p. 271-286.
- Wygard, G.T., 1986, Deposition and early diagenesis of a Middle Devonian marine shale: Ludlowvill Formation, Western New York: *in* Brett, C.E., (ed.), Dynamic stratigraphy and depositional environments of the Hamilton Group (Middle Devonian) in New York State, Part 1. New York State Museum Bulletin, Nos. 457, p. 78-101.
- Zachara, J.M., Kittrick, J.A., and Harsh, J.B., 1988, The mechanism of Zn²⁺ adsorption on calcite: *Geochimica et Cosmochimica Acta*, v. 52, p. 2281-2291.
- Zeigler, A.M., 1965, Silurian marine communities and their environmental significance: *Nature*, v.1207, p. 270-272.
- Zeigler, A.M., Cocks, L.R.M., and Bambach, R.K., 1968, Composition and structure of Lower Silurian marine communities: *Lethaia*, v.1, p. 1-27.
- Zeigler, A.M., Cocks, L.R.M., and McKerrow, W.S., 1968, The Llandovery transgression of the Welsh Borderland: *Journal Geological Society London*, v. 11, p. 736-

Zemann, J., 1969, Crystal chemistry, *in* Wedepohl, K.H., (ed.), Handbook of Geochemistry: Springer Verlag, Berlin, v. **1**, p.

Appendix I

Locality and stratigraphic information

1A. Hungry Hollow Area

Widder Formation. (Fig. A-1)

Abandoned brick pit on north side of the Ausable River, 3.5 km east of Arkona, Ontario. Shales exposed in new diggings on west side of quarry.

- i) Widder Formation. Calcareous dark grey fissile shales with scattered *Devonochonetes*, *Mucrospirifer mucronatus*, and *M. thedfordensis*. Brachiopods are predominantly articulated and not deformed. Fine disseminated pyrite is common often coating valves. *Greenops boothi* and *Phacops rana*. are commonly articulated. Sampled from the metre interval above base of the Widder Formation.

1B. Hungry Hollow Area

Hungry Hollow and Arkona Formations. (Fig. A-1)

Hamilton Group outcropping along the south bank of the Ausable River, 500 m west of the Hungry Hollow brick pit, 3.0 km east of Arkona, Ontario.

- ii) Hungry Hollow Formation. Light grey claystone with abundant favositid corals and disarticulated *Mucrospirifer mucronatus*. From shale interval 50 cm above encrusted crinoidal grainstone hardground (see Landing and Brett 1987).
- iii) Arkona Formation. Light grey claystone with abundant articulated and disarticulated *Mucrospirifer mucronatus* and *Devonochonetes*. Shale interval 0.75-1.0 m below the base of Hungry Hollow Formation grainstone.
- iv) Arkona Formation. Thin (4 cm), lenticular brachiopod and crinoid dominated packstone. A winnowed fossil hash bed approximately 5-6m below the base of the Hungry Hollow Formation. Alate and disarticulate *Mucrospirifer arkonensis* are abundant. The bed may represent a winnowed *Mucrospirifer* patch community?

2. Lake Erie shoreline bluffs

Eden Quadrangle

Ludlowville Formation (Fig. A-2)

10-12 m outcrop along Lake Erie near mouth of Eighteen Mile Creek. Approximately 600 m northwest along creek north of abandoned Lakeshore Boulevard bridge. Wanakah, Erie Co., New York State.

- i) Lower Wanakah Shale. Grey mudstone 15 cm-30 cm above Murder Creek Trilobite Bed (Miller et al., 1988). Collected over 15 cm interval. Abundant articulated *Athyris spiriferoides*, and *Rhipidomella vanuxemi*; *Mediospirifer audacula* and *Spinocyrtia granulosa* predominantly disarticulated and fragmented.
- ii) Lower Wanakah Shale. Prominent shell layer (5-10 cm thick) within sequence of calcareous grey mudstones, 60 cm below base of "Murder Creek Trilobite Bed". Many brachiopods are in life position and still articulated. *Mediospirifer audacula*, *Athyris spiriferoides* dominant. Large *Spinocyrtia* are commonly encrusted
- iii) "Pleurodictyum" Bed (Grabau, 1899) or Darien Coral Bed (Miller et al., 1988). Lower Wanakah Shale. Scattered brachiopods from grey calcareous shales approximately 1.5 m below "Murder Creek Trilobite Bed". 40 cm above Lakeview (*Nautilus*) Bed. *Athyris*, *Mucrospirifer*, *Spinocyrtia*, *Rhipidomella*, and *Stropheodonta* sp. are abundant. Most are articulated and *Athyris* are commonly in life position.

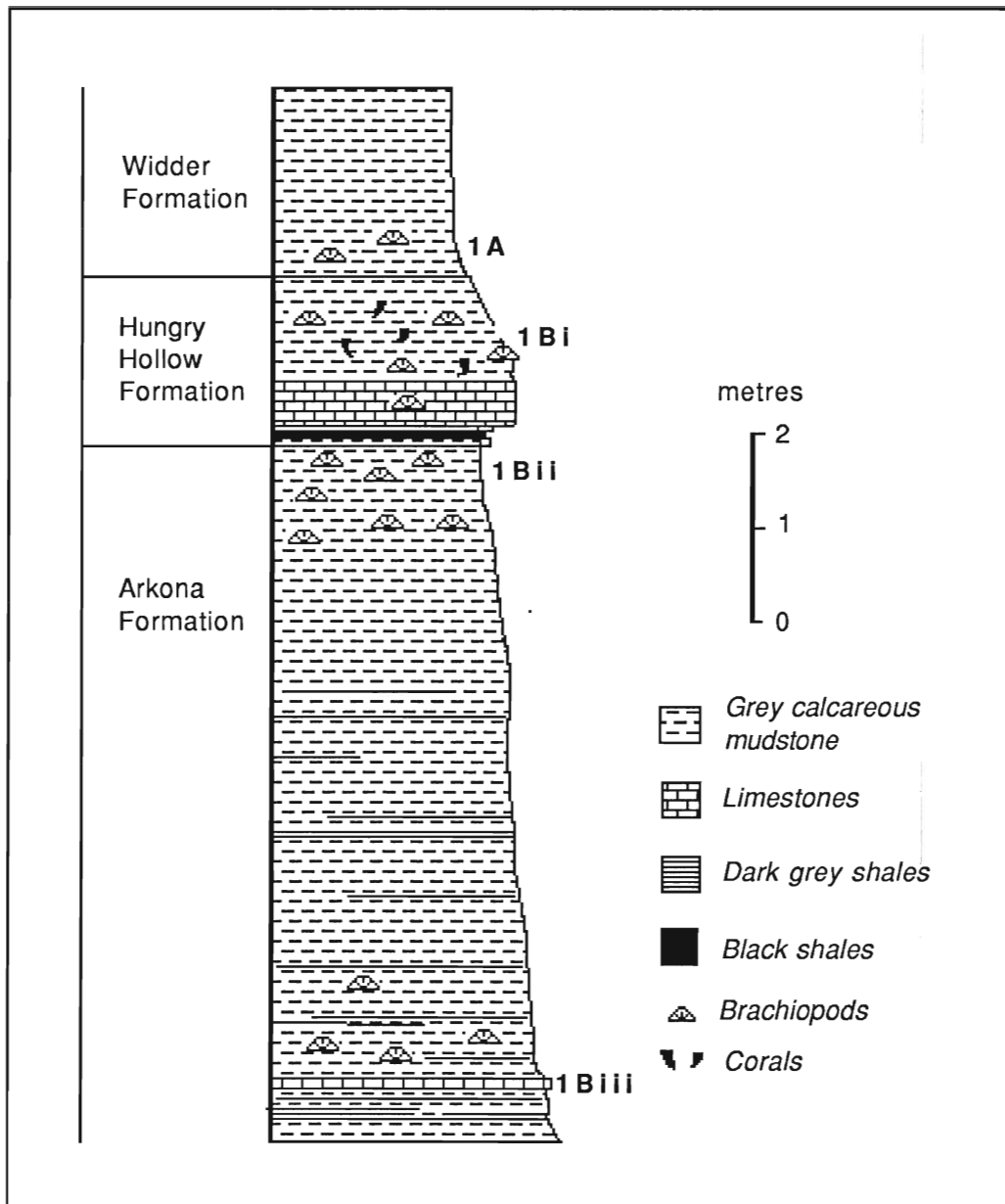


Figure A-1. Stratigraphic section of Hamilton Group (Middle Devonian) units at Hungry Hollow Quarry. Numbers refer to sampling intervals listed in Appendix I. Modified from Landing and Brett (1987).

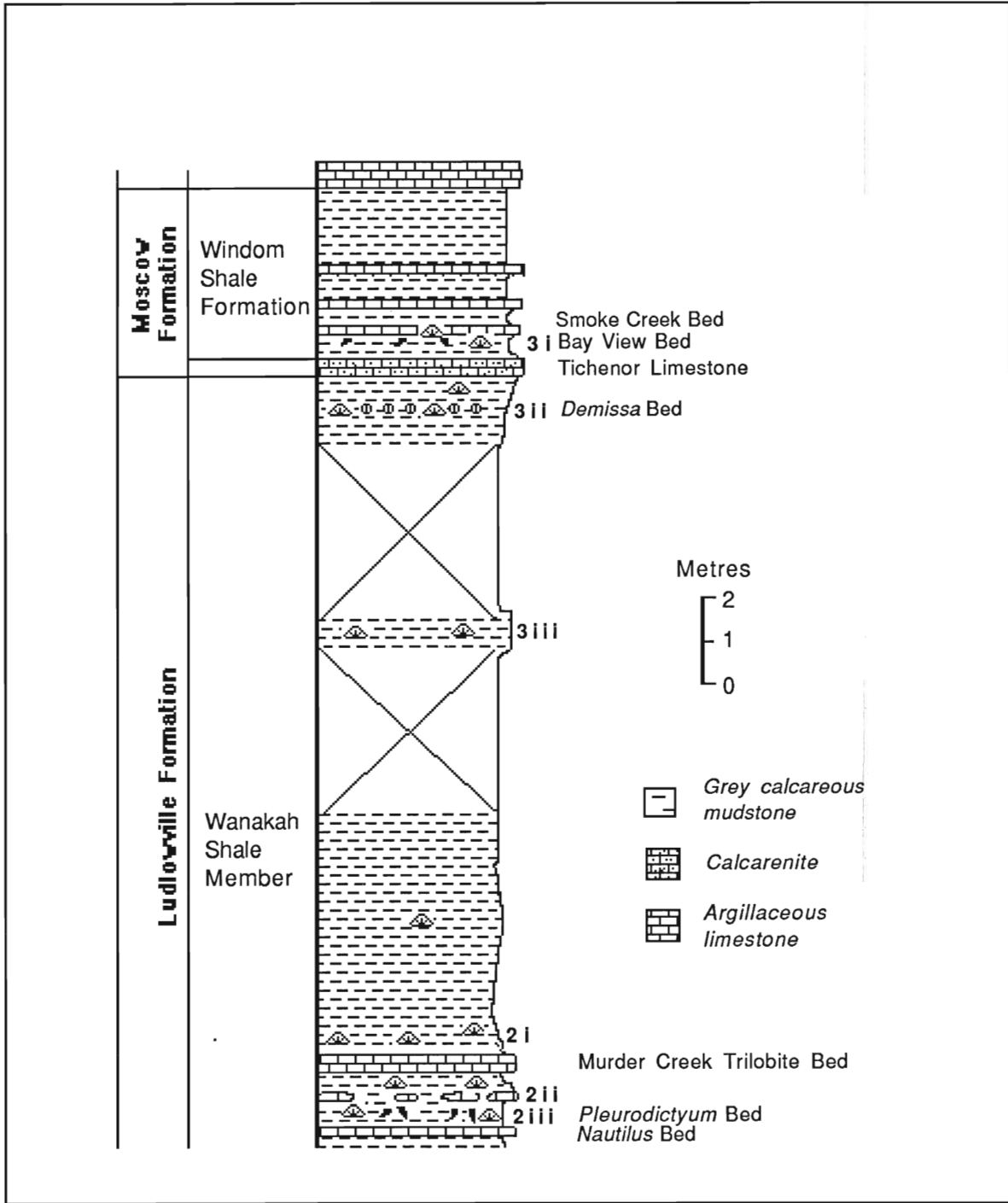


Figure A-2. Stratigraphic section of Wanakah and Windom Shale Members at Eighteen Mile Creek. Numbering refers to sampling horizons listed in Appendix I.

3. Eighteen Mile Creek

Eden Quadrangle

Ludlowville Formation and Moscow Formation (Fig. A-2)

Exposure on west bank of Eighteen Mile Creek; 100 m south of abandoned Lakeshore Boulevard bridge. Wanakah, Erie Co., New York State. 7-8 m vertical face with 10m talus slope. Middle Wanakah outcrops at base of talus slope.

- i) Lowest Windom Shale Member. Calcareous grey mudstones 30-50 cm above Tichenor Limestone with abundant small, juvenile *Athyris spiriferoides*, *Mucrospirifer mucronatus* and *Ambocoelia umbonata*. Between this bed and the Tichenor Limestone are dark grey shales dominated by thin pavements of small *Ambocoelia umbonatas*. Overlying is the Bay View Bed with abundant corals and diverse brachiopods.
- ii) "Dimissa" Bed. Upper Wanakah Shale Member. Grey shales, approximately 0.8-1.0 m below Tichenor Limestone. Prominent shell layer with abundant disarticulated brachiopods *Athyris spiriferoides*, *Mediospirifer audacula*, *Rhipidomella vanuxemi*, and *Mucrospirifer mucronatus*. Fragments of *Phacops rana* are also common.
- iii) Middle Wanakah Shale. Dark-grey calcareous fissile mudstones containing scattered *Ambocoelia* and small *Athyris spiriferoides*, *Mucrospirifer mucronatus*, orthids. Approximately 5-6 m below Tichenor Limestone.

4. Athol Springs.

Buffalo S.E. Quadrangle

Ludlowville Formation.

Shoreline exposure along Lake Erie. 300 m south of Big Tree Road and Lakeshore Road junction. 3m outcrop below bar parking lot. Wanakah, Erie Co., New York State.

- i) Wanakah Shale Member. Dark-grey calcareous fissile mudstones with rare disarticulated *Ambocoelia umbonata*.

5. Big Tree Road shale pit.

Buffalo S.E. Quadrangle

Ludlowville Formation.

100m east of railway bridge and 100 m south of Big Tree Road. Small unnamed creek south of pit. Blasdell, Erie Co., New York State. 0.6-1.0 m outcrop of dark-grey Wanakah Shale.

6A. Penn Dixie quarry

Buffalo S.E. Quadrangle

Moscow Formation. (Fig. A-3)

South side of abandoned Penn Dixie quarry, 500 m northwest of intersection of Big Tree Road and Bay View Road, Blasdell, Erie Co., New York State. Exposure of Penn Dixie Bed forms a small escarpment (0.5 m) along the quarry floor.

- i) "Penn Dixie Bed", Windom Shale. Dark-grey, pyritic mudstones containing abundant *Ambocoelia umbonata* and small, juvenile articulated *Athyris spiriferoides*. Disarticulated trilobites *Greenops boothi* and *Phacops rana* are common.

6B. Penn Dixie quarry

Buffalo S.E. Quadrangle

Moscow Formation. (Fig. A-3)

North part of quarry, 300 m north of locality 5A. Blasdell, Erie Co., New York State. Exposures of lower Windom Shale in sides of shale pits.

- ii) "Smoke Creek Bed". Lower Windom Shale. Fissile, grey, calcareous mudstone containing abundant *Mucrospirifer mucronatus*, *Mediospirifer audacula* and *Rhipidomella vanuxemi*. The Smoke Creek Bed is subdivided into three subunits (Speyer and Brett, 1985). A lower subunit A of bioturbated, fossiliferous mudstones. Subunit B is a thin poorly defined bedding plane that yields articulated and clustered trilobites. Sampling was from subunit C, a platy, calcareous mudstone.
- iii) "Bay View Bed". Lower Windom Shale. Grey calcareous mudstones between the Smoke Creek Bed and the Tichenor Limestone below. Diverse brachiopods assemblage, containing *Pseudoatrypa* sp., *Strophodonta* sp., *Mucrospirifer mucronatus*, *Athyris spiriferoides*, and *Mediospirifer audacula* amongst others
- iv) Tichenor Limestone. Brown calcarenite. Rare *Mediospirifer audacula* present on upper erosion surface.

6C. Penn Dixie quarry

Buffalo S.E. Quadrangle

Ludlowville Formation. (Fig. A-3)

Small creek, flowing northwards out of quarry, towards Rush Creek. 150 m northeast of locality 6B, Blasdell, Erie Co., New York State. The Tichenor limestone forms the cap to a small 1m waterfall, a feature common to most exposures of the uppermost Wanakah Shale

- v) "*Dimisa* " Bed. Upper Wanakah Shale. Grey shales with prominent shell layer approximately 0.8-0.9 m below Tichenor Limestone. Epibionts attached to some brachiopod valves. Contains abundant *Athyris spiriferoides*, *Mediospirifer audacula*, *Pseudoatrypa* sp. *Mucrospirifer mucronatus*, *Rhipidomella vanuxemi*, *Tropidoleptus* sp.
- vi) "Concretion Bed". Upper Wanakah Shale. Large calcareous concretions (15-35 cm thick) occur as distinct horizons within generally fissile grey mudstones. *Athyris spiriferoides* sampled directly from the second main concretion horizon, approximately 3.0-3.5 m below the Tichenor Limestone.
- vii) Middle Wanakah Shale. *Athyris spiriferoides* and *Mucrospirifer mucronatus* sampled from grey shales approximately 1.0-1.3 m below second "Concretion Bed".
- viii) Middle Wanakah Shale. *Devonochonetes* and *Mucrospirifer mucronatus* sampled from grey shales approximately 2.5-2.8 m below second "Concretion Bed".

7A. Smoke Creek.

Buffalo S.E. Quadrangle

Ludlowville Formation.

Small waterfall over Tichenor Limestone, 100 m south of Mile Strip Road and 150 m east of Abbott Road/Mile Strip Road intersection. Upper 2 m of Wanakah Shale exposed in shale banks on both sides of creek.

- i) "*Dimissa* " bed. Upper Wanakah Shale. Grey shales with an abundant brachiopod bearing horizon 0.9 to 1.0 m below the base of the Tichenor Limestone.

7B. Smoke Creek.

Buffalo S.E. Quadrangle

Ludlowville Formation.

2 m outcrop along small tributary of Smoke Creek South Branch (west side). Along California Road, 170 m east of Abbott Road and 650 m north of Mile Strip Road, Orchard Park, Erie Co., New York State

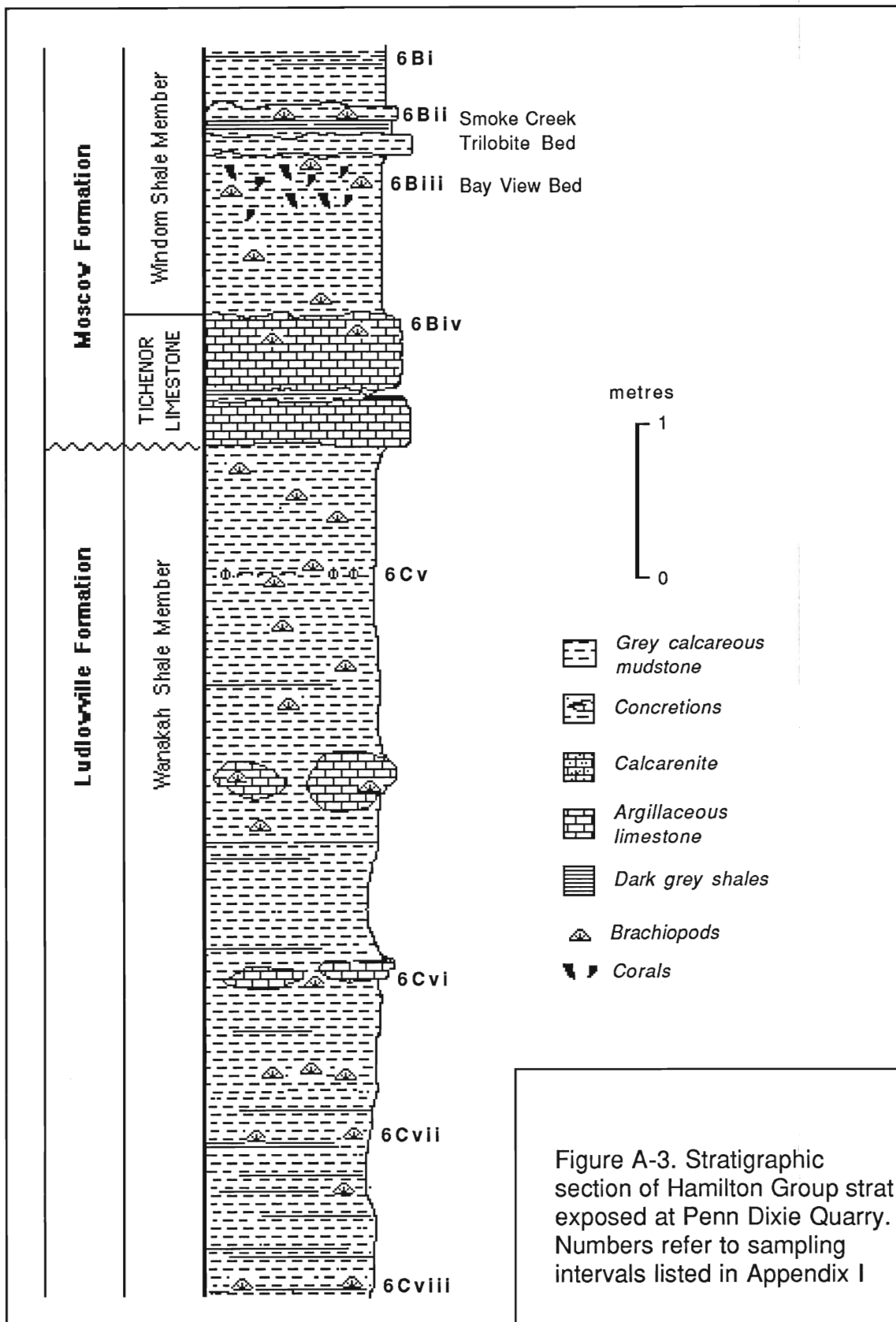


Figure A-3. Stratigraphic section of Hamilton Group strat exposed at Penn Dixie Quarry. Numbers refer to sampling intervals listed in Appendix I

- ii) Middle Wanakah Shale. 20-35 cm sampling interval from grey calcareous shales, containing scattered *Mucrospirifer mucronatus*, *Athyris spiriferoides*, *Mediospirifer audacula*, *Rhipidomella vanuxemi*, *Pseudoatrypa* sp., *Stropheodonta*, *Spinocyrtia* sp., approximately 1.4-1.6 m above creek bed. 25-30 cm beneath a minor concretion horizon and approximately 2.5-3.0 m below Tichenor Limestone.

7C. Smoke Creek.

Buffalo S.E. Quadrangle

Ludlowville Formation

5-6 m bank exposure on east side of Smoke Creek South Branch. 100 m west of Abbott Road, behind the Fire Station. 550 m north of Mile Strip Road, Orchard Park, Erie Co., New York State.

- iiiii) Middle Wanakah Shale. Sampling from dark grey fissile shales approximately 1.5-2.5 m above creek bed and between two prominent concretion horizons. *Mucrospirifer mucronatus* is the only common brachiopod, with *Devonochoonetes* present.

8A. Cazenovia Creek.

Orchard Park Quadrangle

Ludlowville Formation (Fig. A-4)

Small falls over Tichenor Limestone in Cazenovia Creek, 50 m east of Northup Road, Spring Brook, Erie Co., New York State.

- i) Moscow Formation. Tichenor and Michenor limestone are separated by a thin dark grey calcareous shale. This represents the most easterly outcrop of the condensed Jaycox and Deep Run Shales. The Tichenor is a crinoidal packstone with scattered disarticulated *Mediospirifer audacula* valves. Large colonial corals are common to the Michenor upper surface.
- ii) Upper Wanakah Shale. *Mucrospirifer mucronatus*, *Athyris spiriferoides*, *Mediospirifer audacula*, *Rhipidomella vanuxemi* sampled from grey mudstones 10 cm below Tichenor Limestone.
- iii) "Dimissa Bed". Upper Wanakah Shale. Fissile, grey mudstones and thin lenticular limestones. Sampled from grey mudstones approximately 0.8 m below Tichenor Limestone. Diverse brachiopod assemblage of *Mucrospirifer mucronatus*, *Athyris spiriferoides*, *Pseudoatrypa* sp. *Mediospirifer audacula*, *Rhipidomella vanuxemi*, *Spinocyrtia* sp. *Tropidoleptus* and *Rhipidomella vanuxemi* are all articulated. Articulation ratio of other species is variable, but some *Athyris* appear to be in life position

8B. Cazenovia Creek.

Orchard Park Quadrangle

Moscow Formation.

Bank exposure along Cazenovia Creek, approximately 700 m east of Northup Road, Spring Brook, Erie Co., New York State. Over 10 m of Windom Shale.

- iv) Windom Shale. Dark calcareous mudstones
Approximately 1.5-1.8 m above Tichenor Limestone.
Small *Ambocoelia umbonata*

9. Tributary of Buffalo Creek

Orchard Park Quadrangle

Ludlowville Formation.

Small, unnamed creek flowing north into Buffalo Creek. Immediately north of Bullis Road and 1.1 km east of Pound Road and Bullis Road intersection. Spring Brook Station, Erie Co., New York State.

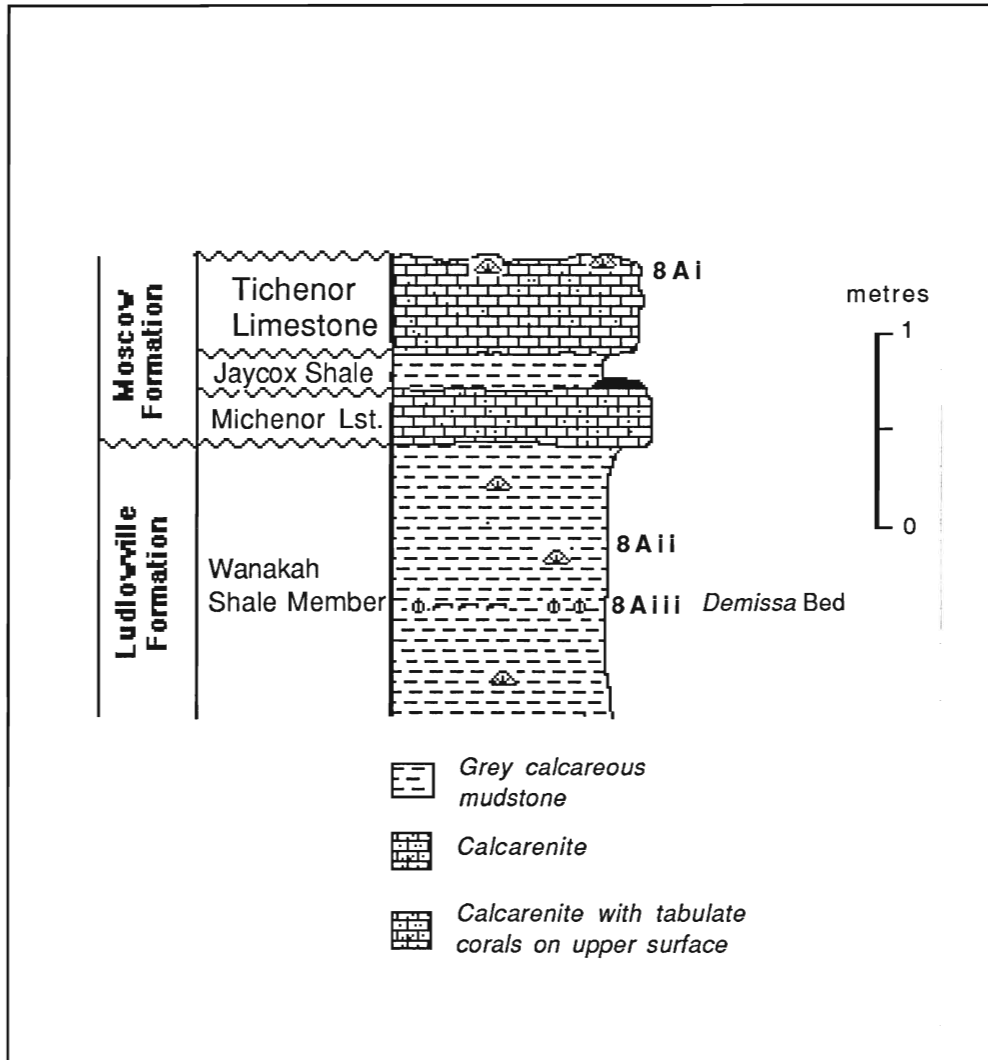


Figure A-4. Stratigraphic section of Hamilton Group strata exposed at Cazenovia Creek. Numbers refer to sampling intervals listed in Appendix I.

- i) Lower Wanakah Shale (above "*Pleurodictyum*" and "Murder Creek Trilobite Bed"). *Mucrospirifer mucronatus*, *Athyris spiriferoides*, and *Mediospirifer audacula* collected.
10. Girdle Road, Buffalo Creek. East Aurora Quadrangle
- Ludlowville Formation.**
Low bank (4.5 m outcrop) of Buffalo Creek, immediately below Girdle Road bridge. Elma, Erie Co., New York State.
- i) Upper Ledyard Shale. Medium grey calcareous mudstones 50 cm above base of outcrop dominated by scattered *Athyris spiriferoides* and *Mediospirifer audacula*.
- ii) Upper Ledyard Shale. Medium grey calcareous mudstones 1.5 m above base of outcrop. More diverse dominated by *Athyris spiriferoides*, *Mucrospirifer mucronatus*, *Mediospirifer audacula*, *Rhipidomella vanuxemi*, orthids and *lingula*.
11. Bowen Road, Buffalo Creek. East Aurora Quadrangle
- Ludlowville Formation.**
South bank of Buffalo Creek, 200 m east of Bowen Road. Elma, Erie Co., New York State.
- i) Lower Wanakah Shale. Sampling of *Athyris spiriferoides*, *Mucrospirifer mucronatus*, *Mediospirifer audacula*, *Rhipidomella vanuxemi* from shales in sequence of medium grey fissile shales and thin lenticular limestones. Approximately 60 to 120 cm above prominent Murder Creek Trilobite Bed.
12. Bullis Road, Buffalo Creek. East Aurora Quadrangle
- Moscow Formation.**
Banks of Buffalo Creek, 150 m south of the abandoned Old Bullis Road bridge. Elma, Erie Co., New York State. 3-5 m outcrop from top with 5-7 m talus slope to creek floor.
- i) Windom Shale. Dark grey calcareous mudstones with numerous concretion horizons. *Ambocoelia umbonata* collected from dark shales. Fragments of *Athyris spiriferoides*, *Mucrospirifer mucronatus*, *Mediospirifer audacula* from shell hash horizon 3.2 m above base of outcrop
- 13A. Eleven Mile Creek Alexander Quadrangle
- Moscow Formation.**
Bed of Eleven Mile Creek, approximately 500 m south of U.S. Highway 20. Genesee Co., New York State.
- i) Lower Kashong Shale. 20 cm interval of dark grey calcareous mudstones approximately 0.5-1.0 m above Tichenor Limestone. *Mediospirifer audacula*, *Athyris spiriferoides*.
- 13B. Eleven Mile Creek Alexander Quadrangle
- Ludlowville Formation.**
Small waterfall over Tichenor Limestone in bed of Eleven Mile Creek, 25 m south of U.S. Highway 20. Genesee Co., New York State. 5 metre outcrop of Wanakah Shale below Tichenor and Michenor Limestones. Thin (15 cm) condensed highly calcareous Deep Run Shale between these limestones not sampled.

- ii) "*Dimisa* Bed". Upper Wanakah Shale. Medium grey to dark grey calcareous mudstones. Brachiopod horizon approximately 0.85-1.0 m below the Tichenor Limestone. Many *Athyris* brachiopods are in life position. Less diverse brachiopod community than "*Dimissa*" Beds outcropping to the west. *Athyris spiriferoides*, *Mediospirifer audacula*.
14. Spring Creek Alexander Quadrangle
- Ludlowville Formation.**
Banks of Spring Creek, 1.2 km south of Alden Municipal Park. Alden, Genesee Co., New York State.
- i) Middle Ledyard Shale. Very fissile, dark grey shales approximately 1.0-1.5 m below Alden Pyrite beds. *Mucrospirifer mucronatus* is the only common brachiopod.
- 15A. Murder Creek Alexander Quadrangle
- Kashong Shale Fm.** (Fig. A-5)
Shale bank along west branch of Murder Creek. 650 m south of U.S. Highway 20, Darien, Genesee Co., New York State. 3 m outcrop.
- i) Kashong Shale. 75 cm sampling interval from dark grey fissile shales, 1.0 m above base of creek. Dominated by articulated and pyritized *Mucrospirifer mucronatus*, *Devonochonetes* and crinoids.
- 15B. Murder Creek Alexander Quadrangle
- Moscow Formation.** (Fig. A-5)
Small waterfall (1 metre high) along west branch of Murder Creek. Beneath wooden footbridge, 350-400 m north of U.S. Highway 20, Darien, Genesee Co., New York State. Outcrop of Jaycox Shale between Tichenor and Michenor Limestones. Deep Run Shale found between Michenor Limestone and upper Menteth limestone bed.
- ii) Menteth Limestone. Grey brown crinoidal calcarenite (25-30 cm thick)
- iii) Deep Run Shale. Dark grey, highly calcareous mudstones. 50 cm thick condensed section of Deep Run Shale between limestones. Low brachiopod diversity i.e. *Mucrospirifer mucronatus*
- iv) Michenor Limestone. 65 cm thick limestone bed. *Mediospirifer audacula*.
- v) Jaycox Shale. 45 cm thick condensed section of highly calcareous mudstones.
- vi) Tichenor Limestone. 45-50 cm thick limestone bed. *Mediospirifer audacula*.
- 15C. Murder Creek Alexander Quadrangle
- Ludlowville Formation.** (Fig. A-5)
Shale bank along west branch of Murder Creek. Approximately 750-850 m north of U.S. Highway 20 and 750 m south of Sharrack Road. Darien, Genesee Co., New York State. 3.5 m outcrop on east side of creek.
- vii) Upper Wanakah Shale. Medium grey calcareous mudstones. 50 cm interval, 2.0-2.5 m above base of exposure. Possibly approximately 1.5-2.0 m below base of Tichenor Limestone. *Athyris spiriferoides*, *Mucrospirifer mucronatus*, *Mediospirifer audacula*.

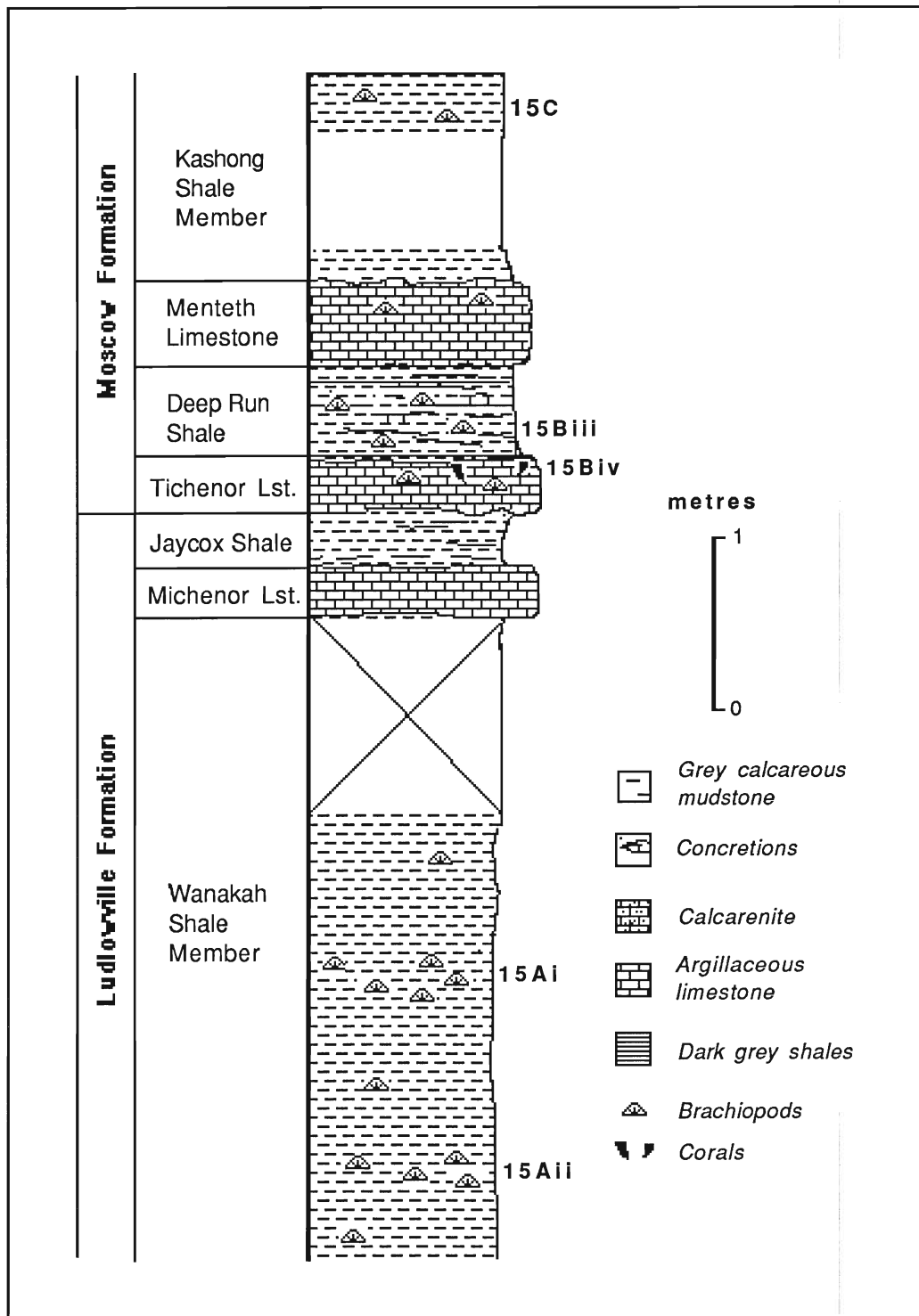


Figure A-5. Stratigraphic section of Hamilton Group strata exposed at Murder Creek. Numbers refer to sampling intervals listed in Appendix I.

- viii) Upper Wanakah Shale. Medium grey calcareous mudstones. Base of exposure, 30-35 cm sampling interval and approximately 3.5-4.5 m below Tichenor Limestone. *Athyris spiriferoides*, *Mucrospirifer mucronatus*.

16. Bowen Creek Alexander Quadrangle

Ludlowville Formation.

Banks of west branch of Bowen Creek, 0.4 km south of Walker Road and 0.6 km west of Gilate Road, Alexander, Genesee Co., New York State. Dark grey Wanakah Shale in creekbed.

17. Bethany railcut Batavia South Quadrangle

Ludlowville Formation

Railroad cut along the abandoned Erie-Lackawanna line, just east of Francis Road. 2.5km north of U.S. Highway 20, Bethany, Genesee Co., New York State. North cut of railroad. Talus slope, 6-7m vertically. Francis Road pyrite in lower part of section (Dick and Brett, 1986).

- i) Middle Wanakah Shale. Brachiopods collected from a 50 cm interval. *Athyris spiriferoides*, and rare *Mediospirifer audacula*. Fresh outcrop dug out from talus debris at 5.5m up slope.
- ii) Middle Wanakah Shale. Fresh outcrop dug out from talus debris at 4.5m up slope. Brachiopods collected from a 40 cm interval of dark grey, pyritized mudstones. *Athyris spiriferoides*, and rare *Mediospirifer audacula*.

18. Retsof Leicester Quadrangle

Moscow Formation.

Railroad cut and shale dumps beside the International Salt Company mine, 400 m south of N.Y. Route 63, Retsof, Livingston Co., New York State.

- i) Upper Kashong Shale Member. Macrofossils sampled from dark grey calcareous mudstones. This outcrop represents the upper Kashong Shale (Brett and Cottrell, 1982). *Tropidoleptus carinatus*, *Mucrospirifer mucronatus*, crinoids, and rare *Athyris spiriferoides* are present.

19A. Fall Brook Genesee Quadrangle

Moscow Formation.

Shale banks of Fall Brook Creek, just below Fall Brook Falls. Locality is 650 m north of 18A along Fall Brook Creek, Genesee, Livingston Co., New York State. 18-20 m outcrop and 10m talus slope. Smoke Creek Bed exposed at base of falls.

- i) Windom Shale Member. Brachiopods sampled from base of Windom outcrop. *Mediospirifer audacula* is most common brachiopod.

19B. Fall Brook Genesee Quadrangle

Moscow Formation.

Shale bank of Fall Brook Creek, 150 m east of N.Y. Route 39. 1.1 km south of N.Y. Route 63 and 39 intersection and 2.6 km south of Genesee, Livingston Co., New York State. 3.5m outcrop.

- i) Kashong Shale Member. Sampling from lowest metre of grey calcareous mudstones. *Tropidoleptus carinatus* is common brachiopod, and *Mucrospirifer mucronatus* is present.

20A. Jaycox Creek

Geneseo Quadrangle

Moscow Formation. (Fig. A-6)

Shale banks of Jaycox Creek, above small waterfall (3.0 m) over Tichenor Limestone. 850 m west of N.Y. Route 39, near horse farm and 3.5 km north of Geneseo, Livingston Co., New York State. 3m outcrop.

- i) Deep Run Shale Member. Approximately 2 m of dark, fissile calcareous mudstones with scattered articulated and disarticulated brachiopods are scattered. *Mediospirifer audacula* sampled from lowest 50-75 cm of Deep Run Shale and are predominantly

20B. Jaycox Creek

Geneseo Quadrangle

Moscow Formation. (Fig. A-6)

Shale banks of Jaycox Creek, below first waterfall over Tichenor Limestone. 100 m west of locality 19A, Geneseo, Livingston Co., New York State. 2.5 m outcrop.

- ii) Jaycox Shale Member. Approximately 2.5 m outcrop of medium grey mudstones and occasional thin nodular limestones. Corals are abundant in lowest metre of Jaycox. Brachiopods sampled from lower metre interval of Jaycox Shale *Mediospirifer audacula*, *Tropidoleptus carinatus*.

20C. Jaycox Creek

Geneseo Quadrangle

Ludlowville Formation. (Fig. A.6)

Shale banks of Jaycox Creek, below second waterfall (4.0-4.5 m), 150 m west of locality 19B, Geneseo, Livingston Co., New York State.

- iii) "Dimisa Bed". Upper Wanakah Shale. Dark fissile calcareous mudstones with concretion horizons beginning several metres below Michenor Limestone. *Mediospirifer audacula*, *Athyris spiriferoides*, *Mucrospirifer mucronatus* are abundant in Dimissa Bed approximately 0.9-1.0 m below the Michenor Limestone.

21. Wheelers Gully
Quadrangle

Geneseo

Moscow Formation.

Shale bank of Wheelers Gully, 150m west of N.Y. Route 39, 4.8 km north of Geneseo, Livingston Co., New York State. 3.5 m outcrop.

- i) Kashong Shale Member. *Mediospirifer audacula*, *Tropidoleptus carinatus*, crinoids collected from a 50 cm interval of sparsely fossiliferous dark grey calcareous mudstones within 50 cm interval, 1.5 m above creek floor. Minor pyritization of matrix present.

22A. Menteth Gully

Canandaigua Lake Quadrangle

Moscow Formation.

Shale banks upstream of high waterfalls (15-17 m), along Menteth Creek, 350 m west of West Lake Road, west side of Canandaigua Lake, Ontario Co., New York State.

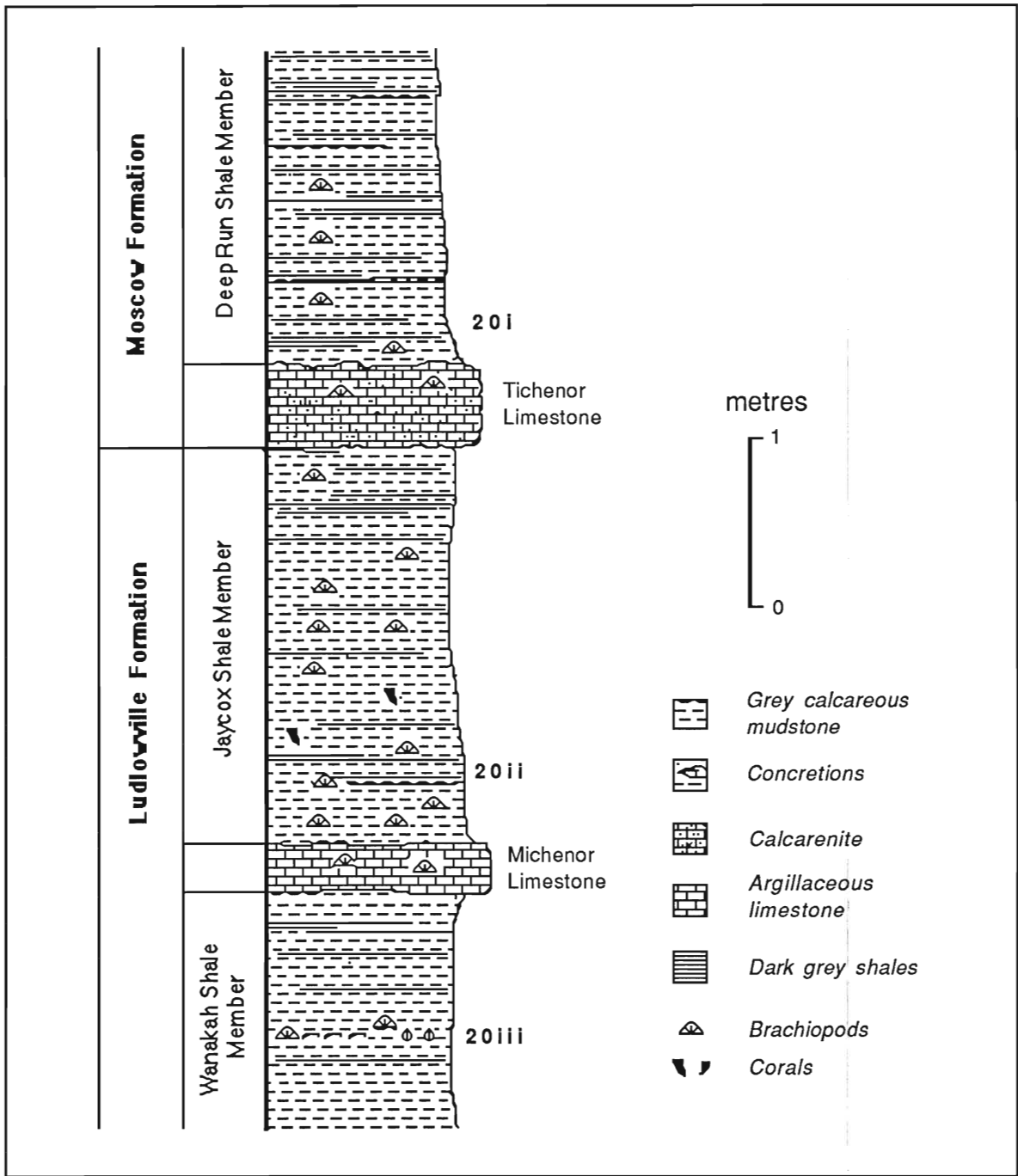


Figure A-6. Stratigraphic section of Hamilton Group strata exposed at Jaycox Creek. Numbers refer to sampling intervals listed in Appendix I.

- i) Kashong Shale Member. Shale bank 3.5 m high, east side of creek, just above falls.
Tropidoleptus carinatus is dominant brachiopod in medium grey fissile, calcareous mudstones. Position in unit unknown.

22B. Menteth Gully Canandaigua Lake Quadrangle

Moscow Formation.

Shale banks downstream of high waterfalls (15-17 m), along Menteth Creek, 250 m west of West Lake Road, west side of Canandaigua Lake, Ontario Co., New York State.

- i) Kashong Shale Member. *Tropidoleptus carinatus*, *Mucrospirifer mucronatus* are sampled from base of waterfall, 9-10m below top of falls.

23. Kashong Creek Geneva South Quadrangle

Ludlowville Formation.

Shale banks of Kashong Creek, 500 m west of N.Y. Route 14, south of Geneva, Ontario Co., New York State.

- i) Wanakah Shale Member. Position in unit unknown.
Ambocoelia umbonata.

24. Indian Creek Dresden Quadrangle

Moscow Formation.

Shale banks along north side of Indian Creek, 150 m west of N.Y. Route 96A and 3.5km north of Willard, Ontario Co., New York State. 3.5 m outcrop.

- i) Kashong Shale Member. Dark grey, highly fissile calcareous mudstones. Thin pavements with abundant *Ambocoelia umbonata* are sampled 30-50 cm above creek floor.

25. Big Hollow Creek Ovid Quadrangle

Ludlowville Formation.

Shale banks of Big Hollow Creek, east of Swick Road and 3.5 km north of Hayt Corners, Seneca Co., New York State.

- i) King Ferry Shale Member. Lateral equivalent of the Wanakah Shale Member (Brett and Cortrell, 1982). Dark fissile calcareous mudstones with scattered *Mucrospirifer mucronatus*.

26. Stoney Creek Ontario.

Rochester Shale Formation

Stoney Creek Member. Road cut, 1 km east of King Street East. Lateral equivalent of the Burleigh Hill Member of the Rochester Shale. Fine grained and thin bedded shaley dolostones of Stoney Creek Member .

27. Dewitt Road, Stoney Creek. Ontario.

Rochester Shale Formation.

Thin bedded, shaley dolostones of Stoney Creek Member exposed.

28. Vinemount Ontario.
Rochester Shale Formation.
 Road cut, 2.4 km west of Winona. Fine grained dolostones of Stoney Creek member exposed.
29. Wolverton Mountain Road, Grimsby. Ontario.
Rochester Shale Formation.
 2 km west of Grimsby, a reduced section of Rochester Shale. A 1.2-1.6 m outcrop is exposed above Irondequoit Formation. Dark grey calcareous mudstones and several thin micritic limestones.
30. Beamers Falls, Grimsby. Ontario.
Rochester Shale Formation.
 Stream cut on 40 Mile Creek, 1 km south of Grimsby. Upper 3 m of Burleigh Hill member exposed in east face of gorge below upper waterfall. This sequence of dark gray fissile calcareous shale is essentially barren of macrofossils. Articulated *Atrypa reticularis* were collected from Lewiston E Member in exposure further down gorge towards Grimsby.
31. 15 Mile Creek. Ontario.
Rochester Shale Formation.
 Stream cut at top of escarpment, 5 km southwest of St. Catharines. Exposes upper 2-3m of Burleigh Hill member. Grey calcareous shales, thin micritic limestones and thin shaley dolostones are essentially unfossiliferous. Single *Coolinia subplana* found in lowest calcareous shales.
32. Rockway Falls. Ontario.
Rochester Shale Formation.
 3.5 km southwest of St. Catharines along Highway 69. Complete section of Lewiston and Burleigh Hill members exposed. Here Lewiston Member is essentially a sequence of dark grey fissile calcareous mudstones, thin bedded calcisiltites and micritic limestone (bryozoa common). Burleigh Hill Member consists of dark grey barren mudstones, which in upper part of unit grade into thin bedded dolostones of the Decew Formation.
33. Decew Falls. Ontario.
Rochester Shale Formation.
 1 km southwest of Brock University, St. Catharines. Complete section of Lewiston and Burleigh Hill members.
- i) "*Coolinia subplana*" horizon. Burleigh Hill Member. This horizon is a 10-15 cm fossiliferous amalgamated calcarenite layer, within a sequence of barren grey calcareous mudstones.
34. Brock-Decew, St. Catharines. Ontario.
Rochester Shale Formation. (Fig. 4.18)
 Hydro road cut to Power House Dam, 0.5 km west of Brock University. Grey calcareous shales and thin-bedded dolostones of the upper Burleigh Hill member.
- i) "*Coolinia subplana*" horizon. Burleigh Hill Member. Brachiopods collected from two calcarenite layers (15 cm thick), approximately 2.5-3.0 m below beginning of gradational

contact of Burleigh Hill shaley dolostones with the Decew Dolostone. This is the laterally equivalent horizon to that seen in the Burleigh Hill, Decew Falls and Old Welland Canal sections. Disarticulate *Dalejina* and *Resserella elegantula* valves are common.

35. Highway 406 stream cut, St. Catharines. Ontario

Rochester Shale Formation.

150 m east of the 406 highway, on the escarpment between Burleigh Hill and Sanatorium Hill. Middle and upper Burleigh Hill calcareous shales exposed. Disarticulated *Dalejina* and *Whitfieldella* valves were common.

36. Burleigh Hill, St. Catharines. Ontario.

Burleigh Hill Member (Fig. 4.18)

Road section along Burleigh Hill Road, 1km south of St. Catharines, exposing the complete Burleigh Hill member.

6.5 m outcrop of the Burleigh Hill Member. (type locality) with gradational upper contact with the dolomitic Decew Dolostone. *Coolinia subplana* was the only brachiopod collected in the calcareous shales above and below the "*Coolinia subplana*" horizon.

- i) "*Coolinia subplana*" horizon. Burleigh Hill Member.
Fossils sampled from eroded calcareous shale horizon, 40-50 cm thick, 5.2-5.4 m above base of Burleigh Hill Formation and approximately 2-2.5 m below beginning of gradational contact of Burleigh Hill shaley dolostones with the Decew Dolostone. Here this collecting horizon represents 3 and/or 4 separate storm bed layers. Brachiopods collected were *Dalejina*, *Whitfieldella nitida*, *Resserella elegantula*, strophomenids *Leptaena rhomboidalis*, *Coolinia subplana*, a few fragments of *Atrypa reticularis*. Other fossils collected were *Dalmanites limulurus* and *Naticonema niagarensis*.

37. Lock 5 Railway Cut, Thorold. Ontario.

Merritton Formation.

Railway cut exposure, approximately 300 m west of Welland Canal Lock 5. 5-6 m outcrop of Clinton Group limestones and shales.

- i) Merritton Formation. *Pentameroides* sp. brachiopods sampled from uppermost Merritton phosphatized hardground (2-3 cm thick) to 15 cm below top of unit. Valves are abraded, disarticulate and corroded.

38. Old Welland Canal exposure, Thorold. Ontario.

Rochester Shale Formation.

Cliff section, behind abandoned power station dam. At the junction of the old Welland Canal and the St. Lawrence Seaway Haulage Road, 1.2 km south of the General Motors Plant.

- i) "*Coolinia subplana*" horizon. Dark grey calcareous shales of the Burleigh Hill Member. Section destroyed by percolating leachate from dump along escarpment.

39. Niagara Falls Gorge Ontario.

Rochester Shale Formation.

Hydro road cut along Niagara gorge. Upper calcareous shale section of Burleigh Hill member. Essentially barren, except for a few fragments of *Coolinia subplana*.

Clinton Group. (Fig. 4.9)

Excised block on east side of gorge along old railway line, approximately 800 m south of the Artpark complex.

- i) Lewiston A Member.
Thin calcisiltite beds 10-15 cm above base of Lewiston A. Abundant *Atrypa reticularis*, *Eospirifer radiatus*, *Whitfieldella nitida* and *W. oblata*, *Coolinia subplana*, *Eoplectodonta transversalis*, large *Leptaena*.
- ii) Irondequoit Formation.
Uppermost 5 cm pink crinoidal biosparite with *Atrypa reticularis*, *Whitfieldella nitida*, *Eospirifer radiatus*,
- iii) Irondequoit Formation.
Sampling interval from 5-15 cm below top of formation. Brachiopod dominated crinoidal biosparite. *Whitfieldella nitida*, *Eospirifer radiatus*, *Atrypa reticularis*.
- iv) Irondequoit Formation.
1m below upper contact with *Whitfieldella nitida*, *Eospirifer radiatus*, *Atrypa reticularis*.
Sampled from crinoidal wackestones and packstones.
- v) Irondequoit Formation.
2.0-2.4 m below upper contact. Disarticulate *Whitfieldella nitida*, and articulated *Eospirifer radiatus*, *Atrypa reticularis* are present. *Whitfieldella* are dominant, and commonly abraded.

Rochester Shale Formation. (Fig. 4.9)

Vertical exposures on east side of gorge along an abandoned railway line. Below the Robert Moses Parkway, close to the Hydroelectric facility and directly opposite the Sir Adam Beck Hydroelectric Station. Exposure of Upper Queenston (Upper Ordovician), Medina Group, Clinton Group and Lockport Group. The upper contact of the Rochester Shale with the Decew Formation is a gradational transition from dolomitic gray shales to thin bedded argillaceous dolostones to massive fine grained dolostone.

Burleigh Hill Member/Lewiston E Member.

- i) 9.20 m above basal Rochester Shale contact. Pyritized hardground 8cm thick containing abundant *Resserella elegantula*, *Whitfieldella nitida* and *Coolinia subplana*.

Lewiston E Member.

- ii) 9.0 m above basal Rochester Shale contact. *Whitfieldella nitida* and *Eospirifer radiatus*.
- iii) 8.20 to 8.28 m above contact. *Eospirifer radiatus*.
- iv) 7.72 to 7.82 m above contact. *Eospirifer radiatus*.

Lewiston D Member.

- v) 7.00 m above contact. *Eospirifer radiatus*.
- vi) 6.60 to 6.70 m above contact. *Eospirifer radiatus*.

Lewiston C member.

- vii) 4.0 m above contact. *Eospirifer radiatus*.

- viii) 3.70-3.81 m above contact. Calcisiltite bed with *Striispirifer niagarensis*, *Whitfieldella nitida*, *Eospirifer radiatus*.
- ix) 3.55 to 3.59 m above contact. Thin calcisiltite bed *Atrypa reticularis*, *Eospirifer radiatus*, *Striispirifer niagarensis*, *Whitfieldella nitida*,
- x) 3.40 to 3.45 m above contact. Calcisiltite bed *Whitfieldella nitida*, *Eospirifer radiatus*, *Striispirifer niagarensis*.

Lewiston B member.

- xi) 2.32 to 2.35 m above contact. *Atrypa reticularis*.
- xii) 2.01 to 2.02 m above contact. *Atrypa reticularis*.
- xiii) 1.72 to 1.75 m above contact. *Atrypa reticularis*, *Eospirifer radiatus*.
- xiv) 1.47 to 1.58 m above contact. *Atrypa reticularis*, *Eospirifer radiatus*.
- xv) 1.25 m above contact. *Atrypa reticularis*, *Whitfieldella nitida*.
- xvi) 1.00 to 1.25 m above contact. *Atrypa reticularis*, *Whitfieldella nitida*.

Lewiston A Member.

- xvii) 0.90 m above contact. *Atrypa reticularis*, *Eospirifer radiatus*.
- xviii) 0.80 to 1.00 m above contact. *Atrypa reticularis*, *Eospirifer radiatus*. *Leptaena rhomboidalis* occurs from this horizon into the Lewiston B member.
- xix) 0.70 to 0.75 m above contact. *Atrypa reticularis*, *Whitfieldella nitida* and *Eospirifer radiatus*. *Coolinia subplana* occurs from this horizon into the Lewiston B member.
- xx) 0.40 to 0.50 m above contact. *Atrypa reticularis*, *Whitfieldella nitida*.
- xxi) 0.25-0.35 m above contact. *Atrypa reticularis*, *Whitfieldella nitida* and *Eospirifer radiatus*.
- xxii) 0.20 to 0.25 m above contact. *Atrypa reticularis*, *Whitfieldella nitida* and *Eospirifer radiatus*.
- xxiii) 0.10 to 0.25 m above contact. *Atrypa reticularis*, *Whitfieldella nitida* and *Eospirifer radiatus*.
- xxiv) 0 to 0.10 m above Irondequoit contact. *Atrypa reticularis*, *Whitfieldella nitida* and *Eospirifer radiatus*.

42. Bree Road, Cambria County

New York State.

Irondequoit Formation.

Road cut along Bree Road. Outcrop 1.5 m. Dolomitized wackestones with visibly altered brachiopods .

43. Canal Road, Lockport

New York State.

Rochester Shale Formation.

Road cut along canal running through Lockport city centre. Burleigh Hill Member and Upper Lewiston member units exposed.

- i) Lewiston E Member. Brachiopods collected from thin and slightly nodular calcarenite and calcisiltite beds within a generally unfossiliferous grey calcareous mudstone sequence. The abundance of bryozoa within these "storm bed" layers in addition to *Coolinia subplana*, *Atrypa reticularis*, *Eospirifer radiatus*, *Resserella elegantula* suggests these beds to be Lewiston E in character.

44. Brewer Street, Rochester

New York State.

Rochester Shale Formation.

Overhanging cliff exposure, excised by the Genesee River on east side of gorge. Directly below the west end of Brewer Street and church.

- i) The Rochester Shale exposed here is undifferentiated into its separate members recognized further west along the Niagara Escarpment. Brachiopods collected from a horizon approximately 5.5 m above Genesee River waterline. The poor condition of the exposure did not enable further collecting. *Coolinia subplana*, *Resserella elegantula*, and *Whitfieldella nitida*.
45. Hydro Road, Rochester New York State.
- Reynales Formation.**
Exposure along access road to the R.G. & E. Power Station, 350 m south of the junction of Seth Green Drive and Norton Street, Rochester.
- i) Wallington Limestone Member. Thin beds of light grey crystalline limestone with shale partings containing abundant *Pentameroides* sp.
46. Sodus Creek New York State.
- Rochester Shale Formation.**
Sodus Creek exposure of the bryozoa Lewiston E member beds. *Atrypa reticularis*, *Eospirifer radiatus*, and *Howellella* from collection of D. Tetrault (University of Rochester, N.Y.)
- 47A. Goat Island Manitoulin Island.
- Verulam Formation.**
An old railway cutting on the west side of Goat Island, just south of Highway 6 exposes Verulam Formation (about 5-6 m). Thin bedded, fossiliferous, nodular wackestones, packstones and calcareous mudstones with thin shale partings. These limestones are dominated by strophomenid brachiopods.
- i) Verulam Formation. *Rafinesquina* sp. (*deltoidea* ?) and *Dalmanella rogata*. collected from nodular skeletal grainstone beds (crinoidal biosparites; 5-10 cm thick) at base of exposure. These crinoidal grainstones are partially dolomitized (fine grained euhedral dolomite) and can be tentatively interpreted as shoal edge facies (cf. Brookfield and Brett, 1988).
- 47B. Goat Island Manitoulin Island.
- Cobourg Formation.**
Cobourg formation is exposed along an abandoned railway cutting on the northeast side of Goat Island. Take a dirt track off Highway 6, just north of Little Current swing bridge. A 4-5m exposure is seen.
- i) Cobourg Formation. Sequence consists of greenish grey shales interbedded with skeletal wackestones and calcareous mudstones. The upper part consists of greyish brown nodular packstones and wackestones with thin greenish grey shale partings. Dominated by small articulate rhyconellid and large strophomenid brachiopods (notably *Rafinesquina deltoidea*). Trilobite fragments are common. Sampling of *Rafinesquina* from partially dolomitized wackestones.
48. Little Current Manitoulin Island.
- Cobourg Formation.**
Just south of Little Current swing bridge on Highway 6 are old railway cuttings, exposing Cobourg Formation. 3.5 to 4 m exposures seen on both sides of road.

- i) Cobourg Formation. Greenish grey nodular calcareous mudstones, wackestones and occasional packstones (biomicrites, biopelsparites and biosparites; 5-15 cm thick) are interbedded with thin green shales. Trilobite fragments, corals and small rhyconellid brachiopods are common in some of the thicker wackestone beds.
49. Little Current Manitoulin Island.
- Cobourg Formation.**
Along Harbour Road East, 250 m east of Little Current Harbour, a 4.5 m exposure of Cobourg Formation is seen.
- i) Cobourg Formation. Greenish grey, nodular calcareous mudstones and wackestones (both biomicrites and crinoidal biosparites; 5-15 cm thick) are interbedded with thin green shales. Small articulated rhyconellids are very abundant, whereas strophomenids are rare. Large orthocone nautiloids (5-8 cm) are present with small solitary corals and trilobite fragments (possibly *Isotelus* sp.). Sampling was from upper 1.5 m of section.
50. South of Little Current Manitoulin Island.
- Whitby Formation.**
Low banks of small creek, approximately 5 km south of Little Current along Highway 6. 1.5 to 2 m of dark grey, fissile shales exposed.
- i) Sheguiandah Member. These shales are essentially barren of macrofossils except for a 25-30 cm thick sequence of brachiopod pavements at top of exposure. Very abundant layers of predominantly articulated *Dalmanella* sp (*rogata* ?). Most are coated by iron oxides, limonite crusts.
51. South of Little Current Manitoulin Island.
- Georgian Bay Formation.**
Approximately 250 m south of locality 50 is a 5 to 6 m outcrop of weathered shale on the west side of Highway 6.
- i) Wikwemikongsing Member. Light grey, green and brown shales. Brachiopods (predominantly *Dalmanella rogata*), crinoids, bryozoans and gastropods are weathered in relief.
52. Sheguiandah Manitoulin Island.
- Cobourg Formation.**
Cobourg Formation unconformably overlies Precambrian Lorraine Quartzite along Highway 6; section about 10 km south of Little Current. Boulders (up to 1.5 m size) of Lorraine Quartzite are incorporated into lowest 1.0 to 1.5 m of Cobourg Formation. At this section, Cobourg Formation is a light brown, medium bedded dolostone. Karstic? porosity is evident.
53. Sheguiandah Manitoulin Island.
- Whitby Formation.**
Black shales assigned to the Collingwood Member of the Whitby Formation overly Cobourg Formation in road section 100 m south of locality 52 along Highway 68. Shales here are essentially devoid of macrofossils.

54. Sheguiandah Manitoulin Island.
- Georgian Bay Formation.**
Road setion along Highway 6 as it climbs escarpment overlooking Sheguiandah Bay. 1.5 km north of Ten Mile Point. 3-4 m exposed on both sides of road.
- i) Meaford Member. Thin bedded greenish gray calcareous mudstones and wackestones with abundant but scattered small articulated rhyconellids.
55. High Falls Manitoulin Island.
- Georgian Bay Formation.**
About 30 km south of Little Current along Highway 6, a waterfall over the escarpment on the east side of road exposes approximately 10 m of the Kagawong Member.
56. Kagawong Village Manitoulin Island.
- Georgian Bay Formation.**
A 14-15 m outcrop at Bridal Veil Falls exposes the uppermost Wekwemikongsing Member (1.5 m) and the Meaford Member (12.5-13.5 m).
- i) Meaford Member. A sequence of grey medium-bedded (5 to 15 cm thick) fossiliferous calcareous mudstones and skeletal wackestones (biomicrites). Interbedded with thin greenish grey shaley partings in lowest 3 m of Meaford. Beds close to base of section are extremely fossiliferous (almost "coquinite" packstones) consisting of predominantly single valves of *Sowerybella* sp. These brachiopods are however silicified and coated with thick layer of iron oxides (1-2 mm).
- ii) Wikwemikongsing Member. A sequence of dark grey shales with hard, thinly bedded (1-2 cm) calcareous mudstones. Large *Sowerybella* sp. brachiopods from both the shales and calcareous mudstones (hard biomicrites) are silicified and oxide coated.
57. Keppel Township Bruce Peninsula.
- Georgian Bay Formation.**
18 km north of Owen Sound town centre, along County road 26 that fringes Owen Sound. On the waterline of the Keppel Township Park, 1 m of Georgian Bay Formation is exposed.
- i) Georgian Bay Formation. Medium bedded (10-15 cm thick) greenish grey packstones, wackestones and calcareous mudstones are extremely fossiliferous, but singular in diversity, dominated by strophomenid brachiopods (notably *Rafinesquina* sp.) and coral fragments. Many of these beds are almost coquinite packstones (biomicrites). Sampling of *Rafinesquina* sp. from planar pelloidal wackestones (biopelsmicrites; 5-8 cm thick).
58. East Meaford Creek Bruce Peninsula.
- Georgian Bay Formation.**
Exposures of Georgian Bay Formation are seen along East Meaford Creek, just north of Highway 26, 3 km east of Meaford.
- i) Upper Georgian Bay Formation. Sampling from upper section at East Meaford Creek that comprises of sequences of grey to greenish grey thin to thick bedded (4-20 cm) wackestones and calcareous mudstones (biomicrites) interbedded with thin green and grey shales. Fossiliferous wackestones are often singularly dominated by *Rafinesquina deltoidea*. Sampling of *Rafinesquina* restricted to planar wackestones (8 to 10 cm thick).

59. Craigeleith Ontario.

Whitby Formation

The Collingwood Beds of the Whitby Formation are exposed 1 km east of Craigeleith Provincial Park, along the shoreline of Nottawasaga Bay, .

- i) Collingwood Member. From the waterline the first metre of Whitby Formation is characterized by thin (1-3 cm), fissile, fossiliferous (brachiopod pavements), dark grey calcareous mudstones interbedded with thin black shales (1-5 cm thick). The brachiopod pavements are dominated by *Dalmanella* sp. in a wide range of taphonomic conditions, from articulated to disarticulated to abraded to shell hash. Geochemical sampling was restricted to the best taphonomically preserved specimens. The majority of very thin calcareous mudstones (<1 cm thick) are a shell hash. The thin black shales are generally devoid of brachiopods but contain trilobites, especially large disarticulate *Isotelus gigas* and *Pseudogygites canadensis*.
- ii) Collingwood Member. Lower grey calcareous mudstones and shales, of the Collingwood grade into predominantly fissile black shales with a few very thin shell hash layers. Trilobite faunas dominate these black shales.

60. Collingwood Ontario.

Cobourg Formation.

A 6 metre exposure of Cobourg Formation is seen in an abandoned quarry along Lakefield Avenue, just off Highway 26, close to the Batteaux River.

- i) Cobourg Formation. Sequence consists of thin to thick bedded (5-15 cm) skeletal wackestones and calcareous mudstones (biomicrites). The lower part consists of greyish brown nodular packstones with thin greenish grey shale partings and grades upwards into predominantly barren hard, calcareous mudstones. Brachiopod fauna is restricted to small rhynchonellids.

61. Beaverton Ontario.

Cobourg Formation.

Cobourg outcrops at the intersection of Highway 12/48 and Thorah Line 4, as road cuts through Cobourg escarpment. 2.5 m outcrop.

- i) Cobourg Formation. Planar bedded grey, crinoidal packstones, grainstones (5-10 cm) and thin calcareous mudstones with thin shale partings. Strophomenids dominate, *Rafinesquina deltoidea* and are sampled from crinoidal grainstones (coarse crinoidal biosparites).

62. Mara Quarry Ontario.

Verulam Formation.

11 m section in Mara limestone quarry, 300 m west of Highway 12 in Gamebridge. Sequence of grey grainstones, pelloidal mudstones and hard, calcareous mudstones, irregularly bedded with thin grey shale partings. This section has been assigned to the lower Verulam Formation (Liberty, 1969) and is interpreted by Brookfield and Brett (1988) as a proximal to distal shoal lithofacies.

- i) Verulam Formation. Sequence of light grey, thin, irregularly bedded skeletal wackestones, packstones and calcareous mudstones (5-10 cm thick) commonly with greenish grey thin shale partings. Brachiopods are sampled from crinoidal packstones (biomicrites). Single valved strophomenid brachiopods predominate within the basal parts

of these beds i.e. *Rafinesquina deltiodea* and *Sowerybella* sp. Commonly *Dalmanella rogata* cluster on upper surfaces.

63. Bolsover

Ontario.

Verulam Formation. (Fig. A-7)

Road cut along Highway 48, 2 km south of Bolsover. 2 m section on either side of road. Brookfield and Brett (1988) have interpreted this outcrop as representative of a distal shoal cycle. Tentatively interpreted as Upper Verulam Formation.

- i/ii) Verulam Formation. Sequence of thin grey shaley beds with thin calcareous mudstones weathering to rubbly brown. Sampling horizons are referred to in Fig. A.7. Articulate brachiopods i.e. predominantly *Dalmanella rogata*. are common to these shaley and mudstone beds (Beds A and D). Outcrop has five thin, irregularly bedded, grey crinoidal wackestones and hard, nodular mudstones (3-10 cm thick) within two metre section (Beds B, C and E). *Dalmanella rogata* is present in uppermost wackestone bed (crinoidal biomicrite). This bed is an irregular and undulating hardground.

64. Dalrymple

Ontario.

Bobcaygeon Formation.

Road cut along Highway 503 south of Dalrymple. Weathered dark grey section of thinly bedded calcareous mudstones with single valved brachiopods present often at tops of beds. Predominantly *Dalmanella rogata* sampled from thin planar wackestones (skeletal biomicrites). Brachiopods are partially silicified.

65. Kirkfield Quarry

Ontario.

Verulam Formation. (Fig. A-8)

Abandoned quarry north of Kirkfield. Take first eastward dirt road just north of the Trent Canal lock. Quarry is water filled and only the lower Verulam Formation is exposed (2.5 m thick). The contact between Bobcaygeon and Verulam Formations is at the waterline.

- i) Lower Verulam Formation. Thick to thin bedded crinoidal grainstones and packstones (5-20 cm thick) and peloidal mudstones interbedded with rare shale partings. Some beds exhibit graded fabric. The lowermost beds are cross-laminated. Articulate *Dalmanella* sp. and crinoids are abundant in uppermost 20 cm of quarry section (from a crinoidal biosparite with minor micrite. These beds are interpreted by Brookfield and Brett (1988) to be shoal-edge lithofacies.
- ii) Upper Bobcaygeon Formation. Uppermost half metre of thick, cross-bedded (20-25 cm thick) grey crinoidal packstones, wackestones and calcareous mudstones.

66A. Trent Canal Lock

Ontario.

Bobcaygeon Formation.

North of Kirkfield, 100m south of Trent Canal Lock along County Road 503. Road section exposes 2.5 m of weathered dark grey calcareous mudstones with thin lenses of crinoidal grainstones and packstones. Articulate *Dalmanella rogata* are common but are variably silicified.

- i) Bobcaygeon Formation. Thin bedded (3-6 cm thick), grey, planar calcareous mudstones (biomicrites) and peloidal wackestones (fine biopelsparite). *Dalmanella rogata*. sampled from upper 50 cm of section (biomicrites).

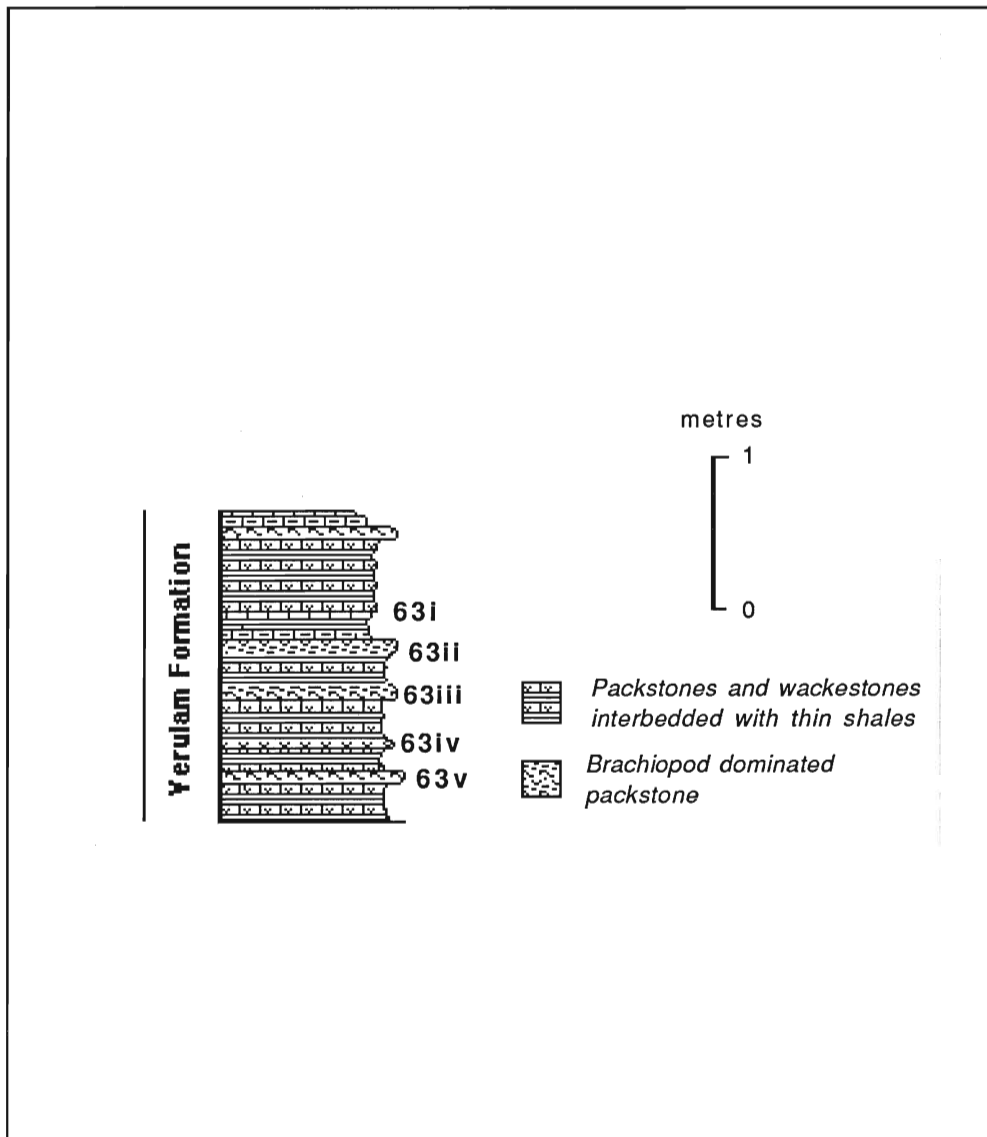


Figure A-7. Stratigraphic section of Verulam Formation from the Bover roadcut. Numbers refer to sampling intervals listed in Appendix I. Modified from Brookfield and Brett, 1988.

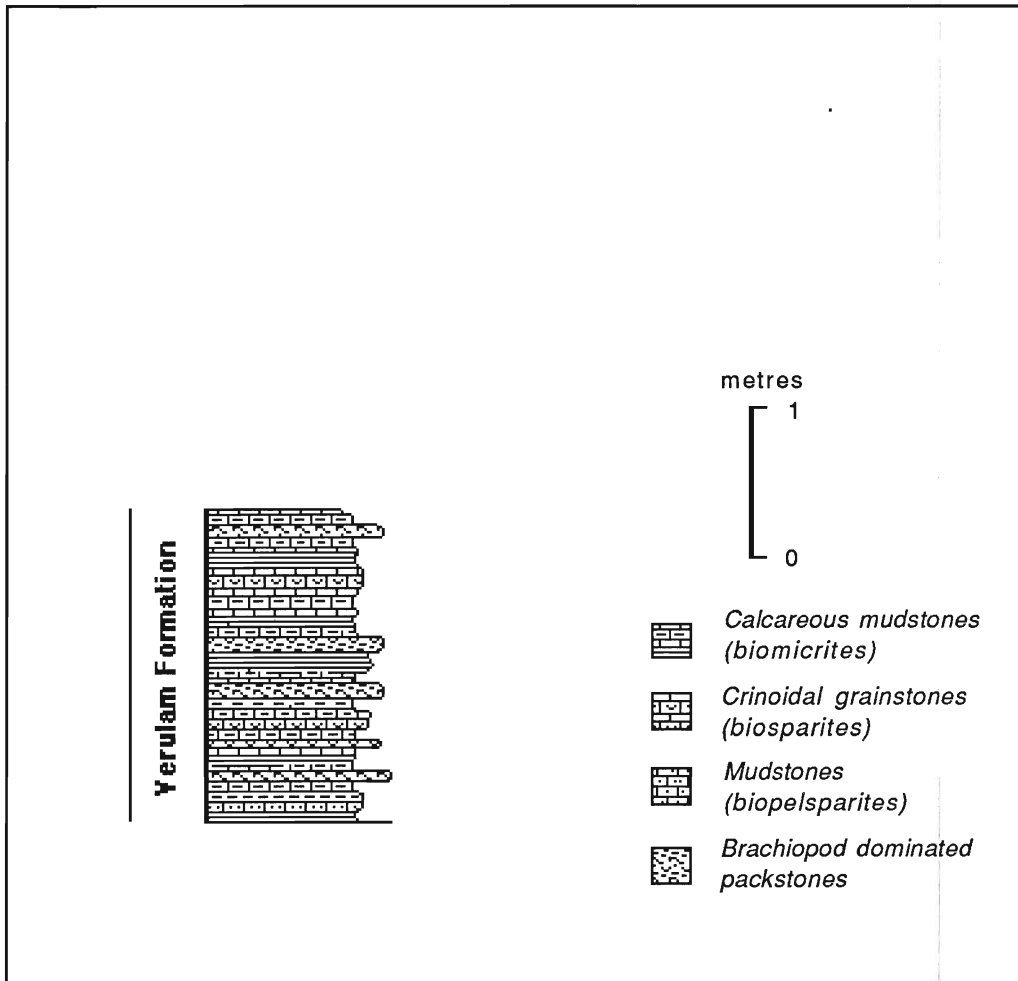


Figure. A-8. Stratigraphic section of Verulam Formation at Kirkfield Quarry.

- 66B. North of Kirkfield Ontario.
- Verulam Formation**
North of Kirkfield, 250 m south of the Trent Canal Lock along County Road 503. Road section exposes 1.8 m of lower Verulam Formation
67. Kirkfield Ontario.
- Verulam Formation.**
4 km south of Kirkfield along County Road 6. Liberty's (1969) S5 locality and interpreted as Upper Verulam. Possibly belongs to Brookfield and Brett's (1988) shoal edge-shoal bar biofacies of uppermost Verulam.
- i) Verulam Formation. 1.8 m outcrop in ditch of thick bedded, low angle cross-bedded crinoidal packstones (i.e. crinoidal biosparites)
68. Glenam Ontario.
- Cobourg Formation.**
Road cut 5.5 km south of Kirkfield along County Road 6. Liberty's (1969) S6 locality.
- i) Cobourg Formation. Liberty's (1969) S6 locality. Greenish grey skeletal packstones, wackestones and calcareous mudstones. Thin, weathered shaley partings present between beds.
- ii) Verulam Formation. 500 m north of Cobourg Formation outcrop. Cross-bedded crinoidal grainstones outcropping in ditch. Can be tentatively interpreted as Upper Verulam Formation and in accordance with Brookfield and Brett (1988) part of shoal edge lithofacies.
69. Eldon Hill Ontario.
- Cobourg Formation.**
6.5 km south of Kirkfield along County Road 6. Liberty 's (1969) H1 locality.
- i) Cobourg Formation. Greenish grey, nodular skeletal packstones and wackestones, with pelloidal mudstones. Appears in this section to be sparsely fossiliferous. *Rafinesquina* sp sampled from medium bedded, planar, coarse pelloidal grainstones (coarse biopelsparite).
70. Fenelon Falls Ontario.
- Bobcaygeon Formation.**
8.5 m outcrop at Fenelon Falls below the Trent Canal locks.
- i) Upper Bobcaygeon Formation. Five metre sequence of thin bedded brown wackestones with thin blue grey calcareous mudstones. Brachiopods are rare and limited to lowermost interval. *Dalmanella rogata* and *Onniella* sp. are present.
- ii) Lower Verulam Formation. Upper part of section dominated by thin to medium bedded planar crinoidal packstones and calcareous mudstones (biomicrites) with thin greenish grey shale partings.

71. County Road 21 Ontario.
- Verulam Formation.**
4 km southwest of Cameron, along County Road 21. 1.5m exposure at east side of road.
- i) Upper Verulam Formation. Thin to medium bedded planar crinoidal packstones and wackestones (crinoidal biosparites).
72. Lindsay Ontario.
- Cobourg Formation.**
Road cut 4 km north of Lindsay along Highway 35/115. Section through Cobourg escarpment exposes 5- 6m.
- i) Cobourg Formation. Grey, medium, planar bedded crinoidal grainstones and packstones (i.e. crinoidal biosparites). Low-angle cross lamination often developed in thicker beds.
73. Dunsford Ontario.
- Trenton Group.**
2.5 km southwest of Dunsford along Highway 36. 10 m section cuts through Cobourg escarpment. Contact between Cobourg and Verulam Formations hidden beneath talus slope.
- i) Lower Cobourg Formation. Coarse pelloidal packstones (biopelsparites; 5-10 cm thick) with fine skeletal fragments of gastropods, bivalves and trilobites. Interbedded with nodular calcareous mudstones.
- ii) Upper Verulam Formation. Medium bedded, planar, grey coarse crinoidal biosparite, grainstones and packstones.
74. Cedar Glen Road Ontario.
- Verulam Formation.**
Four outcrops of Verulam Formation along Cedar Glen Road between Highway 36 and Sturgeon Lake.
- i) Lower Verulam Formation. At waterfront of Sturgeon Lake.
ii) Verulam Formation. 250 m from waterfront along Cedar Glen Road.
iii) Verulam Formation. 100 m north of County Road 24.
iv) Verulam Formation. At the intersection of Cedar Glen Road and Highway 36.
- 75A. Dunsford Ontario.
- Verulam Formation.**
1.5 km north of Dunsford along Highway 36.
- i) Verulam Formation. Sequence of thin planar grey calcareous mudstones with thin grey shaley partings.
- 75B. Bobcaygeon. Ontario.
- Bobcaygeon Formation**
3/4 km south of the town of Bobcaygeon. Highway close to Little Bob quarry.

76A. County Road 7

Ontario.

Cobourg Formation.

Road section 4 km north of Downeyville along County Road 7 between Downeyville and Dunsford.

- i) Cobourg Formation. Coarse, planar pelloidal wackestone and packstone beds (coarse biopelsparite; 5-10 cm thick) with fine skeletal fragments of gastropods, bivalves and trilobites. Interbedded with nodular calcareous mudstones (fine biomicrites).

76B. Highway 17.

Ontario.

Bobcaygeon Formation

6km south of Bobcaygeon, along Highway 17. Cross-bedded grey crinoidal packstones and wackestones in ditch exposure.

77. Lakefield Quarry

Ontario.

Verulam Formation. (Fig. A-9)

Abandoned quarry west of Lakefield. 1.5 km east of Highway 28. Approximately 9m of grey medium bedded planar biosparite grainstones, wackestones and packstones interbedded with thin biomicrite mudstones and grey shale partings. Dominated by *Rafinesquina deltoidea* and *Sowerybella* sp. Interpreted by Brookfield and Brett (1988) as part of a proximal shoal lithofacies.

- i) Verulam Formation. Thick crinoidal grainstone bed. Abundant strophomenid brachiopods, and trilobite fragments.
- ii) Verulam Formation. Thin crinoidal grainstones. Brachiopods, trilobites
- iii) Verulam Formation. Thin crinoidal grainstones. Brachiopods, trilobites
- iv) Verulam Formation. Thin crinoidal packstone
- v) Verulam Formation. Skeletal wackestones (biomicrite)

78. Trenton

Ontario.

Verulam Formation.(Fig. A-10)

On the off ramp for highway 33 along Highway 401. North of Trenton. Approximately 4m of alternating thin to thick crinoidal packstones and thin calcareous mudstones with green shaley partings.

- i) Verulam Formation. At top of section. Crinoidal packstones, with abundant corals, bivalves
- ii) Verulam Formation. (30-35 cm from top). Crinoidal packstones, with abundant corals, bivalves.
- iii) Verulam Formation. (50-55 cm). Crinoidal packstones, with abundant corals, bivalves
- iv) Verulam Formation. (105 cm). Skeletal packstones.
- v) Verulam Formation. (2.20 m). Skeletal packstone, with abundant corals, bivalves, gastropods and brachiopods. Minor silicification of brachiopods evident.
- vi) Verulam Formation. (2.70 m). Crinoidal packstones, with abundant corals, bivalves

79. Belleville

Ontario.

Verulam Formation.

Abandoned quarry off Highway 401, close to the Moira River and Highway 62.

- i) Verulam Formation. Skeletal crinoidal packstones. Minor silicification of brachiopods present.

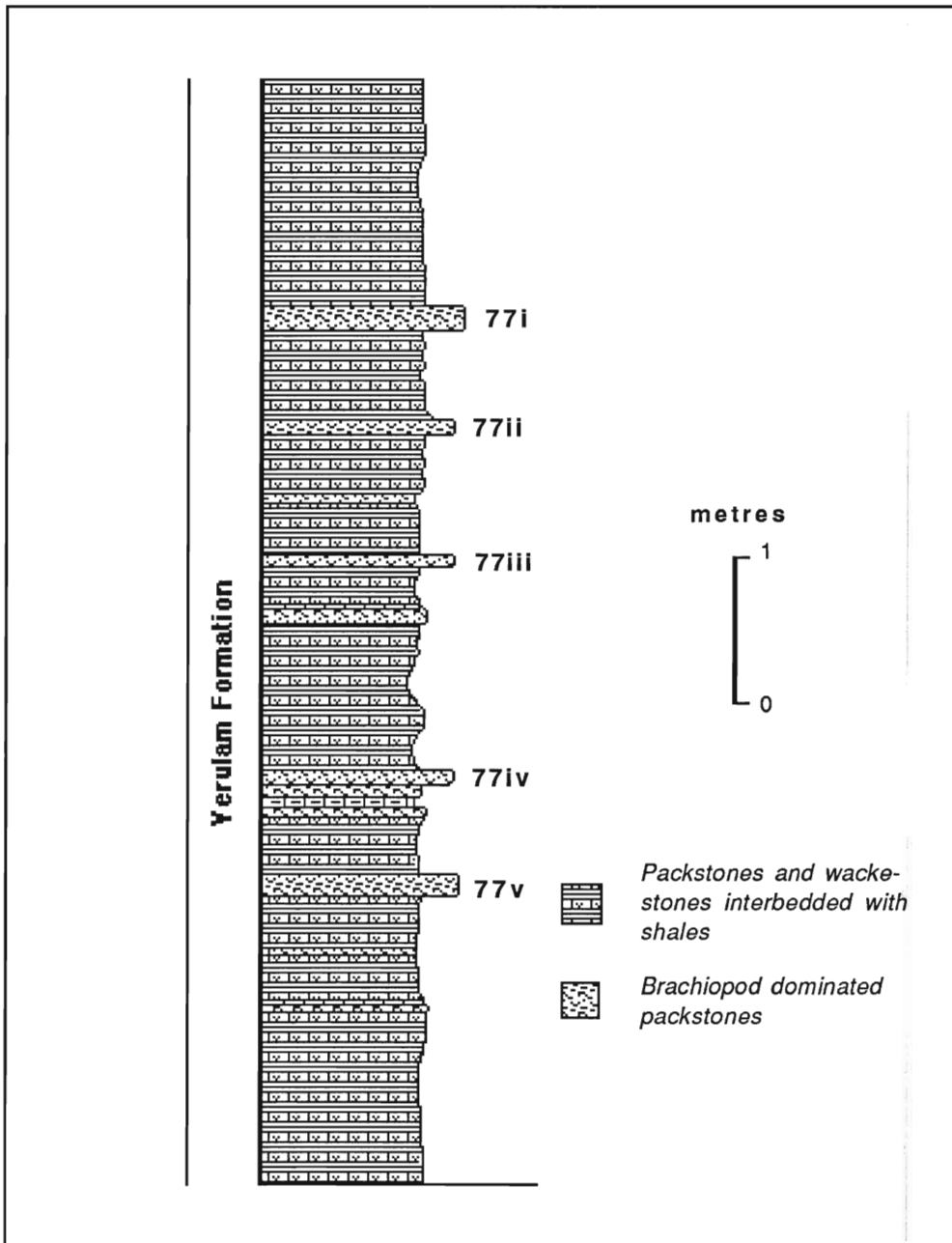


Figure A-9. Stratigraphic section of Verulam Formation at Lakefield Quarry near Peterborough. Numbering corresponds to sampling intervals listed in Appendix I. Modified from Brookfield and Brett (1988).

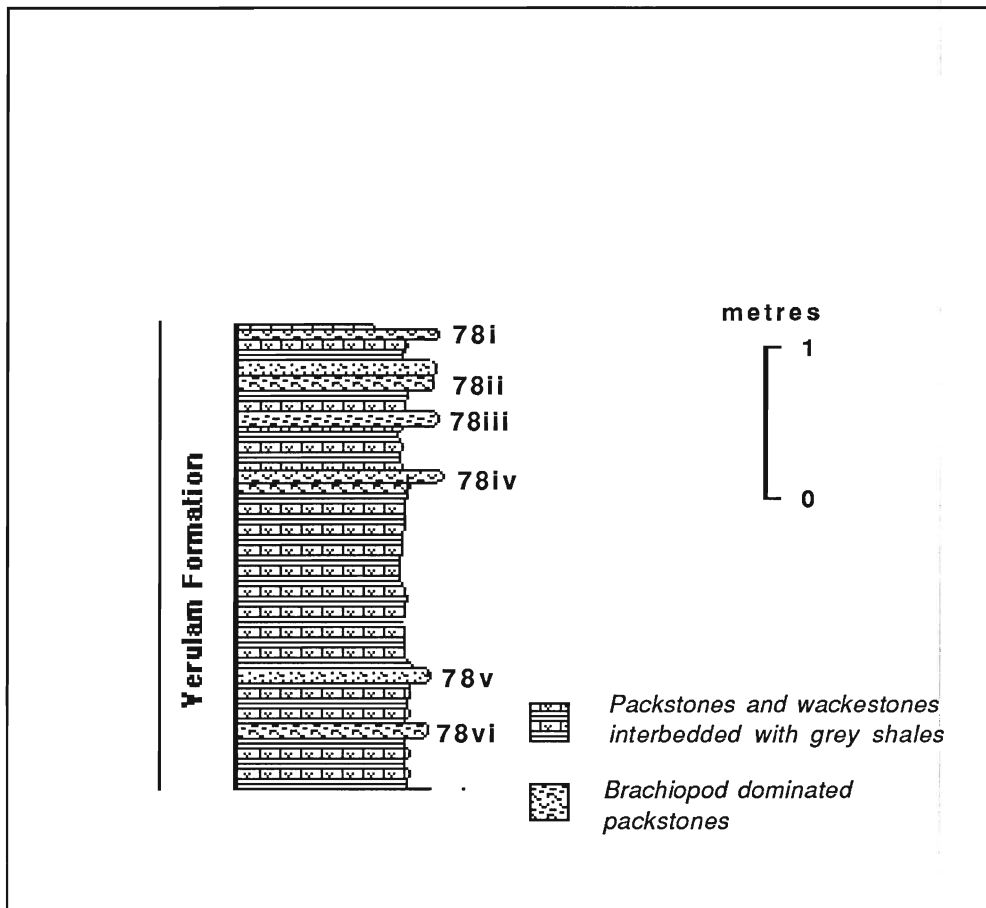


Figure A-10. Stratigraphic section of Verulam Formation outcropping along roadcuts at the intersection of Highways 33 and 401. Numbers refer to sampling intervals.

Appendix II

Key to species identification

<u>No.</u>	<u>Species</u> (SP)
1.	<i>Athyris spiriferoides</i>
2.	<i>Mucrospirifer mucronatus</i>
3.	<i>Mediospirifer audacula</i>
4.	<i>Rhipidomella vanuxemi</i>
5.	Orthid
7.	<i>Tropidoleptus carinatus</i>
8.	<i>Strophomena</i>
9.	Crinoid
10.	Cement
11.	<i>Mucrospirifer arkonensis</i>
12.	<i>Dalmanella rogata</i>
14.	<i>Rafinesquina deltoidea</i>
15.	Rhynchonellid
16.	<i>Sowerybella</i>
21.	<i>Pentameroides</i> sp.
22.	<i>Eospirifer radiatus</i>
23.	<i>Whitfieldella nitida</i>
24.	<i>Atrypa reticularis</i>
25.	<i>Strispirifer niagarensis</i>
27.	<i>Coolinia subplana</i>
28.	<i>Dalejina</i>
29.	<i>Resserella elegantula</i>
30.	<i>Leptaena rhomboidalis</i>
31.	<i>Rhyncotretra americanus</i>
M.	Matrix

LM = locality, see appendix ??.

Sample number superscripts refer to

80¹ = pedicle valve

80² = brachial valve

80³ = matrix from within brachiopod

80⁴ = replicate

I.R. = %; Elemental contents are reported in ppm;

BD = below detection limits

$\delta^{18}\text{O}$ and $\delta^{13}\text{C}$ are reported in ‰ (PDB).

APPENDIX III. Elemental and isotopic data.

Sample	SP	LM	IR	Ca	Mg	Sr	Mn	Na	Fe	Al	$\delta^{18}\text{O}$	$\delta^{13}\text{C}$
2	1	3ii	7.3	363070	1030	900	200	1040	110	BD		
3	1	3ii	8.5	357800	1580	865	205	840	210	BD		
4	1	3ii	6.7	340640	1315	840	145	1140	250	BD	-3.55	+2.41
5	1	3ii	3.7	317600	1185	795	150	995	380	BD	-4.36	+2.46
6	1	3ii	6.5	341740	1545	815	225	1060	370	BD		
16	M	3ii	89.9	193140	7450	370	1130	605	10270	BD		
18	3	3ii	12.5	330620	1000	800	220	1325	555	BD		
20	3	3ii	11.6	340430	980	860	210	1555	510	BD		
21	2	3ii	10.1	350710	1190	910	180	1340	365	BD		
22	2	3ii	11.7	372890	1250	960	140	1430	530	90		
24	2	3ii	9.1	356670	1060	970	140	1720	475	50		
25	3	3ii	10.5	337880	1260	890	265	1255	1365	160		
26	3	3ii	7.6	371610	805	920	205	1215	390	BD		
27	2	3ii	9.8	362150	940	910	170	1360	230	70		
30	3	3ii	12.0	298060	1190	920	215	1455	950	145		
33	2	3ii	10.6	339790	1480	950	230	1250	945	185		
40	4	3ii	7.3	317580	4300	775	1030	1470	2165	315		
41	4	3ii	25.6	331580	3720	880	620	1515	2760	25		
42	1	3i	3.9	373010	990	735	95	850	280	BD	-4.14	+1.84
43 ¹	1	3i	4.0	369410	1045	805	80	1050	350	260	-3.79	+2.02
44	3	3i	4.5	352190	890	950	130	1670	505	140		
45	1	3i	11.8	352160	820	710	140	735	720	120		
46	2	3i	10.1	352990	975	730	170	950	1200	70		
51	5	3iii	11.0	346750	3020	1040	780	930	2375	60		
53	5	3iii	12.8	356380	3170	1195	375	1120	1860	165		
56 ¹	1	3iii	4.9	362600	1160	830	105	1020	525	200		
56 ²	1	3iii	17.0	375900	1510	810	270	680	2480	20		
57	1	3iii	8.5	343680	855	780	40	965	160	40		

Sample	SP	LM	IR	Ca	Mg	Sr	Mn	Na	Fe	Al	$\delta^{18}\text{O}$	$\delta^{13}\text{C}$
58	2	3iii	9.8	355660	1340	1025	80	1025	385	BD		
60	1	7ii		6.1	354900	2175	795	100	1320	200	BD	
61	1	7ii		6.1	356200	1450	795	120	1190	275	55	
62	1	7ii	4.1	371160	1530	820	130	1325	300	170		
63	1	7ii	9.0	355610	1920	950	120	1760	260	180		
64	1	7ii	5.6	356240	1440	845	250	1395	700	125		
66	2	7ii	4.3	355620	1090	890	90	1330	240	110		
67	2	7ii	5.9	371720	960	870	160	1400	475	110		
68	2	7ii	8.3	352720	650	695	150	1150	320	85		
69	2	7ii	12.5	352240	1045	940	190	1680	560	125		
70	3	7ii	32.9	354150	705	615	85	940	80	75		
71	3	7ii	4.2	365860	725	840	110	1670	140	BD		
72	2	7ii	7.6	375400	950	990	160	1650	695	BD		
80 ¹	3	7ii	3.7	362570	785	850	210	1900	600	BD		
80 ²	3	7ii	8.5	354810	880	720	250	1560	1305	75		
80 ³	M	7ii	87.4	111760	2810	355	445	1180	14860	540		
81	3	7ii	7.3	311310	625	615	105	1235	445	BD		
83	4	7ii	11.3	310700	3490	880	350	2195	940	BD		
84	4	7ii	8.5	307140	2810	865	185	1490	790	BD		
85	4	7ii	7.2	311310	3970	910	350	2155	1510	20		
86	4	7ii	11.8	294350	3390	910	195	1650	1250	BD		
87	4	7ii	28.9	268970	2310	635	135	1214	210	90		
88	2	7iii	7.4	363720	1045	885	105	1670	375	90		
89	2	7iii	3.5	361400	670	810	110	1670	375	120		
90	2	7iii	7.8	365990	850	820	95	1410	410	45		
91	2	7iii	7.1	360580	760	835	90	1505	325	BD		
95 ²	2	7iii	6.4	369420	855	980	160	1490	860	40		
98	1	8ii	5.1	364510	1510	780	250	1565	535	60		
99	1	8ii	9.0	378400	1585	820	120	1400	275	BD	-3.86	+2.40
100 ¹	1	8ii	3.9	377730	1420	880	205	1520	690	BD		

Sample	SP	LM	IR	Ca	Mg	Sr	Mn	Na	Fe	Al	$\delta^{18}\text{O}$	$\delta^{13}\text{C}$
100 ²	1	8ii	3.8	392680	1225	835	205	1595	500	80		
100 ³	M	8ii	90.8	150510	5465	600	865	1420	14710	4400		
101	1	8ii	2.7	246830	1270	870	110	1500	140	50		
104 ¹	1	8ii	9.1	322630	1075	800	120	1250	330	BD	-3.65	3.02
104 ²	1	8ii	5.2	321040	1605	805	350	1330	1170	120		
106	2	8ii	5.2	315310	1065	960	130	2000	310	280		
107	2	8ii	5.2	213280	1225	935	150	1720	525	220		
109	3	8ii	5.4	393940	700	860	150	1310	245	BD		
110	2	8ii	13.6	394730	1290	1030	230	1545	310	BD		
112	2	8ii	11.9	374880	1150	920	130	1335	250	BD		
113	4	8ii	7.6	379730	2855	920	360	1510	445	BD		
115	4	8ii	5.8	348200	2810	830	270	1400	350	BD		
116	4	8ii	10.7	392720	4235	1020	380	1525	495	BD		
126 ¹	3	8ii	6.3	388730	835	860	50	1150	110	BD		
126 ²	3	8ii	8.4	401140	1050	880	135	1270	265	BD		
127	7	8ii	9.6	369370	2015	880	295	1510	420	95		
128	7	8ii	7.4	365720	1200	755	850	985	670	100		
129 ¹	7	8ii	9.1	368010	2340	850	520	1450	710	40		
129 ²	7	8ii	6.1	369660	2300	880	275	1575	480	140		
149	1	9	5.2	369780	985	860	125	1200	240	60		
150	3	9	4.9	370970	760	870	65	1490	160	75		
151	1	9	3.6	362720	970	850	120	1205	250	90		
152	2	9	6.1	365700	1230	940	130	1370	365	155		
154	2	9	8.5	335880	1190	815	35	1135	595	150		
158	3	9	6.4	362790	1145	1015	170	1660	240	145		
159	3	9	4.0	394560	610	880	15	1345	90	BD		
160	2	9	5.8	390460	1245	920	160	1255	290	BD		
161	2	9	3.8	379810	1140	1020	75	1410	215	BD		
162	2	9	5.7	394590	1300	1040	165	1560	320	BD		

Sample	SP	LM	IR	Ca	Mg	Sr	Mn	Na	Fe	Al	$\delta^{18}\text{O}$	$\delta^{13}\text{C}$
164 ¹	1	10i	6.7	373130	1420	950	750	1420	320	BD		
164 ²	1	10i	9.4	399900	1450	970	510	1410	350	BD		
165	1	10i	6.0	377930	1540	1010	70	1550	230	BD		
166	3	10i	8.4	369850	875	855	70	1325	175	BD		
167	1	10i	5.2	373160	1390	875	260	1200	350	BD		
168	3	10i	6.9	382780	590	840	50	1260	180	17		
170 ¹	1	10i	5.9	352430	1540	850	1645	1210	820	130		
170 ²	1	10i	5.4	355370	1450	870	1140	1225	700	165		
171	1	10i	7.0	343030	1715	910	250	1405	370	180		
172	1	10i	2.5	351550	1365	840	5	1170	95	170		
173	2	10i	5.4	340750	1040	875	215	1465	420	240		
176	2	10i	4.4	355640	785	1045	75	1410	260	220		
177 ¹	2	10i	9.2	344850	1150	980	360	1465	715	260		
177 ²	2	10i	4.5	340810	1180	955	510	1425	825	240		
178	2	10i	6.2	343540	1075	960	90	1675	370	290		
179	2	11	9.0	381540	1645	1080	80	1720	270	170		
180	2	11	4.2	386710	1190	880	160	1190	270	130		
181	1	11	3.2	383280	1245	855	70	1080	240	130		
182 ¹	3	11	6.6	389850	845	895	<1	1130	130	150		
182 ²	3	11	2.4	387140	680	920	<1	1110	130	75		
184	2	11	7.5	365600	1040	890	200	1210	370	180		
185 ¹	1	11	6.4	361250	1420	770	80	900	330	180		
185 ²	1	11	12.0	365360	1885	805	430	1020	640	270		
187	4	12	5.9	376860	1095	830	855	1120	950	220		
188	8	12	11.6	383450	1910	960	320	1390	440	325		
190	1	15viii	5.7	356730	955	850	185	1235	145	BD		
191	1	15viii	5.3	371590	1205	860	195	1250	145	BD		
192	1	15viii	6.7	326190	940	750	225	1090	250	BD		
193	7	15viii	6.5	372190	1220	920	280	1480	290	15		

Sample	SP	LM	IR	Ca	Mg	Sr	Mn	Na	Fe	Al	$\delta^{18}\text{O}$	$\delta^{13}\text{C}$
194	2	15viii	7.3	385230	920	995	280	1430	170	BD		
195	2	15viii	7.3	380750	750	885	295	1285	185	BD		
196	2	15viii	10.5	354930	880	1000	320	1705	205	30		
197	7	15viii	13.0	393090	1205	840	270	1310	875	100		
199 ¹	2	15viii	3.7	353020	950	795	400	1140	360	30		
199 ²	2	15viii	7.7	403940	970	760	770	1180	740	70		
201	1	15vii	5.9	420240	1315	905	180	1150	150	35		
204	1	15vii	5.3	381020	1205	855	260	1165	130	50		
205	1	15vii	5.0	215740*	580*	865	295	1125	120	60		
206	1	15vii	7.2	366740	1560	810	110	1125	120	65		
207	1	15vii	5.4	388040	1380	830	165	1185	115	65		
207 ⁴	1	15vii	5.7	385920	1580	825	180	1150	110	65		
210	3	15vii	6.9	385850	655	1030	190	1345	100	BD		
211	3	15vii	5.3	394320	730	1070	215	1465	160	BD		
212	3	15vii	5.3	383290	700	1005	280	1265	160	BD		
213	2	15vii	4.1	375840	890	1040	240	1290	330	BD		
217	3	15vii	8.1	390830	745	990	320	1320	370	BD		
218	2	15vii	7.8	386150	1090	1050	210	1310	350	BD		
223	2	15vii	5.9	389780	800	1105	310	1315	310	BD		
224	2	15vii	5.7	384650	1080	1150	140	1505	145	BD		
225	2	15vii	6.4	391620	895	975	300	1310	470	BD		
226	2	15vii	4.9	391620	1030	1075	230	1290	860	BD		
227	7	15vii	8.0	357690	1275	920	945	1120	860	BD		
228	7	15vii	4.6	365620	850	750	625	870	500	BD		
230	7	15vii	5.0	368720	810	830	690	1020	890	BD		
231	2	15iii	8.2	357500	3495	1335	330	1365	475	BD		
232	2	15i	14.0	349980	1695	1140	330	1720	1035	BD		
233	2	15i	19.9	363240	1835	1050	595	1540	1225	BD		
234	9	15i	9.0	354240	7105	1090	2680	1160	2940	BD		
235	1	17ii	3.3	364750	1215	895	165	1225	100	BD		

Sample	SP	LM	IR	Ca	Mg	Sr	Mn	Na	Fe	Al	$\delta^{18}\text{O}$	$\delta^{13}\text{C}$
236	1	17ii	4.6	360130	1150	945	205	1380	135	BD		
238	1	17ii	5.0	367480	1290	880	170	1230	80	BD		
243	3	17ii	7.5	395830	680	930	255	1365	190	BD		
244	3	17i	6.9	405160	580	890	170	1290	70	BD		
245	2	17i	4.6	350990	1285	880	170	1255	70	BD		
246 ¹	1	17i	6.1	417920	1350	860	180	1250	160	BD		
246 ²	1	17i	3.9	402030	1240	865	115	1180	90	BD		
249	1	17i	4.8	396900	1065	860	220	1250	185	BD		
250	1	13ii	4.3	412360	1165	820	135	1055	115	BD		
251	1	13ii	3.4	387780	1620	815	210	1240	190	BD		
252	1	13ii	4.7	401370	1080	860	190	1260	130	BD		
253	1	13ii	5.5	406670	1210	800	150	1120	130	BD	-4.02 -3.74	+2.45 +2.33
254	1	13ii	3.7	386640	1330	840	150	1200	80	BD	-4.30	+2.68
255	2	13ii	5.2	376100	1060	920	240	1630	270	17		
256	2	14	2.1	374760	925	880	160	1430	100	BD		
257	2	14	2.1	383670	870	855	110	1430	145	BD		
258	2	14	2.1	373430	730	845	90	1470	160	BD		
260	3	13i	25.4	358190	830	820	220	1560	390	BD		
261	3	13i	43.0	361740	585	1095	130	1280	320	195	-2.77	+5.46
262	3	13i	37.9	363710	1820	790	390	505	1715	600		
263	1	13i	7.6	378960	1070	1180	150	1595	430	210	-2.73	+5.15
270	3	19i	5.4	406460	800	1005	160	1410	220	125		
271	3	19i	5.0	402340	620	1050	160	1385	250	100		
272	3	19i	5.8	391920	970	1105	210	1530	305	125		
273	3	19i	6.0	395120	1240	1070	280	1380	590	210		
275	M	19i	58.1	393660	4340	780	1440	525	5225	1940		
276	3	19i	4.8	410870	810	975	130	1490	305	90		
280	2	20iii	4.5	392000	1020	1040	140	1600	430	95		
282	2	20iii	4.6	411170	1140	1080	100	1640	330	100		

Sample	SP	LM	IR	Ca	Mg	Sr	Mn	Na	Fe	Al	$\delta^{18}\text{O}$	$\delta^{13}\text{C}$
283	3	20iii	13.0	265360	670	610	90	1170	255	45	-2.70	+4.85
284	3	20iii	2.1	377310	940	1100	140	1590	430	150		
285	2	20iii	14.8	388580	1070	1110	170	1610	520	120	-3.17	+5.07
286	1	20iii	3.9	390670	1020	1035	80	1400	190	40	-3.42	+4.81
287 ¹	7	20ii	6.5	405210	1550	1020	245	1625	700	80		
287 ²	7	20ii	9.2	390830	1475	1025	215	1640	625	80		
288	3	20ii	10.4	412910	1355	980	210	1570	880	100		
289	3	20ii	6.5	377550	1045	1055	240	1655	610	170	-3.44	+4.44
291	M	20ii	79.9	367830	7495	750	1340	875	8210	1440		
292	9	20ii	11.1	367830	5810	650	2490	920	3365	180		
293	9	20ii	6.4	407870	6755	1550	2110	625	6040	60		
294	3	20i	42.5	391430	1800	570	1030	805	3500	180		
295	3	20i	22.9	373655	720	895	60	425	350	70	-2.57 -2.65	+4.80 +4.79
301	11	1iv	7.0	391370	1040	1035	640	1465	935	60		
302	11	1iv	4.4	405180	985	1000	480	1330	665	30		
305	2	1ii	4.6	404540	750	1035	80	1460	180	40		
306	2	1ii	5.2	412270	740	970	110	1295	220	30		
308	2	1ii	6.6	394500	1055	1065	175	1495	345	60		
309	2	1ii	13.3	389650	870	880	115	1195	165	10		
310	2	1ii	6.3	416390	840	1045	70	1405	130	30		
312	11	1iv	7.4	396420	1425	840	995	1310	1990	100		
313	11	1iv	10.6	385000	1390	850	905	1280	2190	180		
314	11	1iv	5.2	373920	1020	920	955	1355	1090	60		
370	7	18	0.1	366210	1350	850	820	1425	2300	110		
371	7	18	0.1	405690	1450	930	710	1465	1495	19	-2.84 -3.18	+4.41 +4.58
372	7	18	5.0	363790	1250	820	725	1350	2090	140		
373	7	18	0.3	401950	1510	895	1060	1340	2040	105		
374	7	18	4.4	395090	1575	870	660	1395	1535	30	-2.61	+4.69
375	7	18	8.3	379400	1650	765	600	1390	2480	150		
376	2	18	4.8	376650	1350	1070	765	1500	2095	160		

Sample	SP	LM	IR	Ca	Mg	Sr	Mn	Na	Fe	Al	$\delta^{18}\text{O}$	$\delta^{13}\text{C}$
377	2	18	4.6	375730	1155	1070	170	1660	420	140		
378	1	18	2.8	371340	1505	1145	440	1625	980	140		
379	2	18	10.0	361530	1550	655	1665	980	3710	280		
380	3	18	7.5	372310	1685	1050	530	1750	1650	170		
381	9	18	8.0	378680	6900	1150	3295	835	5220	14		
382	9	18	9.9	363310	7180	1150	3315	730	6410	50		
383	9	18	9.0	360520	6955	905	4010	1140	6210	50		
383 ⁴	9	18	9.8	362430	6830	870	3740	1110	6320	55		
400	3	6v	2.8	394080	650	880	185	1380	325	100	-4.61	+2.45
401	1	6v	11	389150	1140	860	170	1245	240	30	-3.89 -4.16	+2.91 +2.79
401 ⁴	1	6v	3.2	391590	1180	900	140	1180	235	60		
402	1	6v	11.3	399930	1215	830	385	1115	825	130	-5.21	+2.15
403	1	6v	9.7	437260	1420	960	170	1330	275	45		
404	1	6v	3.5	390020	845	920	230	1200	330	40		
405	2	6v	4.5	404940	1220	1050	175	1495	250	155		
406	2	6v	3.8	404840	960	980	180	1400	210	160		
407	2	6v	3.7	405650	905	910	140	1245	235	115		
408	2	6v	4.2	404790	975	1025	120	1370	270	70		
409	7	6v	12.6	374920	2200	850	225	1440	420	170		
410	7	6v	19.3	376990	2010	980	320	1570	1230	310		
411	7	6v	8.1	369480	1900	890	210	1445	1340	55		
412	4	6v	5.1	381460	2975	915	340	1540	850	50		
413	4	6v	10.5	391910	2870	900	305	1510	930	90		
414	4	6v	8.1	387270	2945	940	290	1640	850	50		
415	2	6i	8.7	396650	770	885	130	1380	195	19		
416	2	6i	3.2	398970	1380	960	200	1500	320	85		
417	2	6i	2.9	387030	1040	970	110	1620	180	60		
418	4	6i	8.1	390230	2400	910	235	1595	200	20		
419	4	6i	1.5	378220	3035	1000	295	1670	320	15		
420	3	6ii	9.5	375960	660	870	50	1190	65	BD	-3.18	+3.66

Sample	SP	LM	IR	Ca	Mg	Sr	Mn	Na	Fe	Al	$\delta^{18}\text{O}$	$\delta^{13}\text{C}$
421	3	6ii	6.8	365980	595	910	50	1255	65	BD		
421 ⁴	3	6ii	9.4	370660	590	920	50	1290	70	BD		
422	3	6ii	6.6	374530	340	940	30	880	70	BD	-2.85	+3.74
423	3	6ii	10.3	390210	805	870	170	1185	280	90		
424	3	6ii	10.2	377550	900	940	80	1445	120	90		
425	2	6viii	0.1	336220	1460	875	210	1410	410	240		
426	1	6viii	14.7	381270	1730	860	280	1055	940	230		
427	1	6viii	5.1	369040	1935	860	500	750	2060	180		
428	1	2ii	7.4	374270	1205	960	130	1360	195	20	-3.36	+3.12
429	1	2ii	9.8	396640	1135	870	130	1025	205	BD		
430	1	2ii	9.3	368220	1320	955	190	1345	405	50	-3.05	+3.25
431	1	2ii	12.9	385640	1275	1040	185	1380	350	30		
432	3	2ii	7.0	370270	620	950	85	1420	205	35	-4.76	+3.53
433	3	2ii	0.8	392460	650	1110	55	1240	115	BD		
434	3	2ii	9.8	394090	610	935	75	1380	140	BD		
435	3	2ii	6.7	372470	715	890	120	1350	300	40		
436	3	2ii	11.5	391400	740	1020	100	1420	215	30		
438	1	2i	4.0	393350	1120	890	125	1125	310	50		
439	1	2i	9.1	398620	1135	820	160	1055	320	80		
440	1	2i	8.1	388470	1160	860	105	1200	185	45		
441	1	2ii	8.5	371790	1355	980	85	1200	165	65		
442	1	2iii	10.1	366780	1665	980	170	1400	575	80		
442 ⁴	1	2iii	10.0	361790	1705	995	165	1395	580	70		
443	1	2iii	12.4	379790	1610	1080	110	1490	330	65		
444	1	2iii	6.3	370220	1390	860	70	1135	155	55		
445	1	2iii	8.4	370280	1695	925	95	1290	200	70		
446	3	2iii	10.1	369780	1000	1070	130	1600	520	95		
447	3	2iii	6.6	362070	1240	1040	150	1620	545	100		
448	3	2iii	9.4	360670	1020	930	125	1405	520	100		
449	3	2iii	5.0	384040	1135	1110	95	1610	460	120		

Sample	SP	LM	IR	Ca	Mg	Sr	Mn	Na	Fe	Al	$\delta^{18}\text{O}$	$\delta^{13}\text{C}$
450	1	6vi	3.5	406110	1500	875	550	1045	840	135		
451	1	6vi	7.1	401610	940	760	90	955	135	100		
452	1	6vi	6.5	399940	1210	770	130	990	220	60		
453	1	6vi	5.4	382970	1420	770	145	1055	230	80		
454	1	6vi	1.3	393670	1120	810	135	1060	210	110		
1001	2	1iii	4.0	369340	985	1165	130	1650	185	40		
1003	2	1iii	2.9	400380	980	1110	130	1450	185	40		
1004	2	1iii	2.4	409400	945	1050	180	1410	280	9		
1007	2	1iii	3.2	402210	1640	1070	495	1520	1270	150		
1008	2	1iii	1.0	335910	895	850	90	1275	160	50		
1009	2	1iii	4.6	413940	1095	1240	120	1840	160	45		
10111	10	1iii	7.8	395620	1205	130	2460	290	4340	15		
10112	10	1iii	7.6	386890	2245	170	2380	340	5060	BD		
1050	2	1i	11.4	396020	810	1050	100	1570	100	20		
1051	2	1i	1.1	411040	870	1080	90	1540	115	4		
1051 ⁴	2	1i	2.2	408440	860	1090	120	1580	105	16		
1054	2	1i	10.8	409920	940	1100	95	1630	115	13		
1055	2	1i	8.9	409980	1160	1045	160	1605	230	25		
1056	2	1i	4.2	407100	1220	1100	155	1725	275	45		
501	14	61	0.1	346390	3280	1270	70	1580	390	30		
502	14	61	4.6	359710	11100	1320	95	1575	285	30		
503	14	61	4.9	379820	11080	1170	90	1610	225	15		
504	12	63ii	3.0	400230	5500	745	130	830	200	50		
505	12	63ii	15.4	343910	8245	830	90	1250	120	8		
506	12	63ii	10.8	388280	5610	880	110	1175	260	310		
507	12	63ii	2.8	380060	1935	810	120	1075	155	60		
509	12	63ii	5.8	368320	2520	810	110	1010	200	290		
510	M	63i	34.6	393050	3120	550	210	315	750	435		
512	12	63i	5.2	389950	3345	810	100	930	195	85		
513	12	63i	4.9	383320	3925	540	155	345	180	120		
514	12	63i	5.0	388450	3170	825	135	880	230	77		

Sample	SP	LM	IR	Ca	Mg	Sr	Mn	Na	Fe	Al	$\delta^{18}\text{O}$	$\delta^{13}\text{C}$
515	12	63i	6.4	366460	3675	1135	35	1620	130	140		
701	12	51	24.9	324470	3080	785	290	1200	2340	400		
702	12	51	11.3	365500	1470	780	345	1140	2485	250		
703	12	51	2.6	361120	3000	740	405	1110	2610	140	-6.56	-0.47
704	12	51	3.2	301300	2490	660	285	920	2190	50		
705	12	51	6.4	292970	1135	700	300	1030	2595	245		
706	12	51	4.8	342470	4320	805	325	1160	2370	80		
707	12	51	1.8	335560	3440	665	365	940	2260	100	-6.37 -6.85	-0.11 -0.32
711	9	51	3.9	361380	9050	130	2220	230	3400	70		
712	9	51	0.9	378840	5250	130	1185	345	2895	40		
713	9	51	1.0	379650	8625	230	1960	290	4180	40		
730	12	50	6.6	368140	16225	410	590	685	5485	160		
731	12	50	16.8	398330	12020	370	410	860	5825	135	-8.50	-0.76
732	12	50	6.6	368770	18740	415	610	645	6455	140	-7.73	-0.79
736	12	50	7.5	404300	13030	450	510	710	3900	130		
737	12	50	5.1	398350	16545	590	590	840	5340	145		
738	12	50	13.5	355860	16760	800	520	815	4950	BD	-7.84	-0.66
739	12	50	12.5	405400	19670	455	600	630	6700	100		
746	15	49	6.3	382880	7495	785	25	1270	480	210		
747	15	49	7.3	391930	4685	850	6	1480	325	45		
748	15	49	1.3	312820	3620	750	1	1300	225	60		
749	15	49	6.7	378040	5320	710	120	1200	960	450		
750	15	49	2.0	407230	4450	900	0	1495	530	170		
752	15	49	3.5	373730	7360	790	130	1260	560	0		
760	14	77iv	9.6	341710	3710	840	180	1030	380	305		
761	14	77iv	15.3	401430	4395	730	45	1415	315	490	-5.73	+0.83
762	14	77iv	12.4	365490	3670	820	160	1050	370	140	-5.34	+0.78
763	14	77iv	6.9	440450	3720	855	150	1250	350	280		
764	14	77iv	15.2	387890	3810	820	160	1100	520	220		
765	16	77iii	15.6	397340	4270	720	205	1055	680	80		

Sample	SP	LM	IR	Ca	Mg	Sr	Mn	Na	Fe	Al	$\delta^{18}\text{O}$	$\delta^{13}\text{C}$
766	16	77iii	6.4	397270	3050	755	175	1025	450	125		
767	16	77iii	8.3	362450	4850	935	270	1505	700	245		
768	16	77iii	8.4	386320	1510	310	85	480	220	70		
769	M	77iiii	11.4	370750	18015	370	530	600	6555	80		
773	12	65i	6.0	415550	3185	590	130	585	120	30	-6.81	+1.15
774	12	65i	6.1	404840	3360	515	120	535	110	70		
775	12	65i	10.6	404870	3105	615	130	740	130	70	-5.84	+1.15
776	12	65i	4.2	358590	3990	640	150	650	130	100		
777	12	65i	15.8	397200	3150	475	155	365	135	40		
778	12	65i	8.4	378470	3640	530	135	480	120	80		
784	12	66i	4.0	215150	1685	550	30	1070	170	110		
785	12	66i	66.7	621040	4970	1395	50	3565	470	740		
786	12	66i	69.9	437690	3700	970	90	2560	540	550		
788	14	73	13.0	317000	3910	710	240	940	690	430		
789	14	73	6.0	384870	3850	830	280	1040	875	170		
791	14	81	8.1	381920	2780	630	200	590	360	75		
792	14	81	11.4	373400	4360	835	185	990	510	225		
793	14	81	5.3	375360	2610	560	230	330	350	75		
794	14	81	7.6	376290	3790	945	115	1490	665	95		
795	14	81	2.4	400550	2970	670	185	675	410	75		
796	10	81	1.5	408610	2470	310	250	180	610	70		
797	16	79	3.7	403700	3570	650	160	850	400	150		
798	16	79	10.7	401200	3240	850	100	1350	310	70		
799	16	79	2.0	413690	2780	860	50	1525	105	120		
801	16	78v	9.3	388650	2980	720	115	1195	790	55		
803	16	78v	12.0	398010	3165	770	105	1260	620	130		
804	16	78v	14.0	387310	2825	710	100	1010	610	340		
805	16	78v	6.2	402010	2985	760	110	1130	670	420		
806	16	78v	5.4	382020	2855	680	100	1175	570	135		
807	16	78vi	4.2	369020	2730	795	130	1070	480	90		
808	16	78vi	12.0	365060	3085	775	130	1115	460	210		

Sample	SP	LM	IR	Ca	Mg	Sr	Mn	Na	Fe	Al	$\delta^{18}\text{O}$	$\delta^{13}\text{C}$
809	16	78vi	8.2	365560	3200	610	225	785	550	120		
810	M	78vi	10.5	382610	3200	415	285	110	660	40		
810 ⁴	M	78vi	6.3	382080	2700	380	290	130	710	65		
811	10	78vi	6.3	370300	1510	470	260	75	885	40		
812	14	78i	5.1	380030	3480	975	80	470	640	BD		
813	14	78i	1.5	397360	3500	1010	110	1060	645	40		
814	14	78i	3.1	408770	3705	905	90	1010	620	BD		
815	14	78i	2.3	390190	3200	875	50	1320	450	BD		
816	14	78i	9.0	389660	3690	840	70	1050	830	60		
818	15	78i	1.4	380830	2615	700	0	1460	370	120		
819	15	78i	0.1	374090	2660	370	0	1300	700	4890		
822	14	78iii	3.7	404390	3160	1010	50	1330	495	80		
823	14	78iii	4.9	375210	3690	1185	120	1230	575	110		
824	10	78iii	3.7	359220	1495	220	350	135	1670	85		
825	14	78iv	13.2	380660	4295	490	300	215	700	105		
826	14	78iv	4.5	347220	263	1095	80	1260	525	175		
827	14	78ii	9.0	381990	3945	570	255	330	430	80		
827 ⁴	14	78ii	8.9	376300	3905	570	240	335	425	80		
828	14	78ii	3.5	386560	2490	795	400	715	500	95		
829	M	78ii	12.5	374390	3890	590	240	335	895	130		
830	14	69	4.3	351590	3675	1010	80	1270	620	220		
831	14	69	4.8	352000	3660	1120	70	1450	390	260		
832	14	69	5.1	376400	3070	1000	180	1230	595	205		
835	16	66ii	2.3	396550	2975	1040	40	1365	50	160		
836	16	66ii	1.3	412450	3230	1070	70	1460	85	290		
837	16	66ii	3.7	407920	2620	1100	40	1360	170	150		
839	12	66ii	0.9	360090	3350	685	110	540	90	65		
840	12	676ii	12.1	401790	3290	740	100	740	125	130		
841	12	66ii	1.9	400540	3420	730	100	720	120	70		
842	12	66ii	8.4	403820	3485	970	90	1245	100	30		

Sample	SP	LM	IR	Ca	Mg	Sr	Mn	Na	Fe	Al	$\delta^{18}\text{O}$	$\delta^{13}\text{C}$
843	14	66ii	14.8	381740	2940	1090	180	1070	165	130		
844	16	66ii	2.6	388920	2910	1000	55	1150	95	120		
845	16	66ii	8.1	380490	3195	1095	85	1300	120	85		
851	10	68	5.3	385000	1150	400	160	80	560	130		
855	14	80ii	5.1	373850	2630	1020	110	1045	135	95	-6.37	+1.51
856	14	80ii	13.0	387570	2580	940	125	940	220	30	-5.11	+1.68
861	14	57	5.9	380010	5180	960	935	1230	230	60		
862	14	57	15.6	383000	5065	1185	525	1540	1230	165	-6.48	+0.23
863	14	57	5.8	380840	4305	1140	450	1420	1065	90		
864	14	57	12.8	351850	6010	1040	520	1325	1650	35		
866	14	57	12.7	420560	5680	1105	670	1595	1550	1300		
867	14	57	10.4	392990	4710	1045	580	1550	1300	55		
867 ⁴	14	57	11.7	402070	4740	1125	595	1680	1335	45		
873	14	58	8.3	384960	4105	1220	460	1765	565	10		
874	14	58	3.8	400860	4160	1485	340	2370	370	25		
875	14	58	8.5	390150	4865	1050	1180	1535	960	12		
876	14	58	9.6	384510	4405	1155	830	1770	790	10		
877	14	58	10.3	387360	4195	1320	595	1900	620	19	-6.69 -6.25	-0.04 +0.25
878	14	58	4.8	395100	4010	1330	510	2000	670	20		
879	14	58	4.8	368640	3965	1135	715	1375	720	16	-5.60	+0.17
880	14	47	5.0	347840	4260	1195	465	1500	755	30	-7.10	+0.59
881	14	47	4.9	356080	2740	1080	90	1160	345	45	-5.99	+0.79
882	14	47	5.0	367210	3310	1080	80	1060	335	10		
883	14	47	6.2	361450	4560	955	90	955	520	5	-6.17 -6.01	+0.53 +0.51
885	14	47	5.7	356680	6355	925	170	970	735	15		
890	14	47	6.2	368110	4310	980	95	860	550	20	-4.53	+1.74
891	14	47	6.7	364980	3930	805	180	335	695	20	-5.63 -5.61	+1.18 +1.07
892	14	47	4.7	365620	3815	690	140	525	575	65		
893	14	47	2.1	376400	5075	1160	80	1090	470	30		

Sample	SP	LM	IR	Ca	Mg	Sr	Mn	Na	Fe	Al	$\delta^{18}\text{O}$	$\delta^{13}\text{C}$
894	14	47	3.4	386720	5700	1160	70	1490	550	10		
895	14	47	9.0	363320	6590	1075	70	1235	640	17		
898	12	59	8.5	371280	5335	1135	100	1550	785	20		
899	12	59	10.7	367030	4810	1220	80	1650	690	40		
900	12	59	9.6	349960	5340	1110	85	1440	575	70		
901	12	59	6.2	369260	4250	1305	115	1630	880	75		
1501	16	68	8.8	303810	2435	430	130	100	300	80		
1502	14	68	9.1	356580	2800	765	120	590	530	270		
1503	14	68	11.6	375140	3010	665	135	490	660	200		
1504	14	68	7.9	375890	2840	550	160	310	710	30		
1505	14	68	12.2	385590	3670	620	60	850	1260	390		
1506	9	68	3.6	382790	4580	350	145	175	270	80		
1512	6	68	9.8	364450	4740	445	220	70	845	80		
1512 ⁴	6	68	9.5	364520	4820	445	220	110	840	25		
2000	21	37	0.0									
2003	21	37	1.6	377490	5955	895	285	395	540	40	-6.16	+2.48
2006	21	37	0.8	334570	12300	780	300	450	895	55		
2007	21	37	2.1	353150	12330	790	300	405	870	50	-5.55 -5.97	+2.33 +2.33
2010	21	37	1.4	369400	2260	920	130	415	265	300		
2013	21	37	0.9	320410	2025	720	380	580	830	90		
2100	22	40i	3.6	373360	1090	1260	19	1330	30	110	-1.74	+5.15
2101	22	40i	2.6	378760	1735	1195	75	1290	175	170	-2.84	+5.64
2102	22	40i	2.6	353640	3745	1210	195	1490	485	70		
2103	M	40i	36.2	277500	30650	215	1450	320	5050	140		
2104	22	40i	2.7	380090	3060	1070	165	1150	295	60		
2105	22	40	2.2	373170	3875	1230	190	1330	370	50		
2106	22	40i	3.1	377340	2350	1130	140	1165	280	65		
2108	23	40i	5.6	377730	2120	1185	75	840	230	30		
2109	23	40i	2.4	364370	3350	1160	110	940	385	90		
2110	23	40i	5.0	373110	1680	1290	20	950	140	30		

Sample	SP	LM	IR	Ca	Mg	Sr	Mn	Na	Fe	Al	$\delta^{18}\text{O}$	$\delta^{13}\text{C}$
2110 ²	23	40i	2.2	377630	1650	1250	15	970	150	65		
2112	23	40i	7.4	374090	1985	1220	40	1265	155	180		
2115	23	40i	1.5	372900	2290	1215	80	1340	275	65		
2116	23	40i	4.6	368720	2810	1235	115	1375	290	260		
2117	23	40i	6.4	374310	1585	1235	1	1270	90	100		
2118	23	40i	7.6	359800	1745	830	50	1140	220	30		
2119	24	40i	1.8	371040	2910	1240	50	1440	180	70		
2120	24	40i	5.5	376510	4580	1235	110	1400	290	140		
2121	24	40i	1.5	373350	2835	1250	160	1430	560	75		
2123	24	40i	1.2	356410	2980	1140	140	1220	475	90		
2131	23	40iv	3.0	371790	4040	1035	240	1150	385	70		
2132	23	40iv	7.3	366600	4050	950	220	820	385	70		
2134	23	40iv	4.8	390580	4070	1115	280	765	200	40		
2138	23	40iv	6.1	413680	6685	1010	585	820	610	40		
2143	23	40iv	6.6	404150	1800	1175	75	825	60	50		
2160	23	40v	6.8	412060	2890	1240	215	920	150	25		
2161	23	40v	5.7	385570	2370	1210	165	920	130	35		
2162	23	40v	5.3	405550	1555	1105	70	805	50	30		
2163	23	40v	6.5	416520	1945	1170	110	990	60	30		
2164	23	40v	4.7	317590	2055	1135	80	780	50	45		
2170	23	40iii	4.4	369110	3770	1240	255	1410	280	135		
2171	23	40iii	4.8	384210	1840	1240	90	1500	95	70		
2172	24	40iii	9.2	409550	3670	1105	340	1260	400	90		
2173	24	40iii	8.7	418250	1990	1120	180	1420	250	100		
2174	22	40iii	15.0	370100	5280	1205	310	1350	380	190	-4.17	+4.58
2175	24	40iii	3.1	360150	3550	1240	265	1360	290	135		
2176	22	40iii	11.3	346910	1880	1275	140	1310	135	130	-3.29	+5.36
2177	24	40iii	4.5	411340	2445	1150	230	1390	205	115		
2180	24	40iii	10.6	355520	3740	1260	295	1485	310	120		
2181	23	40iii	11.8	366050	6080	940	705	740	565	125		
2182	23	40iii	8.0	409660	15520	1000	930	815	1280	100		

Sample	SP	LM	IR	Ca	Mg	Sr	Mn	Na	Fe	Al	$\delta^{18}\text{O}$	$\delta^{13}\text{C}$
2183	23	40iii	6.5	394150	4850	1170	375	1410	400	65		
2190	23	40ii	3.0	414980	1320	1220	80	900	90	35		
21904	23	40ii	12.0	367650	1250	1260	75	945	80	70		
2191	24	40ii	6.7	408610	6720	1125	360	1190	490	100		
2193	24	40ii	4.2	377880	2970	1180	115	1265	225	50		
2194	24	40ii	11.1	404500	22020	870	1390	1000	2230	150		
2195	24	40ii	12.5	282990	2860	1290	120	1545	210	40	-3.61	+5.65
2300	22	40xxiv	14.5	318340	1670	1260	35	1390	90	1	-3.25	+5.32
2301	22	40xxiv	4.6	364770	3240	1090	90	1175	150	30	-3.46	+4.98
2302	22	40xxiiv	7.5	383380	3455	4260	190	1260	270	90		
2303	23	40xxiv	6.5	369560	2415	1250	90	1450	125	70		
2304	23	40xxiv	6.9	404340	5225	1240	205	1020	330	115		
2305	23	40xxiv	6.1	413100	1865	1280	60	930	100	90		
2306	24	40xxiv	7.1	378200	5160	1220	215	1430	375	155		
2307	24	40xxiv	3.6	341390	3210	1285	160	1340	250	140		
2308	24	40xxiv	5.7	428500	3975	1220	220	1480	320	160		
2320	22	40xxiii	7.6	429190	4940	1175	170	840	315	115		
2322	23	40xxiii	2.7	380040	1205	1165	30	750	1150	95		
2323	23	40xxiii	4.5	441070	1335	1240	35	1070	70	45		
2324	23	40xxiii	5.8	412250	2460	1225	50	1090	70	50		
2325	23	40xxiii	8.2	391860	3160	1210	235	1520	490	70		
2326	24	40xxiii	7.0	408550	3550	1115	180	1535	340	65		
2327	24	40xxiii	9.6	380250	4690	1285	175	1800	365	30		
2328	24	40xxiii	10.0	367250	3670	1155	165	1530	330	85		
2340	23	40xxi	6.0	428373	1590	1265	1	1030	55	120		
2341	23	40xxi	5.5	439360	1880	1170	1	900	140	140		
2342	23	40xxi	8.3	312770	8230	970	490	1330	740	125		
2344	24	40xxi	13.1	353200	4855	1550	170	1830	330	160		
2346	22	40xxi	5.9	320680	2830	1330	140	1140	295	130		
2351	23	40xx	6.1	398210	1160	1625	2	920	65	70		

Sample	SP	LM	IR	Ca	Mg	Sr	Mn	Na	Fe	Al	$\delta^{18}\text{O}$	$\delta^{13}\text{C}$
2352	23	40xx	6.6	421960	7015	1455	220	930	415	125		
2353	23	40xx	6.8	428180	3605	1360	50	925	215	175		
2354	23	40xx	8.3	400890	5295	1500	110	1365	460	100		
2355	24	40xx	12.0	414330	3680	1360	100	1385	285	140		
2356	24	40xx	15.3	412310	4970	1560	70	1540	430	85		
2370	24	40xix	4.7	439500	2985	1440	35	1630	265	150		
2371	24	40xix	13.2	446840	3815	1110	260	1580	330	120		
2372	24	40xix	6.9	394620	3685	1195	130	1535	300	165		
2373	24	40xix	6.1	405740	3260	1170	100	1570	270	175		
2373 ²	24	40xix	4.5	435050	3290	1130	110	1560	270	145		
2374	23	40xix	3.7	419610	1595	1060	1	865	70	110		
2375	23	40xix	7.4	329250	7760	1110	50	890	470	250		
2376	23	40xix	5.3	397080	4475	1190	150	910	240	165		
2377	22	40xix	5.3	399100	1960	1360	40	1200	110	190	-3.61 -3.28	+4.56 +4.88
2378	22	40xix	8.8	392750	3220	1285	140	1420	235	135	-2.71	+5.02
2380	22	40xviii	11.1	385030	3800	1225	110	1340	225	170		
2381	24	40xviii	4.6	404260	4110	1170	130	1300	340	180		
2382	24	40xviii	10.3	418770	4010	1200	270	1450	310	190		
2383	24	40xviii	13.9	382230	3910	855	330	1160	360	115		
2385	24	40xviii	8.1	416180	3685	1210	100	1570	230	160		
2387	24	40xviii	3.9	399860	2875	1195	200	1465	280	85		
2400	24	40xvi	5.8	365380	3710	1120	480	1255	300	60		
2401	24	40xvi	5.3	370440	3890	1280	160	1565	310	85		
2402	24	40xvi	6.4	376860	4125	1150	320	1380	420	50		
2403	24	40xvi	10.6	385650	4320	1310	190	1750	370	40		
2450	24	40xv	9.8	390000	3970	1150	290	1330	360	45		
2451	24	40xv	7.8	421180	2670	1315	110	1630	220	BD		
2452	24	40xv	6.5	382310	5300	1310	370	1545	70	90		
2460	23	40x	6.2	392800	2480	1095	70	850	130	35		
2461	23	40x	8.3	415420	5915	1175	130	820	435	50		

Sample	SP	LM	IR	Ca	Mg	Sr	Mn	Na	Fe	Al	$\delta^{18}\text{O}$	$\delta^{13}\text{C}$
2462	23	40x	7.1	422670	6620	1220	140	910	450	105		
2463	25	41 x	9.6	396060	1930	1315	110	1635	110	30	-3.61	+4.67
2464	25	41 x	3.9	434420	2140	1230	80	1325	165	30	-3.92	+4.88
2465	25	41 x	5.0	412410	2575	1230	75	1390	175	40		
2470	24	41 x iii	8.3	426570	3460	1265	160	1675	325	60		
2471	24	41 xiii	2.9	412390	2980	1155	160	1620	380	60		
2472	22	41 xiii	5.6	406400	2680	1200	140	1310	225	30	-3.91	+5.46
2473	22	41 xiii	5.4	384370	2790	1250	90	1370	190	25		
2474	22	41 xiii	9.5	390180	2240	1215	80	1300	140	60	-3.53 -3.49	+5.10 +4.99
2480	22	40xiv	10.2	395540	1835	1290	90	1335	110	60		
2481	24	40xiv	4.8	409050	3790	1215	135	1450	230	25		
2485	24	40xii	9.9	358010	5835	1115	410	1200	770	60		
2486	24	40xii	5.1	283870	1150	880	220	905	130	9		
2490	25	41 ix	4.7	348890	2725	975	150	810	270	BD		
2491	25	41 ix	1.4	361420	1725	1340	40	1410	80	5		
2491 ²	25	41 ix	12.5	436710	1935	1545	55	1575	80	14		
2492	25	41 ix	9.9	397760	4545	1290	185	1505	525	BD		
2495	24	40xi	3.3	369720	2740	1340	240	1570	220	19		
2496	24	40xi	10.3	349500	3630	1105	805	1320	390	50		
2497	24	40xi	10.2	392350	3720	1240	110	1535	245	40		
2498	24	40xi	6.1	387480	3975	1190	420	1470	545	115		
2500	25	40vii	2.6	417500	1670	1340	60	1440	135	65		
2501	25	40vii	3.3	420300	2610	1275	110	1520	350	85		
2510	22	40vi	2.8	406390	2140	1190	70	1265	190	115	-2.85 -2.87	+4.91 +4.75
2511	22	40vi	8.7	416460	2625	1205	95	1370	275	70		
2512	22	40vi	3.7	407620	3100	1215	170	1450	445	140		
2513	22	40vi	7.1	416670	4780	1120	225	1250	580	100	-4.50	+4.85
2520	22	40ii	7.7	413960	7265	1290	190	1400	685	185	-3.48	+4.79
2521	23	40ii	7.8	400270	1540	1235	65	920	110	70		
2524	22	40ii	6.5	411730	2175	1240	90	1440	175	95		

Sample	SP	LM	IR	Ca	Mg	Sr	Mn	Na	Fe	Al	$\delta^{18}\text{O}$	$\delta^{13}\text{C}$
2530	29	40i	10.3	348990	9250	1130	420	1470	1000	125		
2531	29	40i	6.4	351020	5750	1205	385	1450	605	90		
2532	29	40i	11.6	369340	12860	1010	425	1285	1240	125		
2533	29	40i	4.2	373940	7780	1130	420	1495	765	100		
2534	23	40i	7.1	356030	9860	1110	260	900	1035	105		
2536	22	40v	5.6	370820	1865	1145	120	1350	185	90		
2540	22											
2541	22	40iv	3.2	341620	1970	1220	95	1320	220	100		
2545	22	40iii	7.5	356630	1905	1300	95	1380	210	120	-3.39	+5.13
2546	22	40iii	4.4	355560	9185	1240	210	1225	775	180		
2600	21	45	5.0	417840	1520	985	180	700	380	75	-5.12	-0.46
2601	21	45	6.1	417130	1915	690	1065	575	2980	60	-7.58	-0.60
2602	21	45	10.1	421330	3900	990	370	860	1235	40		
2603	21	45	7.9	420270	3430	535	1340	460	3200	60		
2605	21	45	5.1	418290	1840	705	920	630	2935	140		
3001	27	36	6.2	404704	4100	1755	280	1370	1185		-5.02 -5.26	+4.15 +3.97
3002	28	36	11.1	352962	3650	2900	70	1860	650			
3003	27	36	10.6	407260	5820	1915	270	1490	1300		-5.23	+3.91
3004	27	36	12.4	373588	9130	3160	285	1500	1305			
3005	30	36	8.6	380111	7660	2745	240	1280	1060		-5.06	+4.02
3006	30	36	11.2	294098	9825	3340	410	1130	1505			
3007	28	36	7.3	338606	4060	2155	105	1540	690			
3008	28	36	6.2	370013	5895	2975	110	1390	820			
3009	28	36	9.8	422530	3910	2640	100	1635	600			
3010	27	36	16.1	396613	3420	1890	230	1600	890			
3011	28	36	13.7	288792	3610	1600	180	1075	470		-5.05	+4.16
3012	29	36	8.0	367282	5175	2655	250	1540	855			
3013	28	36	7.8	345019	4140	1600	150	1420	680			
3014	29	36	6.6	415025	4960	2685	175	1390	610		-4.57	3.90
3015	29	36	6.6	383962	4070	2750	215	1590	550			

Sample	SP	LM	IR	Ca	Mg	Sr	Mn	Na	Fe	Al	$\delta^{18}\text{O}$	$\delta^{13}\text{C}$
3016	29	36	3.8	371906	5400	2610	190	1340	790		-4.73	+4.03
3017	28	36	8.5	383079	8775	2550	270	1340	1170			
3018	28	36	5.9	389297	3390	2720	120	1470	660		-4.61 -4.57	+4.00 +4.01
3019	28	36	9.6	371393	8770	2550	270	1340	1170			
3020	30	36	8.1	376568	3765	3750	140	1580	620			
3021	27	36	10.7	346568	10080	2740	360	1335	1570			
3022	27	36	13.9	356914	5175	3315	210	1420	1605			
3023	29	36	4.6	356000	6360	2520	170	1325	915			
3024	29	36	4.4	323816	3980	1255	195	1540	895			
3025	28	36	6.6	302975	4410	1165	130	1680	720			
3026	23	36	6.4	351754	5790	2510	205	1450	670			
3027	29	36	4.5	383882	5190	2495	210	1330	535		-4.96	+4.21
3028	29	36	6.3	285087	4220	1365	210	1610	795			
3029	30	36	11.6	275664	5030	1170	190	1350	1025			
3030	30	36	13.4	289653	4025	750	370	1525	1465			
3031	28	36	10.8	363172	11400	1940	440	1070	1750			
3032	28	36	6.5	356395	6260	1705	330	1275	790			
3033	M	36	35.9	279905	27120	130	850	280	5340			
3034	M	36	24.0	325087	22427	190	1140	325	4230			
3035	29	34	4.4	348611	3410	1315	215	1500	645			
3036	28	34	5.6	355059	3170	1620	180	1595	695			
3037	28	34	6.9	355618	3320	1610	160	1490	570			
3038	29	34	5.2	392357	2940	2665	140	1390	620			
3039	29	34	7.7	359787	3760	1850	220	1565	695			
3040	29	34	7.5	379202	6765	1960	235	1340	900			
3041	29	34	5.8	332486	8470	1765	265	1405	930			
3042	28	34	6.2	376040	5990	2600	305	1580	750			
3043	23	34	2.1	342316	2260	810	460	740	4380			
3044	28	34	8.9	365826	6015	2530	400	1340	870			
3045	28	34	6.8	355683	6810	2015	415	1310	930			

Sample	SP	LM	IR	Ca	Mg	Sr	Mn	Na	Fe	Al	$\delta^{18}\text{O}$	$\delta^{13}\text{C}$
3046	28	34	9.3	384267	12110	1695	530	1030	2500			
3047	28	34	11.4	335145	5435	1000	385	1350	1000			
3048	28	34	7.1	326996	4930	920	560	1370	1000			
3049	29	34	9.7	304152	7595	1800	390	1385	1160			
3050	28	34	8.1	342014	4275	1610	390	1440	650			
3051	M	34	30.0	420030	31551	145	840	320	5220			
3052	28	35	17.7	318623	31286	550	805	990	4810			
3053	28	35	17.9	342000	23689	620	900	715	5015			
3054	23	35	6.9	328444	21348	410	1350	615	4205			
3055	23	35	17.7	322444	4150	770	640	900	1120			
3056	28	35	12.9	341072	2150	880	465	1470	675			
3057	23	41	12.3	378400	4735	1830	330	775	840			
3058	23	41	15.6	399560	10550	1185	820	1260	1460			
3059	23	41	12.0	362270	11490	675	570	760	1570			
3060	23	41	11.2	407610	3620	930	870	1690	995			
3061	24	41	25.4	368650	14595	680	1150	1960	2525			
3062	24	41	6.6	384090	5125	530	360	1370	770			
3063	22	46	8.5	390140	1815	1740	290	1585	1120			
3064	23	46	8.3	379550	1810	935	570	505	6945			
3065	24	46	19.7	358470	1985	620	970	1590	2550			
3066	31	46	9.6	377010	2375	685	560	800	5530			

Appendix IV
Statistical Tables

Table A-1. Factor analysis (varimax rotated factor matrix; Nie et al., 1975) of Devonian brachiopod elemental chemistries (n= 253). Interpretations are based on applied and theoretical geochemical considerations (cf. Brand and Veizer, 1980).

	Factor 1	Factor 2	Factor 3	Communality
log Ca	-.075	.154	<u>-.732</u>	.565
log Mg	.718	.163	.193	.581
log Sr	-.197	<u>.816</u>	.291	.789
log Mn	<u>.881</u>	-.066	.102	.791
log Na	.107	<u>.910</u>	-.053	.841
log Fe	<u>.850</u>	.163	.104	.759
log Al	.267	.136	.485	.325
log I.R.	-.089	.033	<u>.705</u>	.506
% of variation explained	30.3	21.5	12.7	
Eigenvalue	2.425	1.717	1.016	
Interpretation	Diagenetic alteration?	Environmental control?	Silicification/ Minor leaching?	

Table A-2. Factor analysis (varimax rotated factor matrix; Nie et al., 1975) of *Athyris spiriferoides* (Middle Devonian) elemental chemistries (n= 83). Interpretations are based on applied and theoretical geochemical considerations (cf. Brand and Veizer, 1980).

	Factor 1	Factor 2	Factor 3	Communality
log Ca	.052	-.080	<u>.714</u>	.519
log Mg	<u>.595</u>	.404	-.283	.597
log Sr	-.057	<u>.832</u>	.366	.830
log Mn	<u>.796</u>	.050	.004	.637
log Na	-.081	<u>.921</u>	-.149	.876
log Fe	<u>.820</u>	-.225	.012	.724
log Al	.487	.097	<u>.544</u>	.542
log I.R.				
% of variation explained	25.9	22.3	17.6	
Eigenvalue	2.107	1.782	1.407	
Interpretation	Diagenetic alteration?	Environmental control?	?	

Table A-3. Factor analysis (varimax rotated factor matrix; Nie et al., 1975) of *Mucrospirifer mucronatus* (Middle Devonian) elemental chemistries (n= 74). Interpretations are based on applied and theoretical geochemical considerations (cf. Brand and Veizer, 1980).

	Factor 1	Factor 2	Communality
log Ca	-.351	<u>.688</u>	.596
log Mg	<u>.777</u>	.451	.712
log Sr	-.159	<u>.921</u>	.857
log Mn	<u>.635</u>	.008	.903
log Na	.064	<u>.715</u>	.605
log Fe	<u>.831</u>	-.314	.790
log Al	<u>.745</u>	-.157	.579
log I.R.	.415	.233	.221
% of variation explained	35.9	23.7	11.9
Eigenvalue	2.873	1.896	
Interpretation	Diagenetic alteration?	Environmental control?	

Table A-4. Factor analysis (varimax rotated factor matrix; Nie et al., 1975) of *Mediospirifer audaculus* elemental chemistries (n= 59). Interpretations are based on applied and theoretical geochemical considerations (cf. Brand and Veizer, 1980).

	Factor 1	Factor 2	Communality
log Ca	.229	<u>.705</u>	.549
log Mg	<u>.865</u>	-.023	.749
log Sr	.022	<u>.851</u>	.725
log Mn	<u>.769</u>	-.049	.593
log Na	-.137	<u>.706</u>	.518
log Fe	<u>.884</u>	-.124	.797
log Al	<u>.681</u>	.023	.464
log I.R.	.337	<u>-.783</u>	-.727
% of variation explained	36.9	27.1	
Eigenvalue	2.955	2.169	
Interpretation	Diagenetic alteration?	Environmental control?	

Table A-5. Factor analysis (varimax rotated factor matrix; Nie et al., 1975) of *Tropidoleptus carinatus* elemental chemistries (n= 20). Interpretations are based on applied and theoretical geochemical considerations (cf. Brand and Veizer, 1980).

	Factor 1	Factor 2	Factor 3	Communality
log Ca	.111	.312	.782	.721
log Mg	.866	-.186	.119	.799
log Sr	.179	-.217	.868	.833
log Mn	-.428	.733	-.349	.843
log Na	.754	-.085	.586	.919
log Fe	.223	.871	-.046	.810
log Al	.915	.121	.076	.858
log I.R.	.163	.803	-.274	.746
% of variation explained	41.1	25.8	14.7	
Eigenvalue	3.286	2.064	1.179	
Interpretation	Taxonomic control and storage in shell calcite?	Diagenesis alteration?	Environmental control?	

Table A-6. Factor analysis (varimax rotated factor matrix; Nie et al., 1975) of *Rhipidomella vanuxemi* elemental chemistries (n= 17). Interpretations are based on applied and theoretical geochemical considerations (cf. Brand and Veizer, 1980).

	Factor 1	Factor 2	Factor 3	Communality
log Ca	<u>.905</u>	.011	-.141	.839
log Mg	-.163	.184	<u>.887</u>	.847
log Sr	<u>.867</u>	.041	.456	.962
log Mn	.152	<u>.935</u>	-.171	.927
log Na	.277	.055	<u>.921</u>	.929
log Fe	-.095	<u>.918</u>	.242	.911
log Al	-.272	.497	<u>-.620</u>	.705
log I.R.	<u>-.813</u>	.041	-.094	.672
% of variation explained	37.4	24.7	22.7	
Eigenvalue	2.995	1.979	1.817	
Interpretation	Environmental control?	Diagenesis alteration?	Taxonomic control and storage in shell calcite?	

Table A-7. Factor analysis (varimax rotated factor matrix; Nie et al., 1975) of Middle Devonian brachiopod elemental chemistries (N = 19). Interpretations are based on applied and theoretical geochemical considerations (cf. Brand and Veizer, 1980).

	Factor 1	Factor 2	Factor 3	Communality
log Ca	.388	-.152	-.765	.759
log Mg	.123	-.738	.159	.576
log Sr	.731	.124	-.201	.589
log Mn	.244	-.740	.381	.753
log Na	.863	-.146	.000	.766
log Fe	.339	-.213	.837	.861
log Al	.727	.150	.240	.609
log I.R.	.258	.804	.255	.777
$\delta^{18}\text{O}$.311	.792	.087	.732
$\delta^{13}\text{C}$.645	.663	.043	.858
% of variation explained	33.9	23.8	15.2	
Eigenvalue	3.389	2.376	1.515	
Interpretation				

Table A-8. Factor analysis (varimax rotated factor matrix; Nie et al., 1975) of Silurian brachiopod elemental chemistries (n= 205). Interpretations are based on applied and theoretical geochemical considerations (cf. Brand and Veizer, 1980).

	Factor 1	Factor 2	Factor 3	Communality
log Ca	-.110	.055	.779	.623
log Mg	.844	.105	.123	.738
log Sr	-.390	.733	.078	.695
log Mn	.853	-.018	-.085	.735
log Na	-.073	.848	-.017	.724
log Fe	.868	.222	.163	.830
log Al	.249	.042	.692	.542
log I.R.	.210	.634	.082	.452
% of variation explained	32.7	21.1	13.0	
Eigenvalue	2.617	1.686	1.038	
Interpretation	Diagenetic alteration?	Environmental control?	?	

Table A-9. Factor analysis (varimax rotated factor matrix; Nie et al., 1975) of *Eospirifer radians* elemental chemistries (n= 31). Interpretations are based on applied and theoretical geochemical considerations (cf. Brand and Veizer, 1980).

	Factor 1	Factor 2	Factor 3	Communality
log Ca	.057	.171	<u>.780</u>	.641
log Mg	<u>.908</u>	.065	.166	.856
log Sr	.036	<u>.699</u>	.081	.496
log Mn	<u>.933</u>	.059	.115	.888
log Na	.040	.245	-.476	.289
log Fe	<u>.962</u>	-.095	.115	.947
log Al	.257	-.053	<u>.719</u>	.586
log I.R.	.001	<u>.782</u>	-.172	.641
% of variation explained	36.9	16.2	13.8	
Eigenvalue	2.948	1.299	1.101	
Interpretation	Diagenetic alteration?	?	?	

Table A-10. Factor analysis (varimax rotated factor matrix; Nie et al., 1975) of *Whitfieldella nitida* elemental chemistries (N= 48). Interpretations are based on applied and theoretical geochemical considerations (cf. Brand and Veizer, 1980).

	Factor 1	Factor 2	Factor 3	Factor 4	Communality
log Ca	.047	-.215	<u>.902</u>	.085	.869
log Mg	<u>.891</u>	.240	-.028	.168	.880
log Sr	-.404	.438	<u>.617</u>	-.219	.784
log Mn	<u>.850</u>	-.253	.048	-.011	.789
log Na	.001	.402	-.053	<u>-.734</u>	.704
log Fe	<u>.867</u>	.219	-.099	.052	.813
log Al	.186	<u>.893</u>	.110	.012	.844
log I.R.	.134	.239	-.038	<u>.815</u>	.741
% of variation explained	33.6	19.1	14.3	13.2	
Eigenvalue	2.690	1.527	1.147	1.059	
Interpretation	Diagenetic alteration?	?	Environmental control?	?	

Table A-11. Factor analysis (varimax rotated factor matrix; Nie et al., 1975) of *Atrypa reticularis* elemental chemistries (n= 50). Interpretations are based on applied and theoretical geochemical considerations (cf. Brand and Veizer, 1980).

	Factor 1	Factor 2	Factor 3	Communality
log Ca	.215	.766	.014	.632
log Mg	-.233	.556	.639	.772
log Sr	.861	.060	.001	.745
log Mn	-.677	-.031	.535	.745
log Na	.867	.179	.114	.797
log Fe	-.487	.510	.397	.654
log Al	.094	.793	-.011	.638
log I.R.	.129	-.051	.869	.774
% of variation explained	32.6	26.3	13.0	
Eigenvalue	2.612	2.103	1.044	
Interpretation	?	?	?	

Table A-12. Factor analysis (varimax rotated factor matrix; Nie et al., 1975) of Ordovician brachiopod elemental chemistries (n= 133). Interpretations are based on applied and theoretical geochemical considerations (cf. Brand and Veizer, 1980).

	Factor 1	Factor 2	Factor 3	Communality
log Ca	.039	.411	.430	.362
log Mg	<u>.696</u>	.144	.001	.506
log Sr	-.088	<u>.890</u>	.201	.841
log Mn	<u>.778</u>	-.079	-.004	.612
log Na	.037	<u>.898</u>	.052	.810
log Fe	<u>.847</u>	-.099	.129	.743
log Al	-.163	-.185	<u>.804</u>	.708
log I.R.	.230	.029	<u>.670</u>	.503
% of variation explained	24.7	22.8	16.0	
Eigenvalue	1.974	1.826	1.284	
Interpretation	Diagenetic alteration?	Environmental control/	Laboratory leaching/	

Table A-13. Factor analysis (varimax rotated factor matrix; Nie et al., 1975) of *Dalmanella rogata* elemental chemistries (n= 40). Interpretations are based on applied and theoretical geochemical considerations (cf. Brand and Veizer, 1980).

	Factor 1	Factor 2	Factor 3	Communality
log Ca	-.138	.176	<u>.880</u>	.824
log Mg	<u>.522</u>	-.093	<u>.688</u>	.755
log Sr	<u>-.625</u>	<u>.598</u>	-.042	.750
log Mn	<u>.914</u>	-.218	.069	.887
log Na	-.227	<u>.886</u>	.001	.836
log Fe	<u>.903</u>	.273	-.019	.891
log Al	.376	<u>.631</u>	-.031	.540
log I.R.	-.104	<u>.660</u>	.184	.470
% of variation explained	34.7	25.7	14.6	
Eigenvalue	2.775	2.011	1.167	
Interpretation	Diagenesis alteration (meteoric)	Environmental control/ lab leaching?	?	

Table A-14. Factor analysis (varimax rotated factor matrix; Nie et al., 1975) of *Rafinesquina deltoidea* elemental chemistries (n= 64). Interpretations are based on applied and theoretical geochemical considerations (cf. Brand and Veizer, 1980).

	Factor 1	Factor 2	Factor 3	Communality
log Ca	.332	.024	<u>.612</u>	.485
log Mg	.421	.406	-.367	.476
log Sr	<u>.925</u>	.024	-.184	.890
log Mn	.153	<u>.792</u>	.070	.656
log Na	<u>.924</u>	.098	.059	.866
log Fe	.014	<u>.830</u>	-.052	.692
log Al	-.322	.077	<u>.717</u>	.625
log I.R.	-.270	.437	.494	.508
% of variation explained	31.0	20.3	13.7	
Eigenvalue	2.477	1.626	1.095	
Interpretation	Environmental control?	Diagenetic alteration?	Laboratory leaching?	

Table A-15. Factor analysis (varimax rotated factor matrix; Nie et al., 1975) of *Sowerybella* sp. elemental chemistries (n= 21). Interpretations are based on applied and theoretical geochemical considerations (cf. Brand and Veizer, 1980).

	Factor 1	Factor 2	Communality
log Ca	<u>.655</u>	-.379	.573
log Mg	<u>.723</u>	.492	.764
log Sr	<u>.845</u>	-.290	.798
log Mn	-.053	<u>.929</u>	.866
log Na	<u>.893</u>	-.154	.822
log Fe	-.039	<u>.907</u>	.824
log Al	<u>.516</u>	.012	.267
log I.R.	-.262	<u>.789</u>	.690
% of variation explained	42.0	28.0	
Eigenvalue	3.363	2.241	
Interpretation	Environmental control?	Diagenetic alteration?	

Appendix V. Table of summarized taphonomic features for selected beds from the Hamilton Group (Middle Devonian) of New York and Ontario.

Locality	Bed	Bio facies	Deform.	Taph.	Articulation Ratios					
					<i>Mucro.</i> A/D	<i>Ath.</i> A/D	<i>Medio.</i> A/D	<i>Rhip.</i> A/D	<i>Trop.</i> A/D	
		1.	2.	3.	4.					
1A (i)	Widder	N/A	N/A		47/52					
1B (ii)	Hungry Hollow	N/A	N/A		5/53					
1B (iii)	Arkona		N/A	N/A		35/16				
1B (iv)	Arkona		N/A	N/A		-/63				
2 (i)		4A			-/10	10/-	9/-			
2 (ii)		5A			26/7	6/55	12/-			
2 (iii)	Pleurodictyum	5B	S>C>T	B/E		14/4	5/7			
3 (i)	Ambocoeliid	3A	T>S			5/-	4/-			
3 (ii)	Demissa	5A	S>C>T		-/58	8/52	-/46	6/-		
3 (iii)		5A				9/3				
6 (ii)	Smoke Creek	4A	C>S		12/7					-/6
6 (iii)	Bay View Bed	5B		B/E/F					-/45	22/2
6 (v)	Demissa	5A	S>C>T		-/52	25/-	-/2	6/4	6/2	
6 (vi)	Concretion	4A	S>T			17/-	5/-			
7 (ii)	Demissa	5A	S>T		20/58	12/12	-/5	10/-	12/10	
7 (iii)	Mucrosp.	4B			2/35					
8 (ii)					5/15	3/10	7/29			
8 (iii)	Demissa	5A	S>T		36/65	37/-		8/-	39/-	
13 (ii)	Demissa	5A	S>T		13/35	59/115	-/14			
20 (iii)	Demissa	4A	S>T			8/3	5/3			

- n.b.
1. Brachiopods belong to biofacies association listed in Fig. 3.1
 2. Dominance of type of shell deformation. S = splayed; C = carinate; T = telescoped (Alexander, 1986).
 3. Presence of significant B = boring; E = encrustation; F = shell fragmentation
 4. Articulation ratios i.e. articulated valves to disarticulated